Year : 2019

Impact of TCR-ligand avidity for viral and tumor antigens on human CD8 T cell potency and long-term persistence

Couturaud Barbara

Département d'Oncologie Fondamentale

Impact of TCR-ligand avidity for viral and tumor antigens on human CD8 T cell potency and long-term persistence

Doctoral Thesis in Life Sciences (PhD)

presented to the Faculty of Biology and Medicine

of the University of Lausanne by

Barbara COUTURAUD

MSc. in Biotechnology

Ecole Nationale Supérieure de Technologie des Biomolécules de Bordeaux

Jury

Prof. Renaud Du Pasquier   President

Dr. Nathalie Rufer   Thesis director

Prof. Fabienne Tacchini-Cottier   Internal expert

Prof. Annette Oxenius   External expert

Lausanne, 2019

Imprimatur

Vu le rapport présenté par le jury d'examen, composé de

Président·e	Monsieur	Prof.	Renaud	**Du Pasquier**
Directeur·trice de thèse	Madame	Dre	Nathalie	**Rufer**
Expert·e·s	Madame	Prof.	Fabienne	**Tacchini-Cottier**
	Madame	Prof.	Annette	**Oxenius**

le Conseil de Faculté autorise l'impression de la thèse de

Madame Barbara Couturaud

Master d'ingénieur, École nationale supérieure de technologie des biomolécules de Bordeaux, France

intitulée

Impact of TCR-ligand avidity for viral and tumor antigens on human CD8 T cell potency and long term-persistence

Lausanne, le 30 août 2019
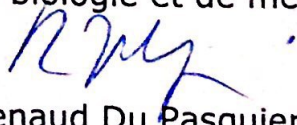
pour le Doyen
de la Faculté de biologie et de médecine

Prof.   Renaud Du Pasquier

Table of Contents

Summary

The development of immunotherapies against viral infections and cancer requires a better understanding of the key parameters that control T cell-mediated immune responses, such as TCR-ligand binding avidity. The overall aim of this thesis was to improve our knowledge regarding the contribution of TCR binding avidity in mediating the functional potency and maintaining the long-term memory of antigen-specific CD8 T cells. We first performed a comprehensive study of TCR-pMHC binding avidity (i.e. off-rates) combined with various functional assays on large libraries of tumor- and virus-specific CD8 T cell clones from melanoma patients and healthy donors. We demonstrated that TCR-pMHC off-rates accurately predicted the functional potential of antigen-specific CD8 T cells. Our data also confirmed the superior binding avidities of virus-specific compared with tumor–specific T cell clonotypes. The TCR-pMHC off-rate is a more stable and robust biomarker of CD8 T cell potency than frequently used functional assays that depend on multiple parameters, including T cell activation state. Together, our data show that the TCR-pMHC binding avidity is a reliable biophysical parameter for patient monitoring during immunotherapy. In the second part of this thesis, we investigated whether TCR-ligand avidity is a determining factor for the clonal selection and evolution of antigen-specific T cells over time. We studied TCRαβ clonotype composition and persistence over a period of 15 years combined with TCR-pMHC binding avidity analyses on large repertoires of cytomegalovirus (CMV)- and Epstein-Barr virus (EBV)-specific CD8 T cell clones from healthy donors. Within CMV-specific T cell repertoires, we observed the progressive contraction of clonotypes of higher TCR-pMHC avidity and lower CD8 binding dependency during chronic antigen exposure. Strikingly, we identified a unique transcriptional signature preferentially expressed by high-avidity T cell clonotypes, including elevated expression of the inhibitory receptor *LILRB1*. Enhanced proliferative capacity was also observed upon LILRB1 blockade. This was not the case for the EBV-specific T cell clonal composition and distribution that, once established, displayed an unprecedented stability for at least 15 years, independently of TCR-pMHC avidity. Our findings reveal an overall long-term avidity decline of CMV- but not EBV-specific T cell clonal repertoires, highlighting the differing role played by TCR-ligand avidity over the course of these two latent herpesvirus infections. We propose that the mechanisms regulating the long-term outcome of CMV- and EBV-specific memory CD8 T cell responses in humans are distinct.

Résumé

Le développement des immunothérapies ciblant les infections virales et les cancers requiert une meilleure compréhension des paramètres-clés qui contrôlent les réponses cellulaires T, tel que l'avidité des TCRs pour leur ligand. L'objectif global de cette thèse était d'améliorer nos connaissances sur la contribution de l'avidité du TCR à la médiation des fonctions cellulaires et au maintien de la mémoire à long terme des cellules T CD8. Nous avons initialement mené une étude analytique sur l'avidité du TCR combinée à divers essais fonctionnels sur des lymphocytes T CD8 dirigés contre des antigènes viraux et tumoraux chez des donneurs sains et des patients atteints de mélanome. Nous avons démontré que l'avidité du TCR prédisait avec précision les fonctions cellulaires des cellules T CD8. Nos résultats confirment également que les cellules T CD8 spécifiques pour les antigènes viraux sont de plus haute avidité que celles spécifiques pour les antigènes tumoraux. De plus, l'avidité du TCR est un biomarqueur de la capacité fonctionnelle des cellules T, qui est plus stable et robuste que les tests fonctionnels habituellement utilisés. Dans l'ensemble, nos résultats montrent que l'avidité du TCR est un paramètre biophysique fiable pour le suivi des patients traités par immunothérapie. Par la suite, nous avons évalué si l'avidité du TCR était un facteur déterminant pour la sélection clonale des cellules T CD8 au cours du temps. Sur une période de 15 ans, nous avons étudié la composition et la persistance des répertoires clonotypiques dirigés contre le cytomégalovirus (CMV) et l'Epstein-Barr virus (EBV) ainsi que l'avidité du TCR chez des donneurs sains. Dans le cas de la réponse lymphocytaire T contre le CMV, nous avons observé la contraction progressive des clonotypes de plus haute avidité et peu dépendants de l'interaction avec le corécepteur CD8, au cours du temps. Nous avons identifié une signature transcriptionnelle distincte chez les clonotypes de plus haute avidité, avec notamment de l'expression élevée du récepteur inhibiteur *LILRB1*. Une augmentation de la capacité proliférative des cellules T a également été observée lors du blocage de LILRB1. Cela n'était pas le cas des répertoires des cellules T CD8 dirigées contre l'EBV qui, une fois établis, sont maintenus de façon stable pendant au moins 15 ans, indépendamment de l'avidité du TCR. Nos résultats révèlent un déclin global à long terme de l'avidité des répertoires clonaux de lymphocytes T spécifiques du CMV, mais non de l'EBV, soulignant le rôle différent joué par l'avidité des TCRs au cours des infections latentes induites par ces deux virus. Nous suggérons que des mécanismes distincts régulent l'évolution à long terme des réponses lymphocytaires mémoires T CD8 spécifiques du CMV et de l'EBV chez l'homme.

Abbreviations

2D	Two-dimensional
3D	Three-dimensional
AIDS	Acquired immune deficiency syndrome
AP-1	Activator protein 1
APC	Antigen presenting cell
C	Constant
CARs	Chimeric antigen receptors
CCR7	C-C motif chemokine receptor 7
CD	Cluster of differentiation
CD62L	L-selectin
CDR	Complementarity determining region
CM	Central-memory T cell
CMV	Cytomegalovirus
CpG ODN	CpG oligodeoxynucleotides
CTLA-4	Cytotoxic T lymphocyte antigen 4
D	Diversity
DN	Double negative
DNA	Deoxyribonucleic acid
DP	Double positive
EBV	Epstein–Barr virus
EC_{50}	Half maximal effective concentration
EM	Effector-memory T cell
EMRA	Effector-memory CD45RA+ or Effector T cell
hCMV	Human cytomegalovirus
HCV	Hepatitis C virus
HIV	Human immunodefiency virus
HLA	Human leukocyte antigen
ICAM-1	Intercellular adhesion molecule 1
IE1	Immediate-early protein 1
IFA	Incomplete Freund's adjuvant
IFN	Interferon

IL	Interleukin
IM	Infectious mononucleosis
IS	Immunological synapse
ITAM	Immunoreceptor tyrosine-based activation motif
ITIM	Immunoreceptor tyrosine-based inhibitory receptor
J	Joining
K_D	Dissociation equilibrium constant
KLRG1	Killer-cell lectin like receptor G1
k_{off}	Dissociation rate
k_{on}	Association rate
LAG-3	Lymphocyte-activation gene-3
LAT	Linker of activated T cells
Lck	Lymphocyte-specific protein tyrosine kinase
LCMV	Lymphocytic choriomeningitis virus
LFA-1	Lymphocyte function-associated antigen 1
LILRB1	Leukocyte immunoglobulin-like receptor subfamily B member 1
MCMV	Mouse cytomegalovirus
MHC	Major histocompatibility complex
MP-SPR	Multiparametric surface plasmon resonance
N	Naive T cell
NFAT	Nuclear factor of activated T cells
NFκB	Nuclear factor-kappa B
NK	Natural killer
NTA	Nitrilotriacetic acid
NTAmers	NTA-His tag-containing multimer
NY-ESO-1	New York esophageal squamous cell carcinoma 1
PD-1	Programmed cell death 1
PDL-1	PD ligand-1
pMHC	Peptide-MHC complex
pp65	65kDa phosphoprotein
RAG	Recombination-activating gene
RNA	Ribonucleic acid
RNASeq	RNA sequencing

RSS	Recombination signal sequences
SHP	Src homology region 2 domain-containing phosphatase
SLO	Secondary lymphoid organ
SLP-76	SH2 domain containing leukocyte protein of 76kDa
SP	Single positive
SPR	Surface plasmon resonance
$t_{1/2}$	Half-time
TCR	T cell receptor
TGF-β	Tumor growth factor β
TIGIT	T cell immunoreceptor with Ig and ITIM domains
TNF	Tumor necrosis factor
TRAV	T cell receptor alpha variable
TRBV	T cell receptor beta variable
Treg	Regulatory T cell
V	Variable
VLA-1	Very late antigen-1
VZV	Varicella-Zoster Virus
WT	Wild-type
ZAP-70	Zeta-chain-associated protein kinase 70

Introduction

1.   T cell immunity

1.1.   T cells in the immune system

The human immune system comprises organs, cells and molecules, which serve to defend the body against invasion and infection by foreign pathogens and molecules. The immune system can be divided into an innate immune component, which acts rapidly and in a non-adaptive way, and the adaptive immune component, which takes days to develop but may provide lifelong protection against a particular pathogen. The two systems work closely together to shape an efficient immune response against a foreign organism whilst each having distinct functions (reviewed in [1]).

The innate immune system provides the first line of defense against pathogens, through anatomical and physiological barriers and innate immune cells such as macrophages, dendritic cells, neutrophils or natural killer (NK) cells. These cells provide an immediate response by detecting and neutralizing or eliminating invading pathogens as well as alerting other components of the immune system. In addition, humoral innate immune proteins, such as the complement proteins, can recognize and induce the destruction of foreign organisms.

On the other hand, adaptive immune responses are mediated by T and B lymphocytes, which recognize components of pathogens or abnormal self-cells (known as antigens) in a highly specific manner through their cell surface T and B cell receptors, respectively. T and B lymphocytes collectively possess an enormous repertoire of specificities enabling recognition of virtually any antigen they could encounter. Upon antigen recognition, they proliferate to generate large pools of lymphocytes sharing the same antigen specificity (i.e. clonal selection and expansion). B lymphocytes will then differentiate into plasma cells to produce antibodies, which neutralize extracellular pathogens and facilitate their elimination by other components of the immune system. T lymphocytes can be divided into either cytotoxic T cells (CD8+ T cells, CD stands for Cluster of Differentiation), able to directly kill infected or abnormal cells, or helper T cells (CD4+ T cells), able to secrete cytokines and to regulate the response of other immune cells. A subgroup of CD4+ T cells named regulatory T cells (Tregs) serve to prevent and limit the extent of immune activation. Some activated B and T cells will persist after the

resolution of the infection and differentiate into memory cells. In the case of a second exposure to the same antigen, memory cells are capable of generating an immune response that is faster and of greater amplitude, in order to efficiently eliminate the pathogen.

1.2. T cell development

B and T lymphocytes are derived from multipotent hematopoietic stem cells in the bone marrow. Whilst B cells undergo a large part of their development there, T cells must migrate from the bone marrow to the thymus in order to undergo thymocyte differentiation (reviewed in [2]). They first start as CD4-CD8- double negative (DN) cells in the thymic cortex, then either evolve into the minor population of γ:δ T cells or into the major population of α:β T cells we will focus on hereafter. α:β T cells then enter a double positive (DP) thymocyte stage, during which they express both CD4 and CD8 coreceptors. Finally, they mature into CD4+ or CD8+ single positive (SP) cells while entering the thymic medulla. This step of maturation is driven by the capacity of T cells to interact via the T cell receptor (TCR) with self-peptide presented in the major histocompatibility complex (MHC) class I and MHC class II, expressed by thymic epithelial cells. DP thymocytes that interact optimally with self-MHC will receive essential survival signals and further mature. This process is known as positive selection. DP thymocytes that are positively selected by interacting with MHC class I will differentiate into CD8+ SP, while thymocytes optimally interacting with MHC class II will differentiate into CD4+ SP (Figure 1). Thymocytes also undergo negative selection which eliminates those that recognize self-antigens too strongly, by apoptosis [3]. This process prevents autoimmune responses in the periphery. Both positive and negative selection, collectively known as central tolerance, lead to the death of the majority of thymocytes and it is estimated that only 2% of mature naive T cells will exit the thymus to form the peripheral T cell repertoire. Nonetheless, some self-reactive T cells specific for self-antigen (such as Melan-A, [4]), although of low affinity, survive negative selection and migrate to the periphery. However, these cells only rarely generate auto-immune responses, demonstrating the existence of mechanisms of peripheral tolerance that limit their activation. Such mechanisms can be clonal deletion of self-reactive T cells or their conversion into Tregs by antigen presenting cells (APCs) that present self-antigen in secondary lymphoid organs, or the depletion of the growth-factor interleukin-2 (IL-2) from the environment and secretion of immuno-suppressive cytokines, such as IL-10 and tumor growth factor β (TGF-β) by Tregs [5].
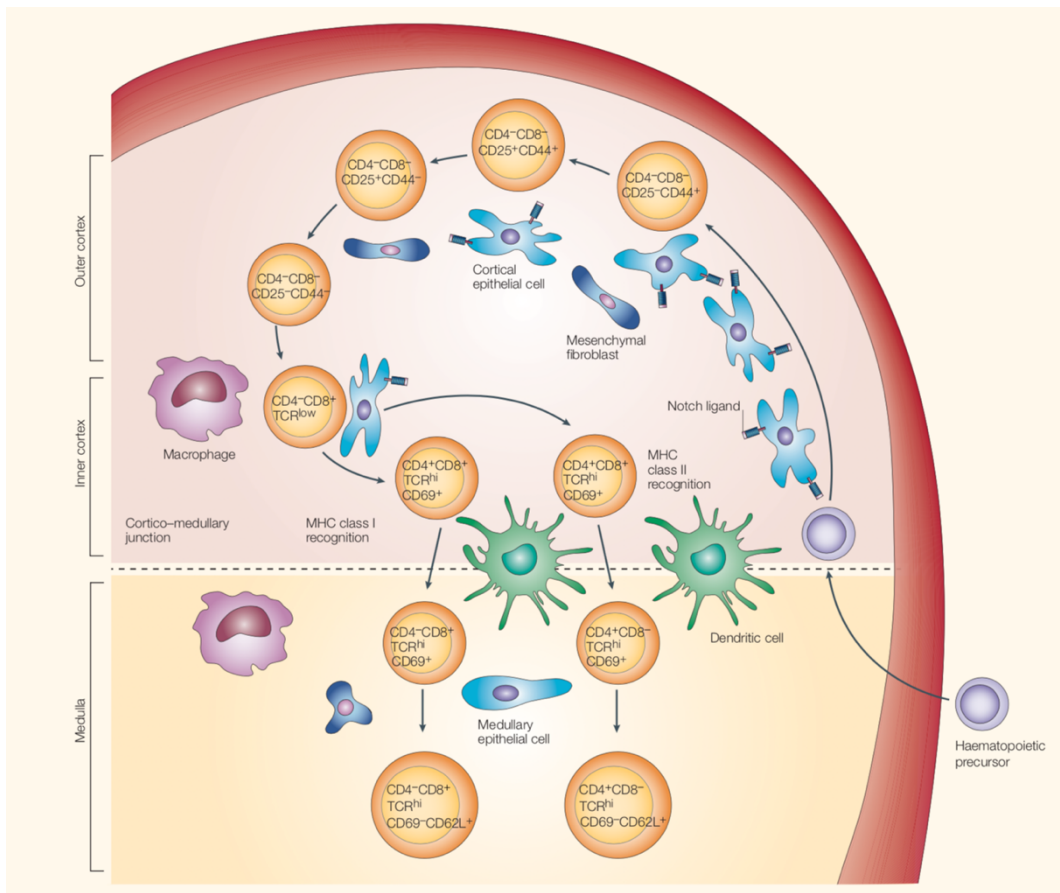
Figure 1: T cell development in the thymus. *Haematopoietic precursors migrate from the bonne marrow to the thymus, where T cell lineage commitment occurs. They first start as CD4-CD8- double negative (DN) cells in the thymic cortex, then enter a CD4+CD8+ double positive (DP) thymocyte stage, and finally mature into CD4+ or CD8+ single positive cells while entering the thymic medulla. Mature single positive T cells have been positively and negatively selected to generate self-tolerant CD4+ helper T cells and CD8+ cytotoxic T cells. Adapted from Zúñiga-Pflücker 2004 [2].*

1.3.   The T cell receptor and co-receptors

During T cell development, the TCR undergoes a process of gene-segment rearrangement to give rise to a heterodimer consisting of two transmembrane glycoprotein chains, the α and β chains. Both α and β chains are composed of a variable region, a constant region, a transmembrane region and a short cytoplasmic tail. The TCRα gene locus contains several variable (V) and joining (J) gene segments and one constant (C) region, whereas the TCRβ locus contains two diversity (D) gene segments in addition to several V and J gene segments and two C regions (Figure 2). The gene segments of each chain are randomly combined. First,

8

in double negative thymocytes, the β chain gene undergoes Dβ-Jβ rearrangement followed by Vβ-DβJβ rearrangement. Next, Vα-Jα rearrangement takes place in double positive thymocytes. Gene rearrangements are driven by the recognition of recombination signal sequences (RSS), which flank all TCR gene segments, by the recombination-activating genes RAG1 and RAG2. After the introduction of double strand breaks in RSS by RAG1/2, DNA repair machinery completes the recombination process [6]. During gene rearrangement, the diversity of the receptors is further increased by the addition and deletion of nucleotides at the junction between the Vα-Jα and Vβ-Dβ-Jβ gene segments. Finally, the rearranged VJα and VDJβ regions are transcribed and spliced to join their respective C regions. After translation, the two chains pair to form the α:β T cell receptor, which is expressed at the cell surface. The whole process of combinatorial and junctional diversity, as well as the random α:β chain pairing, leads to a high diversity of sequences especially in the so-called complementarity determining regions (CDRs) that make up the antigen binding site. The CDR1 and CDR2 are generated by the recombination of the two variable regions Vα and Vβ, and make contact mostly with the MHC molecule. The CDR3, formed by the Jα and Dβ-Jβ regions, is the most variable part of the TCR and thus mainly interacts with the antigenic peptide [7]. We use the CDR3 sequence to define a unique TCR clonotype, which is a population of T cells that carry identical TCR α and β chains.
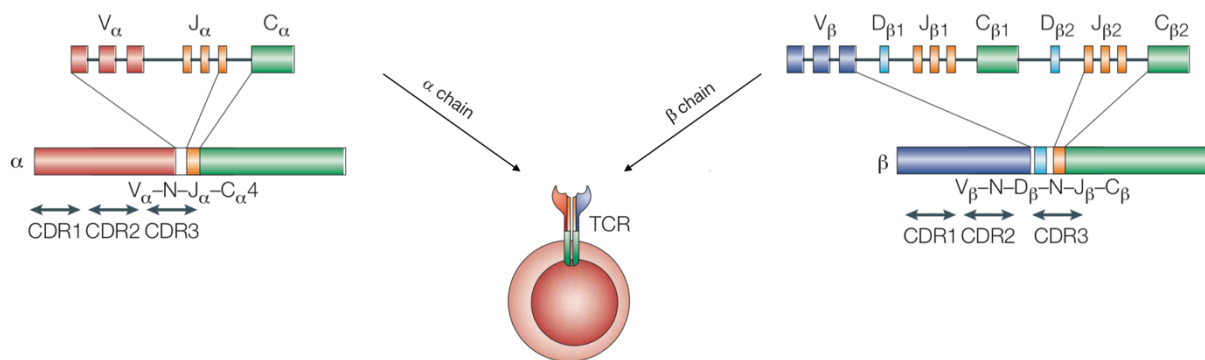
Figure 2: T-cell receptor gene rearrangement. *Variable (Vα), joining (Jα) and constant (Cα) gene segments constitute the TCRα gene locus, whereas the TCR β locus contains diversity (D) gene segments in addition to several Vβ and Jβ and two Cβ gene segments. Segments from each region are recombined, with additional nucleotide additions, to generate the final TCR sequence. Adapted from Nikolich-Zugich et al. 2004 [7].*

The recombination process has the potential to create between 10^{15} and 10^{20} different TCRs [7-9], though a more recent study has even estimated this number as high as 10^{61} [10]. However, due to stringent positive and negative selection, the real TCR repertoire diversity is much lower. In fact, while the number of T cells circulating in a human body is estimated to be between 10^{12} and 10^{13} [11], the number of different TCRs has been shown to be between 10^7 [12] and 10^8 [13]. This discrepancy indicates that a relatively high number of T cells bearing an identical TCRαβ, or clonotypes, are circulating, due to homeostatic proliferation and clonal expansion after antigen recognition.

The TCR has only short cytoplasmic tails that do not allow it to directly signal after binding to a peptide-MHC complex (pMHC). Therefore, to be functional the TCR has to be in association with the CD3 molecule to form a TCR/CD3 complex [14] (Figure 3). CD3 is a protein complex made up of a γ and a δ chain, two ε chains and two ζ chains. The γ, δ and ε chains are cell-surface proteins with transmembrane regions and cytoplasmic tails that contain immunoreceptor tyrosine-based activation motifs (ITAMs). The two ζ chains are mainly intracellular dimers linked by disulfide bonds which each contain three ITAMs. The transmembrane regions of the CD3 chains are negatively charged due to the presence of aspartate residues, a characteristic that allows these chains to associate with the positively charged residues in the transmembrane region of the TCR. To induce a T cell response upon TCR triggering, the CD3 ITAMs become phosphorylated and recruit a complex set of intracellular signaling molecules (the precise T cell signaling process is detailed in section 1.4).
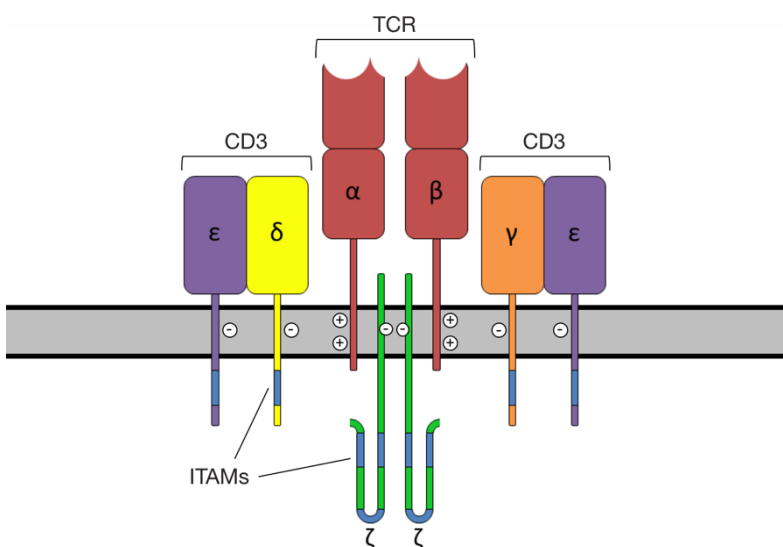
Figure 3: The T cell receptor complex. *The T cell receptor (TCR) complex comprises the TCR αβ heterodimer in association with the CD3 co-receptor, composed of six signaling chains (two ε, two ζ, one γ and one δ). CD3 chains contain one to three immunoreceptor tyrosine-based activation motifs (ITAMs). TCR and CD3 chains interact via their respective positively and negatively charged residues. Adapted from Murphy 2012 [1].*

In addition to the interaction between the TCR and the peptide-MHC, T cell co-receptors also participate in interactions with the MHC to increase antigen sensitivity (Figure 4). Indeed, the co-receptors CD4 and CD8 are cell surface glycoproteins, which associate with the TCR complex on the T cell surface and bind to MHC to stabilize and increase the avidity of the TCR-pMHC interaction [15-17]. The CD4 is a single chain with four immunoglobulin-like domains including the D1 domain which interacts with the MHC class II molecule. On the other hand, CD8 can be found in an αα homodimeric or αβ heterodimeric form. The latter is found on the vast majority of T lymphocytes and we will be focused on thereafter. CD8 interacts through its α chain with the α3 domain of MHC class I molecules. In the context of Human Leukocyte Antigen (HLA)-A*0201, residues 223-229 of the α3 domain have been shown to be of particular importance for this interaction [18]. The CD8 α chain, in addition to its critical role in binding MHC I, also holds the docking site for the lymphocyte-specific protein tyrosine kinase (Lck) p56, essential for the initiation of TCR signaling. In contrast, it is the β chain, and especially the palmitoylated part of its cytoplasmic tail, that partition CD8 into lipid rafts to bring it close to the TCR complex [19].

The CD28 costimulatory molecule, found in association with the TCR complex (Figure 4), is an important co-receptor for T cell activation and survival. It has two ligands, CD80 expressed on activated APCs early during an immune response, and CD86 expressed on APCs later during the immune response [20]. CD86 is also the ligand for the inhibitory receptor cytotoxic T lymphocyte antigen 4 (CTLA-4), thus playing a role in regulating T cell immune responses [21]. CD28 expression varies between the different T cell subsets and will be described in section 1.5.

CD45 is a transmembrane tyrosine phosphatase expressed by hematopoietic cells known to regulate TCR-mediated signaling (Figure 4). It has been shown to be capable of both downregulating and enabling Lck activity [22], to facilitate T cell signaling and to suppress the hyperactivation of peripheral T cells, respectively. CD45 has several isoforms depending on the inclusion or exclusion of alternatively spliced exons, A, B and C. The different isoforms are specific to the stage of T cell activation and differentiation, and thus are used to identify different T cell subsets. For instance, the isoform containing exon A, and so called CD45RA, is expressed on naive T cells [23] and activated effector T cells [24]. CD45RO, which does not contain any of the exons, is expressed on memory T cells [25].

1.4.   Antigen recognition and T cell signaling

The TCR can only recognize antigen in the form of peptide properly processed and presented in MHC molecules at the surface of APCs. The two classes of MHC, MHC class I and MHC class II differ in their structure, their expression on cells and the type of antigenic peptides they present. MHC class I molecules comprise a transmembrane heavy chain α which contains three domains (α1, α2, α3) associated non-covalently with the β2 microglobulin chain. MHC class I molecules present peptides derived from cleaved endogenous proteins, such as self-peptides or viral peptides produced during viral replication, to the TCR of CD8 T cells [26]. MHC class I molecules are expressed by all nucleated cells with a higher expression on immune cells such as dendritic cells or B and T cells. MHC class I molecules are encoded, in humans, by three main genes HLA-A, -B, and -C. The HLA genes are highly polymorphic resulting in a unique set of HLA alleles in each individual, with the exception of identical twins [27]. MHC class II molecules consist of two transmembrane chains, α and β, each containing two domains (α1, α2, β1, β2), encoded by the HLA-DR, -DP and -DQ genes. They are specialized in the presentation of extracellular antigens derived from proteins degraded in the endocytic pathway of APCs, to the TCR of CD4 T cells [28]. Therefore, MHC II expression is highly restricted to phagocytic APCs such as dendritic cells, macrophages or B cells.

After recognition by the TCR of a peptide presented by MHC molecules, a protein reorganization occurs at the interface of the T cell and APC to form an immunological synapse (IS) (Figure 4). This is a tight molecular junction whose formation is driven by the engagement of adhesion receptors such as the T cell integrin Lymphocyte Function-associated Antigen 1 (LFA-1) to its ligand, Intercellular Adhesion Molecule 1 (ICAM-1) on the APC [29, 30]. This organized interface also contains diverse regulatory elements that fine-tune T cells activation, such as the coreceptor CD45 [31] or the inhibitory receptors PD-1 (Programmed Cell Death 1) or CTLA-4 [32].
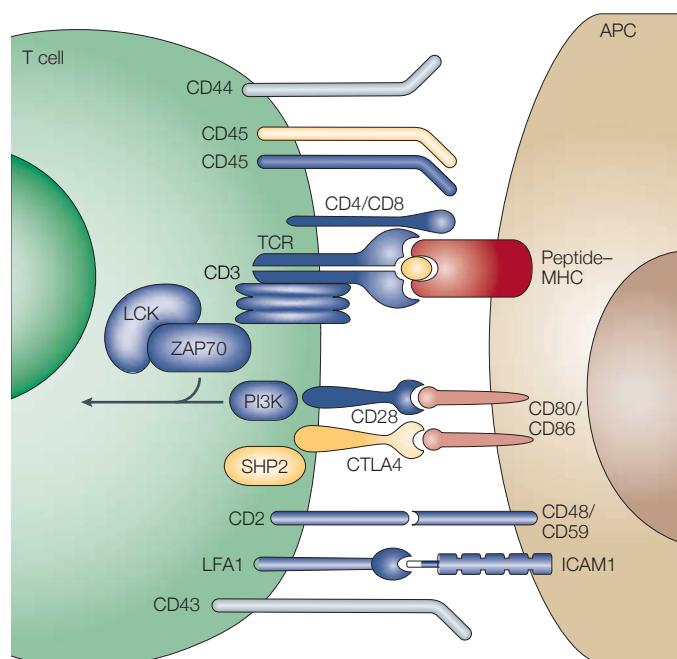
Figure 4: Immunological synapses between T cells and antigen presenting cells. *A representative view of the antigen recognition signal (TCR-peptide/MHC), co-stimulatory (shown in blue) and -inhibitory (shown in yellow) molecules found in an immunological synapse and involved in T-cell recognition. Adapted from Huppa and Davis, 2003 [33].*

Following TCR-pMHC interaction and the formation of the IS, an intracellular signaling cascade is initiated in the T cell. In the case of naive T cells, pMHC recognition is not sufficient for T cell activation, and requires the additional engagement of CD28 costimulatory receptors by cognate ligand expressed on APCs (Figure 4). In the absence of such costimulation, naive T cells will become anergic and will not be able to proliferate or to differentiate. Anergy is one of the processes that induces tolerance and prevents excessive self-reactivity of T cell-based immune responses, as CD80 and CD86 are mainly expressed on activated APCs during infection. For effector T cells, on the other hand, TCR-pMHC interaction is sufficient to initiate T cell activation. TCR-mediated cell signaling starts with the activation of the Src-family Lck and Fyn kinases by the tyrosine phosphatase CD45, which removes their inhibitory phosphatase groups. Lck and Fyn then phosphorylate the ITAMs of the CD3 chains of the TCR complex, which results in the recruitment of the Syk-family zeta-chain-associated protein kinase 70 (ZAP-70) [34]. After being activated by Lck, ZAP-70 will phosphorylate the transmembrane proteins LAT (linker of activated T cells) and SLP-76 (SH2 domain containing leukocyte protein of 76kDa), which together activate phospholipase C-γ (PLC-γ) [35]. The activation of PLC-γ leads to the activation of three distinct signaling branches, culminating with the transcription factors (i) nuclear factor-kappa B (NFκB), (ii) nuclear factor of activated

T-cells (NFAT) and (iii) activator protein 1 (AP-1) [36]. These transcription factors regulate gene transcription involved in cell activation, proliferation, and differentiation.

1.5. CD8 T cell differentiation and subsets

Following activation, naive T cells will rapidly proliferate to generate a large pool of effector cells with the same antigen specificity, a process known as clonal expansion. At the end of the primary response, the majority of effector T cells will die by apoptosis and only a small fraction will remain as long-term memory T cells. During a second exposure to the same antigen, memory T cells are mobilized in a recall response that is faster and more efficient than the primary response [37]. The different subsets of T cells (naive, memory and effector) can be distinguished based on their differential expression of cell-surface molecules.

Naive (N) T cells express high levels of homing receptors such as L-selectin (CD62L) and C-C motif chemokine receptor 7 (CCR7), which promote T cell trafficking to secondary lymphoid tissues where they encounter activated APCs. Thus, N T cells are generally defined as CD62L+CCR7+ and CD45RA+.

Effector T cells lose the capacity to migrate to lymph nodes and are thus defined as CCR7-, CD62L-, and CD45RA+ and are termed EMRA T cells. EMRA T cells preferentially home to peripheral tissues and exhibit strong effector functions such as cytokine production and killing capacity to eliminate infected or abnormal cells. Expression of the coreceptor CD28, involved in T cell co-stimulation, further defines intermediate stages of differentiation of EMRA T cells. EMRA CD28+ (EMRA28+) T cells display phenotypic and functional features that are intermediate between naive and differentiated effector, while EMRA CD28- (or EMRA28-) T cells is a subset evolving toward a more differentiated effector stage [38].

The memory CD8 T cell subset also consists of a highly heterogeneous population of cells that differ in phenotype, function and response to a particular antigen. Sallusto *et al.* [39] were the first to discriminate two types of CD8 memory T cells based on their expression of CCR7: the central-memory (CM) cells which are CCR7+ and the effector-memory (EM) cells which are CCR7-. CM T cells lack immediate effector function but recirculate between blood and lymphoid tissues to eventually re-encounter antigen and rapidly proliferate at high magnitude. In response to antigen re-encounter they will differentiate into effector or effector-memory T cells. EM T cells circulate between blood and peripheral tissues where they can exert effector

functions. Based on expression of the costimulatory receptor CD28, EM T cells subset can be further divided in two subsets [40]. CD28 expressing memory cells or EM28+, resemble CM T cells with a short replicative history, low expression of effector molecules, but an increase survival potential. On the other hand, CD28- memory cells or EM28-, express more cytokines and have an advanced replicative history, thus being closer to effector T cells [40]. Finally, several other memory T cell subsets have been more recently described, such as tissue-resident memory T cells, which stably occupy peripheral tissues and do not re-enter blood circulation. They exert effector functions to provide immediate protection against local infection at body surfaces to accelerate pathogen clearance (reviewed in [41]).

1.6.   CD8 T cell effector functions

As previously described, following antigenic challenge, naive CD8 T cells undergo a program of clonal expansion and differentiation, during the course of which they acquire effector functions to become cytotoxic T cells and kill infected or tumor cells [42]. One way for CD8 T cells to exert their cytotoxic function is by delivering cytotoxins, mainly perforin and granzyme, to target cells. Perforin generates pores in the target cell membrane, and granzyme, a serine protease, enters target cells via perforin-mediated pores to induce apoptosis. These proteins are synthesized and stored in granules inside CD8 T cells. To avoid damage to surrounding tissue that effector molecules could induce, cytolytic granules are released within an immunological synapse between the T cell and the target cell [43]. Activated CD8 T cells also express the transmembrane protein Fas ligand, which can bind to Fas expressed on target cells. This interaction leads to the death of the target cell by apoptosis through the death domain of the cytoplasmic tail of Fas [44]. Finally, CD8 T cells can also act by releasing cytokines such as interferon-γ (IFNγ), tumor necrosis factor α and β (TNFα and TNFβ) [45]. IFNγ inhibits viral replication, and increases the expression of MHCI as well as the presentation of viral peptides. IFNγ also recruits and activates macrophages to act as phagocytes and antigen presenting cells. TNFα and TNFβ cytokines are as well able to activate macrophages and can directly kill target cells by apoptosis through the interaction with TNF receptor-I.

2.   Non-self and self T cell-specific immune responses

2.1.   Anti-viral versus anti-tumoral responses

From an immunological point of view, chronic infections and cancer are comparable in many ways. In addition to giving rise to a specific immune response, they are also characterized by continuous antigenic stimulation of immune cells. They are also known to escape immune control through various mechanisms such as the downregulation of immunogenic antigens, as well as MHC downregulation. The drastic difference between the viral and tumoral context is the ability of the immune system to efficiently control chronic infections, while tumor cells are often invasive and can only rarely be spontaneously controlled. In fact, while cancer vaccines in melanoma patients have shown successful induction of T cells at high frequencies and with similar phenotype and effector characteristics to those associated with long-lasting, protective anti-viral responses [46-48], they have so far obtained only limited clinical success. This could be due to the persistence of an immunosuppressive tumor microenvironment [49, 50]. Indeed, tumors induce strong local immune suppression through several mechanisms such as the secretion of immunosuppressive factors including the cytokines TGF-β [51] or IL-10, or by the depletion of nutrients essential for CD8 T cell activity [52, 53]. Another major difference between chronic viral infections and tumors is the origin of their respective antigens. Virally infected cells are recognized by T cells through the presentation of non-self antigens, while tumor-specific T cells respond to self-antigen, and are therefore largely eliminated by both central and peripheral tolerance mechanisms to prevent auto-immunity. As a result, tumor-specific CD8 T cells typically exhibit weaker TCR-pMHC binding avidity (dissociation equilibrium constant (K_D) between 300-10 μM) compared to pathogen-specific CD8 T cells (K_D of up to 1 μM) [54, 55].

Despite the differences described hereabove, chronic viral infections such as Epstein-Barr virus (EBV) and Cytomegalovirus (CMV) have proven to be essential tools in the study of highly-efficient memory T cell responses, and for the identification of T-cell correlates of protection in humans.

2.2.   T cell-based parameters for protective immunity

The development of immunotherapies, such as adoptive cell transfer, for the treatment of cancer and viral infection has been of growing interest in recent decades. To better exploit the therapeutic potential of T cells, numerous studies have focused on defining key parameters and their synergy for an optimal protective immune response (Figure 5, reviewed in [56, 57] and [58]). After being activated by their cognate antigen, T cells must proliferate to reach high frequencies. The magnitude of the response is, in part, driven by naive CD8 T cell frequencies, which have been correlated with the number of CD8 T cells generated upon primary antigenic challenge (reviewed in [59]), though this finding remains controversial [60-62]. Similarly, it is not clear whether the magnitude of the response is a protective parameter as it has been associated with protection in some studies [63-65], while this is not the case in others reports [66, 67]. In addition, the affinity of a given peptide-MHC interaction has been shown to shape the magnitude of the response and has been associated with efficient protection [68, 69].

Importantly, the magnitude of a T-cell response does not necessarily reflect its functional potential. In this regard, T cell functional avidity, which describes how well a T cell responds *in vitro* to its cognate antigen, has been used to assess the quality of a T cell response. It is defined by functional readouts such as cytokine production, target cells lysis or proliferation at different doses of peptide antigen [70]. Numerous studies have associated high T cell functional avidity with efficient viral control and clearance in both animal models [71-73] and patients with human immunodeficiency viruses (HIV) [74, 75] and hepatitis C (HCV) [76-78] infections. In addition, T cell functional avidity has been associated with better tumor control in mice [79, 80] and in melanoma patients [81, 82]. On the other hand, high functional avidity T cells may be more prone to activation-induced cell death, senescence, or exhaustion (reviewed in [70]). Nonetheless, a greater proportion of polyfunctional CD4 or CD8 T cells (i.e. which exert multiple effector functions) have been observed in HIV [83, 84], hepatitis C [85] and CMV [86] patients with controlled infection, compared to patients with progressive disease. The functional avidity of T cells is primarily controlled by the strength of TCR-pMHC interactions (or TCR–pMHC binding affinity/avidity), and this key parameter will be extensively discussed in section 3.

The quality of a T cell response also depends on the T cell capacity to migrate to the tumor or infection sites, as well as to survive and persist over time. Finally, it is generally accepted that greater diversity of the TCR repertoire is associated with better protection [87], as a polyclonal

response targeting multiple epitopes should ensure long-term protection even if some clonotypes are poorly functional or do not survive. In addition, it helps minimize opportunities for mutation-driven pathogen or tumor escape [88]. A relatively diverse TCR repertoire has been shown to be a predictor of better disease outcome in mouse models [89], whereas in humans the advantage of having a diverse repertoire is not always apparent, especially during viral infection. Indeed, highly skewed repertoires with clonotypes shared between individuals have been observed in EBV, CMV [90-92] or HIV [93] patients who show disease control.

This non-exhaustive list of criteria and their importance for a protective immune response can greatly vary depending on many parameters such as the type of infection or malignancy, as well as the patient HLA background and immunocompetent status.
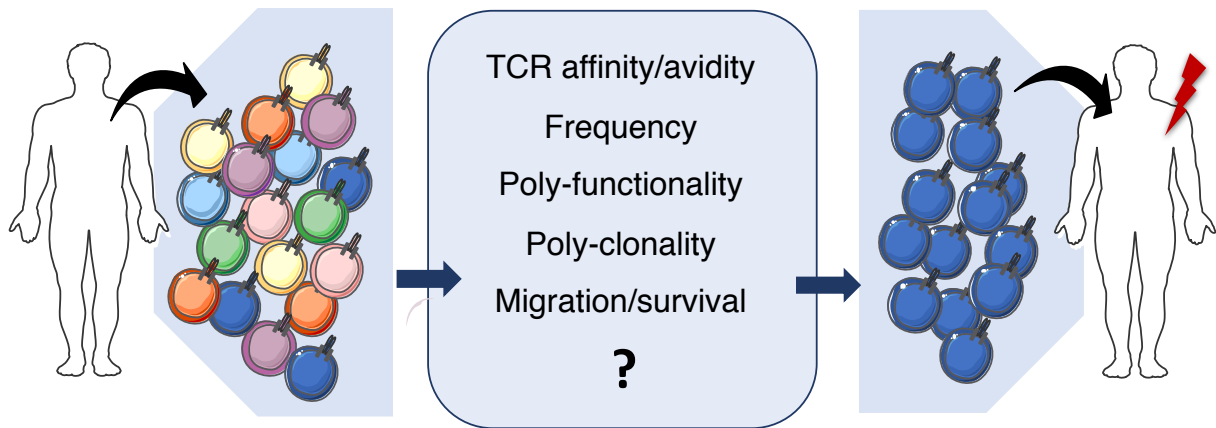
Figure 5: Identifying T cell correlates of protection for adoptive cell transfer immunotherapy. *Selection of autologous T cells from a patient based on correlates of protection such as TCR affinity/avidity, T cell frequency, poly-functionality, poly-clonality, capacity to migrate to the tumor or sites of infection, as well as survival. After in vitro selection and expansion, T cells are re-infused to the patient. Adapted from Hebeisen et al. [94].*

3.   TCR-pMHC binding affinity/avidity

3.1.   Definitions

The strength and kinetics of TCR-pMHC recognition are central parameters that impact numerous aspects of T cell biology. Due to technological limitations, these parameters are often translated in terms of functional avidity, which is the antigen sensitivity measured by functional readouts such as cytotoxic activity, proliferation or cytokine production. These functional assays are often limited to experiments of fixed stimulation doses and do not directly measure the TCR-pMHC affinity/avidity. In addition, many parameters can influence functional assays such as the chosen readouts, the activation state of the cells as well as intra-experimental variability.

In contrast to functional avidity, the structural binding strength of the TCR to pMHC is defined as the TCR affinity or avidity (Figure 6). The TCR-pMHC affinity refers to the strength with which a monovalent receptor binds to its ligand, in this case a single TCR to a peptide–MHC complex [95], and this value is inversely proportional to the dissociation equilibrium constant K_D. At steady-state, K_D is defined as the ratio of the dissociation rate (k_{off}) and association rate (k_{on}). The dissociation rate k_{off}, or the speed at which the TCR dissociates from the pMHC complex can also be expressed as a half-life ($t_{1/2}$), by the equation $t_{1/2} = \ln2 \, / \, k_{off}$ [96].

Conversely, TCR-pMHC avidity is the association constant of multiple TCRs bound to their respective pMHC complexes, in the cellular context [70]. This measure takes into account the potential contribution of co-receptors, TCR density on the cell surface or the T cell activation state [94]. TCR-pMHC avidity was commonly assessed by multimers while monomeric pMHC-TCR dissociation kinetic measurements are assessed by reversible multimers such as Nitrilotriacetic acid (NTA)-His tag-containing multimer (NTAmers) [97, 98] or Streptamers [99] and define TCR structural or binding avidity.
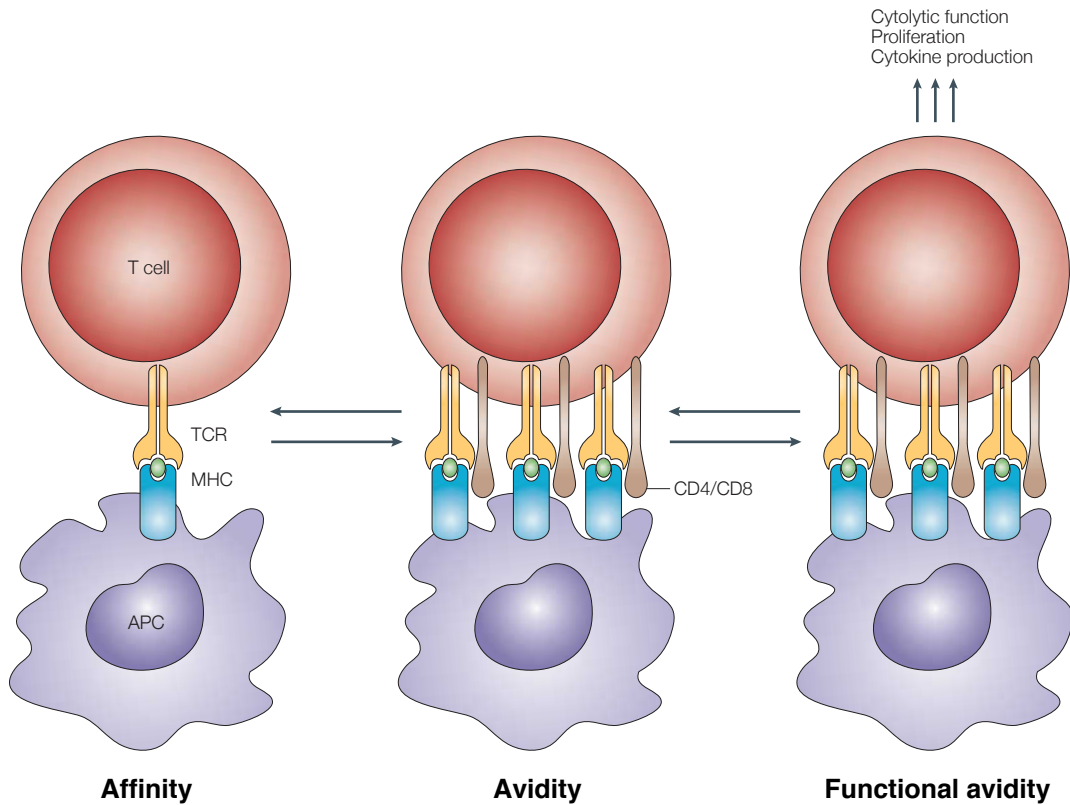
Figure 6: Parameters of the TCR-pMHC interaction. *The TCR-pMHC affinity refers to the association constant of a monovalent receptor bound to its ligand, while TCR-pMHC structural avidity is the association constant of multiple TCRs bound to their respective pMHC complexes in the cellular context. Functional avidity depends on the antigen sensitivity translated into functional readouts such as proliferation, cytokine production or cytotoxic function. Adapted from Nikolich-Zugich et al. 2004 [7].*

3.2. Measurement of TCR-pMHC binding affinity/avidity

TCR-pMHC affinity kinetics (i.e. k_{on}, k_{off} and K_D) were first assessed by surface plasmon resonance (SPR). SPR assays require the production of soluble TCRs which are perfused through a three-dimensional (3D) space to interact with pMHC attached to a sensor chip (also defined as 3D interactions) (Figure 7A). A major limitation of this technique is the expensive and laborious production of soluble molecules. Moreover, SPR measurements do not take into account the contribution of the CD8 coreceptor to TCR–pMHC binding strength. Novel technologies have been more recently developed to measure association and dissociation constants in a more physiological way, at the interface between a living T cell and an APC or a membrane linked pMHC at the two-dimensional (2D) level [100, 101], using fluorescent-based or micropipette adhesion frequency assays (Figure 7B). 2D interaction analyses have been

shown to correlate well with functional avidity of T cells [102, 103], however they require highly specialized equipment and are time-consuming.

TCR-pMHC avidity was originally estimated based on the staining intensity of soluble pMHC multimers of well-defined valencies (Figure 7C) directly on living cells [98, 104]. However, pMHC multimer staining intensity does not consistently correlate with the TCR-pMHC affinity/avidity [79, 105, 106]. In the past, these discrepancies were overcome by performing multimeric association and dissociation rate measurements on living T cells, monitored by flow cytometry generally during several hours. Nonetheless, multimeric off-rate does not consistently correlate with functional capacity and *in vivo* protection [79, 106], mainly due to the multivalent nature of pMHC complexes and their capacity to rebind TCRs during dissociation assays [107].
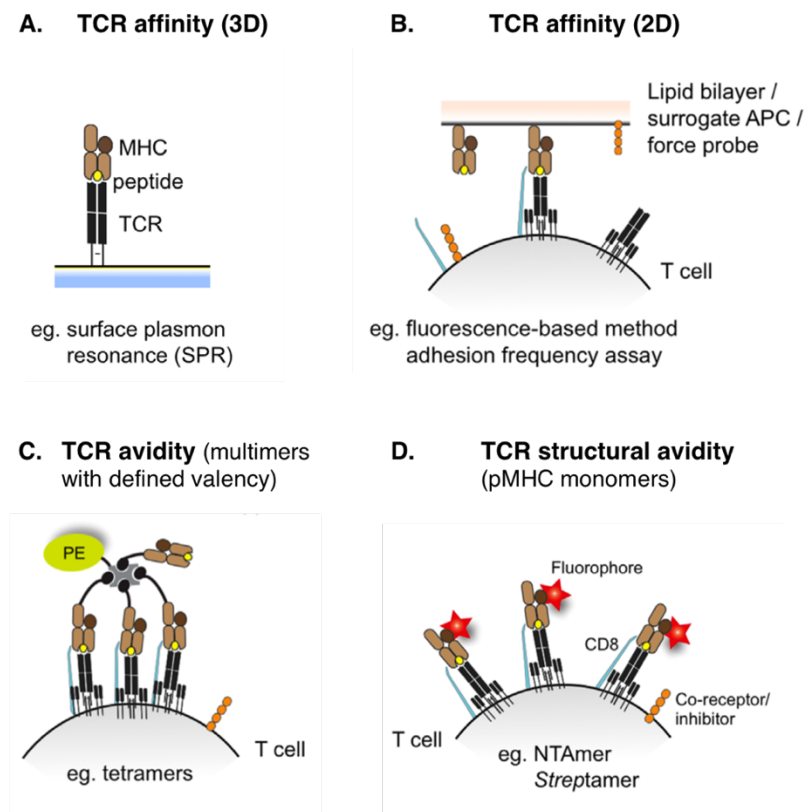
Figure 7. Representation of TCR-pMHC binding affinity/avidity measurements. *TCR-pMHC affinity refers to the association constant of a monovalent receptor bound to its ligand and can be assessed by (A) 3D interactions (commonly done by SPR) or (B) directly at the interface between a living T cell and an APC or a membrane linked pMHC at the 2D level. TCR-pMHC avidity is the association constant of multiple TCRs bound to their respective pMHC complexes in the cellular context using multimers with defined valency (C). Due to the caveats induced by the multivalency of multimers, reversible multimers have been developed to assess TCR structural avidity defined as the strength of interaction between monovalent TCR-pMHC complexes at the cellular level (D). Adapted from Hebeisen et al. [94].*

To overcome these limitations and to measure TCR structural avidity at the monomeric level, reversible multimers such as NTAmers [97, 98] and Streptamers [99] have recently been developed. These complexes consist of fluorescently labelled pMHC monomers linked together in a multimeric complex that can be disrupted upon addition of a stimulus (Figure 7D). Reversible multimers allow the quantitative and reproducible measurements of monomeric TCR-pMHC dissociation kinetics (k_{off}) on living T cells. In the case of Streptamers, multimer complexes dissociate following addition of D-biotin through a binding site competition process that can take up to 60 seconds to reach total complex disruption. Monomeric dissociation rate of pMHC from TCRs can be then monitored as a decay in fluorescence measured by real-time microscopy [99]. The more recently developed reversible multimers, NTAmers [97], are made of pMHC monomers bearing Cy5-labeled β2m complexed with PE-streptavidin carrying an engineered NTA linker (Figure 8). These complexes are highly stable but rapidly decay to monomers in several seconds (2-3 sec) upon addition of imidazole.
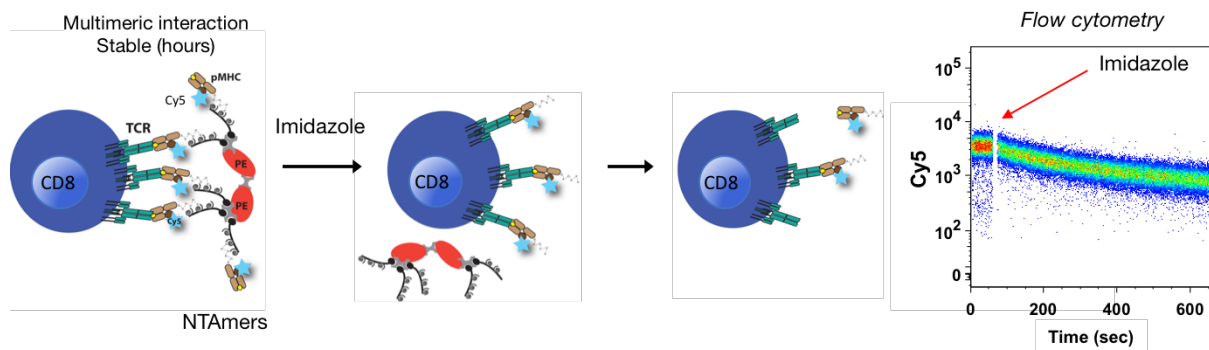
Figure 8: Representation of reversible NTAmer-based dissociation assay. *Individual antigen-specific CD8 T cell clones were stained with HLA-A0201 antigen-specific NTAmers composed of a PE-labeled backbone (grey) and Cy5-labeled monomers (brown) carrying imidazole-sensitive Ni^{2+}-NTA4 moieties. Upon addition of imidazole, the NTAmer multimeric complex rapidly dissociates into Cy5-labeled pMHC monomers and Cy5 fluorescent decay can be measured by flow cytometry over time. Adapted from Hebeisen et al. 2015 [108].*

Owing to the faster decay of the multimeric complex into monomeric pMHC when compared with Streptamers, NTAmers offer an increased sensitivity to detect T cells with low avidity TCRs (reviewed in [94]), such as those typically found in self/tumor–specific CD8 T cell repertoires. Our lab recently showed that NTAmer-based dissociation rates strongly correlate

with the killing capacity of TCR-engineered and natural tumor-specific human CD8 T cells [108, 109].

3.3. Relationship between TCR avidity and function

The strength of TCR-pMHC interaction has been shown to influence multiple facets of T cell activity, including thymic selection, priming by APCs, activation, proliferation and differentiation. During priming in secondary lymphoid organs (SLOs), T cells expressing high avidity TCRs engage in longer interactions with APCs than do their low avidity counterparts [110]. Such high avidity T cell-APC interactions lead to a greater degree of expansion within SLOs, and to a slower acquisition of effector functions compared to low avidity T cells [110, 111]. Thus, high-avidity T cells exit the lymphatic system and enter blood circulation later but in greater number and with superior effector functionality [111]. This mechanism allows for a rapid response to early infection by low avidity T cells, followed by more robust control mediated by high avidity T cells. Indeed, it has been shown that greater diversity of recruited TCR affinities is associated with improved host protection in mice [111, 112].

Using various engineered models, such as affinity-optimized TCR variants or altered peptide ligands, several studies have shown that within the physiological affinity range (K_D 100–1 µM), strong TCR-pMHC interactions correlate with enhanced T cell responsiveness (e.g. cell activation, signaling, proliferation, cytokine/chemokine secretion, and target cell killing) [113-118]. Furthermore, seminal clinical trials demonstrated the importance of TCR-pMHC affinity/avidity in cancer patients treated with engineered T cells of enhanced TCR affinity (reviewed in [119]). Clinical studies performed with affinity-enhanced T cells against the cancer testis HLA-A2/NY-ESO-1$_{157-165}$ (NY-ESO-1 stands for "New York esophageal squamous cell carcinoma 1") antigen provided augmented *in vivo* functional capacity and improved tumor growth control [120-122].

However, most of these reports including the clinical studies are based on artificial models (e.g., using affinity-optimized TCR variant panels or altered peptide ligand models), and thus only limited information is available on the overall impact and clinical relevance of TCR-pMHC binding avidity or kinetics (e.g. off-rates) in the context of naturally occurring antigen-specific CD8 T cell responses. Using Streptamers, Nauerth *et al.* have shown that virus-specific CD8 T cells bearing TCRs of high affinity conferred better protection against *Listeria monocytogenes* infection in mice [99]. Moreover, in the tumor model, our group recently documented that the

half-lives determined by NTAmers accurately predicted the killing capacities of large panels of tumor-specific T cell clones that were isolated prospectively from patients with cancer [108] as well as following therapeutic vaccination [109].

Thus, whilst T cells bearing both low and high affinity TCRs are likely crucial for an efficient immune response *in vivo*, high affinity T cells are essential for complete and/or prolonged pathogen control. Moreover, identifying and selecting TCRs of higher avidity may be of particular importance in the tumoral setting, since most high avidity/affinity self/tumor antigen–reactive T cells are naturally eliminated or silenced by mechanisms of central and peripheral tolerance, emphasizing the need to select the remaining rare high-avidity cells for immunotherapy.

4.   Herpes virus

Herpes viruses are genetically stable, large double stranded DNA viruses. Following primary/replicative infection in a permissive cell type, they are able to establish lifelong latency in a second cell type. γ herpesviruses, such as EBV, use the proliferative capacity of the latently infected cell to amplify their stable reservoir, while α and β herpesviruses, such as CMV, do not have this capacity. In hosts able to mount a proper immune response, herpesviruses are generally well controlled reflecting the fine balance between host immune mechanisms and the capacity of the virus to evade those controls.

4.1.   Biology of infection of the Epstein-Barr Virus

EBV infection is restricted to human beings and characterized by latent infection in B cells. EBV is mainly transmitted in saliva and is wide spread, with more than 95% of adults over 30 being seropositive in Europe and North America [123, 124]. Primary infection typically occurs in childhood and is usually asymptomatic. However, in adolescents or adults primary EBV infection may lead to symptomatic infection (known as infectious mononucleosis (IM)) in 25% to 70% of cases [125, 126], characterized by fever, sore throat, enlarged lymph nodes in the neck, and tiredness. Following oral transmission, the virus undergoes lytic replication in oral epithelial cells and locally-infiltrating B lymphocytes associated with lytic gene expression programs. Two immediate early proteins (acting as transcriptional activators) are first expressed, followed by several early proteins (essential for viral DNA replication) and finally several late proteins (mainly virus structural components). At the same time, the virus induces

a growth-transforming infection in B cells leading to their expansion in lymphoid tissues and blood. Some of these cells will survive the immune response and allow the virus to established a life-long persistence in the circulating memory B cell pool. This latent phase is associated with a highly restricted latent gene expression profile which serves to avoid immune detection by minimizing antigen exposure [127]. Periodically, EBV virus can re-enter into the lytic phase, leading to host cell lysis and the release of new virions.

4.2. EBV-associated diseases

EBV is characterized as an oncogenic virus. However, while it is never cleared by the immune system after primary infection, it is well controlled and immunocompetent individuals usually carry it as a lifelong asymptomatic infection. Nonetheless, in an immunosuppressive context, such as HIV infection or autoimmune disease treatment, EBV infection can lead to severe and life-threatening disease and malignancy. Since epithelial cells and B cells are the primary target cells, most common EBV-derived cancers are nasopharyngeal carcinomas and B cell lymphomas such as Burkitt's lymphoma as well as Hodgkin's and non-Hodgkin's lymphoma. Moreover, EBV is one of the major causes of post-transplant lymphoproliferative disorder due to the use of immunosuppressive drugs leading to donor- or recipient-derived EBV reactivation. To date, no antiviral drugs have been approved for the specific treatment of EBV infection, yet several candidates have proven to inhibit EBV replication *in vitro* [128].

4.3. Immune control of EBV

The immune response to EBV comprises, primarily, the induction of cellular immunity mediated by T and NK cells, as well as humoral immunity mediated by antibody-secreting B cells. During the acute phase of infection, NK cells significantly expand, in parallel with the viral load [129]. They mediate control over primary EBV infection by targeting lytically-infected cells to limit virus replication, but can also prevent or delay B cell transformation by EBV [130, 131].

During the lytic phase, a dramatic expansion of specific CD8 T cells is observed in the periphery, with responses to any one lytic epitope accounting for up to 50% of the circulating CD8+ population. CD8 immunodominance follows the sequential pattern of expression of lytic proteins in target cells, with immediate early and some early antigens dominating over late antigens. This suggests that CD8 T cell responses are mounted through direct contact with

lytically infected cells. During the lytic phase, a significantly smaller population of CD8 T cells (up to 5% of the circulating pool) [132] is directed against latent antigens, especially epitopes from the EBNA3 family. At the end of the acute phase and with the decline in viral load, lytic and latent antigen specific CD8 T cells contract to below 2% and 0.5% of the circulating CD8+ T cell compartment, respectively [133-135].

CD4 T cell expansion also occurs during the acute phase of the infection but to a lesser extent, and it is mainly directed against latent epitopes, though CD4 T cells respond to a broader range of available lytic and latent antigens. Finally, the host humoral response consists mainly of the production of antibodies against a wide range of lytic antigens such as viral capsid antigens and early antigens which are highly immunogenic [136].

4.4.　　Biology of infection of the Cytomegalovirus

Human cytomegalovirus (hCMV) is a β herpesvirus infecting between 60% and 90% of the population worldwide, with higher frequencies found in developing countries [137]. The virus is spread between individuals via body fluids such as saliva, blood, breast milk, via sexual contact or from an infected mother to her child during pregnancy. Primary infection is usually asymptomatic in immunocompetent hosts, with rare cases of infectious mononucleosis symptoms. After primary infection, the virus establishes a lifelong asymptomatic latency in the host, through a fine homeostatic balance between viral determinants and immune surveillance. Following transmission, the virus infects mainly epithelial and endothelial cells [138] but also several other cell types such as smooth muscle cells, fibroblasts, leukocytes and dendritic cells [139, 140]. However, it establishes a lifelong latency in vascular endothelial cells, epithelial cells and primarily in immature cells of the myeloid lineage [141, 142], the latter are found in the bone marrow and in blood circulation. These infected cells can spread the latent infection by circulating and infiltrating many organs. Reactivations from the latent state occur regularly and studies have shown that inflammation was the leading cause. Indeed, in an inflammatory context, cells from the myeloid lineage are stimulated and will differentiate into macrophages or dendritic cells where reactivation can occur [143, 144]. These constant CMV reactivations throughout life require constant and efficient immune control to keep the host disease free.

4.5. CMV-associated diseases

CMV infection can cause severe and sometimes fatal disease in immunocompromised individuals or neonates. Indeed, hCMV is a major infectious cause of congenital abnormalities, including hearing loss, visual impairment, mental retardation or morbidity, and it is estimated to affect 1 to 5% of all live births in developed countries [145]. In adults, severe cases of CMV-associated disease occur in the majority of acquired immune deficiency syndrome (AIDS) patients without anti-CMV prophylactics, with the most common being retinitis and subsequent blindness. Transplant patients are also at high risk of CMV reactivation and 30 to 75% of organ recipients will develop symptomatic disease during the year following transplant [146, 147]. The risk of fatal disease depends on the type of transplantation. For example, bone marrow transplants have a much higher risk of fatal pneumonia compared to kidney transplants [148, 149]. Many other pathologies are related to CMV-infection such as colitis, hepatitis or central nervous system disease. These risks can be significantly reduced with the prescription of anti-viral prophylactics. However, they have been associated with toxicity, and patients can still develop late-onset CMV diseases when the treatment is stopped [150]. As T cell-mediated immunity is the main correlate of protection (detailed in section 4.6), adoptive transfer of CMV-specific T cells in immunocompromised patients has been investigated. Several clinical trials have established the safety and efficacy of simultaneous adoptive transfer of both CMV-specific CD8 and CD4 T cells for prophylaxis and treatment of CMV infection following transplant [151-154]. Finally, CMV infection is thought to increase the risk of development of other fungal and bacterial infections [155] as CMV interferes with the host immune system, especially in the more impaired immune systems of older individuals [156]. Aging of the immune system with CMV infection will be discussed in more details in section 5.6.

4.6. Immune control of CMV

hCMV infection induces a robust immune response where both the innate and adaptive immune systems play a role. The innate immune system, especially NK cells, provides the first line of defense by eliminating infected cells to contain the infection. The adaptive immune system then comes into play, in the form of both humoral and cell-mediated immunity. Antibodies neutralize viral proteins and prevent viral entry into new cells, and are thought to be essential to limit viral dissemination and symptomatic infection [157, 158]. On the other hand, CMV-specific CD4 and CD8 T cells play a critical role in the control of latent and

reactivating CMV. It has been shown in mouse CMV (MCMV) models that while CD8 T cells and NK cells are sufficient to control lytic infection in most organs, CD4 T cells are essential for the control of viral replication in the salivary glands [159, 160]. CMV-specific T cells can recognize over 150 antigens but are mainly directed against two dominant epitopes, the 65kDa phosphoprotein (pp65), derived from the virus matrix, and the immediate-early protein 1 (IE1), presented by HLA-A2 and HLA-B7, respectively [161, 162]. The magnitude of the CD8 response is highly variable between individuals, but CMV-specific CD8 T cells represent on average 5% and up to 35% of the circulating pool of CD8 T cells in seropositive healthy adults [162]. Indeed, it has been shown that CMV-specific CD8 T cells generally persist in large numbers after the contraction phase and, in the case of certain specificities, can even slowly accumulate over time in a process that has been termed "memory inflation" [163-165].

The phenomenon of memory inflation has been primarily described in the MCMV model, where "conventional CD8 T cells" contract following the acute phase, resulting in a pool of memory T cells stably maintained during the latent phase. In contrast, CD8 T cells specific for certain antigens such as $M38_{316-323}$, $m139_{419-426}$, $IE3_{416-423}$, $IE3_{461-475}$, $M102_{486-500}$, accumulate gradually over time during the latent phase and, as such, are termed "inflationary CD8 T cells" [163, 166, 167]. In human CMV, some epitope-specific CD8 T cell responses have also been shown to increase in magnitude with age [168-170]. The distinct frequency and phenotypic patterns of conventional versus inflationary CD8 T cell responses against CMV are represented in Figure 9.
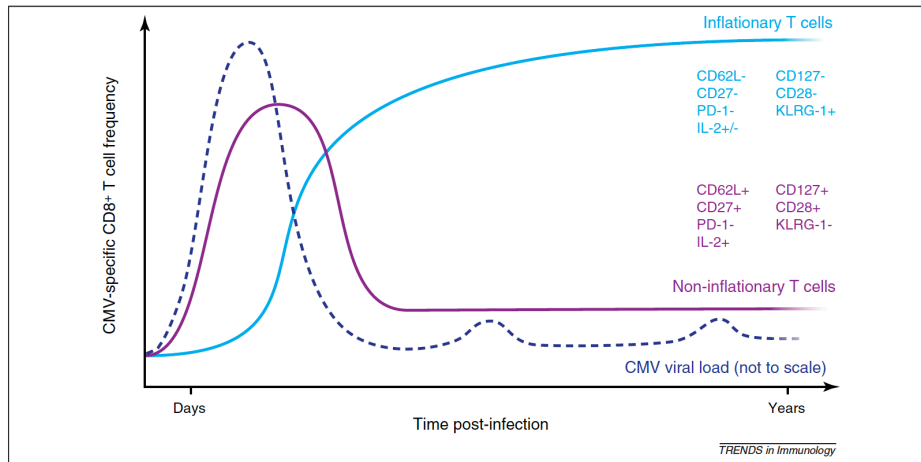
Figure 9: CMV-specific T cell response dynamics. *Representative kinetics of CMV-specific T cells during the acute and latent phases of infection. While non-inflationary T cells contract following the acute phase, inflationary T cells continuously accumulate during the latent phase aided by regular viral transcriptional activity and T cell stimulation. Adapted from O'Hara G et al. 2012 [171].*

While long-lived classical memory CD8 T cells are mainly maintained over time with a central memory T cell phenotype, inflationary effector-memory cells are usually terminally differentiated, characterized by the downregulation of co-receptors such as CD27 and CD28 as well as homing receptors like CD62L and CCR7 (Figure 9 and 10). They also express several inhibitory receptors such as killer-cell lectin like receptor G1 (KLRG-1) [166] and leukocyte immunoglobulin-like receptor subfamily B member 1 (LILRB1, also known as CD85j or ILT-2) [172], but not PD-1 [173] (Figure 9 and 10). In addition, they maintain their effector functions, secrete cytotoxins such as perforin and granzyme [174] and are able to proliferate [173, 175], in contrast to the features of exhausted T cells generally observed in other persistent chronic viral infections such as HIV or hepatitis B and C virus [176].
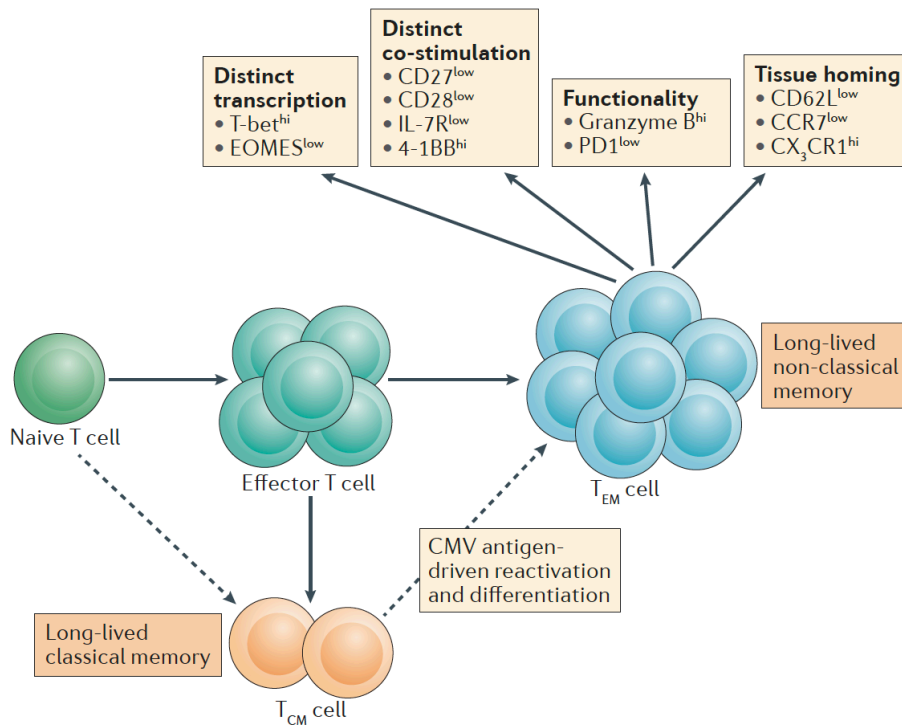
Figure 10: Classical and non-classical CMV-specific CD8 T cells. *Long-term conventional memory CD8 T cells are maintained with a central memory T cell phenotype, while inflationary T cells (non-classical memory) have an effector-memory phenotype characterized by the downregulation of co-receptors such as CD27 and CD28 as well as homing receptors like CD62L and CCR7 and the maintenance of effector functions. Adapted from Klenerman and Oxenius, 2016 [177].*

While CMV reactivation events are well controlled by humoral and cell-mediated immunity, resulting in the virtual absence of new virion production unless the infected host is severely immunocompromised [178], the main driver of memory inflation is thought to be repetitive antigen exposure via detection of transcriptional reactivation [179]. Indeed, when MCMV-specific CD8 T cells were transferred into naive hosts, they failed to divide and persist, suggesting that antigen stimulation is required for their accumulation and maintenance at high frequencies [173]. Mouse models have also demonstrated that CM T cells are a primary source of new EM T cells, thus sustaining memory inflation (Figure 10). MCMV-specific CM T cells are thought to be re-activated both in SLOs, by non-hematopoietic, latently infected cells [180], as well as in blood circulation, by latently infected vascular endothelial cells [181] (Figure 11). After reactivation, they undergo proliferation and differentiation and ultimately accumulate in peripheral tissues where they can exert effector functions (Figure 11).
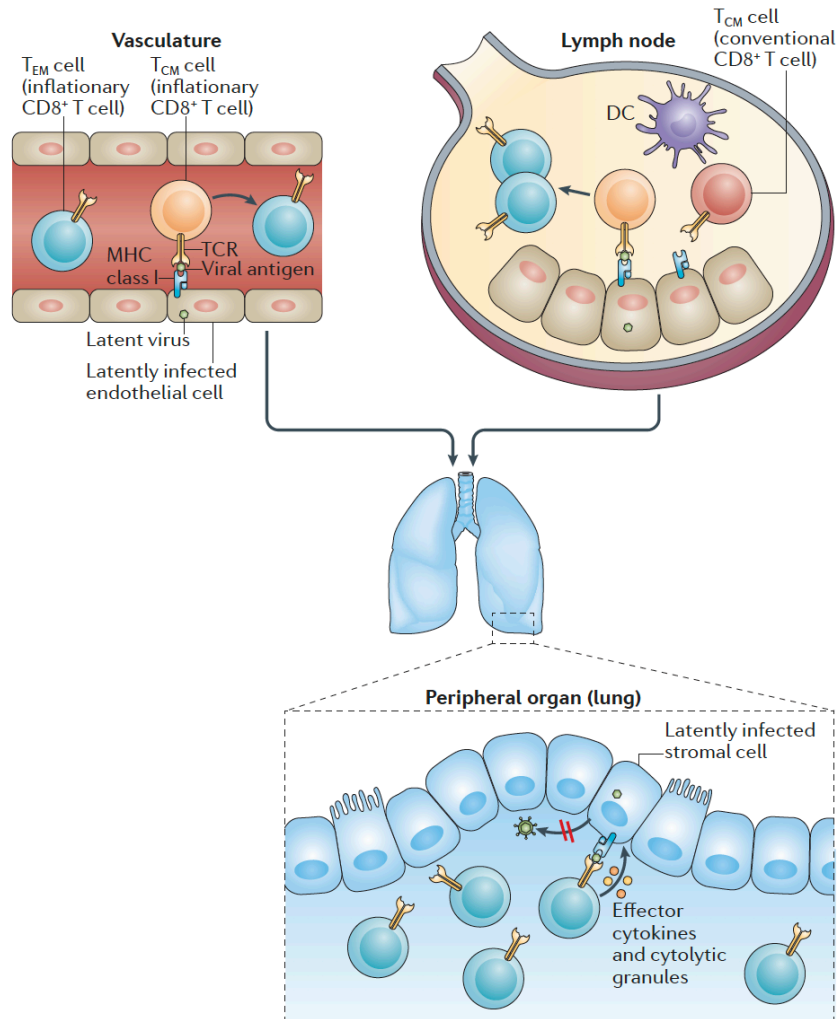
Figure 11: Model of CMV-inflationary cell activation and maintenance. *Non-hematopoietic latently infected cells present viral antigens to inflationary central memory (CM) T cells in lymph nodes or in the vasculature. Activated CM T cells proliferate and differentiate into inflationary effector memory T cells and ultimately accumulate in peripheral tissues where they can exert effector functions. Adapted from Klenerman and Oxenius, 2016 [177].*

Despite mounting a strong response, the immune system is not able to eliminate the infection due to its latency and the multiple immune-evasion strategies employed by hCMV. Indeed, of the 751 CMV proteins thus far identified in infected cells [182] only a few are essential for viral replication. The vast majority are thought to be immune evasion proteins, which profoundly interfere with both the innate and adaptive components of the host, impeding viral clearance [183]. For example, the hCMV US11, US2 and US3 proteins down-regulate MHC-I and MHC-

II molecules on T cells and APCs, while hCMV-UL18 is a surface-expressed MHC-I homologue. The expression of such viral proteins in infected cells avoids immune recognition by CD4 and CD8 T cells, as well as NK cells [184-187]. Furthermore, CMV-UL111.5A is a potent immunosuppressive interleukin homologous to IL-10, that has been demonstrated to suppress anti-CMV immunity [188]. Finally, many hCMV proteins also inhibit the activation of NK cells by blocking activatory receptors or preventing the expression of activatory ligands [184, 187].

5. Memory CD8 T cell immune response to EBV and CMV

5.1. Differences in frequency and phenotype between EBV- and CMV-specific memory CD8 T cells

As previously mentioned, some CMV-specific memory CD8 T cells can go through memory inflation during the latent phase of infection, resulting in a continuous expansion overtime. Conversely, irrespective of their antigen specificity, the pool of EBV-specific memory CD8 T cells remains relatively stable over time. Nonetheless, CD8 T cells specific for EBV lytic antigens are found in higher frequencies and harbor a more terminally differentiated phenotype (i.e. CCR7-, CD62L- and CD45RA+) compared to EBV latent antigen-specific CD8 T cells which are largely CD45RA- and express higher levels of CCR7 and CD62L. However, even CD8 T cells specific for EBV lytic antigens remain generally less differentiated than CMV-specific CD8 T cells, being CD27^{high} and CD27^{low}, respectively [189-192]. In addition, CMV-specific memory T cells generally exhibit high levels of expression of CD57, a marker of replicative senescence [193, 194]. These phenotypic differences are not reflected by functional capacity, since both CMV- [173] and EBV-specific [195] memory T cell clones are cytotoxic and have the capacity to secrete cytokines such as TNFα, and IFNγ as well as perforin.

These differences in frequency and phenotype between EBV- and CMV-specific memory CD8 T cells could, in part, be due to differences in the biology of the two viruses. Indeed, during latency, EBV reactivation in B cells occurs only sporadically, leading to cycles of T cell rest and stimulation thus maintaining a pool of functional CD8 T cells over time. Conversely, CMV latent infection is characterized by continuous low level of transcriptional activity leading to the constant stimulation of CD8 T cells with infrequent rest [196, 197].

5.2. TCR repertoire characteristics of EBV- and CMV-specific responses

One way to study T cell immune responses against specific epitopes is to assess the TCR repertoire diversity in terms of the number, the frequency and the distribution of clonotypes within an antigen-specific T cell pool. T cell clonotypes are defined as the progeny of a given naive precursor cell sharing the same antigen-specific TCRα and β chains. Several studies have shown that the degree of diversity in the EBV- [90-92, 198-203] and CMV-specific [91, 199, 202, 204, 205] TCR repertoires is generally highly restricted, ranging from 1 to 16 clonotypes, though some studies suggest that this number may be somewhat higher [206]. This discrepancy depends, at least in part, on the targeted epitope and the method used to study the repertoire. Indeed, TCR repertoires are often studied based on either the β or the α chain sequence of the clonotypes and not both, thus potentially incorporating a bias in the estimated diversity.

Preferential T cell receptor beta variable (TRBV) and alpha variable (TRAV) gene segment usage (according to Arden's nomenclature [207]) has been observed in epitope-specific TCR repertoires, such as the large proportion of TR-BV2, -BV4, -BV16, -BV22 and TRAV15 in EBV A2/GLC-specific CD8 T cell clonotypes [90, 91, 201-203]. Similarly, the CMV A2/NLV-specific repertoire has been associated with a biased usage of TRBV and TRAV genes segments including TR-BV8, -BV13 and TRAV18 [91, 199, 202, 205]. Finally, so-called "public" TCRs against CMV and EBV have been reported in several studies, based on the shared TCRα or β chain rearrangements or features between various individuals [204, 205, 208-211]. Clonotypes bearing such public TCRs have been shown in some cases to preferentially expand [205, 208], possibly because public TCRs may be evolutionarily selected for optimum interactions with certain viral epitopes. However, "true" public TCRs defined as the exact same TCRαβ found in unrelated individuals may be relatively rare [208].

5.3. TCR repertoire selection of EBV- and CMV-specific responses between acute and latent phases

Upon primary viral infection, antigen-specific T cells expand during the acute phase, followed by a contraction phase when the viral load decreases. During the contraction phase, 90% of T cells are lost and the remaining cells constitute the memory pool and will persist into the latent phase of the infection. The parameters driving the selection of certain T cells from the acute to the chronic phase remain elusive.

In the context of hCMV infection, data describing the T cell repertoire between the acute and chronic phases are very limited, since the primary infection is generally asymptomatic. One study, however, including both patients after organ transplant as well as rare cases of symptomatic primary hCMV infection, has shown that the diversity of the polyclonal CD8 T cell response rapidly diminishes when entering the chronic phase. The TCR repertoire is then limited to the usage of only a few TCR Vβ segments within which dominant clones frequently had public TCR usage [212]. This observation was reinforced in the context of hCMV reactivation and/or chronic inflammation. In this clinical setting, a dramatic clonal focusing of HLA-A*0201/NLV-pp65-specific T cells has been observed, with selection of single clonotypes displaying similar public TCR features in several patients [205].

As EBV primary infection is more often symptomatic, in the form of infectious mononucleosis, compared to hCMV primary infection, several studies have investigated the repertoire evolution between IM and the latent phase of the infection. Some studies observed a relative conserved TRBV usage, yet with significative dominance shift [213, 214]. Others have shown at the clonotype level that highly dominant CD8 T cell clonotypes present during acute IM are poorly represented [215], if at all [90] in the chronic phase and are often overtaken or replaced by other clonotypes specific for the same epitope after 1 to 2 years after the primary infection.

Together, these studies suggest that a change of repertoire occurs in human CMV and EBV infections between the two phases, with some clones being less likely to contribute to the memory pool during latency. However, the repertoires in these studies are mostly based on TRBV staining and on very few TCR sequences at the clonotype level. A more recent study using tetramer sorting and next-generation sequencing found that, in both hCMV- and EBV-infection in renal transplant recipients, the CD8 T cell clonal repertoires in the early phase of infection were mostly similar to those found after one year, both in terms of clonal composition and dominance hierarchy [216].

Collectively, whether the TCR repertoire is conserved or undergoes selection during the transition from the acute to the latent phase of EBV and CMV infections still remains controversial.

5.4. TCR repertoire evolution of EBV and CMV specific responses over time during the latent phase

Several studies have focused on the maintenance of the clonal repertoire during the latent phase of herpes virus infection. In both hCMV and EBV infection, it has been demonstrated that, once established, the CD8 T cell clonal composition appears to be relatively stable for at least several years with only minor alterations in dominance [91, 198, 212, 216, 217]. Nevertheless, it is important to note that the maximal time span analyzed in those studies was of about 5 years, whereas hCMV and EBV immune responses persist for decades and small changes in the repertoire may only be observed over longer periods of time. In this regard, Miles and colleagues [92] have observed in two EBV-positive donors, the persistence of single CD8 T cell clonotypes against the HLA B*0801/FLR and HLA B*4405/EEN epitopes for 18 and 11 years, respectively. However, in most reported cases, EBV specific responses are oligoclonal, and the long-term (i.e. more than 5 years) persistence and shift in dominance between clonotypes has thus far not been extensively investigated.

Collectively, following primary infection and initial TCR repertoire focusing, herpes virus-specific T cell responses revealed a high stability of the TCR clonotype repertoire over time [216] as well as during homeostatic immune reconstitution [218]. Nonetheless, in depth analysis of the precise clonotype composition, as defined by both TCR α and β chains, and its persistence over long periods of time in healthy humans with chronic infection are still required to better understand long-term memory T cell responses.

5.5. Impact of TCR-pMHC affinity/avidity on clonal repertoire selection

Despite major efforts, the parameters underlying the clonal selection after the acute phase to enter the memory pool as well as the long-term maintenance of virus-specific CD8 T cell repertoires remain poorly understood.

Several studies have proposed the TCR-pMHC affinity/avidity as a major determinant of the TCR repertoire selection and dominance in virus-specific CD8 T cell responses. Indeed, Day and colleague have shown that hCMV-specific dominant clones selected from the acute phase into the memory pool showed higher functional avidity (based on half maximal effective concentration or EC_{50} from target cell lysis assays) compared to contracted clones, suggesting a functional avidity threshold to enter the memory pool [212]. These results were reinforced in

the context of hCMV reactivation and/or chronic inflammation, where it has been shown that the preferentially expanded and dominant clonotypes were of higher avidity for their cognate antigen compared to subdominant clonotypes, based on CD8-mutated tetramer binding and tetramer dissociation rates [205, 219]. On the other hand, one study has shown that CD8 T cell repertoires against the EBV HLA-B8/RAKFKQLL epitope displayed no significant differences in terms of global avidity (measured by tetramer staining and dissociation kinetics) between the acute and chronic phases of infection, thus contrasting with the concept of avidity maturation observed in CMV infection [220].

Similarly, the impact of TCR-pMHC affinity/avidity has been investigating for the persistence of CMV- and EBV-specific clonal repertoire during latency. While the repertoire is kept stable for several years, dominant and subdominant clonotypes appear to have comparable functional avidity but display heterogeneous levels of CD8 binding dependency. This suggests a compensatory role for the CD8 co-receptor to preserve clonotypic diversity while maintaining high functional capacity [91, 198, 202, 212]. The impact of the TCR avidity on long-term evolution of the repertoire and eventual shift in clonal dominance has been so far mainly estimated by mathematical models. Indeed, Davenport *et al.* [220] have proposed a model to predict the evolution of EBV-specific T cell repertoires throughout the course of an infection. This model takes into account variations in TCR avidity and thus in cell division rate of the different clonotypes, but also integrated a decline in survival with increased cell division number. This senescence model is characterized by a primary contribution from several clones, the gradual senescence of high-avidity T cell clones, and their slow replacement by clones of intermediate avidity (in a process termed clonal succession) during life-long latent infection. This theory was partially supported in hCMV infection by the more recent work of Griffiths and colleagues, who reported that highly differentiated CMV/pp65-specific CD8 T cells that re-express CD45RA and which are of relatively low avidity (based on CD8-null tetramer binding) are significantly more prevalent in older individuals [221]. In addition, Ouyang *et al.* have observed a large expansion of functionally impaired CD8 T cells directed against a CMV epitope in the elderly, which was not observed in younger donors [222]. These data suggest a skewing of the T cell repertoire avidity during aging.

Nonetheless, further investigations are needed to determine the precise criteria for antigen-specific CD8 T cell repertoire selection into the memory pool following acute infection as well as their evolution during lifelong latency.

## 5.6.	Immune responses with aging

It is commonly accepted that human aging is characterized by an increased vulnerability to infection and a decrease in vaccine efficacy [223, 224] due a deterioration of the immune system, also termed immunosenescence [225]. One of the main features of the cellular immunity with aging is the change in T-cell composition. In both blood and SLOs, the proportion of naive T cells in older individuals has been shown to be markedly decreased in the CD4 and CD8 T cell compartments [226, 227], mainly due to thymic involution. This age-related decrease of thymic output of naive T cells, in addition to an age-related loss in the capacity to prime naive T cells [228], reduces the hosts ability to respond to novel antigen encounter, thus rendering them more prone to a variety of diseases [229].

Concurrent with the decrease of the naive T cell pool, the relative proportion of other subsets, especially effector-memory T cells, increases [230]. Moreover, the phenotype of T cells has been shown to evolve with increasing age, with the gradual loss of the costimulatory receptors CD28 and CD27, while the expression of markers such as CD57 and KLRG1 is enhanced with aging. In addition, telomere length of T cells also tends to decrease with time [231]. This phenotype has been associated with T cell senescence, characterized by a low or inexistent proliferative capacity, despite high functional properties. The overall decline of the immune system with aging is also characterized by low-grade inflammation in the absence of explicit infection (or inflamm-aging). Inflamm-aging and immunosenescence are interrelated processes [232] that may be reinforced by many factors such as metabolic changes, tissue injury or latent infections.

Latent infections with continued T cell stimulation, such as CMV, is believed to accelerate the aging of the immune system and thus to compromise its ability to control new infections or latent reactivation in the elderly. As previously mentioned, in normal aging the proportion of naive CD4 T cells decreases, whereas this does not hold true for the absolute number of naive CD4 T cells. However, in CMV seropositive individuals a decrease in the absolute number of naive CD4 T cells is observed [227]. On the other hand, for CD8+ cells, a reduction in the absolute number of CD8 naive-T cells in older individuals has been reported [229] regardless of their CMV serostatus [233], probably due to decreased homeostatic proliferation [234, 235]. Proportionally, the increase in effector-memory T cells is more pronounced in CMV+ individuals than in their seronegative counterparts. This is in part due to the phenomenon of memory inflation over time and the accumulation of CMV-specific memory T cells [177].

Latent hCMV infection, especially with significant memory inflation, is suspected to accelerate immunosenescence in seropositive elderly individuals. Moreover, since CMV-specific inflationary T cells are generally terminally differentiated, with low proliferative potential but high functional capacity, their large contribution to the T cell pool could also be responsible for the observed global increase of senescent- and/or exhausted- like T cells in the elderly. Indeed, several studies have shown that persistent viral infections such as HIV [174, 236-238], HCV [239], and CMV [224, 240] correlate with an increased proportion of highly differentiated, exhausted and/or senescent T cells already in early life and with time. This phenomenon was not observed in latent EBV or Varicella-Zoster Virus (VZV) infections, probably due to a less stringent and continued T cell stimulation.

While a modest age-related decrease in TCR repertoire diversity has been demonstrated [13, 241-243], the large expansion of oligoclonal hCMV-specific CD8 T cells during memory inflation has been proposed to further constrain the overall T cell repertoire diversity [244], although the physiological impact of this change remains unclear [245]. Whether the persistence of CMV infection over time reduces the hosts ability to mount an effective and protective immune response to other pathogens, or increases the risk of cancer or other diseases, remains to be elucidated. On one hand, CMV-infection has been associated with an increased risk of cardiovascular disease in elderly individuals through several mechanisms, including direct vascular damage due to infection of vascular endothelial cells [246], or by increasing the background level of inflammation thus enhancing inflammation-mediated vascular pathology [247]. Large cohort studies have also associated high levels of CMV-specific immunoglobulin G with mortality in the elderly [247, 248]. On the other hand, CMV infection has been shown to be beneficial in aged mice, by conferring an increased resistance to bacterial infection through the mobilization of a broader TCR repertoire [249] and a higher basal activation state of the innate immune system [250, 251]. Finally, conflicting studies have reported both a beneficial [252] and detrimental [253] impact of latent hCMV infection on influenza vaccination, further confounding our understanding of the effect of chronic CMV infection on human immune system potency.

Objectives

This thesis is divided into two main objectives. The first objective focusses on the impact of TCR-ligand binding avidity on T cell functional potency among viral and tumor-specific CD8 T cells. This part has been recently published in Allard M, Couturaud B *et al.*, JCI Insight 2017 [254] (see Manuscript 1 in the results section). The second objective addresses the impact of TCR-ligand binding avidity on the evolution of human CD8 TCR repertoires specific for persistent herpes viruses over extended periods of time. The data collected from the second aim are compiled into a manuscript in preparation (see Manuscript 2 in the results section).

1.   Impact of TCR binding avidity on CD8 T cell function among different antigenic specificities

In the last few decades, immunotherapy has played a leading role in innovative treatments against cancers such as melanoma, or viral infections such as CMV. In most immunotherapy-related strategies, cytotoxic CD8 T-cells play a central role, due to their capacity to kill tumor or infected cells. Therefore, extensive research has been undertaken to investigate which properties of these cells are essential to generate protective and durable immune responses. In that regard, high T cell functional avidity, which is the antigen sensitivity measured by functional readouts, has been associated with better control of viral infections in both animal models [71-73] and humans [74-78], as well as better tumor control in mice [79, 80] and melanoma patients [81, 82]. However, *ex vivo* functional avidity and polyfunctional assessments remain laborious and time consuming, and are often not possible because relatively large number of cell numbers must be withdrawn from patients. Furthermore, the TCR-pMHC binding avidity remains often neglected, mainly due to technical limitations. In fact, TCR-ligand avidity may offer a better biometric by which the quality of the antigen-specific T cell response can be directly evaluated, since it controls numerous aspects of T cell biology such as T-cell activation, differentiation, and functional efficacy (reviewed in [255]) as well as *Listeria monocytogenes* infection control in mice [99].

1.1. Strong relationships between TCR-pMHC binding avidity and T cell functional potency

To better characterize the relationship between the physical interaction of the TCR-pMHC complex and the ensuing T cell activation, we used the recently developed NTAmer technology. This novel flow cytometry-based approach allows for the quantification of monomeric TCR-pMHC dissociation kinetics (k_{off}) directly on living antigen-specific CD8 T cells. Using this technology, our group documented robust correlations between NTAmer kinetic values (k_{off}) and those obtained by SPR [108]. Moreover, we showed that NTAmer-based k_{off} measurements strongly correlate with the killing capacity of TCR-engineered CD8 T cells [108] as well as following therapeutic vaccination [109]. In the latter study, we found differences in TCR-pMHC binding avidity depending on the type of Melan-A$_{26-35}$ peptide used for vaccination [109]. To elucidate the precise causality between TCR-pMHC binding avidity and the overall CD8 T cell functional profile, NTAmer-based k_{off} measurements of antigen-specific CD8 T cell clones were combined with multiple functional assays including killing capacity, CD107a degranulation, cytokine production, proliferation, costimulatory and inhibitory receptor expression, as well as the ability of tumor-specific CD8 T cells to control tumor growth *in vivo*. This part of the study was performed on large libraries of HLA-A*0201–restricted effector-memory CD8 T cell clones specific for self/tumor antigen (i.e. Melan-A$_{26-35}$ and NY-ESO-1$_{157-165}$) and viral antigen (i.e. CMV/pp65$_{495-504}$ and EBV/BMFL1$_{259-267}$). Results obtained from these experiments show that TCR-pMHC off-rate is a major determinant controlling the functions of CD8 T cells *in vitro* and *in vivo*. These observations further enhance our understanding of the impact of TCR avidity on CD8 T cell activation and function.

1.2. Variations of TCR-pMHC avidity according to the antigenic specificity of CD8 T cells

Only limited information is available on the overall quality of TCR-pMHC binding avidity of self/tumor–specific versus non–self/pathogen–specific CD8 T cell repertoires [54, 55]. The most detailed study investigating this question was carried out by Aleksic *et al.* [55] who compared the TCR affinities of 14 tumor-specific TCRs directed against various tumor antigens, versus 10 TCRs that bind to different viral antigens. Using the SPR approach, they observed that TCRs that bind viral antigens fall within a higher affinity range than those that bind cancer-related antigens [55]. However, one of the major caveats of SPR analysis is that it

ignores the contribution of CD8 coreceptor and/or other molecules present in the vicinity of the TCR to the overall TCR-pMHC avidity. In addition, this study focused on only one TCR sequence per antigenic specificity due to technical limitations (i.e. the laborious and expensive production of soluble TCRs and their cognate pMHC), thus introducing a strong selection bias, as it is known that TCRs directed against the same epitope can cover a large range of TCR affinities [256]. To better address the question of whether or not TCR avidity depends on the antigenic origin (i.e. self/tumor versus non-self/viral), we performed a comprehensive analysis of TCR-pMHC off-rates using the novel NTAmer technology on large panels of effector-memory CD8 T cell clones (n = 414) specific for (i) the differentiation antigen A2/Melan-A$_{26-35}$, (ii) the cancer testis antigen A2/NY-ESO-1$_{157-165}$, (iii) the viral A2-CMV/pp65$_{495-504}$ antigen and (iv) the viral A2-EBV/BMFL1$_{259-267}$ antigen isolated from five melanoma patients and two healthy donors. In addition, we investigated potential differences in terms of TCR binding avidity between the type of tumor antigen (i.e. Melan-A versus NY-ESO-1) as well as following peptide vaccination in combination with CpG oligodeoxynucleotides (CpG ODN) and incomplete Freund's adjuvant (IFA) (i.e. Melan-A) or from patients with naturally occurring anti-tumoral T cell responses (i.e. NY-ESO-1). Our data highlight superior TCR-ligand binding avidities of virus-specific T cell repertoires compared with self/tumor-specific T cell ones. Moreover, higher avidity T cells were found in melanoma patients with natural responses against NY-ESO-1 tumor antigen than following therapeutic vaccination with the Melan-A peptide. Nevertheless, several clones with enhanced TCR binding avidity could still be detected, indicating the presence of rare self/Melan-A-specific CD8 T cells that are selected upon vaccination, emphasizing the relevance of therapeutic vaccination approaches in enhancing the quality of a tumor-specific repertoire.

## 1.3.	Stability and robustness of TCR-pMHC off-rates

T cell functional avidity can greatly vary depending on the chosen functional readouts and the laboratory protocols used to assess them, the activation state of the T cells, their differentiation status or the expression of inhibitory and costimulatory receptors [70]. In this regard, the TCR-pMHC off-rate may provide a more reliable biophysical parameter to assess T cell potency. To investigate this question, we assessed the reproducibility of NTAmer-derived TCR-pMHC off-rate measurements in parallel with T cell functional capacities, in separate experiments. In addition, we investigated the impact of the T cell activation state on TCR-pMHC off-rate and on T cell functional avidity. Our results revealed that the TCR-pMHC off-rate is a more stable

and robust biomarker of CD8 T cell potency than the frequently used functional assays/metrics, that depend on T cell activation state, and therefore show major intra- and inter-experimental variability. The identification of novel T cell-based parameters able to overcome some of the limitations associated with functional assays, and thus to resolve the lack of universal standards of T cell potency assessment, is of great interest. Indeed, the efficient and reproducible identification and isolation of high avidity T cells is of significant value to improve the therapeutic potential of T cells for immunotherapy. In this line, TCR-pMHC off-rate represents an interesting candidate as a biomarker of T cell therapeutic efficacy.

2. Impact of TCR-ligand binding avidity on the persistence of viral-specific CD8 T cell clonotypes over time

2.1. Progressive fluctuations over time of CMV- but not EBV-specific memory CD8 T cell clonotype repertoires

Whether CD8 memory T cell repertoires are stably maintained over prolonged periods, periodically "renewed", or slowly remodeled remains a matter of debate. It is a particularly difficult question to address in humans, since it requires in-depth longitudinal analysis of protective immune responses over extended periods of time. In this regard, the unique signature of a TCR defined by its α and β chain sequences is an excellent marker to track individual clonotypes and follow antigen-specific responses in a straightforward manner over time [257]. Antigen- specific CD8 T cell repertoires are generally composed of highly frequent (also defined as dominant) as well as less frequent (defined as non-dominant) T cell clonotypes [202]. In humans, changes in TCRαβ clonotype dominance have been observed between the acute and the chronic phases of persistent EBV and CMV infection [90, 198, 212]. In addition, several studies have revealed the persistence of dominant and non-dominant CMV and EBV-specific T cell clonotypes in healthy donors over periods of 2 to 5 years [91, 198, 212, 216, 217]. However, the repertoires in most of these studies were mostly based on TRBV staining and on very few TCR sequences at the clonotype level. In addition, fluctuations in the repertoires may be observed only after longer periods of time.

To reinforce our knowledge about the precise persistence of dominant and non-dominant CMV- and EBV-specific CD8 T cell clonotypes over extended periods of time in asymptomatic virus-infected individuals, we studied the TCRαβ clonotype composition and selection of large

panels of CMV- and EBV-specific CD8 T-cell clones from six healthy donors over a period of 15 years, i.e. between early (2002) and late (2017) time-points. The TCRαβ repertoires were assessed by several techniques to minimize experimental bias. These analyses allowed us to examine whether the presence of continuous antigenic stimulation (i.e. during latent CMV infection) versus sporadic stimulation (i.e. during latent EBV infection) over extended periods of time leads to intermittent shifts in the dominance hierarchy of TCR clonotypes. Whereas T cell clonal repertoires against HLA-A2/pp65 (i.e. CMV) were highly restricted (i.e. 2 to 6 clonotypes), the clonal T cell repertoires for EBV (HLA-A2/BMFL1) showed more diversity (i.e. 15 to 25 co-dominant clonotypes), in agreement with our previous report [91]. We found that the TCRαβ clonotype composition of both CMV- and EBV-specific T cell responses remains remarkably stable over the 15 years. Nevertheless, significant fluctuations within the CMV-specific clonotype repertoires were observed during this observed period of time, highly contrasting to the great stability of the EBV-specific ones.

2.2. Progressive long-term avidity decline of CMV- but not EBV-specific memory CD8 T cell clonotype repertoires

We next investigated how TCR-pMHC binding parameters could influence T cell selection, expansion and persistence over extended periods of time (i.e. 15 years). As previously described, several studies have linked clonal selection and expansion during infection and the respective TCR-pMHC binding affinity/avidity. While some studies have shown the selective expansion of particular TCR clonotypes of high avidity for virus-specific MHC following secondary acute virus infection in mice [258-260], others have found an enrichment of virus-specific CD8 T cells of low affinity/avidity in older individuals, suggesting a T cell repertoire skewing towards an overall lower avidity during aging [221, 222, 256]. However, all of these studies are based on classical multimer staining and functional assays and mostly characterized T cell clonotypes at the TCR-Vβ level, without including accurate measurements of the TCR-pMHC binding affinity/avidity or kinetics, nor the complete TCRαβ clonotype repertoire analysis. Importantly, almost no longitudinal studies of more than 5 years have been carried out in humans. Thus, available data on long-term repertoire and overall avidity evolution is limited to studies comparing groups of individuals of different age. Therefore, the precise impact of TCR-pMHC-CD8 avidity on well-defined virus-specific T cell clonotype selections and their persistence in humans remains largely unknown.

In our study, we took advantage of NTAmer based off-rate measurements on CMV- and EBV-specific clones from the repertoires of our healthy donors followed during 15 years, as well as TCR avidity measurements on total CMV-specific CD8 T cell populations at the two time points (i.e. 2002 versus 2017). We also studied the contribution of CD8 binding to the overall TCR-pMHC binding avidity of each co-dominant clonotypes, using NTAmers bearing the D227K/T228A mutations in the HLA-α3 domain preventing CD8 binding (i.e. CD8-null NTAmers; [108]). Within the CMV-specific TCRαβ clonotype repertoires, we observed the preferential selection and expansion over time of clonotypes of lower TCR-pMHC binding avidity and higher CD8 binding dependency. In contrast, the clonal evolution of the EBV-specific clonotype repertoires was highly preserved, with the same clonotype distribution (i.e. dominant versus sub-dominant, low versus high TCR avidity, CD8 binding-independent versus -dependent) during the observation period of 15 years. Interestingly, for the EBV model, TCR-pMHC off-rates correlated to distinct TRBV family usage (e.g. TRBV20 versus TRBV29) rather than to individual clonotype selection, as it is the case for the CMV-specific T cell responses. Similar data were found when we performed off-rate measurements on global virus-specific T cell populations from 2002 versus 2017, with an overall avidity decline over time of CMV- but not of EBV-specific CD8 T cell clonotype repertoires. Together, these experiments allowed us to better understand to which extent structural TCR binding avidity governs the selection, expansion and survival of particular T cell clonotypes over extended periods of time, as well as the evolution of overall TCR avidity of the repertoire during EBV- and CMV latency. Specifically, our findings revealed distinct features of the highly sophisticated control of persistent CMV- versus EBV-specific CD8 T cell clonotypes over extended periods of time in healthy adults.

2.3. Accumulation of LILRB1 expression over time in high avidity CMV-specific CD8 memory T cell clonotypes

Several studies have shown a progressive change in the phenotype of virus specific CD8 T cells during CMV and EBV latency, as well as in general aging. Indeed, CMV- and EBV-specific T cells that accumulate in older individuals have been shown to have a more differentiated phenotype with, for example, the re-expression of CD45RA [221]. Moreover, T cells directed against chronic infections such as CMV, HCV or HIV are often described as exhausted or senescent T cells, characterized by high expression of inhibitory receptors such as PD-1, CTLA-4 or KLRG1 [174, 236-240]. On the other hand, it has been shown that inhibitory

receptor expression depends on differentiation and activation rather than the exhausted state of human CD8 T cells [261]. This suggests that their sustained expression in chronic infection may rather reflect CD8 T cell activation and differentiation, which may need to be down-tuned in order to prevent chronic tissue damage [262].

Here, we first evaluated the functional capacity of high versus low avidity CMV and EBV-specific CD8 T cell clones generated from our healthy donors at both time-points (i.e. 2002 versus 2017). We found that both CMV- and EBV-specific T cell clonotypes bearing TCRs of higher binding avidities exhibited improved functional potential in terms of killing, and CD107a degranulation capacity as well as cytokine (IFNγ and TNFα) production, compared to clonotypes of lower TCR avidities. Again, functional avidity was related in the EBV model, to the distinct TRBV usage, rather than to particular TCRαβ clonotypes.

Finally, we assessed the whole gene expression from CMV-specific CD8 T cells of defined TCRαβ clonotypes and of known characteristics for TCR binding avidity, clonal dominance and persistence over time by *ex vivo* RNA sequencing (RNASeq). We identified a distinct molecular signature, including elevated expression of *LILRB1,* preferentially expressed by the high avidity T cell clonotypes in three out of the four studied donors. LILRB1/CD85j is a negative regulatory receptor, known to accumulate in antigen-specific CD8 T cells with aging [263]. The RNASeq analyses also revealed a progressive increase in *LILRB1* expression in CMV-specific clonotypes over time. Similar observations were made when we assessed the surface expression of LILRB1 by flow cytometry with a preferential expression found again in high avidity T cell clonotypes. Finally, the functional impact of LILRB1 on proliferation and cytokine production was investigated in blocking experiments.

Collectively, these experiments, combined to the careful evaluation of the clonotype repertoires and the overall TCR avidity evolution over time should improve our knowledge of the fine-tuned control of protective virus-specific T cell immune responses in healthy adults over extended periods of time. Understanding the biological parameters (i.e. TCR-pMHC binding avidity, T cell functional potential, or the presence of checkpoint regulatory receptors) involved in the long-term persistence of CD8 T cell clonotypic responses under chronic antigen exposure should further help us to identify specific deficiencies in anti-tumor T cell responses, and thus guide the rational development of T cell-based therapies against cancer and/or infections.

Results

1. Manuscript 1

The following article, published in The Journal of Clinical Investigation Insight in July 2017, corresponds to the first aim of this thesis. This study was mainly done in collaboration with Dr. Mathilde Allard and supported by all co-authors.

JCI insight

TCR-ligand dissociation rate is a robust and stable biomarker of CD8+ T cell potency

Mathilde Allard,[1] Barbara Couturaud,[1] Laura Carretero-Iglesia,[1] Minh Ngoc Duong,[1] Julien Schmidt,[2] Gwennaëlle C. Monnot,[2] Pedro Romero,[2] Daniel E. Speiser,[1,2] Michael Hebeisen,[1] and Nathalie Rufer[1,2]

[1]Department of Oncology, Lausanne University Hospital Center (CHUV) and University of Lausanne, Epalinges, Switzerland. [2]Ludwig Cancer Research, University of Lausanne, Epalinges, Switzerland.

Despite influencing many aspects of T cell biology, the kinetics of T cell receptor (TCR) binding to peptide-major histocompatibility molecules (pMHC) remain infrequently determined in patient monitoring or for adoptive T cell therapy. Using specifically designed reversible fluorescent pMHC multimeric complexes, we performed a comprehensive study of TCR-pMHC off-rates combined with various functional assays on large libraries of self/tumor– and virus-specific CD8+ T cell clones from melanoma patients and healthy donors. We demonstrate that monomeric TCR-pMHC dissociation rates accurately predict the extent of cytotoxicity, cytokine production, polyfunctionality, cell proliferation, activating/inhibitory receptor expression, and in vivo antitumor potency of naturally occurring antigen-specific CD8+ T cells. Our data also confirm the superior binding avidities of virus-specific T cells as compared with self/tumor–specific T cell clonotypes (n > 300). Importantly, the TCR-pMHC off-rate is a more stable and robust biomarker of CD8+ T cell potency than the frequently used functional assays/metrics that depend on the T cell's activation state, and therefore show major intra- and interexperimental variability. Taken together, our data show that the monomeric TCR-pMHC off-rate is highly useful for the ex vivo high-throughput functional assessment of antigen-specific CD8+ T cell responses and a strong candidate as a biomarker of T cell therapeutic efficacy.

Introduction

Cytotoxic T lymphocytes mediate immune protection against a large number of infectious diseases, and recent developments in oncology confirmed their ability to eliminate cancers. To achieve successful immunity, T cells must be activated through specific interactions between T cell receptors (TCRs) and antigenic peptides presented by major histocompatibility molecules (pMHC) on antigen-presenting cells. This enables T cell expansion and differentiation into large numbers of effector cells with various functional capacities (i.e., killing, cytokine production, proliferation). Furthermore, T cells must migrate and localize to the infected or tumoral tissues, exerting their effector function and finally acquire memory properties, assuring long-lasting immunity.

Extensive research has been undertaken to determine which T cell properties are essential to generate protective and durable immune responses. T cell functional avidity, which measures in vitro T cell responses when exposed to increasing antigen concentrations, has been largely associated with the control of viral (1–3) or tumor (4, 5) load in animal models. In accordance with these observations, several findings in patients with HIV (6, 7) or hepatitis C (8, 9) infections further showed the key role of CD8+ T cells of high functional avidity in efficient viral control and clearance. Yet, others have challenged the functional superiority of such high-avidity cells, which may be prone to increased activation-induced cell death, senescence, or exhaustion (reviewed in ref. 10). In the context of antitumor responses, results obtained from melanoma patients also indicate that T cells of high functional avidities are required for efficient protection (11–13). Besides functional avidity, higher proportions of polyfunctional CD8+ or CD4+ T cells were also found in HIV (14, 15) and hepatitis C (16) controllers, when compared with individuals with progressive disease. Moreover, some reports proposed a direct link between functional avidity (i.e., antigen sensitivity) and polyfunctionality (i.e., T cell capacity to exert multiple effector functions) (17, 18). However, the ex vivo appraisal of T cell functional-

JCI INSIGHT

ity/polyfunctionality is still often limited to assays of fixed stimulation doses and by the lack of universal standards of T cell assessment (reviewed in refs. 19, 20). It is therefore essential to improve our knowledge regarding the contribution of the different aspects of T cell function to clinical efficacy and to identify additional T cell–based parameters that may enable overcoming some of the limitations associated with functional assays.

The functional avidity of T cells is primarily controlled by the strength of TCR-pMHC interactions, a key parameter shown to impact on numerous aspects of T cell biology, including their thymic selection (21), activation and differentiation (22), autoimmune pathogenicity (23), and protection against infection and cancer (24). In fact, TCR-pMHC binding avidity may offer a key metric by which the quality of the T cell response can be directly evaluated, since it controls T cell activation, differentiation, and functional efficacy (25). Numerous studies indicate that, within the affinity range of physiological interactions (K_D 100–1 µM), enhanced TCR-pMHC affinity or off-rate (k_{off}) correlate with improved T cell functionality (26). However, most of these reports are based on artificial models (e.g., using affinity-optimized TCR variant panels or altered peptide ligand models), and thus only limited information is available on the overall impact and clinical relevance of TCR-pMHC binding avidity or kinetics (e.g., off-rates) in the context of naturally occurring antigen-specific CD8+ T cell responses. Moreover, identifying and selecting TCRs of higher avidity may be of particular importance in the tumoral setting, since most high avidity/affinity self/ tumor antigen–reactive T cells are naturally eliminated or silenced by mechanisms of central and peripheral tolerance, emphasizing the need to select the remaining rare high-avidity cells for immunotherapy.

Reversible 2-color multimer-based approaches (i.e., Streptamers, NTAmers) have been developed to precisely quantify monomeric TCR-pMHC dissociation rates (i.e., off-rate or k_{off}) directly on living T cells. Streptamers initially revealed that virus-specific CD8+ T cells with longer off-rates conferred better in vivo protection than T cells with shorter off-rates (27). However, owing to the faster decay of the multimeric complex onto monomeric pMHC when compared with Streptamers, NTAmers offer an increased sensitivity to detect T cells with low-avidity TCRs (26), such as those typically found in self/tumor–specific CD8+ T cell repertoires. Consequently, we recently showed that NTAmer-based k_{off} strongly correlated with the killing capacity of TCR-engineered and natural tumor-specific human CD8+ T cells (28, 29).

With the aim to thoroughly evaluate possible correlations between T cell function and TCR-pMHC binding kinetics, we here undertook a large-scale analysis of combined multiple functions (i.e., killing, CD107a degranulation, cytokine production, proliferation, surface expression of activating/inhibitory receptors, and tumor control) and optimized off-rate measurements using NTAmers to characterize large libraries of tumor- and virus-specific CD8+ T cell clones isolated from melanoma patients and healthy donors. Our large data sets show that the TCR-pMHC off-rate is a major determinant controlling the functions of CD8+ T cells in vitro and in vivo. Our findings are also of practical importance, as we found that the TCR-ligand dissociation rate is a highly stable biomarker, more reliable and reproducible than the usual assessments based on multimer staining levels or functional T cell avidity, which may fluctuate depending on the T cell's activation state.

Results

TCR-pMHC off-rate accurately correlates to overall T cell functional avidity. To precisely address the relationship between the TCR-pMHC off-rate and the overall CD8+ T cell functional profile, we generated large libraries of HLA-A*0201–restricted CD8+ T cell clones, by direct ex vivo sorting and cloning of self/tumor–specific (i.e., Melan-A$_{26-35}$ and NY-ESO-1$_{157-165}$) and virus-specific (i.e., cytomegalovirus CMV/pp65$_{495-504}$ and Epstein-Barr virus EBV/BMFL1$_{259-267}$) effector memory (EM) T cells (Supplemental Figure 1; supplemental material available online with this article; https://doi.org/10.1172/jci.insight.92570DS1). We analyzed all clones for TCR-pMHC dissociation rates using NTAmers loaded with the native Melan-A, NY-ESO-1, EBV/BMFL1, or CMV/pp65 peptide because they provided a more physiological assessment of the TCR-pMHC recognition efficacy as opposed to the corresponding analog peptides (as detailed in Methods). Representative k_{off}-based panels of self/tumor– and virus-specific CD8+ T cell clones were further characterized at the functional level, including assessment of cytotoxic activity, CD107a degranulation, and production of cytokines based on peptide titration assays, as well as proliferation (Supplemental Figure 2). Note that, for the same antigen specificity, most of the different functional readouts/measures were obtained during the same nonspecific restimulation cycle to make use of the antigen-specific CD8+ T cell clones in a similar resting state (>15 days after restimulation).

We observed, for all antigenic specificities, statistically significant correlations between TCR-pMHC off-rates and various functional avidity readouts (EC$_{50}$, defined as the peptide concentration producing half-maximal response) or proliferative capacity (percentage of divided cells) (Figure 1 and Supplemental Fig-

ure 3, A and B). Yet, stronger correlations ($P < 0.01$–0.001, $r > 0.5$, and narrow confidence intervals) were generally found for self/tumor–specific (Melan-A and NY-ESO-1) than non–self/virus–specific (CMV/pp65 and EBV/BMFL1) T cells. By contrast, no positive correlations could be observed between TCR-pMHC off-rates and the maximally reached functions at saturating peptide doses (B_{max}, maximal response) (Supplemental Figure 3C; data not shown). In turn, the maximal response depended on the in vivo differentiation status, with stronger Th2-related cytokine production by clones derived from the early-differentiated EM/CD28+ cells and greater granzyme B expression and killing by those from the late-differentiated EM/CD28− cells (Supplemental Figure 3D). Collectively, these results indicate that, within an antigen-specific repertoire, the kinetics of TCR-pMHC interactions represent a major determinant of the overall functional avidity of CD8+ T cells, regardless of their differentiation status (Supplemental Figure 3D) or function-specific activation thresholds (killing < CD107a < IFN-γ < TNF-α < IL-2) (Supplemental Figure 4A).

TCR-pMHC off-rate closely correlates to CD8+ T cell polyfunctionality. Protective immunity against intracellular pathogens relies on the individual CD8+ T cell capacity to display multiple effector functions or polyfunctionality (10). We hypothesized that the kinetics of TCR-pMHC interactions could also affect their polyfunctionality. The coexpression levels of CD107a, IFN-γ, TNF-α, and IL-2 were characterized on a representative selection of self/tumor– and virus-specific CD8+ T cell clones with relative slow or fast TCR-pMHC off-rates (Figure 2). For all antigenic specificities and peptide titrations tested, the fraction of cells displaying more than 1 single function was always greater in CD8+ T cell clones with slower TCR-pMHC off-rates than with faster ones (Figure 2A). In line with these observations, we found that a significant proportion of antigen-specific CD8+ T cell clones with slow TCR-pMHC off-rates showed increased polyfunctional capacities (in terms of EC_{50} titration curves) when compared with the clones having fast TCR-pMHC off-rates (Figure 2, B–D). However, a strict correlation between off-rates and polyfunctionality was not always found, and limited differences were mostly observed in the EBV-specific CD8+ T cell responses. Taken together, these results show that the TCR-pMHC off-rate not only predicts single functional avidities of self/tumor– and virus-specific CD8+ T cells, but also their capacity to codevelop multiple effector functions.

TCR-pMHC off-rate closely follows costimulatory/coinhibitory receptor expression in activated CD8+ T cells. PD-1 surface expression on CD8+ T cells has been reported to positively correlate with TCR-pMHC binding avidity (30) or functional avidity (31). Here, we explored the relationship between NTAmer-derived off-rates and the expression of various costimulatory (CD28 and CD137) and coinhibitory (LAG-3, PD-1, TIGIT, and TIM-3) receptors (Figure 3). No consistent correlations were found when CD8+ T cell clones were assessed in a resting state (data not shown). In contrast, following 24 hours of stimulation with self/tumor or viral peptides, we observed substantial correlations between TCR-pMHC off-rates and the extent of increased expression of both costimulatory and coinhibitory receptors (Figure 3, A–F). These data indicate a direct impact of TCR-pMHC binding avidities on the susceptibility of CD8+ T cells to antigen-specific activation, and consequently on the upmodulation of both costimulatory and coinhibitory receptors upon stimulation.

We also investigated whether TCR-pMHC off-rates associated with CD5 expression, which is a measure of the strength for self-pMHC selecting ligands during thymocyte development (32). At baseline, most virus-specific CD8+ T cell clones displayed high expression levels of CD5, irrespective of their TCR-pMHC off-rates (Figure 3G). These data are in line with previous reports proposing that T cells with greater TCR sensitivity to self pMHC are most efficiently recruited in response to foreign antigens (33, 34). Positive correlations were only found in the context of self/tumor–specific CD8+ T cell clones, with slower off-rates associating with higher baseline levels of CD5 (Figure 3G and Supplemental Figure 5). This latter observation suggests that the expression levels of CD5 on self/tumor–specific T cells may also predict their capacity for increased homeostatic or antigen-specific response.

TCR-pMHC off-rate predicts the in vivo functional potency of self/tumor–specific CD8+ T cells. To further substantiate the relevance of our in vitro observations, we evaluated the impact of TCR-pMHC off-rates on the ability of self/tumor–specific CD8+ T cells to control tumor growth in vivo. We first adoptively transferred A2/Melan-A$_{26–35}$–specific CD8+ T cell clones of slow versus fast TCR-pMHC off-rates into immunodeficient NSG mice bearing human melanoma Me275 tumors (Figure 4A). The transfer of fast off-rate T cell clones showed intermediate tumor growth control. In contrast, T cell clones with slow off-rates mediated a more significant delay in tumor growth when compared with the untreated (PBS) group (Figure 4B). Furthermore, a significantly prolonged survival was only observed for mice treated with A2/Melan-A$_{26–35}$–specific clones of slow TCR-pMHC off-rates (Figure 4C). To confirm those observations, we then performed similar experiments using the A2/NY-ESO-1 antigenic model, but this time, all mice received s.c. injec-

A | LAU618 A2/Melan-A | LAU155 A2/NY-ESO-1 | BCL4 A2/pp65 | BCL4 A2/BMFL1

A — Killing EC$_{50}$ (M)
n=25 R=0.599 p=0.001
Non-killers
n=32 R=0.654 p<0.0001
n=30 R=0.431 p=0.02
n=26 R=0.236 p=0.2

B — CD107a EC$_{50}$ (M)
n=28 R=0.554 p=0.002
n=30 R=0.645 p=0.0001
n=30 R=0.423 p=0.02
n=25 R=0.708 p<0.0001

C — IFN-γ EC$_{50}$ (M)
n=28 R=0.503 p=0.006
n=30 R=0.621 p=0.0003
n=30 R=0.458 p=0.01
n=25 R=0.438 p=0.03

D — TNF-α EC$_{50}$ (M)
n=28 R=0.586 p=0.001
n=30 R=0.681 p<0.0001
n=30 R=0.483 p=0.007
n=25 R=0.558 p=0.004

E — IL-2 EC$_{50}$ (M)
n=28 R=0.646 p=0.0002
n=30 R=0.681 p<0.0001
Non-IL2
n=29 R=0.398 p=0.03
n=25 R=0.481 p=0.01

F — % of divided cells
n=30 R=0.482 p=0.007
n=27 R=0.574 p=0.002
n=30 R=0.527 p=0.003
n=28 R=0.391 p=0.04
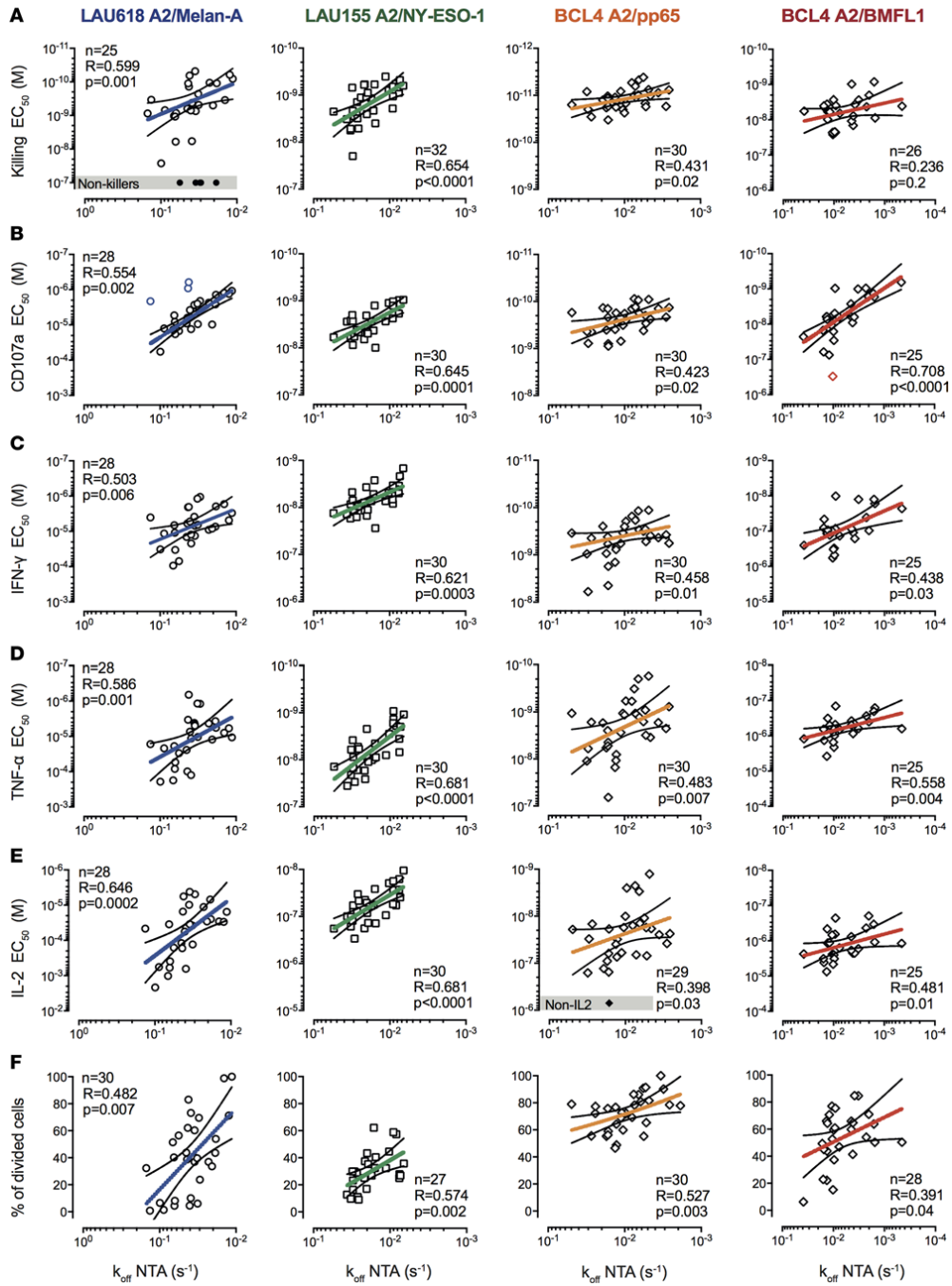
x-axis: k_{off} NTA (s^{-1})

50

JCI insight

Figure 1. Relationship between TCR dissociation rates and functional avidity of self/tumor– and virus-specific CD8+ T cell clones. Correlations between EC_{50} values from (**A**) killing, (**B**) CD107a degranulation, (**C**) IFN-γ–, (**D**) TNF-α–, and (**E**) IL-2–production titration assays and NTAmer-derived TCR dissociation rates (k_{off}). (**F**) Correlations between percentages of proliferating cells upon antigen-specific stimulation and NTAmer-derived TCR dissociation rates (k_{off}). (**A–F**) Antigen-specific CD8+ T cell clones were generated upon direct ex vivo sorting from effector-memory (EM)/CD28+/− and/or EMRA/CD28− subsets. Each data point represents an A2/Melan-A$_{26-35}$– (derived from patient LAU618, ○), A2/NY-ESO-1$_{157-165}$– (patient LAU155, □), A2/pp65$_{495-504}$–, or A2/BMFL1$_{259-267}$– (healthy donor BCL4, ◊) specific individual T cell clone. Nonfunctional clones are represented in gray boxes. The number of clones displaying function *n*, as well as Spearman's correlation (2 tailed, α = 0.05) coefficients *R* and *P* values are indicated. Color-coded and black lines are indicative of regression fitting and 95% confidence intervals, respectively. Of note, only very low numbers of outliers were identified when applying the ROUT method and are highlighted in color (71). The representative TCR-BV-CDR3 clonotype diversity of each antigenic specificity was LAU618/Melan-A, 77%; LAU155/NY-ESO-1, 43%; BCL4/pp65, 57%; and BCL4/BMFL1, 67%.

tions of human recombinant IL-2 to enhance the T cell antitumor efficacy (Figure 4D). In line with the observations made on Melan-A$_{26-35}$–specific T cells, NY-ESO-1$_{157-165}$–specific CD8+ T cell clones of slow TCR-pMHC off-rates provided a significant delay in tumor growth in comparison to the clones with fast off-rates (Figure 4E). Finally, we monitored the peripheral persistence of NY-ESO-1$_{157-165}$–specific T cells at days 2 and 14 following adoptive transfer. Analysis of tail bleeds taken at day 2 revealed that there was a significantly improved engraftment of slow off-rate T cell clones compared with fast off-rate T cell clones (Figure 4F). Yet, tumor-specific T cells did not persist beyond 14 days after T cell transfer (data not shown), in line with a previous report (35). In summary, these data provide further evidence that the TCR-pMHC off-rate represents an excellent biomarker to predict the immunotherapeutic potential of tumor-specific CD8+ T cells, and could therefore be selectively used to enhance the efficacy of adoptive T cell therapy (27).

TCR-pMHC off-rates vary according to the antigenic specificity of CD8+ T cells. Only limited information is available on the overall quality of TCR-pMHC binding avidity of self/tumor–specific versus non–self/pathogen–specific CD8+ T cell repertoires (36, 37). To address this point, we performed a comprehensive analysis of TCR-pMHC off-rates on 414 EM CD8+ T cell clones specific for (a) the differentiation antigen A2/Melan-A$_{26-35}$, (b) the cancer testis antigen A2/NY-ESO-1$_{157-165}$, (c) the viral CMV/pp65$_{495-504}$ antigen, and (d) the viral EBV/BMFL1$_{259-267}$ antigen isolated from 5 melanoma patients and 2 healthy donors (Figure 5, A and B, and Supplemental Figure 6, A and B). TCR-pMHC off-rate repertoires varied according to the T cell antigenic specificity. As such, A2/Melan-A$_{26-35}$–specific CD8+ T cells displayed significantly faster TCR-pMHC off-rates than the A2/NY-ESO-1$_{157-165}$–specific ones. Moreover, both tumor-specific TCR repertoires exhibited significantly faster TCR-pMHC off-rates than repertoires specific for herpes virus antigens (A2/pp65$_{495-504}$ and A2/BMFL1$_{259-267}$). Due to the presence of highly frequent TCR clonotypes potentially biasing the NY-ESO-1– and CMV-specific and to a lesser extent the EBV- and Melan-A–specific CD8+ T cell repertoires (38–40), we performed an extensive TCR-BV-CDR3 clonotyping of 353 EM CD8+ T cell clones (Figure 5C and Supplemental Table 1). We identified 143 individual clonotypes (specific for A2/Melan-A– and A2/NY-ESO-1–tumor antigens, and A2/pp65– and A2/BMLF1–viral epitopes), representing approximately 40% of the clonotype diversity, and depending on the antigenic specificity (Melan-A$_{26-35}$ > EBV/BMFL1$_{259-267}$ > NY-ESO-1$_{157-165}$ and CMV/pp65$_{495-504}$). The same TCR-pMHC off-rate hierarchy (virus-specific > self/tumor–specific CD8+ T cells) was observed when considering all CD8+ T cell clones (Figure 5B) or only the individual TCR clonotypes (Figure 5C). Finally, similar differences were obtained when the CD8+ T cell clones were subdivided according to their ex vivo differentiation status (early-differentiated EM/CD28+ or late-differentiated EM/EMRA/CD28−; Supplemental Figure 6C).

The differences found between A2/Melan-A$_{26-35}$–specific and A2/NY-ESO-1$_{157-165}$–specific repertoires may result from the fact that the A2/Melan-A$_{26-35}$–specific clones were derived following peptide vaccination in combination with CpG and incomplete Freund's adjuvant (IFA) adjuvant (41), when compared with the NY-ESO-1 repertoire obtained from patients with naturally occurring T cell responses. Thus, we investigated the quality of the natural A2/Melan-A$_{26-35}$–specific CD8+ T cell repertoires found in unvaccinated melanoma patients (*n* = 2), as well as in A2-positive and A2-negative individuals without melanoma (*n* = 4), known to express an unusually large peripheral repertoire of naive (CD45RA+CCR7+) A2/Melan-A$_{26-35}$–reactive CD8+ T cells (42). Unvaccinated patients exhibited differentiated A2/Melan-A$_{26-35}$–specific T cell repertoires of significantly faster off-rates when compared with the ones derived from vaccinated melanoma patients (Figure 5D). Strikingly, similar rapid off-rates were observed for the CD45RA+CCR7+ naive-specific T cell repertoires derived from unvaccinated patients as well as from A2-positive and A2-negative healthy individuals. These observations reveal the overall inferior quality of the TCR-pMHC binding repertoires specific for the self–A2/Melan-A$_{26-35}$ epitope, when compared with the ones specific for the cancer testis A2/NY-ESO-1 or viral
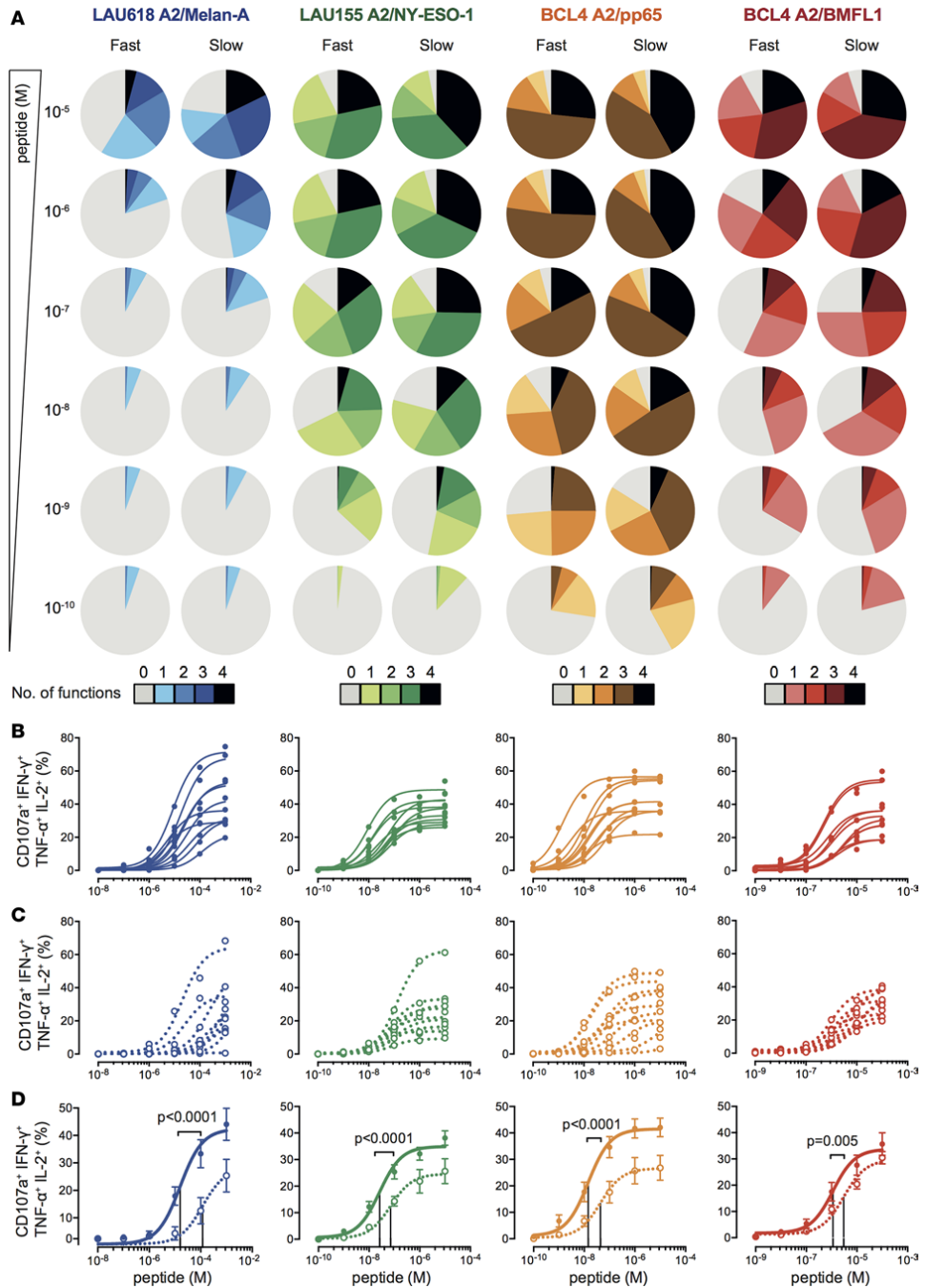
Figure 2. Relationship between TCR dissociation rates and polyfunctionality of self/tumor– and virus-specific CD8+ T cell clones. (A) CD107a, IFN-γ, TNF-α, and IL-2 coexpression titration assays of A2/Melan-A$_{26-35}$– (derived from patient LAU618), A2/NY-ESO-1$_{157-165}$– (patient LAU155), A2/pp65$_{495-504}$–, or A2/BMFL1$_{259-267}$– (healthy donor BCL4) specific clones with slow (n = 10) or fast (n = 10) TCR off-rates. Pie arcs depict the average fraction of cells displaying 0 to 4 functions. **(B** and **C)** Individual and **(D)** average ± SEM polyfunctional (coexpression of CD107a, IFN-γ, TNF-α, and IL-2) titration curves obtained for A2/Melan-A$_{26-35}$– (derived from patient LAU618), A2/NY-ESO-1$_{157-165}$– (patient LAU155), A2/pp65$_{495-504}$–, or A2/BMFL1$_{259-267}$– (healthy donor BCL4) specific clones with slow (n = 10, plain symbols and solid lines) or fast (n = 10, empty symbols and dotted lines) TCR off-rates. Vertical lines indicate EC$_{50}$ values. The P values were determined by the extra sum-of-squares F test (α = 0.05). The representative TCR-BV-CDR3 clonotype diversity of each antigenic specificity was LAU618/Melan-A, 80%; LAU155/NY-ESO-1, 45%; BCL4/pp65, 65%; and BCL4/BMFL1, 80%.

antigens. Yet, several clones with slower off-rates could still be detected, indicating the presence of rare self/Melan-A–specific T cells of high binding avidity within the endogenous unvaccinated repertoire. Finally, our data show that higher-avidity T cells can be selected following therapeutic vaccination, emphasizing the relevance of therapeutic vaccination approaches in enhancing the quality of a tumor-specific repertoire.

TCR-pMHC off-rate is a stable and robust biomarker independent of the activation state of the T cell. CD8+ T cell functional avidity represents a biological readout that is potentially influenced by multiple factors, such as TCR-pMHC binding avidity, TCR and CD8 surface expression, as well as various molecules regulating TCR signaling and T cell function (10). In that regard, the TCR-pMHC off-rate may provide a more reliable biophysical parameter than the widely used functional-related methods to assess T cell potency. To investigate this question, we first compared the variations obtained following separate experimental measurements (n = 4 to 9) of TCR-based dissociation rates, multimer staining intensity levels, and EC$_{50}$ killing avidity of 12 representative Melan-A–specific CD8+ T cell clones. For each individual clone, the interexperimental off-rate values nicely clustered together, in sharp contrast to the repeat multimer staining and functional avidity experiments showing large disparities (Figure 6, A–C). Furthermore, the average dissociation rates of these clones strongly correlated with average EC$_{50}$ killing avidity, but not with average multimer staining intensity (Supplemental Figure 7A). Finally, no correlation was found between functional avidity and multimer staining levels, in agreement with previous reports (reviewed in ref. 26). We next performed longitudinal measurements of TCR-pMHC off-rates and EC$_{50}$ killing avidity on a representative panel of A2/Melan-A$_{26-35}$–specific CD8+ T cell clones following nonspecific in vitro stimulation with phytohemagglutinin (PHA) and feeder cells (Supplemental Figure 7, B and C). We observed a remarkable stability of TCR-pMHC off-rate measurements upon stimulation, even when tested at a 6-month interval on T cell clones that underwent several additional rounds of PHA/feeder expansion (Figure 6D). In contrast and as previously described (43), for a given T cell clone, the killing avidity greatly varied and was augmented up to 10-fold, according to the time elapsed since the last stimulation (Figure 6E). These data indicate that the functional avidity reflects the in vitro activation status of CD8+ T cells, in line with the upregulation of cell-surface expression of TCRαβ, CD8αβ, and VLA-1 integrin, and conversely the downregulation of VLA-4 integrin and several coinhibitory receptors such as CD5, LAG-3, and TIGIT or the costimulatory receptor CD28 (Figure 6F). Importantly, the TCR-pMHC binding off-rate measurement is independent of TCRαβ levels, and stands out as a more stable and reliable biomarker than the usually performed assessments of multimer staining levels (i.e., mean fluorescence intensity) or EC$_{50}$ functional avidity.

Discussion

Several observations support the importance of considering both quantitative (i.e., magnitude of response) and qualitative (i.e., functional avidity, polyfunctionality) determinants of the T cell response, in order to predict in vivo efficacy (reviewed in ref. 10). However, ex vivo functional avidity or EC$_{50}$ (using titrated functional assays) and polyfunctionality assessments remain laborious and time consuming, and are often not possible because relatively large cell numbers must be withdrawn from patients. Importantly, and as shown in the current study, EC$_{50}$ values largely depend on the T cell's activation state, and are thus influenced by intraexperimental (i.e., over-time experimental measurements following T cell stimulation) and interexperimental (i.e., separate experimental measurements) variability/fluctuations (Figure 6). Moreover, functional avidity varies greatly depending on the functional readouts (e.g., cytotoxicity versus cytokine production), which mostly reflects modulation of the function-specific activation thresholds (cytotoxicity < cytokine production) (Figure 1 and Supplemental Figure 4A). Taken together, these observations show that there is a strong need to identify a T cell–based biomarker that overcomes the major limitations associated with functional assays and provides a reliable, simple-to-use, amenable-to-standardization immune metric for immunotherapy of cancer or chronic microbial infections.
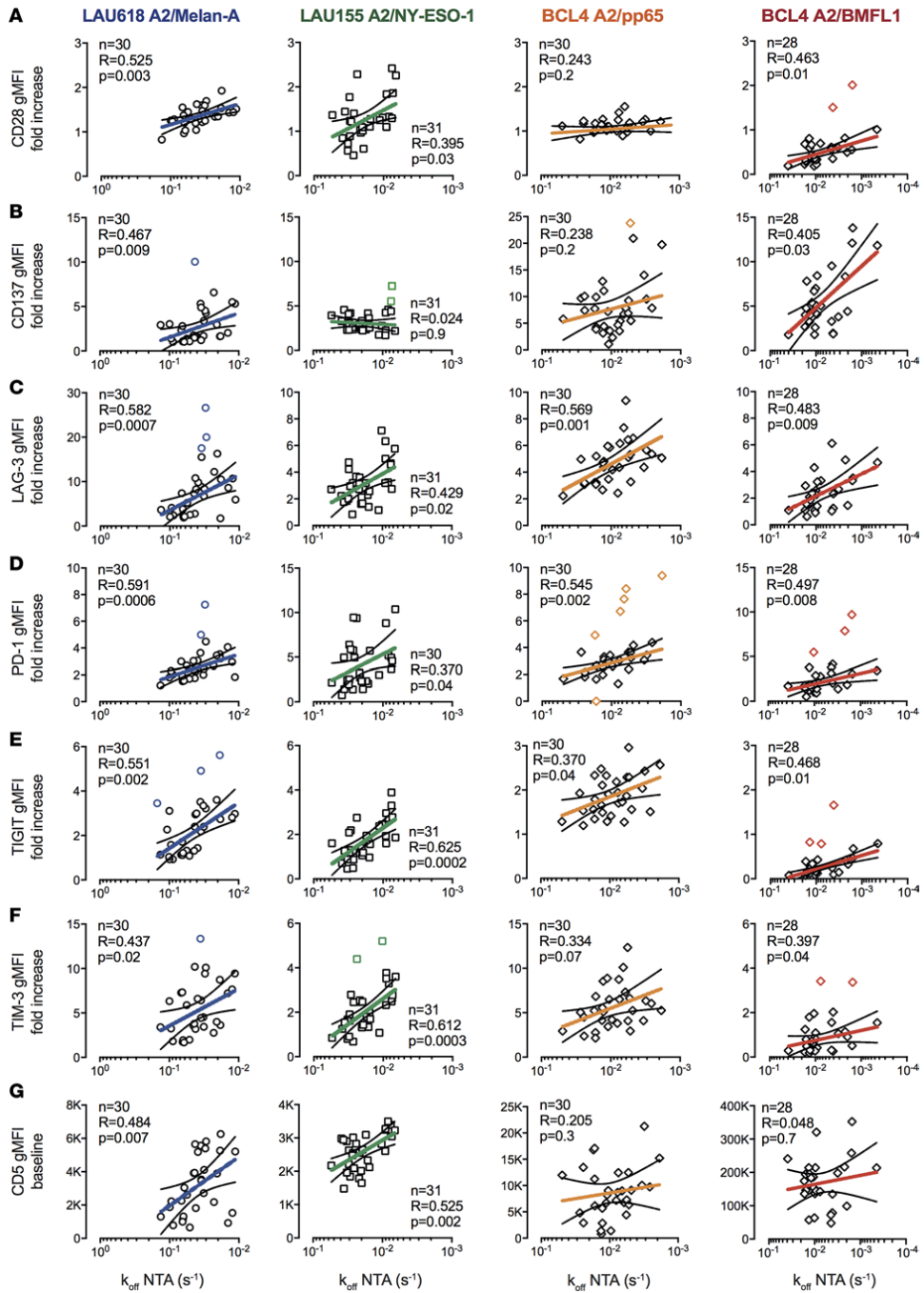
Figure 3. Relationship between TCR dissociation rates and activating/inhibitory receptor expression of self/tumor– and virus-specific CD8⁺ T cell clones. Correlations between fold increases in surface expression of (**A**) CD28, (**B**) CD137, (**C**) LAG-3, (**D**) PD-1, (**E**) TIGIT, and (**F**) TIM-3 upon antigen-specific stimulation and NTAmer-derived TCR dissociation rates (k_{off}). (**G**) Correlations between baseline surface expression levels (geometric mean fluorescence intensity [gMFI]) of CD5 and NTAmer-derived TCR dissociation rates (k_{off}). (**A–G**) Each data point represents an A2/Melan-A$_{26-35}$– (derived from patient LAU618, ○), A2/NY-ESO-1$_{157-165}$– (patient LAU155, □), A2/pp65$_{495-504}$– or A2/BMFL1$_{259-267}$– (healthy donor BCL4, ◊) specific individual T cell clone. The number of clones tested n, as well as Spearman's correlation (2 tailed, $\alpha = 0.05$) coefficients R and P values are indicated. Color-coded and black lines are indicative of regression fitting and 95% confidence intervals, respectively. Outliers were determined by the ROUT method and are highlighted in color (71). The representative TCR-BV-CDR3 clonotype diversity of each antigenic specificity was LAU618/Melan-A, 77%; LAU155/NY-ESO-1, 43%; BCL4/pp65, 57%; and BCL4/BMFL1, 67%.

Here, using an extensive and representative panel of antigen-specific CD8⁺ T cells generated in the context of natural or postvaccination immune responses, we show that the TCR-ligand dissociation rate globally correlated to all aspects of CD8⁺ T cell functions tested (i.e., cytotoxic activity, CD107a degranulation, cytokine production, proliferation and coreceptor modulation; Figures 1 and 3), including polyfunctionality (Figure 2) of both self/tumor– and virus-specific CD8⁺ T cells. Nonetheless, virus-specific T cells displayed weaker, although statistically significant correlations, than tumor-specific T cells, which may in part be the consequence of their overall slower TCR off-rates. These data nicely fit with the model proposing that enhanced TCR affinity or off-rate correlates with improved T cell responsiveness, but that this correlation is no longer linear above a certain TCR binding avidity threshold (reviewed in ref. 26). Specifically, using artificial affinity-enhanced TCRs, several reports (30, 44, 45) have shown that maximal T cell responsiveness occurs within an optimal window of TCR-pMHC binding interactions, usually lying in the upper physiological affinity range (K_D between 10 and 1 μM), and encompassing naturally occurring non–self/virus–specific TCR repertoires (36, 37). Moreover, the monomeric TCR-pMHC off-rate also predicted the relative tumor control activity in vivo (Figure 4). Importantly, as a biophysical readout, the TCR-pMHC off-rate represents a more stable and robust parameter of T cell potency, compared with the fluctuating biological metrics, such as T cell functional avidity or multimer-staining levels, which instead depend on the activation status of the cell (Figure 6). Our observations are in agreement with other studies showing that functional avidity is not a constant parameter in individual T cell clones, but gradually increases with time after in vitro restimulation (43, 46) or during the early course of acute viral infection in vivo (47). Enhanced antigen sensitivity is notably influenced by the differential expression of TCRαβ and accessory molecules (i.e., increased CD8αβ and VLA-1 versus reduced CD28, LAG-3, and TIGIT expression) (Figure 6). Altogether, our data show that the TCR-pMHC off-rate stands out as a major and stable determinant of CD8⁺ T cell function, allowing the accurate monitoring of the quality of naturally occurring or vaccination-induced self/tumor–specific T cell responses, but also for identifying the most potent CD8⁺ T cells for adoptive transfer therapy.

Thus far, a debate remains regarding which parameter(s) of the TCR-pMHC interactions (e.g., K_D, k_{off}, k_{on}) could better predict T cell activation and subsequent response potency. Several studies reported that the dissociation rate (k_{off}) was the most significant factor (27, 45), whereas others proposed that the dissociation constant K_D was the preeminent correlate of T cell responsiveness (44, 48). However, the association rate parameter, k_{on}, may also contribute to the response potency (49, 50). In that regard, Aleksic et al. (51) and Govern et al. (52) proposed that these apparently contradictory observations might in fact reflect the impact of fast versus slow association rates on the TCR-pMHC binding duration. Indeed, at the cell interface, fast k_{on} rates would allow rapid rebinding of the same TCR-ligand complex after dissociation, resulting in enhanced effective dissociation half-lives. Molecular TCR-pMHC binding interactions are usually assessed by surface plasmon resonance (SPR) measurements in solution (3D binding), which fail to take into account the k_{on}-associated rapid rebinding effect of the TCR to the same pMHC. The NTAmer-based approach deviates in that regard from SPR measurements. Using a panel of CD8⁺ T cells engineered to express TCR variants of increasing affinities for pMHC, we previously observed that TCRs with fast k_{on} had prolonged NTAmer-based dissociation half-lives compared with those with slow k_{on} (28). Thus, NTAmers may somehow reflect additional membrane-associated kinetic aspects (i.e., impact of rebinding and CD8 coreceptor), which are typically integrated by the 2D surface–based kinetic analyses (reviewed in ref. 53). Despite its current limitations (T cell cloning requirement, no direct k_{on} readouts), the NTAmer technology allows for rapid and accurate real-time off-rate measurements of large panels of naturally occurring antigen-specific CD8⁺ T cells that may display a broad range of TCR-pMHC affinities, including weak interactions (refs. 28, 29, and current study). Finally, a tight correlation between TCR off-rates and T cell antigenic sensitivity was not always observed, and notably depended on the antigenic specificity of the cells, but
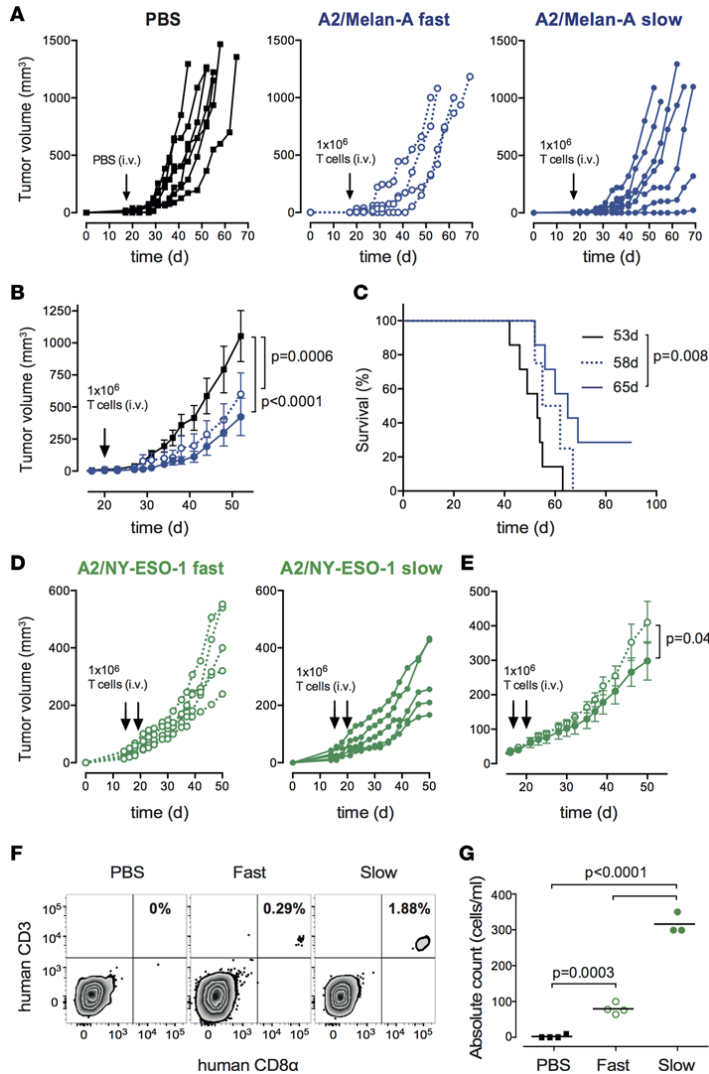
Figure 4. Relationship between TCR dissociation rates and tumor control in immunodeficient mice upon adoptive T cell transfer. (**A**) Individual or (**B**) average ± SEM tumor growth and (**C**) Kaplan–Meier survival curves of tumor-bearing NSG mice adoptively transferred with PBS (control, $n = 7$; black solid lines) or $1 × 10^6$ A2/Melan-A$_{26-35}$–specific T cell clones with fast ($n = 4$; blue dotted lines) or slow ($n = 7$; blue solid lines) TCR off-rates. (**D**) Individual or (**E**) average ± SEM tumor growth curves of tumor-bearing NSG mice adoptively transferred twice with $1 × 10^6$ A2/NY-ESO-1$_{157-165}$–specific T cell clones with fast ($n = 5$; green dotted lines) or slow ($n = 5$; green solid lines) TCR off-rates. Tumor volume and survival curve P values were determined by 2-way ANOVA and log-rank tests, respectively. (**F**) Representative staining and (**G**) absolute counts of human CD8+ T cells from blood taken from tail veins at day 2 following adoptive transfer of $4 × 10^6$ A2/NY-ESO-1$_{157-165}$–specific CD8+ T cell clones with fast ($n = 4$; green empty circles) or slow ($n = 3$; green full circles) TCR off-rates. As control, 3 mice received PBS ($n = 4$; black squares). P values were determined by 1-way ANOVA multiple comparison tests.

also on the T cell functional readout (Figures 1 and 3). However, robust statistical evaluation did not identify consistent outlier clones (i.e., the same clone that behaved as an outlier in one functional assay was not an outlier in the other functional assays). Thus, the few outlier data that we observed might best be explained by the variability/fluctuations related to biological measures (Figure 6), yet we cannot entirely exclude an impact of the k_{on} parameter, possibly influencing T cell responsiveness (49, 50). In-depth k_{on} evaluation of such exceptions would be highly useful, although only feasible once novel technologies that can interrogate all TCR-pMHC binding parameters directly on living T cells become available.

Extending previous studies showing a positive correlation between PD-1 expression and TCR-pMHC avidity (30) or functional avidity (31), NTAmer-based off-rates nicely predicted the upmodulation of both costimulatory (CD28, 4-1BB) and coinhibitory (PD-1, LAG-3, TIM-3, TIGIT) receptors upon antigen-specific stimulation (Figure 3). Thus, our results indicate that T cells of higher binding avidity are more susceptible to activation and
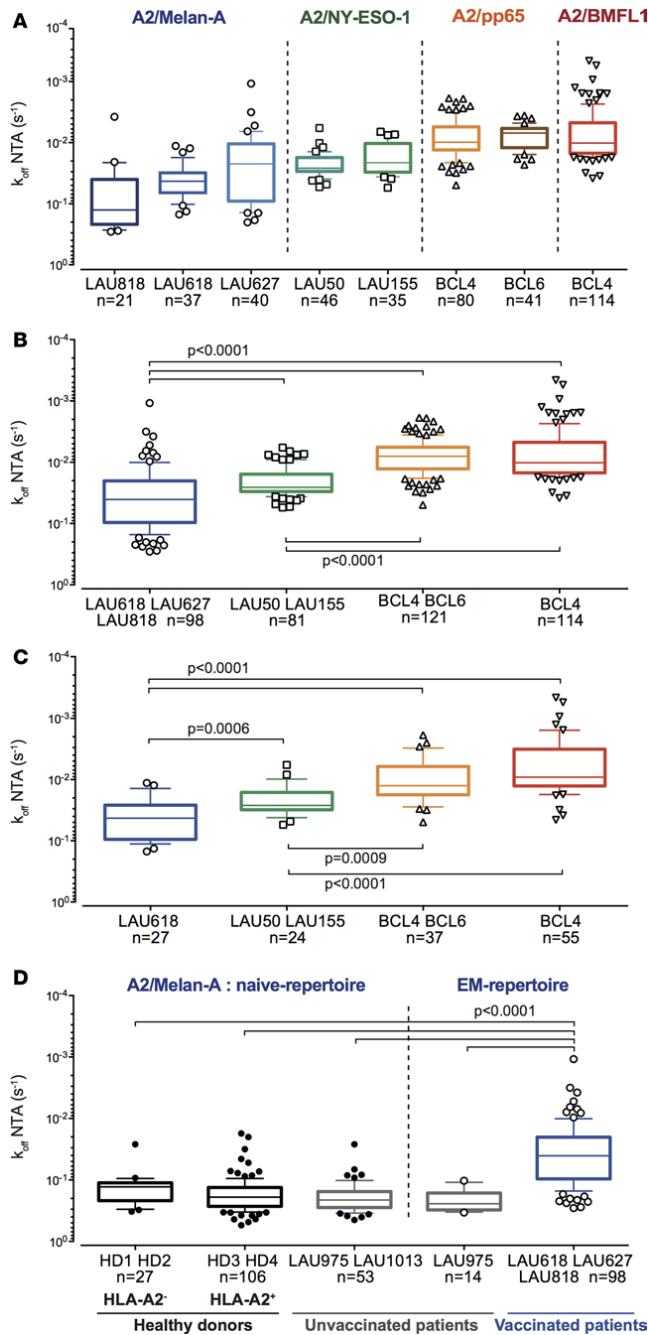
Figure 5. TCR dissociation rates according to the antigenic specificity, clonotype repertoire, and ex vivo differentiation status of CD8+ T cell clones. (A and B) NTAmer-derived TCR dissociation rates (k_{off}) of EM/EMRA CD28+/− clones (n = 414) specific for the differentiation antigen A2/Melan-A$_{26-35}$ (derived from melanoma patients LAU618, LAU627, and LAU818 following vaccination with Melan-A/peptide, incomplete Freund's adjuvant, and CpG), the cancer testis A2/NY-ESO-1$_{157-165}$ (from patients LAU50 and LAU155 with naturally occurring T cell responses), or the persistent herpes viruses A2/pp65$_{495-504}$ or A2/BMFL1$_{259-267}$ (from healthy donors BCL4 and BCL6), categorized according to (**A**) the respective patients and donors or (**B**) antigenic specificity. (**C**) NTAmer-derived TCR dissociation rates (k_{off}) of individual TCR-BV-CDR3 clonotypes specific for the tumor epitopes A2/Melan-A$_{26-35}$ (n = 27) and A2/NY-ESO-1$_{157-165}$ (n = 24), and the persistent herpes virus epitopes A2/pp65$_{495-504}$ (n = 37) and A2/BMFL1$_{259-267}$ (n = 55). (**D**) NTAmer-derived TCR dissociation rates (k_{off}) of A2/Melan-A$_{26-35}$–specific clones derived from HLA-A2–negative (HD1 and HD2), HLA-A2–positive (HD3 and HD4) healthy donors, HLA-A2–positive unvaccinated (LAU975 and LAU1013) and A2/Melan-A$_{26-35}$–vaccinated (LAU618, LAU627, and LAU818) melanoma patients, categorized according to the patient/donor groups and the differentiation status of T cell clones. (**A–D**) Data are depicted as box (25th to 75th percentiles) and whisker (10th to 90th percentiles) with the middle line representing the median. Numbers of clones n, as well as Kruskal-Wallis test (α = 0.05) derived P values are indicated. Significant differences between the A2/Melan-A$_{26-35}$– and the A2/NY-ESO-1$_{157-165}$–specific groups were obtained by Mann-Whitney test (2 tailed).
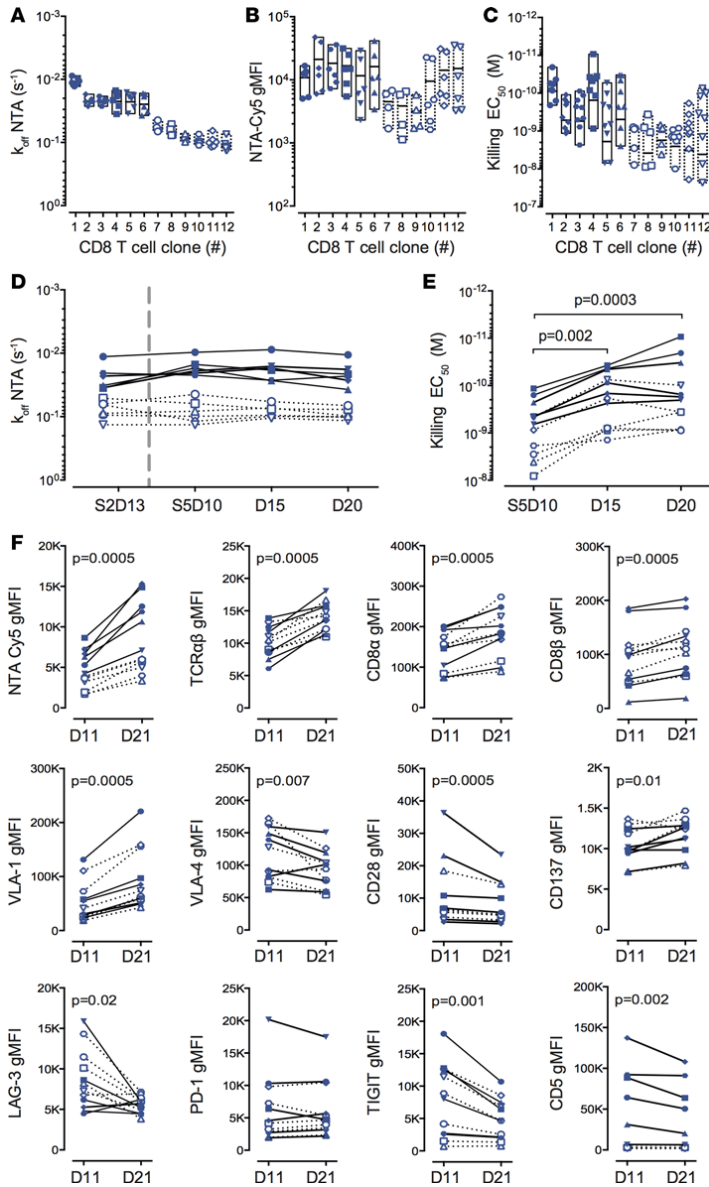
Figure 6. Interexperimental and over-time variations of TCR dissociation rates, pMHC multimer staining, and functional avidity assays. (**A**) NTAmer-derived TCR dissociation rates (k_{off}), (**B**) NTAmer surface staining levels (geometric mean fluorescence intensity [gMFI]) and (**C**) killing avidity values (EC_{50}) obtained in independent assays ($n > 4$) for A2/Melan-A$_{26-35}$–specific CD8$^+$ T cell clones with slow ($n = 6$, plain symbols and solid lines) or fast ($n = 6$, empty symbols and dotted lines) TCR off-rates. (**A**–**C**) Data are depicted as individual values and boxes (minimum to maximum, with the middle line representing the mean). (**D**) NTAmer-derived TCR dissociation rates (k_{off}), (**E**) killing avidity values (EC_{50}), and (**F**) surface staining levels (gMFI) obtained over time (D10/11, D15, and D20/21; D = day) following nonspecific stimulation (by PHA and irradiated feeder cells) for A2/Melan-A$_{26-35}$–specific T cell clones with slow ($n = 6$, plain symbols and solid lines) or fast ($n = 6$, empty symbols and dotted lines) TCR off-rates. S2 represents the off-rate measurements of the same clones 6 months before the fifth round of stimulation (S5). The P values were determined by the Friedman ($\alpha = 0.05$) and Wilcoxon matched-pair signed-rank (2-tailed) tests.

subsequent upregulation of activating/inhibitory receptors than lower-avidity ones. Expression of inhibitory receptors such as PD-1 is usually considered a hallmark of T cell exhaustion in chronic infection and cancer, and consequently high-avidity T cells may be more prone to functional impairment. However, Odorizzi et al. (54) recently found that genetic absence of PD-1 on CD8$^+$ T cells does not prevent exhaustion during chronic LCMV infection. Instead, PD-1 also plays a critical role in protecting T cells from overstimulation, excessive proliferation, and terminal differentiation (54), and identifies highly reactive antitumor T lymphocytes (55). Moreover,

58

JCI insight

T cell differentiation and activation are major drivers of inhibitory receptor expression (56). In line with these observations, the extent of coreceptor upmodulation observed following stimulation (Figure 3) likely reveals the overall antigen sensitivity of the T cells, which is mostly driven by TCR-pMHC binding avidity.

Another major finding is that the TCR-pMHC dissociation rate parameter allows the direct comparison across various antigen-specific T cell repertoires, in contrast to functional assays. The latter ones rely on the stability of the pMHC complexes, which is not the case for monomeric TCR-pMHC dissociation experiments. Indeed, the stability of peptide binding to MHC may highly vary between different antigens even when presented by the same HLA-A*0201 molecule. This may help explaining why direct comparisons of in vitro functional avidities (i.e., EC_{50}) between tumor- and virus-specific T cell clones, or between Melan-A$_{26-35}$ and NY-ESO-1$_{157-165}$ or CMV/pp65$_{495-504}$ and EBV/BMFL1$_{259-267}$ specificities show such divergent differences (Figure 1 and Supplemental Figure 4B). For instance, Melan-A– and EBV-specific T cell clones generally exhibit the lowest EC_{50} functional avidities, whereas NY-ESO-1– and CMV-specific T cell clones share the highest ones. In contrast, this is no longer an issue for the off-rate measurements, which rely by definition on the dissociation rate between the TCR and a given pMHC complex at the monomeric level. Consequently, we were able to directly compare large T cell clonotype repertoires ($n > 300$) across 4 different antigenic specificities and confirm strong binding differences between self/tumor and virus-specific CD8$^+$ T cells (Figure 5 and refs. 36, 37). Specifically, virus-specific CD8$^+$ T cell repertoires were endowed with longer TCR-pMHC dissociation rates than self/tumor–specific ones. These data nicely support the concept that many tumor antigens are in fact self-antigens, and consequently mechanisms of central and peripheral tolerance shape the self/antigen-specific repertoires towards lower TCR avidities by removing high-avidity self-reactive T cells (23, 57).

Fluorochrome-conjugated pMHC reagents are widely used for the detection and analysis of antigen-specific CD8$^+$ T cells. Various reports have previously shown that certain functional antigen-specific CD8$^+$ T cells fail to bind tetrameric MHC ligands, which could represent up to several percent of the CD8$^+$ T cell subset (58–60). Moreover, this is of particular importance when staining tumor-specific CD8$^+$ T cells, known to express lower TCR-pMHC affinity/avidity repertoires than virus-specific cells (Figure 5 and refs. 36, 37). We therefore used pMHC multimer and NTAmer molecules to detect tumor-specific CD8$^+$ T cells, which consistently displayed higher sensitivity than Streptamers or pentamers (Supplemental Figure 1A) or pMHC tetramer molecules (data not shown). However, we cannot entirely exclude that a sizeable fraction of antigen-specific T cells may not be stained by these higher-sensitivity tools and may therefore be ignored in our experimental setting.

The Melan-A/MART-1$_{26-35}$ antigenic peptide is among the best-studied human tumor–associated antigens. We have previously documented that the frequency of naive A2/Melan-A$_{26-35}$–specific CD8$^+$ T cells is unusually high, because of the large numbers selected in the thymus (42). A recent study reported that medullary thymic epithelial cells express a truncated *Melan-A* transcript, which precludes clonal deletion (central tolerance) to this antigen due to the lack of the expression of the immunodominant 26–35 epitope (61). Another interesting explanation might lay in the impact of certain germ line TCR gene segments, notably the *TRAV12-2* gene dominant in the Melan-A antigen–specific T cell repertoire, on contributing substantial binding affinity for the HLA-A2/Melan-A$_{26-35}$ complex (62). One additional plausible cause of the presence of this large Melan-A$_{26-35}$–reactive T cell repertoire is that it could be positively selected through the recognition of unknown Melan-A cross-reactive peptides expressed in the thymus (63, 64). Here, we found that naive Melan-A$_{26-35}$–reactive repertoires isolated from either healthy individuals or unvaccinated melanoma patients depicted an overall poor TCR binding avidity, when compared with the primed repertoires from vaccinated patients (Figure 5). Thus, our observations are compatible with central tolerance mechanisms, possibly involving other cross-reactive self-antigens, and restricting the Melan-A$_{26-35}$–reactive T cell repertoire to the lower-avidity range. Yet, although rare, our large-scale study could identify few self/Melan-A$_{26-35}$–specific naive CD8$^+$ T cells of higher binding avidities within healthy individual's and patient's repertoires, extending and refining prior studies performed using conventional pMHC class-I fluorescent multimers (65). Therefore, it is possible that therapeutic vaccination allows for the selection and expansion of a wide Melan-A–reactive TCR avidity repertoire, which includes highly specific T cells sharing similar binding avidities to those present in the cancer testis A2/NY-ESO-1–specific repertoire.

Finally, our results highlight the importance of optimizing the choice of tumor antigens for the development of cancer-based immunotherapies. Notably, it remains to be determined whether T cell repertoires targeting tumor-derived neoantigens can display greater TCR-pMHC binding avidities than self/tumor–antigen ones, since neoantigen-specific T cells are more likely to escape thymic negative selection (66). It is tempting to speculate that potent neoantigen-specific CD8$^+$ T cells would display TCR off-rates of a magnitude closer to the kinetics of virus-specific CD8$^+$ T cells shown in this study.

JCI insight

Large-scale ex vivo assessment of TCR-pMHC binding kinetics was until recently technically challenging, underestimating the overall impact and clinical relevance of this biophysical parameter in the context of antigen-specific CD8+ T cell repertoires. Based on monomeric TCR-pMHC off-rate measurements (i.e., NTAmers), we here demonstrated that the k_{off} parameter represents a powerful biomarker to characterize in vitro and in vivo CD8+ T cell potency within antigen-specific CD8+ T cell responses. Yet, robust techniques allowing for the rapid identification and isolation of CD8+ T cells of highest avidity and functions directly ex vivo from tissues or blood samples and at the single-cell level are still required. In that regard, Nauerth and colleagues (67) proposed that small polyclonal virus-specific CD8+ T cell populations could be analyzed directly ex vivo without the need of previous TCR cloning or T cell sorting. The recent implementation of an ex vivo platform allowing for the single-cell serial determination of 2D TCR-pMHC affinity (based on micropipette adhesion frequency) and TCR clonotyping is also highly promising (68). In conclusion, recent technological breakthroughs now enable the rapid development of TCR-pMHC binding kinetics–based simple assays as sensitive and reliable biomarkers of CD8+ T cell activity and clinical efficacy.

Methods

Patients, healthy donors, and ethics statement. Peripheral blood samples were collected from HLA-A*0201–negative (HD1 and HD2), HLA-A*0201–positive (HD3 and HD4), HLA-A*0201–positive and CMV/EBV chronically infected (BCL4 and BCL6) healthy donors (HDs) (39) and from HLA-A*0201–positive stage III/IV metastatic melanoma patients included in immunotherapy studies (patient LAU50, NCT00112242; patient LAU155, NCT00002669; and patients LAU975, LAU1013, LAU618, LAU627, and LAU818, NCT00112229; www.clinicaltrials.gov) (38, 41, 69). Patients LAU618, LAU627, and LAU818 received 8 to 12 monthly low-dose vaccinations injected s.c. with 100 μg high-affinity Melan-A$_{26–35}$ (A27L) analog peptide mixed with 0.5 mg CpG 7909/PF-3512676 (Pfizer and Coley Pharmaceutical Group) and emulsified in IFA (Montanide ISA-51, Seppic). Peripheral blood mononuclear cells (PBMCs) centrifuged in Ficoll-Hypaque (Pharmacia) were cryopreserved in 10% DMSO and stored in liquid nitrogen until further use.

Generation of antigen-specific CD8+ T cell clones. Thawed PBMCs were positively enriched using anti-CD8-coated magnetic microbeads (Miltenyi Biotec), stained in PBS, 0.2% BSA, and 5 mM EDTA with PE-labeled HLA-A*0201 multimers (loaded with analog Melan-A$_{26–35}$ (A27L), NY-ESO-1$_{157–165}$ (C165A), and EBV/BMFL1$_{259–267}$ (C260A), or native CMV/pp65$_{495–504}$ peptide) (TCMetrix Sàrl) at 4°C for 45 minutes, followed by cell surface markers (APC anti-CD28, FITC anti-CD45RA [BD Pharmingen], PE-Cy7 anti-CCR7 [BioLegend], and APC-A750 anti-CD8 [Beckman Coulter], Supplemental Table 2) at 4°C for 30 minutes. Cells were then sorted into defined differentiated subpopulations (naive, CD45RA+CCR7+CD28+; EM, CD45RA−CCR7−CD28+/−; or EMRA, CD45RA+CCR7−CD28−) of antigen-specific CD8+ T cells on a FACSAria (BD Biosciences) or Astrios (Beckman Coulter) flow cytometer. Sorted cells were cloned by limiting dilution in Terasaki plates and expanded in RPMI 1640 medium supplemented with 8% human serum, 150 U/ml human recombinant IL-2 (gift of GlaxoSmithKline), 1 μg/ml PHA (Sodiag), and 1 × 10⁶/ml 30-Gy-irradiated allogeneic PBMCs. The antigenic specificity of CD8+ T cell clones was controlled by HLA-A*0201/peptide multimer staining (TCMetrix Sàrl). Extensive TCR-BV-CDR3 clonotyping was performed on the T cells from patients LAU618, LAU155, and LAU50 and from healthy donors BCL4 and BCL6, as previously described (39), allowing selecting representative sets of dominant (with frequency > 5%) and nondominant TCR-BV-CDR3 clonotypes. Clonotype diversity varied from 43% to 80%, depending on the antigenic specificity (Melan-A$_{26–35}$ > EBV/BMFL1$_{259–267}$ > NY-ESO-1$_{157–165}$ and CMV/pp65$_{495–504}$) and is indicated throughout the manuscript.

NTAmer staining and dissociation kinetics measurements. The pMHC multimer and NTAmer molecules used in this study carry 8 to 12 pMHC monomers per conjugate, similarly to Dextramer molecules. Importantly, multimers and NTAmers provided a superior ex vivo detection of A2/Melan-A–specific CD8+ T cells from PBMCs of 2 melanoma patients, when compared with pentamers (5 pMHC monomers) or Streptamers (5–7 pMHC monomers) (Supplemental Figure 1A). NTAmers are dually labeled pMHC multimers built on NTA-Ni²⁺-His-tag interactions (70) and were used for dissociation kinetic measurements as described previously (28, 29). Briefly, individual antigen-specific CD8+ T cell clones were stained for 45 minutes at 4°C in PBS, 0.2% BSA, and 5 mM EDTA with antigen-specific NTAmers, in which the HLA-A*0201 molecules were loaded with the native Melan-A$_{26–35}$, NY-ESO-1$_{157–165}$, EBV/BMFL1$_{259–267}$, or CMV/pp65$_{495–504}$ peptide. Of note, Melan-A– and NY-ESO-1–specific T cells isolated from melanoma patients as well as EBV-specific T cells from healthy donor BCL4 were initially sorted with the analog-peptide multimers. Yet, all Melan-A–, NY-ESO-1–, and EBV-derived T cell clones presented a high degree

of cross-reactivity, since native-peptide NTAmers showed a comparable capacity to stably label each generated specific clone and thus should not have introduced a significant bias in the analysis. NTAmer staining was assessed at 4°C on a SORP-LSR II flow cytometer (BD Biosciences). Following 1 minute of baseline acquisition, imidazole (100 mM) was added and Cy5 fluorescence measured during the following 10 minutes. Data were analyzed using the kinetic module of FlowJo software (v.9.7.6, Tree Star) and modeled (1-phase exponential decay) using Prism software (v.6, GraphPad).

Chromium release cytolytic assay. Chromium release cytolytic assays were performed as previously described (13). Briefly, ^{51}Cr-labeled HLA-A*0201–positive TAP-deficient T2 cells were pulsed with serial dilutions of native Melan-A$_{26–35}$, NY-ESO-1$_{157–165}$, EBV/BMFL1$_{259–267}$, or CMV/pp65$_{495–504}$ peptides, and incubated with antigen-specific CD8$^+$ T cell clones at an E/T ratio of 10:1 for 4 hours. NY-ESO-1$_{157–165}$ and EBV BMFL1$_{259–267}$ peptides were preincubated for 1 hour at room temperature with 2 mM disulfide-reducing agent tris(2-carboxyethyl)phosphine (TCEP, Pierce Biotechnology). Percentages of specific lysis were calculated as 100 × (experimental – spontaneous release)/(total – spontaneous release). EC$_{50}$ and B$_{max}$ values were derived by dose-response curve analysis (log[agonist] versus response) using Prism software. Non–killer clones were defined as displaying a maximal lysis less than 25% and/or for which an EC$_{50}$ value could not be accurately determined. These non–killer clones were excluded from the statistical analyses.

CD107a degranulation and intracellular cytokine staining. HLA-A*0201–positive TAP-deficient T2 cells were pulsed 1 hour at 37°C with serial dilutions of the native Melan-A$_{26–35}$, NY-ESO-1$_{157–165}$, EBV/BMFL1$_{259–267}$, or CMV/pp65$_{495–504}$ peptides, washed, and incubated with antigen-specific CD8$^+$ T cell clones at an E/T ratio of 1:2 for 6 hours in the presence of FITC anti-CD107a (BD Pharmingen; Supplemental Table 2) and brefeldin A (10 μg/ml, Sigma-Aldrich). NY-ESO-1$_{157–165}$ and EBV BMFL1$_{259–267}$ peptides were preincubated for 1 hour at room temperature with the disulfide-reducing agent TCEP (2 mM). Cells were then stained in PBS, 0.2% BSA, 5 mM EDTA, and 0.2% NaN$_3$ with Pacific-Blue anti-CD8α (Beckman Coulter) at 4°C for 30 minutes, fixed in PBS 1% formaldehyde, 2% glucose, and 5 mM NaN$_3$ for 20 minutes at room temperature, and finally stained in PBS, 0.2% BSA, 5 mM EDTA, 0.2% NaN$_3$, and 0.1% saponin (Sigma-Aldrich) with PerCPCy5.5 anti–IL-2, APC anti–IL-13, PE-Cy7 anti–IFN-γ, A700 anti–TNF-α (BD Pharmingen; Supplemental Table 2), and PE anti–IL-4 (Biolegend) for 30 minutes at 4°C before acquisition on a Gallios (Beckman Coulter) flow cytometer. Percentages of CD107a/cytokine–positive T cells were analyzed using FlowJo software (v.10.0.7, Tree Star). EC$_{50}$ and B$_{max}$ values were derived by dose-response curve analysis (log[agonist] versus response) using Prism software. Non-cytokine clones were defined as displaying a maximal response less than 25% and for which an EC$_{50}$ value could not be determined accurately. These non-cytokine clones were not included in the statistical analyses. CD107a, IL-2, IFN-γ, and TNF-α coexpression were analyzed using SPICE software (v.5.35, National Institute of Allergy & Infectious Diseases).

Proliferation assay. 30-Gy-irradiated HLA-A*0201–positive PBMCs were pulsed 1 hour at 37°C with native Melan-A$_{26–35}$ (10 μM), NY-ESO-1$_{157–165}$ (1 μM), EBV/BMFL1$_{259–267}$ (1 μM), or CMV/pp65$_{495–504}$ (0.01 μM) peptides, washed, and incubated with CellTraceViolet-stained antigen-specific CD8$^+$ T cell clones (Thermo Fisher Scientific) at an E/T ratio of 1:2 in RPMI 1640 medium supplemented with 8% human serum and 50 U/ml human recombinant IL-2. NY-ESO-1$_{157–165}$ and EBV/BMFL1$_{259–267}$ peptides were preincubated for 1 hour at room temperature with the disulfide-reducing agent TCEP (2 mM). After 7 days, antigen-specific CD8$^+$ T cell clones were acquired on the Gallios flow cytometer. Percentages of divided cells were analyzed using the proliferation module of FlowJo software (v.9.7.6).

Surface marker expression/modulation assay. For coreceptor modulation assays, antigen-specific CD8$^+$ T cell clones were incubated for 24 hours in the absence or presence of HLA-A*0201 unlabeled tetramers loaded with native Melan-A$_{26–35}$ (1 μg/ml), NY-ESO-1$_{157–165}$ (1 μg/ml), EBV BMFL1$_{259–267}$ (0.1 μg/ml), or CMV pp65$_{495–504}$ (0.01 μg/ml) peptides. Cells were then stained in PBS, 0.2% BSA, 5 mM EDTA, and 0.2% NaN$_3$ with (a) A488 anti-PD1 (Serotec), PE-Cy7 anti-CD5 (BD Pharmingen), APC anti-TIGIT (eBioscience), and BrV421 anti-CD28 (Biolegend), or with (b) FITC anti–LAG-3 (Enzo), PE anti–TIM-3 (R&D Systems), and APC anti-CD137 (BD Pharmingen) at 4°C for 30 minutes and acquired on the Gallios flow cytometer. Marker expression (geometric mean fluorescence intensity [gMFI]) was analyzed using FlowJo software (v.10.0.7) and their modulation was calculated as (gMFI of stimulated cells)/(gMFI of un-stimulated cells).

For over-time expression assays, tumor-specific CD8$^+$ T cell clones were stimulated and expanded upon PHA and irradiated feeder cells, and stained over time (at day 10, 15, and 20) in PBS, 0.2% BSA, 5 mM EDTA, and 0.2% NaN$_3$ with FITC anti-CD8β, PE-Cy7 anti-CD8α, PE anti–pan-TCRαβ (Beckman Coulter), PE anti–VLA-1, PE-Cy7 anti-CD5, APC anti–VLA-4, APC anti-CD137, BrV421 anti-PD1

JCI INSIGHT

(BD Pharmingen), APC anti-TIGIT (eBioscience), BrV421 anti-CD28 (Biolegend), or FITC anti–LAG-3 (Enzo) at 4°C for 30 minutes, and acquired, using identical settings, on the Gallios flow cytometer. Supplemental Table 2 contains a detailed list and information of all antibodies used in this study.

Adoptive T cell transfer in immunodeficient mice. NSG (NOD.Cg-Prkdc^{scid} Il2rg^{tm1Wjl}/SzJ) mice (Jackson Laboratory, stock number 005557) were bred in a conventional animal facility at the University of Lausanne under specific pathogen–free status. Six- to nine-week-old female mice were anesthetized with isoflurane and subcutaneously injected with 1×10^6 A2/Melan-A$_{26–35}$–positive and A2/NY-ESO-1$_{157–165}$–positive human melanoma Me275 tumor cells (grown in DMEM medium supplemented with 10% FCS, and previously passed in NSG mice for A2/NY-ESO-1$_{157–165}$–specific experiments). Once the tumors became palpable (around day 14 to 20), 1×10^6 human tumor-specific CD8 T cell clones were injected intravenously in the tail vein. For A2/NY-ESO-1$_{157–165}$–specific experiments, 1×10^6 T cell clones were administrated twice at day 14 and day 21, followed by 3 daily subcutaneously injections of human recombinant IL-2 (3×10^4 U), starting at the day of T cell transfer. Tumor volumes were measured by caliper twice per week and calculated as follows: volume = length × width × width/2. Mice were sacrificed by CO_2 inhalation before the tumor volume exceeded 1,000 mm^3 or when necrotic skin lesions were observed at the tumor site. In separate experiments, we collected blood from tail veins at day 2 and 14 after infusion of 4×10^6 A2/NY-ESO-1$_{157–165}$–specific T cell clones and analyzed the frequency of persisting human CD8$^+$ T cells by flow cytometry. This study was approved by the Veterinary Authority of the Canton de Vaud (Permit number VD1850.5) and performed in accordance with Swiss ethical guidelines.

Statistics. Data were analyzed using Prism software (v.6, GraphPad) by nonparametric Spearman correlation, nonlinear regression (95% confidence intervals and 10% ROUT coefficient Q; see ref. 71), extra sum-of-squares F, Kruskal-Wallis, Mann-Whitney, Friedman, Wilcoxon-paired, 2-way ANOVA and log-rank tests. The associated P values (2-tailed and α = 0.05 when applicable), as well as numbers of experiments and sample sizes are indicated throughout.

Study approval. Study protocols were designed, approved, and conducted according to the relevant regulatory standards from (a) the ethical commission of the University of Lausanne (Lausanne, Switzerland), (b) the Protocol Review Committee of the Ludwig Institute for Cancer Research (New-York), and (c) Swissmedic (Bern, Switzerland). Healthy donors and patient recruitment, study procedures, and blood withdrawal were done upon written informed consent.

Author contributions

MA, JS, MH, and NR conceived and designed the study. MA, BC, LCI, MND, JS, GCM, PR, DES, and MH acquired data (provided animals, acquired and managed patients, provided facilities, etc.). MA, MH, and NR analyzed and interpreted data. MA, PR, DES, MH, and NR wrote and/or revised the manuscript. NR supervised the study.

Acknowledgments

Address correspondence to: Nathalie Rufer, Department of Oncology, Lausanne University Hospital (CHUV), Biopôle 3 - 02DB92, chemin des Boveresses 155, CH-1066 Epalinges, Switzerland. Phone: 41.21.692.59.77. Email: Nathalie.Rufer@unil.ch.

1. Speiser DE, Kyburz D, Stübi U, Hengartner H, Zinkernagel RM. Discrepancy between in vitro measurable and in vivo virus neutralizing cytotoxic T cell reactivities. Low T cell receptor specificity and avidity sufficient for in vitro proliferation or cytotoxicity to peptide-coated target cells but not for in vivo protection. *J Immunol*. 1992;149(3):972–980.
2. Alexander-Miller MA, Leggatt GR, Berzofsky JA. Selective expansion of high- or low-avidity cytotoxic T lymphocytes and efficacy for adoptive immunotherapy. *Proc Natl Acad Sci U S A*. 1996;93(9):4102–4107.
3. Gallimore A, Dumrese T, Hengartner H, Zinkernagel RM, Rammensee HG. Protective immunity does not correlate with the hierarchy of virus-specific cytotoxic T cell responses to naturally processed peptides. *J Exp Med*. 1998;187(10):1647–1657.

4. Zeh HJ, Perry-Lalley D, Dudley ME, Rosenberg SA, Yang JC. High avidity CTLs for two self-antigens demonstrate superior in vitro and in vivo antitumor efficacy. *J Immunol*. 1999;162(2):989–994.

5. Bullock TN, Mullins DW, Colella TA, Engelhard VH. Manipulation of avidity to improve effectiveness of adoptively transferred CD8(+) T cells for melanoma immunotherapy in human MHC class I-transgenic mice. *J Immunol*. 2001;167(10):5824–5831.

6. Almeida JR, et al. Superior control of HIV-1 replication by CD8+ T cells is reflected by their avidity, polyfunctionality, and clonal turnover. *J Exp Med*. 2007;204(10):2473–2485.

7. Berger CT, et al. High-functional-avidity cytotoxic T lymphocyte responses to HLA-B-restricted Gag-derived epitopes associated with relative HIV control. *J Virol*. 2011;85(18):9334–9345.

8. Yerly D, et al. Increased cytotoxic T-lymphocyte epitope variant cross-recognition and functional avidity are associated with hepatitis C virus clearance. *J Virol*. 2008;82(6):3147–3153.

9. Neveu B, et al. Selection of high-avidity CD8 T cells correlates with control of hepatitis C virus infection. *Hepatology*. 2008;48(3):713–722.

10. Viganò S, Utzschneider DT, Perreau M, Pantaleo G, Zehn D, Harari A. Functional avidity: a measure to predict the efficacy of effector T cells? *Clin Dev Immunol*. 2012;2012:153863.

11. Dudley ME, Nishimura MI, Holt AK, Rosenberg SA. Antitumor immunization with a minimal peptide epitope (G9-209-2M) leads to a functionally heterogeneous CTL response. *J Immunother*. 1999;22(4):288–298.

12. Dutoit V, et al. Heterogeneous T-cell response to MAGE-A10(254-262): high avidity-specific cytolytic T lymphocytes show superior antitumor activity. *Cancer Res*. 2001;61(15):5850–5856.

13. Speiser DE, et al. A novel approach to characterize clonality and differentiation of human melanoma-specific T cell responses: spontaneous priming and efficient boosting by vaccination. *J Immunol*. 2006;177(2):1338–1348.

14. Betts MR, et al. HIV nonprogressors preferentially maintain highly functional HIV-specific CD8+ T cells. *Blood*. 2006;107(12):4781–4789.

15. Harari A, Petitpierre S, Vallelian F, Pantaleo G. Skewed representation of functionally distinct populations of virus-specific CD4 T cells in HIV-1-infected subjects with progressive disease: changes after antiretroviral therapy. *Blood*. 2004;103(3):966–972.

16. Ciuffreda D, et al. Polyfunctional HCV-specific T-cell responses are associated with effective control of HCV replication. *Eur J Immunol*. 2008;38(10):2665–2677.

17. Wilde S, et al. Human antitumor CD8+ T cells producing Th1 polycytokines show superior antigen sensitivity and tumor recognition. *J Immunol*. 2012;189(2):598–605.

18. Almeida JR, et al. Antigen sensitivity is a major determinant of CD8+ T-cell polyfunctionality and HIV-suppressive activity. *Blood*. 2009;113(25):6351–6360.

19. Clay TM, Hobeika AC, Mosca PJ, Lyerly HK, Morse MA. Assays for monitoring cellular immune responses to active immunotherapy of cancer. *Clin Cancer Res*. 2001;7(5):1127–1135.

20. Keilholz U, Martus P, Scheibenbogen C. Immune monitoring of T-cell responses in cancer vaccine development. *Clin Cancer Res*. 2006;12(7 Pt 2):2346s–2352s.

21. Moran AE, Hogquist KA. T-cell receptor affinity in thymic development. *Immunology*. 2012;135(4):261–267.

22. Ozga AJ, et al. pMHC affinity controls duration of CD8+ T cell-DC interactions and imprints timing of effector differentiation versus expansion. *J Exp Med*. 2016;213(12):2811–2829.

23. Zehn D, Bevan MJ. T cells with low avidity for a tissue-restricted antigen routinely evade central and peripheral tolerance and cause autoimmunity. *Immunity*. 2006;25(2):261–270.

24. Hebeisen M, Oberle SG, Presotto D, Speiser DE, Zehn D, Rufer N. Molecular insights for optimizing T cell receptor specificity against cancer. *Front Immunol*. 2013;4:154.

25. Stone JD, Chervin AS, Kranz DM. T-cell receptor binding affinities and kinetics: impact on T-cell activity and specificity. *Immunology*. 2009;126(2):165–176.

26. Hebeisen M, Allard M, Gannon PO, Schmidt J, Speiser DE, Rufer N. Identifying individual T cell receptors of optimal avidity for tumor antigens. *Front Immunol*. 2015;6:582.

27. Nauerth M, et al. TCR-ligand koff rate correlates with the protective capacity of antigen-specific CD8+ T cells for adoptive transfer. *Sci Transl Med*. 2013;5(192):192ra87.

28. Hebeisen M, et al. Identification of rare high-avidity, tumor-reactive CD8+ T cells by monomeric TCR-ligand off-rates measurements on living cells. *Cancer Res*. 2015;75(10):1983–1991.

29. Gannon PO, et al. Quantitative TCR:pMHC dissociation rate assessment by NTAmers reveals antimelanoma T cell repertoires enriched for high functional competence. *J Immunol*. 2015;195(1):356–366.

30. Hebeisen M, et al. SHP-1 phosphatase activity counteracts increased T cell receptor affinity. *J Clin Invest*. 2013;123(3):1044–1056.

31. Simon S, et al. PD-1 expression conditions T cell avidity within an antigen-specific repertoire. *Oncoimmunology*. 2016;5(1):e1104448.

32. Azzam HS, Grinberg A, Lui K, Shen H, Shores EW, Love PE. CD5 expression is developmentally regulated by T cell receptor (TCR) signals and TCR avidity. *J Exp Med*. 1998;188(12):2301–2311.

33. Mandl JN, Monteiro JP, Vrisekoop N, Germain RN. T cell-positive selection uses self-ligand binding strength to optimize repertoire recognition of foreign antigens. *Immunity*. 2013;38(2):263–274.

34. Fulton RB, et al. The TCR's sensitivity to self peptide-MHC dictates the ability of naive CD8(+) T cells to respond to foreign antigens. *Nat Immunol*. 2015;16(1):107–117.

35. Straetemans T, et al. T-cell receptor gene therapy in human melanoma-bearing immune-deficient mice: human but not mouse T cells recapitulate outcome of clinical studies. *Hum Gene Ther*. 2012;23(2):187–201.

36. Aleksic M, et al. Different affinity windows for virus and cancer-specific T-cell receptors: implications for therapeutic strategies. *Eur J Immunol*. 2012;42(12):3174–3179.

37. Cole DK, et al. Human TCR-binding affinity is governed by MHC class restriction. *J Immunol*. 2007;178(9):5727–5734.

38. Derré L, et al. Distinct sets of alphabeta TCRs confer similar recognition of tumor antigen NY-ESO-1157-165 by interacting with its central Met/Trp residues. *Proc Natl Acad Sci U S A*. 2008;105(39):15010–15015.

39. Iancu EM, et al. Clonotype selection and composition of human CD8 T cells specific for persistent herpes viruses varies with

differentiation but is stable over time. *J Immunol*. 2009;183(1):319–331.

40. Speiser DE, et al. Single cell analysis reveals similar functional competence of dominant and nondominant CD8 T-cell clonotypes. *Proc Natl Acad Sci U S A*. 2011;108(37):15318–15323.

41. Speiser DE, et al. Unmodified self antigen triggers human CD8 T cells with stronger tumor reactivity than altered antigen. *Proc Natl Acad Sci U S A*. 2008;105(10):3849–3854.

42. Romero P, Speiser DE, Rufer N. Deciphering the unusual HLA-A2/Melan-A/MART-1-specific TCR repertoire in humans. *Eur J Immunol*. 2014;44(9):2567–2570.

43. Hesse MD, Karulin AY, Boehm BO, Lehmann PV, Tary-Lehmann M. A T cell clone's avidity is a function of its activation state. *J Immunol*. 2001;167(3):1353–1361.

44. Tan MP, et al. T cell receptor binding affinity governs the functional profile of cancer-specific CD8+ T cells. *Clin Exp Immunol*. 2015;180(2):255–270.

45. Kalergis AM, et al. Efficient T cell activation requires an optimal dwell-time of interaction between the TCR and the pMHC complex. *Nat Immunol*. 2001;2(3):229–234.

46. Falcioni F, et al. Influence of CD26 and integrins on the antigen sensitivity of human memory T cells. *Hum Immunol*. 1996;50(2):79–90.

47. Slifka MK, Whitton JL. Functional avidity maturation of CD8(+) T cells without selection of higher affinity TCR. *Nat Immunol*. 2001;2(8):711–717.

48. Tian S, Maile R, Collins EJ, Frelinger JA. CD8+ T cell activation is governed by TCR-peptide/MHC affinity, not dissociation rate. *J Immunol*. 2007;179(5):2952–2960.

49. Huang J, et al. The kinetics of two-dimensional TCR and pMHC interactions determine T-cell responsiveness. *Nature*. 2010;464(7290):932–936.

50. Huppa JB, et al. TCR-peptide-MHC interactions in situ show accelerated kinetics and increased affinity. *Nature*. 2010;463(7283):963–967.

51. Aleksic M, et al. Dependence of T cell antigen recognition on T cell receptor-peptide MHC confinement time. *Immunity*. 2010;32(2):163–174.

52. Govern CC, Paczosa MK, Chakraborty AK, Huseby ES. Fast on-rates allow short dwell time ligands to activate T cells. *Proc Natl Acad Sci U S A*. 2010;107(19):8724–8729.

53. Zhu C, Jiang N, Huang J, Zarnitsyna VI, Evavold BD. Insights from in situ analysis of TCR-pMHC recognition: response of an interaction network. *Immunol Rev*. 2013;251(1):49–64.

54. Odorizzi PM, Pauken KE, Paley MA, Sharpe A, Wherry EJ. Genetic absence of PD-1 promotes accumulation of terminally differentiated exhausted CD8+ T cells. *J Exp Med*. 2015;212(7):1125–1137.

55. Gros A, et al. PD-1 identifies the patient-specific CD8+ tumor-reactive repertoire infiltrating human tumors. *J Clin Invest*. 2014;124(5):2246–2259.

56. Legat A, Speiser DE, Pircher H, Zehn D, Fuertes Marraco SA. Inhibitory receptor expression depends more dominantly on differentiation and activation than "exhaustion" of human CD8 T cells. *Front Immunol*. 2013;4:455.

57. Bouneaud C, Kourilsky P, Bousso P. Impact of negative selection on the T cell repertoire reactive to a self-peptide: a large fraction of T cell clones escapes clonal deletion. *Immunity*. 2000;13(6):829–840.

58. Tungatt K, et al. Antibody stabilization of peptide-MHC multimers reveals functional T cells bearing extremely low-affinity TCRs. *J Immunol*. 2015;194(1):463–474.

59. Khan N, Cobbold M, Cummerson J, Moss PA. Persistent viral infection in humans can drive high frequency low-affinity T-cell expansions. *Immunology*. 2010;131(4):537–548.

60. Huang J, et al. Detection, phenotyping, and quantification of antigen-specific T cells using a peptide-MHC dodecamer. *Proc Natl Acad Sci U S A*. 2016;113(13):E1890–E1897.

61. Pinto S, et al. Misinitiation of intrathymic MART-1 transcription and biased TCR usage explain the high frequency of MART-1-specific T cells. *Eur J Immunol*. 2014;44(9):2811–2821.

62. Cole DK, et al. Germ line-governed recognition of a cancer epitope by an immunodominant human T-cell receptor. *J Biol Chem*. 2009;284(40):27281–27289.

63. Loftus DJ, et al. Identification of epitope mimics recognized by CTL reactive to the melanoma/melanocyte-derived peptide MART-1(27-35). *J Exp Med*. 1996;184(2):647–657.

64. Dutoit V, et al. Degeneracy of antigen recognition as the molecular basis for the high frequency of naive A2/Melan-a peptide multimer(+) CD8(+) T cells in humans. *J Exp Med*. 2002;196(2):207–216.

65. Pittet MJ, et al. Alpha 3 domain mutants of peptide/MHC class I multimers allow the selective isolation of high avidity tumor-reactive CD8 T cells. *J Immunol*. 2003;171(4):1844–1849.

66. Schumacher TN, Schreiber RD. Neoantigens in cancer immunotherapy. *Science*. 2015;348(6230):69–74.

67. Nauerth M, et al. Flow cytometry-based TCR-ligand Koff -rate assay for fast avidity screening of even very small antigen-specific T cell populations ex vivo. *Cytometry A*. 2016;89(9):816–825.

68. Zhang SQ, et al. Direct measurement of T cell receptor affinity and sequence from naïve antiviral T cells. *Sci Transl Med*. 2016;8(341):341ra77.

69. Speiser DE, et al. Rapid and strong human CD8+ T cell responses to vaccination with peptide, IFA, and CpG oligodeoxynucleotide 7909. *J Clin Invest*. 2005;115(3):739–746.

70. Schmidt J, Guillaume P, Irving M, Baumgaertner P, Speiser D, Luescher IF. Reversible major histocompatibility complex I-peptide multimers containing Ni(2+)-nitrilotriacetic acid peptides and histidine tags improve analysis and sorting of CD8(+) T cells. *J Biol Chem*. 2011;286(48):41723–41735.

71. Motulsky HJ, Brown RE. Detecting outliers when fitting data with nonlinear regression - a new method based on robust nonlinear regression and the false discovery rate. *BMC Bioinformatics*. 2006;7:123.

SUPPLEMENTAL MATERIALS

Supplemental Table 1. List of TCR-BV-CDR3 clonotypes and their off-rate values.

Antigenic specificity	Patient/ Donor	Clonotype	BV family	CDR3 (amino acids)	BJ	Mean koff (s-1)
A2/Melan-A	LAU618	clono 1	BV3	SPPGLSGNIQ	2.4	0.03338
		clono 2	BV3	SFQGVGTGEL	2.2	0.02622
		clono 3	BV13	SYGPLSGAGY	1.2	0.02548
		clono 4	BV13	SPGTLADTQ	2.3	0.06173
		clono 5	BV13	SAGYGQPQ	1.5	0.05155
		clono 6	BV14	RAGALQGEQ	2.7	0.10740
		clono 7	BV14	SPAALSGAYEQ	2.7	0.10100
		clono 8	BV17	SPGALNTEA	1.1	0.06438
		clono 9	BV3	SFPRWGRNYSYNEQ	na	0.03492
		clono 10	BV14	SLSAGTGVLDTQ	na	0.09449
		clono 11	BV17	SIGA--EHEQ	na	0.09964
		clono 12	BV17	SIEALQGFTEA	na	0.04187
		clono 13	BV17	RWGVLNTEA	na	0.01835
A2/NY-ESO-1	LAU155	clono 1	BV1	SVATGGDTQ	2.3	0.01875
		clono 2	BV8	NSGSNEQ	2.1	0.02771
		clono 3	BV8	SLGSTEA	1.1	0.00831
		clono 4	BV8	NSGANEQ	2.1	0.02026
		clono 5	BV8	RKGPNEQ	2.1	0.03529
		clono 6	BV13	SYVGAAGEL	2.2	0.02918
		clono 7	BV13	SLTGGLNSPL	na	0.03146
		clono 8	BV1	SLATGEDTQ	na	0.01574
		clono 9	BV13	LGDGDGAYNSPL	1.6	0.03277
	LAU50	clono 10	BV8	QQGGTEA	1.1	0.01572
		clono 11	BV8	SLGGTEA	1.1	0.01975
		clono 12	BV13	RTGLDGY	1.2	0.03094
		clono 13	BV13	SYVGGKAEA	1.2	0.02612
A2/CMV-pp65	BCL4	clono 1	BV1	SVYGGAGNSPL	1.6	0.00866
		clono 2	BV1	SYPGGNTI	1.3	0.01797
		clono 3	BV3	SFLGYTEA	1.1	0.01174
		clono 4	BV8	SSVNEA	1.1	0.00646
		clono 5	BV8	SSAGGAVYGY	1.2	0.02039
		clono 6	BV9	SLLLGTAAEA	1.1	0.00313
		clono 7	BV14	RLLAGGRSAQ	2.5	0.00608
		clono 8	BV3	SFSSPGQGSTDTQ	2.3	0.01285
		clono 9	BV8	SSVLEA	1.1	0.01002
		clono 10	BV8	SLVGGVDGY	1.2	0.03013
		clono 11	BV8	SIMDYGY	1.2	0.03125
		clono 12	BV13	SAVTGAVDQPQ	1.5	0.01642
		clono 13	BV13	SYFYYEQ	2.7	0.00251
		clono 14	BV13	SYSTGTAYGY	1.2	0.00289
		clono 15	BV13	SPKTGVPYEQ	2.7	0.02146
	BCL6	clono 16	BV8	SSANYGY	1.2	0.01505
		clono 17	BV13	SRQTGAAYGY	1.2	0.00617
		clono 18	BV13	SYATGTAYGY	1.2	0.00530
A2/EBV-BMFL1	BCL4	clono 1	BV2	RDRTGNGY	1.2	0.005131
		clono 2	BV2	RDSVGNGY	1.2	0.002706
		clono 3	BV2	RDRVGNGY	1.2	0.001934
		clono 4	BV2	RDSTGNGY	1.2	0.004689
		clono 5	BV2	RVEPGNGY	1.2	0.009871
		clono 6	BV4	VGTGGTNEKL	1.4	0.014417
		clono 7	BV4	VGYGGTNEKL	1.4	0.013503
		clono 8	BV4	VGSGGTNEKL	1.4	0.045620
		clono 9	BV16	SQSPGGTQ	2.5	0.009123
		clono 10	BV16	SQSPGGEA	1.1	0.003469
		clono 11	BV16	SQSPGGTS	na	0.003878
		clono 12	BV18	SPPAVSYEQ	2.7	0.016529
		clono 13	BV2	DGY	1.2	0.017560

Supplemental Table 2. List of antibodies used in this study.

Name	Company	Catalog no	Clone no
APC anti-CD28	BD Pharmigen	559770	CD28.2
FITC anti-CD45RA	BD Pharmigen	561882	HI100
FITC anti-CD107a	BD Pharmigen	555800	H4A3
PerCPCy5.5 anti-IL2	BD Pharmigen	560708	MQ1-17H12
APC anti-IL13	BD Pharmigen	561162	JES10-5A2
PE-Cy7 anti-IFNγ	BD Pharmigen	557844	4S.B3
A700 anti-TNFα	BD Pharmigen	557996	MAb11
PE-Cy7 anti-CD5	BD Pharmigen	348810	L17F12
APC anti-CD137	BD Pharmigen	550890	4B4-1
PE anti-VLA-1	BD Pharmigen	559596	SR84
APC anti-VLA-4	BD Pharmigen	561794	MAR4 .
BrV421 anti-PD1	BD Pharmigen	562516	EH12.1
APC-A750 anti-CD8	Beckman Coulter	A94683	B9.11
Pacific-blue anti-CD8	Beckman Coulter	A82791	B9.11
FITC anti-CD8beta	Beckman Coulter	IM2217U	2ST8.5H7
PE-Cy7 anti-CD8alpha	Beckman Coulter	737661	SFCI21Thy2D3
PE anti-pan-TCRab	Beckman Coulter	A39499	IP26A
PE-Cy7 anti-CCR7	Biolegend	353226	G043H7
PE anti-IL4	Biolegend	500810	MP4-25D2
BrV421 anti-CD28	Biolegend	302930	CD28.2
A488 anti-PD1	AbD Serotech	MCA2628A488	MIH4
APC anti-TIGIT	eBioscience	17-9500-42	MBSA43
FITC anti-LAG-3	Enzo	ALX-804-806F-C100	17B4
PE anti-TIM-3	R&D systems	FAB2365P	344823
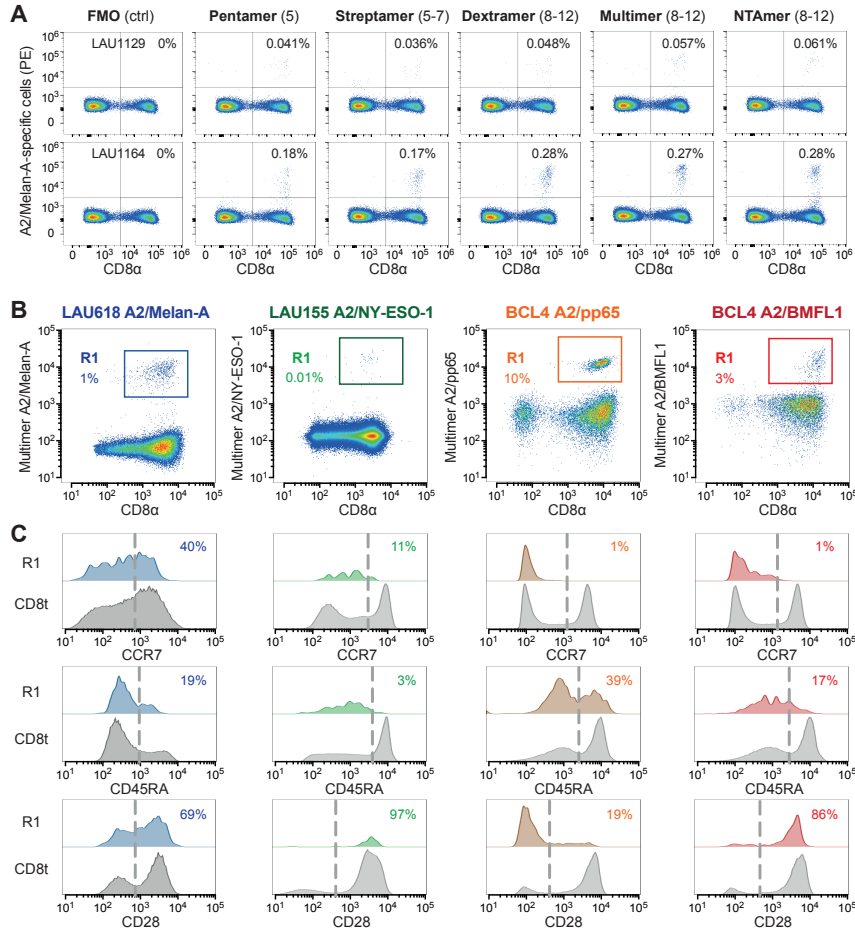
Sup Figure 1 - Allard et al.

Supplemental Figure 1: Ex vivo detection of antigen-specific CD8 T cells using pMHC-based reagents and analysis of blood samples used to generate self/tumor- and virus-specific CD8 T cell clones. **(A)** Comparison of A2/MelanA$_{26-35}$-specific staining from PBMCs obtained from melanoma patients (LAU1129 and LAU1164) using PE-labeled pentamers, streptamers, multimers and NTAmers. Gating was done on live CD14-/CD16-/CD19-/CD3+ lymphocytes. The valence of pMHC reagents is indicated in brackets, as well as percentages of positively stained cells. FMO (fluorescence minus one). **(B)** CD8 and multimer staining of CD8-enriched PBMCs from melanoma patients LAU618 (A2/Melan-A$_{26-35}$), LAU155 (A2/NY-ESO-1$_{157-165}$) and healthy donor BCL4 (A2/pp65$_{495-504}$ or A2/BMFL1$_{259-267}$). **(C)** CCR7, CD45RA and CD28 staining of the corresponding multimer-

specific (*R1*) and total CD8 T cell (*CD8t*) populations. Percentages of positively stained cells are indicated. Melan-A/specific CD8 T cell clones (from patient LAU618) exhibited an EM/CD28$^{+/-}$ phenotype, while NY-ESO-1-specific T cell clones (from patient LAU155) presented mostly an early-differentiated EM/CD28^{+} phenotype. EBV/BMFL1-specific CD8 T cell clones were predominantly EM/CD28^{+}, whereas CMV/pp65-specific clones mostly exhibited a differentiated EMRA/CD28^{-} phenotype.
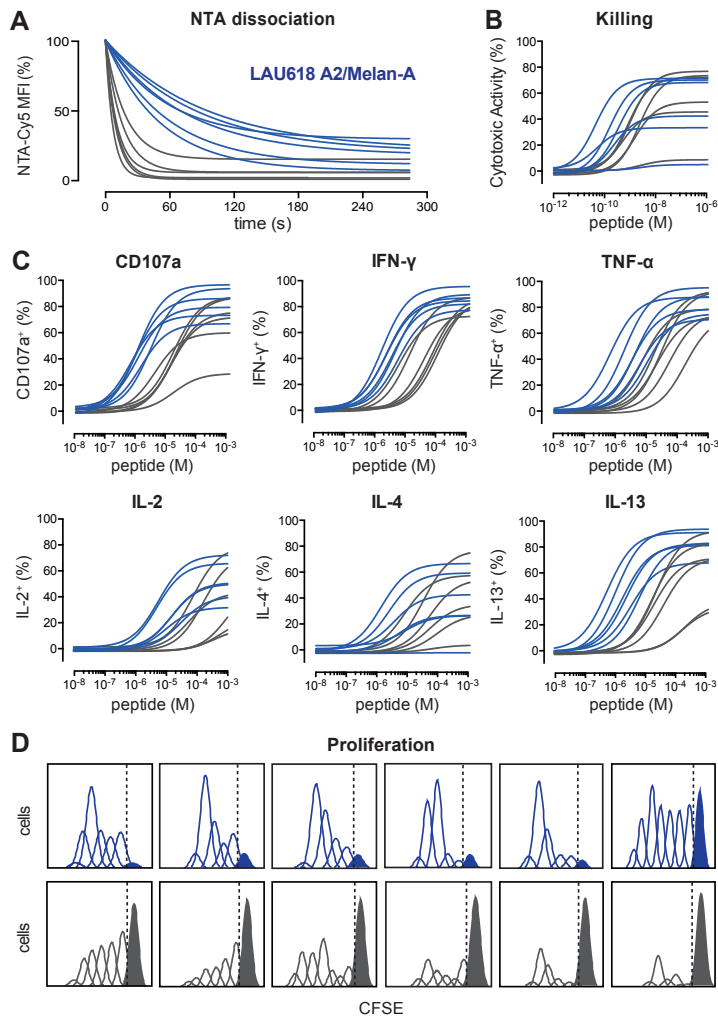
Sup Figure 2 - Allard et al.

Supplemental Figure 2: *In vitro* **analysis of TCR dissociation-rates versus functional avidities of self/tumor- and virus-specific CD8 T cell clones.** Representative (**A**) NTAmer-dissociation curves, (**B**) killing-, **(C)** CD107a degranulation-, IFNγ-, TNFα-, IL-2-, IL-4- and IL-13-production titration curves and **(D)** proliferation analysis (by CFSE fluorescence histograms) obtained for A2/Melan-A$_{26-35}$-specific CD8 T cell clones from patient LAU618, defined as slow (n = 6, blue lines) or fast (n = 6, grey lines) TCR off-rates. Non-divided and divided T cells are represented as plain and empty peaks, respectively.
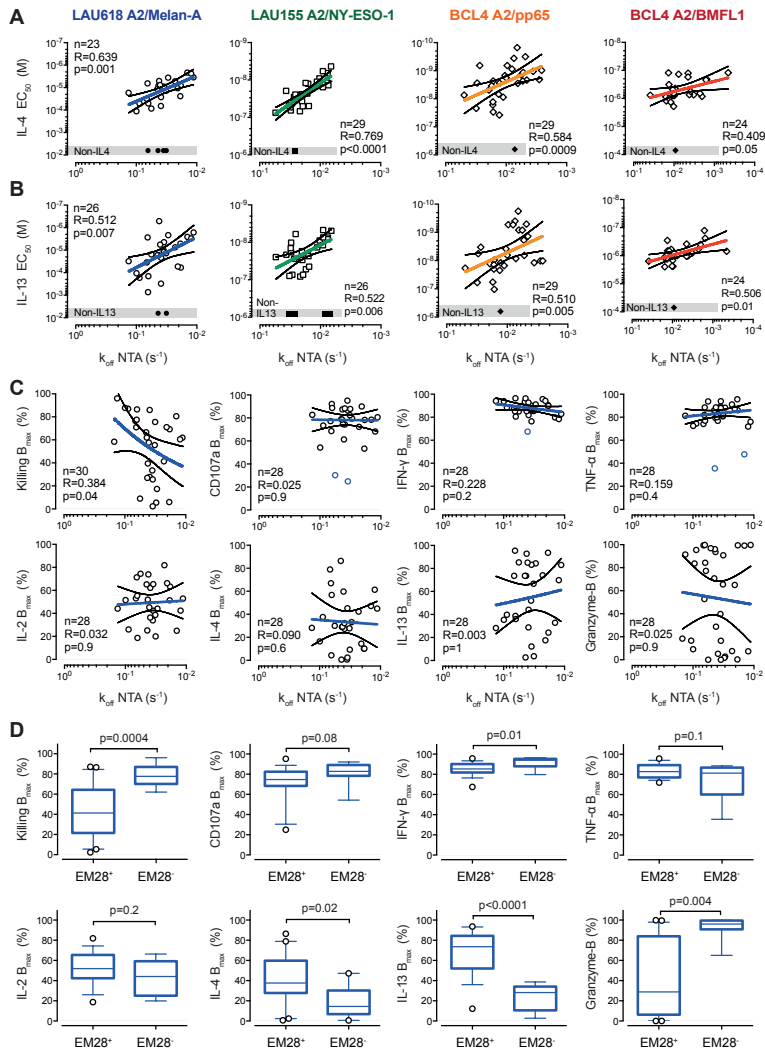
Sup Figure 3 - Allard et al.

Supplemental Figure 3: Relationship between TCR dissociation-rates, functional avidity and maximal function capacity of self/tumor- and virus-specific CD8 T cell clones. Correlations between EC_{50} values from (**A**) IL-4- and (**B**) IL-13-production titration assays, and NTAmer-derived TCR dissociation-rates (k_{off}). (**C**) Correlations between B_{max} values from killing, CD107a-degranulation, IFNγ-, TNFα-, IL-2-, IL-4- and IL-13-production titration assays, or percentages of granzyme-B expressing T cells, and NTAmer-derived TCR dissociation-rates (k_{off}). (**A-C**) Each data-point represents an A2/Melan-A$_{26-35}$- (derived from patient LAU618, ○), A2/NY-ESO-1$_{157-165}$- (patient LAU155, □), A2/pp65$_{495-504}$- or

A2/BMFL1$_{259-267}$- (healthy donor BCL4, ◇) specific individual T cell clone. Non-functional clones are represented in grey boxes. The number of clones displaying function n, as well as Spearman's correlation (two tailed, $α = 0.05$) coefficient R and p values are indicated. Color-coded and black lines are indicative of regression fitting and 95% confidence intervals, respectively. (**D**) B$_{max}$ values from killing, CD107a-degranulation, IFNγ-, TNFα-, IL-2-, IL-4- and IL-13-production titration assays, or granzyme-B expression, of early-differentiated effector-memory EM/CD28$^+$ or late-differentiated EM/CD28$^-$ A2/Melan-A$_{26-35}$-specific T cell clones derived from patient LAU618. Data are depicted as box (25th to 75th percentiles) and whisker (10th to 90th percentiles) with the middle line representing the median. Numbers of clones n, as well as Mann-Whitney (two tailed) derived p values are indicated. Of note, upon high peptide-dose stimulation (at Bmax, maximal response), differentiated EM/CD28$^-$-derived CD8 T cell clones displayed higher granzyme-B expression, cytotoxic and IFN-γ production capacity, but a lower ability to produce IL-2, IL-4 or IL-13 than memory EM/CD28$^+$ T cells.
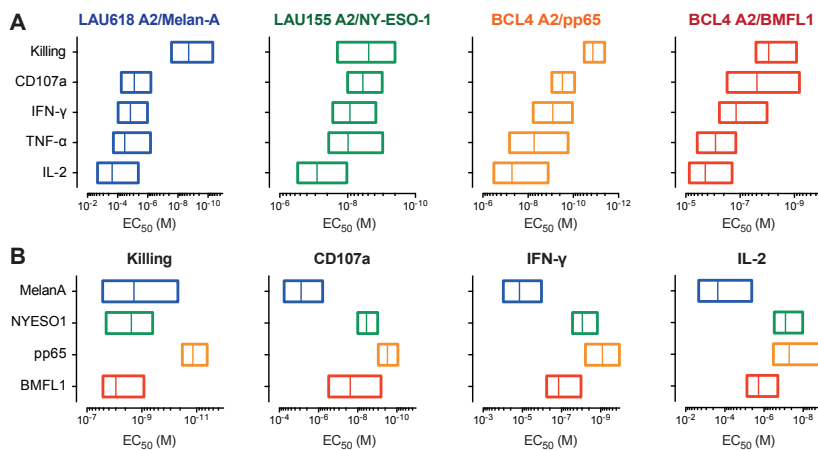
Sup Figure 4 - Allard et al.

Supplemental Figure 4: Functional avidities according to the functional assay or the antigenic specificity of CD8 T cell clones. Comparison of functional avidity (EC$_{50}$) from killing-, CD107a degranulation-, IFNγ-, TNFα- and IL-2-production of A2/Melan-A$_{26-35}$- (derived from melanoma patient LAU618, n = 30), A2/NY-ESO-1$_{157-165}$- (patient LAU155, n = 32), A2/pp65$_{495-504}$- or A2/BMFL1$_{259-267}$- (healthy donor BCL4, n = 30 and 26, respectively) specific CD8 T cell clones classified according to (**A**) the functional assay and (**B**) the antigenic-specificity. Data are depicted as box (minimum to maximum) with the middle line representing the mean. The representative TCR-BV clonotype diversity of each antigenic specificity is as following; LAU618/Melan-A, 77%; LAU155/NY-ESO-1, 43%; BCL4/pp65, 57%; BCL4/BMFL1, 67%.
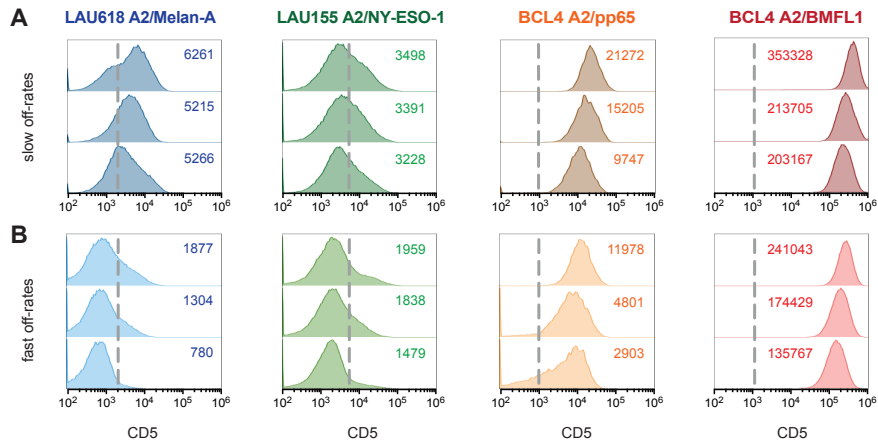
Sup Figure 5 - Allard et al.

Supplemental Figure 5: CD5 expression according to the TCR-dissociation off-rate parameter and antigenic specificity of self/tumor- and virus-specific CD8 T cell clones. CD5 surface staining was obtained at baseline (no antigen-specific stimulation) from representative antigen-specific CD8 T cells of (**A**) slow or (**B**) fast NTAmer-based off-rates. Data are depicted according to the antigenic specificity (A2/Melan-A$_{26-35}$-, A2/NY-ESO-1$_{157-165}$-, A2/pp65$_{495-504}$- and A2/BMFL1$_{259-267}$ antigens). Geometric fluorescence means (gMFI) are indicated.
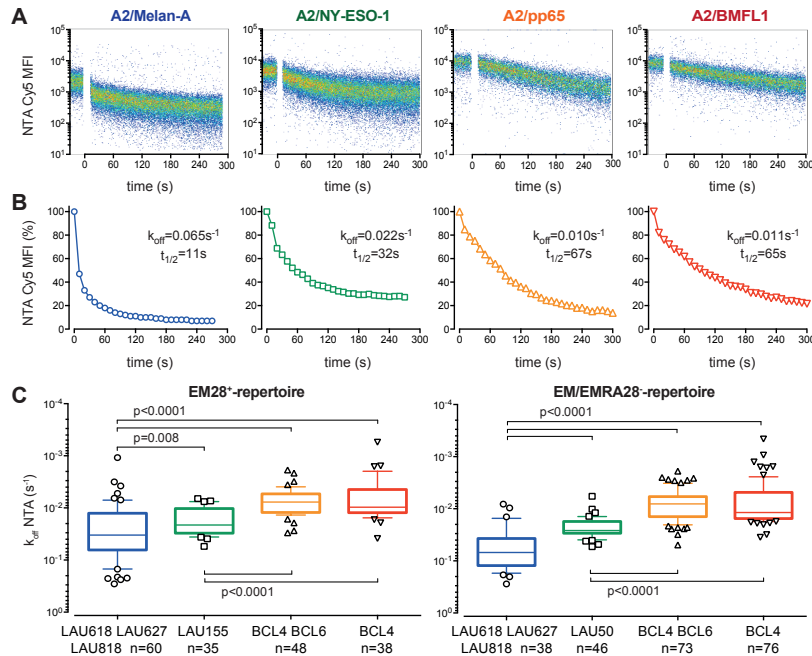
Sup Figure 6 - Allard et al.

Supplemental Figure 6: TCR dissociation-rates according to the antigenic specificity and *ex vivo* differentiation status. Representative (**A**) NTAmer-dissociation staining and (**B**) corresponding fitting curve obtained for A2/Melan-A$_{26-35}$- (○), A2/NY-ESO-1$_{157-165}$- (□), A2/pp65$_{495-504}$- (△) and A2/BMFL1$_{259-267}$- (▽) specific CD8 T cell clones, defined as average TCR off-rates. k$_{off}$ and t$_{1/2}$ derived values are indicated. (**C**) NTAmer-derived TCR dissociation-rates (k$_{off}$) of early-differentiated effector-memory EM CD28$^+$ (left panel) versus late-differentiated EM/EMRA CD28$^-$ (right panel) clones specific for (i) A2/Melan-A$_{26-35}$ (from vaccinated melanoma patients LAU618, LAU627 and LAU818), (ii) A2/NY-ESO-1$_{157-165}$ (from patients LAU50 and LAU155 with naturally occurring tumor-specific T cell responses) or (iii) the persistent herpes viruses A2/pp65$_{495-504}$ or A2/BMFL1$_{259-267}$ (from healthy donors BCL4 and BCL6), categorized according to their antigenic specificity. Data are depicted as box (25th to 75th percentiles) and whisker (10th to 90th percentiles), with the middle line representing the median. Antigen specificity is depicted according to specific colored codes and symbols. Numbers of clones *n*, as well as Kruskal-Wallis test ($\alpha = 0.05$) derived *p* values are indicated. Significant differences between the A2/Melan-A$_{26-35}$- and the A2/NY-ESO-1$_{157-165}$-specific groups were obtained by a Mann Whitney test (two tailed).
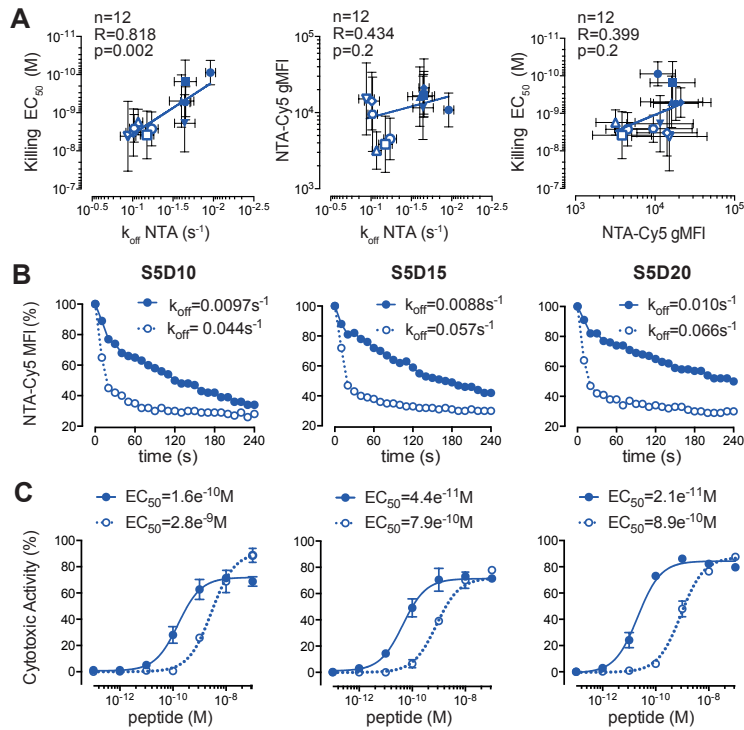
Sup Figure 7 - Allard et al.

Supplemental Figure 7: Correlations between TCR dissociation rates versus pMHC multimer staining versus functional avidity of CD8 T cell clones. (A) Correlations between NTAmer-derived TCR dissociation rates (k_{off}), NTAmer surface staining levels (gMFI) and killing avidity values (EC_{50}) obtained from independent assays (n = 4 to 9) for A2/Melan-A$_{26-35}$-specific CD8 T cell clones, defined as slow (n = 6, plain symbols) or fast (n = 6, empty symbols) TCR off-rates. Each symbol/clone is represented as average ± SD. The number of clones (n), as well as Spearman's correlation (two tailed, $\alpha = 0.05$) coefficients *R* and *p* values are indicated. Lines are indicative of linear regression fitting. Representative **(B)** NTAmer-dissociation and **(C)** killing-titration curves obtained at day 10 (D10), 15 (D15) and 20 (D20) following non-specific stimulation (by PHA and irradiated feeder cells) of A2/Melan-A$_{26-35}$-specific CD8 T cell clones, defined as slow (n =6, plain symbols and solid lines) or fast (n = 6, empty symbols and dotted lines) TCR off-rates. Average and SD percentages are depicted, as well as the corresponding fitting curves and k_{off} or EC_{50} derived values.

2.   Manuscript 2

The following article, in preparation for publication in Autumn 2019, corresponds to the second aim of this thesis.

1 **Progressive long-term avidity decline of CMV- but not EBV-specific memory CD8 T cell**

2 **clonotype repertoires**

3

4 Barbara Couturaud[1], Laura Carretero-Iglesia[1], Mathilde Allard[1,*], Sylvain Pradervand[2], Michael

5 Hebeisen[1] and Nathalie Rufer[1]

6

7 [1]Department of Oncology, Lausanne University Hospital and University of Lausanne,

8 Epalinges, Switzerland

9 [2]Lausanne Genomic Technologies Facility (LGTF), University of Lausanne, Switzerland

10 [*]Current address: Center for Translational Research in Onco-Hematology, University of

11 Geneva, Geneva. Switzerland

12

13 **Corresponding author:** Nathalie Rufer, MD, PhD; e-mail: Nathalie.Rufer@unil.ch

14

15 **Running title:** TCR clonal evolution during latent viral infections

16

17 **Keywords:** Healthy donors, longitudinal studies, herpes viruses, CMV, EBV, latent infection,

18 cytotoxic T cells, TCR clonotype, memory, persistence, TCR off-rate, RNASeq, LILRB1

19

20 **Abbreviations:** NTAmer, NTA-His tag-containing multimer; pMHC, peptide-MHC; CMV,

21 Cytomegalovirus; EBV, Epstein-Barr virus; TCR, T cell receptor

22

1

23 **ABSTRACT**

24 Efficient T cell responses rely on TCR-pMHC binding avidity that controls essential T cell

25 functions. Yet, whether the TCR-ligand avidity is a determining factor for the clonal evolution

26 of virus antigen-specific CD8 T cells, and how this process is determined in CMV against EBV

27 latent infection, remains largely unknown. Here, we quantified TCR-pMHC off-rates on large

28 libraries of well-characterized virus-specific TCRαβ clonotypes isolated from six healthy

29 donors over a period of 15 years. Within CMV-specific T cell repertoires, we observed the

30 progressive contraction of clonotypes of higher TCR-pMHC avidity and lower CD8 binding

31 dependency during chronic antigen exposure. Interestingly, we identified a unique

32 transcriptional signature preferentially expressed by high-avidity T cell clonotypes, including

33 the inhibitory receptor *LILRB1*. Surface expression of LILRB1 was also found to be elevated

34 in the declining clonotypes when compared to the expanding clonotypes, correlating with

35 enhanced proliferative capacity upon LILRB1 blockade. This was not the case for the EBV-

36 specific T cell clonal composition and distribution, that once established, displayed an

37 unprecedented stability for at least 15 years. Taken together, these findings reveal an overall

38 long-term avidity decline of CMV- but not EBV-specific T cell clonal repertoires, highlighting

39 the differing role played by TCR-ligand avidity over the course of these two latent herpesvirus

40 infections. Our data suggest that LILRB1 represents a key checkpoint regulator that limits the

41 life expectancy of high-avidity CMV-specific T cell clonotypes. We conclude that the

42 mechanisms regulating the long-term outcome of CMV- and EBV-specific memory CD8 T cell

43 clonotypes in humans are distinct.

2

44 **INTRODUCTION**

45 Cytomegalovirus (CMV) and Epstein-Barr virus (EBV) are common persistent viruses,

46 infecting, depending on geographical location, 60-90% and over 95% of the human adult

47 population, respectively. Primary CMV and EBV infection is associated with a robust T cell-

48 specific immune response, followed by the establishment of a lifelong latency. In healthy

49 individuals, herpesviruses are generally well controlled, through a fine balance between viral

50 determinants and host immune surveillance, that usually allows immunocompetent individuals

51 to remain asymptomatic throughout their lives. Yet, these viruses remain a major cause of

52 morbidity and mortality in immunocompromised individuals (1, 2).

53 The maintenance of memory CD8 T cell responses during CMV and EBV latent infection has

54 been shown to differ in terms of frequency, phenotype and function. For instance, the number

55 of EBV-specific memory CD8 T cells generally remains stable over time in healthy carriers (3,

56 4), while CMV-specific T cells persist in larger numbers and even slowly accumulate with

57 ageing, in a process named "memory inflation" (5-7). Moreover, CD8 T cells specific for EBV

58 mostly display a T cell central-memory (T_{CM}) phenotype and are thus less differentiated than the

59 predominantly effector-memory (T_{EM}) CMV-specific T cell pool, that typically harbor a more

60 mature phenotype (8, 9). At the functional level, CMV-specific T cells produce cytokines (i.e.

61 IFNγ, TNFα) and effector mediators (i.e. perforin, granzyme B), and show constitutive

62 cytolytic activity, sharing features common among acute effector cells (8, 10-12). It is

63 becoming increasingly clear that repetitive exposure to antigen is a key determinant of memory

64 T cell inflation during CMV latent infection. Indeed, CMV is characterized by intermittent

65 reactivation from latency, inducing a low-level persistent infection, which subsequently

66 impacts on the virus-specific CD8 T cell response (13). In contrast, EBV reactivation during

67 latency is thought to occur only occasionally, with virus-specific T cells showing no sign of

68 inflation/expansion comparable to CMV infection (14). While the factors that drive and

69 maintain these large populations of CD8 T cells are known to diverge between specific herpes

70 viruses (14), there is still a continued need to improve our knowledge about the course of latent

71 CMV and EBV infections and their control by long-term immune responses.

72 The T cell repertoires (TCRs) of CMV- and EBV-specific CD8 T cells during viral infection

73 and latency have been extensively studied over the past two decades (15). Initial skewing of the

74 TCR repertoire towards the HLA-A2 restricted epitope derived from the CMV protein pp65

75 has been observed following primary infection and during CMV reactivation (16, 17), resulting

76 in progressively limited clonal diversity through the latency phase (9, 18). In the EBV context,

3

77   early reports have shown that highly dominant T cell clonotypes present during the primary

78   phase in acute infectious mononucleosis patients were poorly represented in the long-term, as

79   they were often overtaken or replaced by others (19, 20). Nevertheless, longitudinal studies

80   have also revealed that the clonal repertoire against latent CMV and EBV infections, once

81   established, remained stable and did not evolve for at least several years (9, 17, 21-24).

82   However, the maximal time span analyzed in those studies was 5 years, whereas CMV and

83   EBV immune responses persist for decades and small changes in the TCR repertoire may only

84   be observed over longer periods of time. Along this line, Miles et al. (25) have previously

85   reported the long-term persistence of single CD8 T cell clonotypes specific for the HLA-

86   B*0801/FLR and HLA-B*4405/EEN epitopes for 18 and 11 years, respectively, in two EBV-

87   positive donors. Collectively, following primary infection and initial TCR repertoire focusing,

88   herpes virus-specific T clonal repertoires appear to be stably maintained for at least several

89   years (21).

90   Despite major efforts, the parameters underlying the selection and long-term maintenance of

91   virus-specific CD8 T cell subpopulations remain poorly understood. Competition for antigen at

92   the level of the APC (26), as well as between virus-specific T cells (27), have been shown to

93   favor clonal dominance during memory inflation induced by murine CMV (MCMV) infection.

94   Other studies have implicated a dominant role for the immunoproteasome (28) and for the viral

95   gene expression context (29) in defining T cell immunodominance against MCMV. A very

96   recent report found that the inflationary T cell pool is mainly composed of high avidity CD8 T

97   cells that outcompete lower avidity T cells (30). This last observation is in agreement with the

98   assumption that TCR-pMHC avidity represents a major determinant of the TCR repertoire

99   selection and dominance in human CMV-specific CD8 T cell responses (9, 16-18, 23). In

100   addition, investigations of TCR repertoire evolution during aging have shown an accumulation

101   of CMV-specific CD8 T cells of lower avidity or functional potential in elderly individuals (31,

102   32). On the other hand, a dominant CMV/pp65-specific TRBV clonal signature of high avidity

103   has been described in elderly individuals, implying that long-lasting infection does not preclude

104   the establishment of repertoires with increased avidities (33).

105   One of the main limitations in addressing the question on the impact of TCR-pMHC avidity on

106   T cell clonal evolution is that the above-mentioned studies determined avidity using soluble

107   pMHC multimers or functional assays (i.e. specific T cell reactivity was analyzed against

108   increasing antigen concentrations). It is only recently that the precise quantification of TCR

109   binding avidity by NTAmers (34, 35) or Streptamers (36), which provide more reliable tools to

4

110   determine avidity-based TCR repertoire shaping, has become possible (15, 37). Another major

111   restriction lies in the fact that antigen-specific CD8 T cell clonotypes are commonly assessed

112   at the TCR-Vβ chain (i.e. TRBV) level without including complete TCRαβ repertoire analyses.

113   Finally, long-term TCR clonal repertoire and overall avidity evolution have often been

114   restricted to cross-sectional studies comparing individuals of different age groups.

115   Here, we combined TCRαβ clonotypic repertoire with quantitative TCR-pMHC dissociation

116   rate (i.e. off-rate or k_{off}) analyses to characterize the TCR clonal evolution between CMV

117   (HLA-A2/pp65$_{495-503}$) versus EBV (HLA-A2/BMFL1$_{280-288}$) latent infection in longitudinal

118   studies over a period of 15 years. Specifically, we investigated the degree to which this process

119   is determined by TCR-pMHC binding avidity in both viral models. Our findings reveal a

120   progressive long-term avidity decline of CMV- but not EBV-specific memory CD8 T cell

121   clonotype repertoires. This was associated with the preferential expression of the checkpoint

122   regulator LILRB1/CD85j in high-avidity CMV-specific TCRαβ clonotypes. These data

123   highlight a critical role played by TCR avidity-driven repertoire evolution in the long-term

124   outcome of CMV-specific compared to EBV-specific CD8 T cell responses in healthy

125   individuals.

5

126 **MATERIALS & METHODS**

127 **Healthy donors and ethics statement**

128 Leukapheresis were collected from seven healthy individuals latently infected with the CMV

129 and/or EBV viruses (BCL1, BCL2, BCL4, BCL6, BCL7, BCL8 and BCL9) in 2002, as

130 described previously (9) and defined as time-point T_n. Blood samples from the same individuals

131 (except BCL8) were collected 15 years later in 2017, defined as T_{n+15y}. No clinical data were

132 available on their acute infection in the past, but all individuals remained in excellent health

133 during the 15 years of follow-up. Peripheral blood mononuclear cells (PBMCs) centrifuged in

134 Ficoll-Hypaque (Pharmacia) were cryopreserved in 10% DMSO and stored in liquid nitrogen

135 until further use. This study was reviewed and approved according to the relevant regulatory

136 standards from the ethical commission of the University of Lausanne (Lausanne, Switzerland).

137 All healthy donors gave written informed consent.

138 **Generation of virus-specific CD8 T cell clones and direct *ex vivo* single cell sorting**

139 Thawed PBMCs were positively enriched using anti-CD8-coated magnetic microbeads

140 (Miltenyi Biotec), stained in PBS, 0.2% BSA, and 5 mM EDTA with PE-labeled HLA- A*0201

141 multimers loaded with native EBV/BMFL1$_{280-288}$ (GLCTLVAML) or CMV/pp65$_{495-503}$

142 (NLVPMVATV) peptide (Peptide and Tetramer Core Facility, CHUV/UNIL/LICR, Lausanne,

143 Switzerland) at 4°C for 45 minutes, followed by cell surface marker APC-A750 anti-CD8

144 (Beckman Coulter) at 4°C for 30 minutes. Virus-specific CD8 T cells (CD8$^+$multimer$^+$) were

145 then sorted on a FACSAria (BD Biosciences) flow cytometer as single cells for *ex vivo* T cell

146 repertoire analyses or as 300-1000 cells for *in vitro* cloning. For the latter sorting, T cells were

147 further cloned by limiting dilution and expanded in RPMI 1640 medium (Gibco) supplemented

148 with 8% human serum, 150 U/ml human recombinant IL-2 (a gift from GlaxoSmithKline), 1

149 μg/ml PHA (Sodiag), and 1×10^6/ml 30-Gy-irradiated allogeneic PBMCs as feeder cells.

150 Antigen-specific CD8 T cell clones were expanded by periodic (every 20-25 days)

151 restimulation with PHA, irradiated feeder cells and recombinant human IL-2, or cryopreserved

152 in 10% DMSO (Sigma-Aldrich) and stored in liquid nitrogen until further use.

153 **TCR clonotype repertoire sequencing**

154 Extensive *TRBV-CDR3* and *TRAV-CDR3* analysis were performed on *in vitro*-generated T cell

155 clones as well as on e*x vivo* sorted single T cells (9, 38). In brief, single cells were incubated

156 with a lysis/reverse transcription (RT) mix and cDNA preparation mix before undergoing

157 global cDNA amplification as detailed previously (38). T cell clones (2×10^4 cells) were directly

6

158   processed through direct cell lysis and cDNA synthesis without undergoing the global cDNA

159   amplification procedure. Each cDNA sample was then subjected to individual PCR using a set

160   of previously validated forward primers specific for the different known *TRBV* or *TRAV* gene

161   subfamilies and two reverse primers specific for the corresponding *C-beta* or *C-alpha* gene

162   segments (9). PCR products of interest were sequenced from the reverse primer (Fasteris SA).

163   Clonotypes were defined as T cell clones sharing the same *TRBV-CDR3* and *TRAV-CDR3*

164   amino acid sequences. Clonotypic primers for dominant *TRBV-CDR3* sequences were validated

165   and used in clonotypic PCRs for the determination of clonotype frequencies, as described (9).

166   TCR sequences were analyzed using SnapGene (v.4.1.9 GSL Biotech) and described according

167   to the ImMunoGeneTics (IMGT) nomenclature (39).

168   *Ex vivo* **TRBV family and clonotype repertoire analyses**

169   CD8-enriched T cells from PBMCs were initially stained with CMV-specific or EBV-specific

170   multimers as described above, followed by cell surface marker APC-A750, FITC or APC anti-

171   CD8 (Beckman Coulter) and antibodies against the different identified TRBV families as

172   indicated in the Supplemental Table 1 for 30 minutes at 4°C. Samples were acquired on a LCRII

173   cytometer (BD Biosciences) and analyzed using FlowJo 10.4.2 software (v.10.4.2, Tree Star).

174   The frequency of CMV-specific TRBV clonotypes was also assessed for each *ex vivo* TRBV

175   family identified by flow cytometry from donors BCL4 and BCL6. Briefly, antigen-specific

176   CD8 T cells, which stained positive for a given TRBV family were sorted, *in vitro* cloned and

177   *TRBV-CDR3* sequenced as described above.

178   **NTAmer staining and dissociation kinetic measurements**

179   NTAmers (Peptide and Tetramer Core Facility, CHUV/UNIL/LICR, Lausanne, Switzerland)

180   are dual-labeled pMHC multimers built on NTA-Ni^{2+}-His-tag interactions (40) and were used

181   for dissociation kinetic measurements as previously described (34, 35). Individual virus-

182   specific CD8 T cell clones or bulk virus-specific CD8 T cell populations expanded following

183   short-term *in vitro* stimulation (during 20-25 days) with PHA and irradiated feeder cells were

184   stained for 45 minutes at 4°C in PBS, 0.2% BSA and 5 mM EDTA with virus-specific

185   NTAmers, in which the HLA-A*0201 molecules were loaded with native EBV/BMFL1$_{280\text{-}288}$

186   or CMV/pp65$_{495\text{-}503}$ peptides. We also used NTAmers prepared with CD8 binding-deficient

187   HLA-A*0201 monomers (i.e. NTA CD8-null) bearing the D227K/T228A mutations in the

188   HLA α3 domain (34). NTAmer staining was assessed at 4°C on a LSRII cytometer (BD

189   Biosciences). Following 30 seconds of baseline acquisition, imidazole (100 mM) was added

190   and Cy5 fluorescence was measured during the following 10 minutes. Data were analyzed using

7

191   the kinetic module of FlowJo software (v.9.7.6, Tree Star) and modeled (1-phase exponential

192   decay) using Prism software (v.7, GraphPad).

193   CD107a degranulation and intracellular cytokine staining

194   HLA-A*0201-positive TAP-deficient T2 cells were pulsed for 1 hour at 37°C with serial

195   dilutions of native EBV/BMFL1$_{280\text{-}288}$ or CMV/pp65$_{495\text{-}503}$ peptides, washed, and incubated

196   with virus-specific CD8 T cell clones at an E/T ratio of 1:2 for 6 hours in the presence of FITC

197   anti-CD107a (BD Pharmingen) and brefeldin A (10 μg/ml, Sigma-Aldrich). EBV/BMFL1$_{280\text{-}}$

198    $_{288}$ peptide was preincubated for 1 hour at room temperature with the disulfide-reducing agent

199   TCEP (2 mM, Pierce Biotechnology). Cells were then stained in PBS, 0.2% BSA and 5 mM

200   EDTA with Pacific Blue anti-CD8α (Beckman Coulter) at 4°C for 30 minutes, fixed in PBS

201   1% formaldehyde, 2% glucose, and 5 mM NaN$_3$ for 20 minutes at room temperature, and finally

202   stained in PBS, 0.2% BSA, 5 mM EDTA and 0.1% saponin (Sigma-Aldrich) with PE-Cy7 anti-

203   IFNγ and A700 anti-TNFα (BD Pharmingen) for 30 minutes at 4°C before acquisition on a

204   LSRII (BD Biosciences) cytometer. Percentages of CD107a/cytokine-positive T cells were

205   analyzed using FlowJo software (v.10.4.2, Tree Star). EC$_{50}$ values were derived by dose-

206   response curve analysis (log[agonist] versus response) using Prism software (v.7, GraphPad).

207   Chromium release cytolytic assay

208   Chromium release cytolytic assays were performed as following; ^{51}Cr-labeled HLA-A*0201-

209   positive TAP-deficient T2 cells were pulsed with serial dilutions of native EBV/BMFL1$_{280\text{-}288}$

210   or CMV/pp65$_{495\text{-}503}$ peptides, and incubated with virus-specific CD8 T cell clones at an E/T

211   ratio of 10:1 for 4 hours. EBV/BMFL1$_{280\text{-}288}$ peptide was preincubated for 1 hour at room

212   temperature with the disulfide-reducing agent TCEP (2 mM, Pierce Biotechnology).

213   Percentages of specific lysis were calculated as $100 \times$ (experimental − spontaneous

214   release)/(total − spontaneous release). EC$_{50}$ values were derived by dose-response curve

215   analysis (log[agonist] versus response) using Prism software (v.7, GraphPad).

216   Surface marker modulation assay

217   Virus-specific CD8 T cell clones were incubated for 24 hours in the absence or presence of

218   HLA-A*0201 unlabeled multimers loaded with native EBV/BMFL1$_{280\text{-}288}$ (1 μg/ml) or

219   CMV/pp65$_{495\text{-}503}$ (0.01 μg/ml) peptides. Cells were then stained in PBS, 0.2% BSA, 5 mM

220   EDTA and 0.2% NaN$_3$ with A700 anti-CD137 and BV421 anti-PD-1 (Biolegend) at 4°C for 30

221   minutes and acquired on a LSRII flow cytometer (BD Biosciences). Vivid Aqua (Invitrogen)

222   was used to discriminate live/dead cells. The level of expression of each marker (geometric

8

223   mean fluorescence intensity [gMFI]) was analyzed using FlowJo software (v.10.4.2, Tree Star)

224   and their modulation was calculated as (gMFI of stimulated cells)/(gMFI of unstimulated cells).

225   **RNA sequencing analysis**

226   CD8-enriched from PBMCs were stained with CMV-specific multimers followed by cell

227   surface marker APC-A750, FITC or APC anti-CD8 (Beckman Coulter) and antibodies against

228   the different identified TRBV families as described above (Suppl. Table 1). CMV/TRBV-

229   specific CD8 T cells were then sorted on a FACSAria (BD Biosciences) flow cytometer in

230   RNAlater Stabilization Solution (Invitrogen). Total RNA from the *ex vivo* sorted cells (between

231   300 to 8000 cells) was extracted using the RNeasy Micro Kit (Qiagen) according to the

232   manufacturer's protocol. RNA-sequencing libraries were prepared using the Clontech

233   SMART Seq v4 Ultra Low RNA kit (Clontech Laboratories, Inc.) and sequencing was

234   performed on the Illumina HiSeq 2500. Library preparation, sequencing and analyses were

235   performed by the Lausanne Genomic Technologies Facility (UNIL, Lausanne, Switzerland) as

236   described in detail in the Supplemental Data section.

237   **NanoString analysis**

238   Total RNA from CMV-specific CD8 T cell clonotypes of high versus low TCR binding avidity

239   was extracted using the RNeasy Mini Kit (Qiagen) according to the manufacturer's protocol.

240   The NanoDrop spectrophotometer (Thermo Scientific) was used to quantify the RNA. Cell

241   lysates were directly analyzed for the expression of 770 immune-related genes (human

242   PanCancer immune profiling panel) by the NanoString nCounter System and data were further

243   processed using the NanoString nSolver analysis software (v.4) by normalizing with

244   housekeeping genes.

245   **Surface marker expression analysis**

246   Virus-specific CD8 T cell clones were stained in PBS, 0.2% BSA, 5 mM EDTA and 0.2% NaN_3

247   with APC anti-LILRB1/CD85j (eBioscience), PE-CF594 anti-CD57 (BD Horizon), and BV421

248   anti-PD-1 (Biolegend) at room temperature for 30 minutes and acquired on a LSRII flow

249   cytometer (BD Biosciences). Vivid Aqua (Invitrogen) was used to discriminate live/dead cells.

250   The level of expression of each marker (geometric mean fluorescence intensity [gMFI]) was

251   analyzed using FlowJo software (v.10.4.2, Tree Star).

252   ***In vitro* blocking experiments**

253   For T cell proliferation assays, 30-Gy-irradiated HLA-A*0201-positive PBMCs were pulsed 1

254   hour at 37°C with the native CMV/$pp65_{495-503}$ (10^{-8}M) peptide, washed, and incubated with

9

255   CellTraceViolet-stained CMV-specific CD8 T cell clones (Invitrogen) at an E/T ratio of 1:1 in

256   RPMI 1640 medium (Gibco) supplemented with 8% human serum and 50 U/ml human

257   recombinant IL-2 (GlaxoSmithKline) in the presence of monoclonal IgG_{2B} mouse anti-human

258   LILRB1 (CD85j, ILT-2) antibody or an IgG_{2B} isotype control (5 μg/mL, R&D Systems). After

259   3 days, cells were stained in PBS with Near-IR Vivid (Invitrogen) at 4°C for 30 minutes before

260   acquisition on a LSRII (BD Biosciences) cytometer. Percentages of divided cells were analyzed

261   using the proliferation module of FlowJo software (v.10.4.2, Tree Star).

262   For CD107a degranulation and intracellular cytokine staining assays, CMV-specific CD8 T cell

263   clones were incubated for 48 hours in the presence of monoclonal IgG_{2B} mouse anti-human

264   LILRB1 antibody or an IgG_{2B} isotype control (5 μg/mL, R&D Systems). Clones were then

265   incubated with 30-Gy-irradiated HLA-A*0201-positive PBMCs previously pulsed 1 hour at

266   37°C with the native $CMV/pp65_{495\text{-}503}$ (10^{-8}M) peptide, at an E/T ratio of 1:2, in the presence

267   of FITC anti-CD107a (BD Pharmingen) and brefeldin A (10 μg/ml, Sigma-Aldrich). After 6

268   hours, T cell clones were assessed for CD107a degranulation and intracellular cytokine

269   production as described above.

270   **Statistical analyses**

271   Data were analyzed using Prism software (v.7, GraphPad) by nonparametric Mann-Whitney

272   test, Kruskal-Wallis test ($\alpha = 0.05$), Wilcoxon matched-pairs signed rank test and Spearman

273   correlations as indicated throughout the manuscript. All P values were derived using two-tailed

274   tests and $P < 0.05$ were considered significant.

10

RESULTS

Characteristics of the healthy donors

Here, we performed a comprehensive longitudinal study of the TCR-pMHC binding avidities (i.e. off-rates) on well-defined virus-specific CD8 T cell clonotype repertoires from six healthy donors latently infected with (i) both CMV and EBV (BCL4 and BCL9), (ii) CMV only (BCL6 and BCL1) or (iii) EBV only (BCL7 and BCL2). Blood was first withdrawn in 2002 (defined as T_n) when donors had an average age of 30 years (+/- 10 years) and 15 years later in 2017 (defined as T_{n+15y}) (Fig. 1A, Supp. Table 2). The proportion of CMV-specific (HLA-A*0201/pp65$_{495-503}$) and EBV-specific (HLA-A*0201/BMFL1$_{280-288}$) populations within total CD8 T cells over time was monitored by *ex vivo* fluorescent multimer staining (Fig. 1B, Supp. Table 2). No consistent pattern of frequency evolution was found among CMV-specific CD8 T cells, as that of donor BCL6 increased with time (from 1.06% to 4.08%), while the other three individuals showed reduced frequencies across the two time-points with some donor-related variations (between 0.14% to 0.97%). EBV-specific CD8 T cell populations were globally more stable during the period of 15 years, with a maximum frequency variation of 0.15% (Fig. 1B, Supp. Table 2).

TCR clonotype frequencies determined by *in vitro* T cell cloning strongly correlate with direct *ex vivo* TCR β-chain and single-cell clonotype analyses

For detailed analyses of complete TCRαβ repertoires including TCR-pMHC binding avidity characterization, large panels of *in vitro*-generated CMV-specific CD8 T cell clones were generated by single cell sorting from the four healthy individuals latently infected with CMV. The clonal composition was analyzed based on the *TRBV-CDR3* and *TRAV-CDR3* gene sequence ((9, 38), Supp. Table 3). Importantly, for each individual, the cloning procedure from samples obtained at T_n and T_{n+15y} was performed alongside, in the same experiment. To validate the repertoires represented by the *in vitro*-generated clones, we used a panel of TCRβ chain-specific (i.e. TRBV) antibodies combined with multimers for staining of PBMCs directly *ex vivo* (Supp. Fig. 1). Robust correlations were obtained with highly similar relative frequencies of co-dominant TRBV families as determined by both approaches and at the two time-points (Fig. 1C). CMV-specific T cells positive for each TRBV family from donors BCL4 and BCL6 were further sorted, *in vitro* cloned and sequenced for the *TCR-CDR3* gene motif. More than 95% of all TRBV family-recovered clones bore the corresponding *TRBV-CDR3* clonotype (Fig. 1D), demonstrating that for CMV-specific T cell populations, direct *ex vivo* TRBV family staining is a robust indicator of clonotype frequency. In addition, highly comparable

11

308 proportions of individual TCR clonotype signatures were found when using a direct *ex vivo*

309 sorted single-cell approach (Fig. 1E), in agreement with previous studies (9, 38, 41). Altogether,

310 these results indicate that our *in vitro* cloning strategy did not introduce major repertoire biases

311 and allows the high-resolution molecular characterization of the TCR clonotype repertoire in

312 individual virus-specific CD8 T cell sub-populations.

313 **CMV-specific TCRαβ clonotype dominance varies over time**

314 We next assessed the evolution of the TCRαβ clonal repertoire composition and dominance

315 patterns over the observation period of 15 years. In line with our previous observations (9),

316 CMV-specific CD8 T cell repertoires were highly restricted, with the presence of 2 to 6

317 dominant or sub-dominant clonotypes (Fig. 1F). All clonotypes identified in the peripheral

318 blood of the four healthy donors at the early time-point were also found 15 years later (Fig. 1F),

319 indicating a remarkable long-term persistence of a restricted clonal repertoire. Yet, some of

320 these clonotypes were found to decrease in frequency from T_n to T_{n+15y} (clonotypes depicted by

321 grey arcs), whereas others increased (i.e. clono 3, 7, 9 and 11) with time or remained relatively

322 stable (clono 4, 12, 13, 14, and 15). This implies a preferential selection of certain clonotypes

323 over others throughout the course of persistent CMV infection in healthy donors. This

324 observation was particularly evident in donors BCL4, BCL6 and BCL1. In contrast, the TCR

325 clonotype composition of BCL9 remained relatively stable over the 15 years, with only two

326 clonotypes, representing 20% of the repertoire, showing frequency variation over time (clono

327 10 and clono 11; Fig. 1F). Similar changes in frequency were found when analyzing CMV-

328 specific populations at the *ex vivo* TRBV-chain family level (Supp. Fig. 1B).

329 **EBV-specific TCRαβ clonotype dominance and evolution remains highly stable over**

330 **extended periods of time**

331 The TCRαβ clonotype signature of the EBV/BMFL1-specific CD8 T cell repertoire in four

332 healthy individuals, with donors BCL4 and BCL9 sharing T cell responses against CMV/pp65,

333 was determined at T_n and T_{n+15y}. EBV-specific repertoires obtained from single T cells

334 generated by *in vitro* cloning again showed comparable proportions of TRBV family usage by

335 *ex vivo* anti-TRBV staining, resulting in a high correlation coefficient (Fig. 2A). Despite

336 presenting a diverse clonotype composition with 10 to 25 dominant or subdominant clonotypes

337 per donor (Supp. Table 4), EBV-specific T cell repertoires were highly biased in their *TRBV*

338 and *TRAV* family usage, in agreement with previous studies (9, 18, 19, 42, 43). Notably, the

339 TCR clonotypes that dominated EBV-specific T cell responses preferentially used BV20,

12

340   BV29, BV2, BV14 and BV6 as well as AV5 and AV12-1 gene segments (according to IMGT's

341   nomenclature; Fig 2B, Supp. Table 4). In sharp contrast to CMV-specific T cell responses, and

342   despite a high degree of polyclonality, the EBV clonal repertoires showed a remarkable stability

343   during the observation period of 15 years, with only minor changes or fluctuations in their

344   clonotype frequency between the time-points and for each healthy individual (Fig. 2C).

345   **CMV-specific T cell clonotypes that expand over time express TCRs of lower binding**

346   **avidity than those that decrease**

347   To better evaluate how CMV-specific CD8 T cell repertoires evolve during latent infection, we

348   defined three groups of clonotypes based on their frequency changes over time (Fig. 1F, Supp.

349   Fig. 1B), i.e. decreasing, increasing/expanding and stable clonotypes, the latter regrouping

350   clonotypes with frequency variation lower than 5% (Fig. 3A). In donor BCL6, for whom we

351   had two additional time-points (i.e. T_{n+4y} and T_{n+16y}), we observed that the relative frequency

352   increase or decrease of a specific clonotype was a gradual and continuous process during the

353   follow-up (Fig. 3B, left panel). As low-avidity CMV-specific CD8 T cells that re-express

354   CD45RA were reported to accumulate in elderly donors with aging (32), we next sought to

355   determine whether differences in TCR binding avidity between CMV-specific T cell clonotypes

356   could account for the changing patterns of dominance found in healthy donors throughout the

357   course of latent infection. Quantitative TCR-pMHC dissociation rates (i.e. k_{off}) were assessed

358   by two-color reversible NTAmers (NTA) (34, 40) and applied to several clones of each

359   identified CMV-specific TCR$\alpha\beta$ clonotype. Interestingly, as shown in Figure 3C, clonotypes

360   that declined in frequency over time (i.e. decreasing clonotypes) mostly displayed relatively

361   slow off-rates (i.e. low k_{off}/high binding avidity) ranging between 0.015 s^{-1} and 0.0011 s^{-1}, while

362   increasing clonotypes generally showed fast off-rates (i.e. high k_{off}/low binding avidity), with

363   the exception of clono 11 from BCL9 of higher binding avidity. Clonotypes with relatively

364   stable frequencies over the 15 years exhibited variable off-rates (from 0.05 s^{-1} to 0.0007 s^{-1}).

365   Importantly, on average, CMV-specific T cell clonotypes that expanded over time bore TCRs

366   of significantly lower binding avidity (i.e. high k_{off}) compared to those that decreased (Fig. 3D).

367   **Enrichment of CMV-specific T cell clonotypes with reduced functional avidity and higher**

368   **CD8 binding dependency over time**

369   We recently reported that the TCR-ligand off-rate is a stable and reliable biomarker, very useful

370   for assessing *ex vivo* antigen-specific CD8 T cell responses (35). We tested the robustness of

371   this parameter by comparing off-rates from CMV-specific T cell clones expressing the same

372   TCR$\alpha\beta$ clonotype, but isolated from blood samples at different time-points. For instance, each

13

373   identified CMV-specific T cell clonotype derived from donor BCL6 between T_n and T_{n+15y}

374   revealed a highly comparable and stable k_{off} value (Fig. 3B, right panel), in contrast to its

375   frequency variation observed over time (Fig. 3B, left panel). Furthermore, we observed a strong

376   positive correlation between k_{off} rates obtained at T_n and T_{n+15y} from the four CMV-positive

377   individuals studied (Fig. 3E). Similar data (Supp. Fig. 2) were found when assessing off-rates

378   using mutated NTAmers, that were deficient for CD8 binding to pMHC (i.e. CD8-null NTA).

379   These observations demonstrate that for a given TCRαβ clonotype, the TCR-pMHC off-rate

380   remains highly conserved over extended periods of time, while this was not the case for the

381   clonotypic prevalence.

382   To further investigate the parameters driving clonal evolution, we studied the CD8 binding

383   contribution to the overall TCR-pMHC avidity on the different identified CMV-specific

384   TCRαβ clonotypes using CD8 binding-deficient NTAmers. Of note, T cell clonotypes that were

385   highly CD8 binding-dependent could not be stained by mutated NTAmers, thus making

386   dissociation rate measurements technically impossible to record. These non-binder clones are

387   depicted in the grey lower box (Fig. 3F). We found that 100% of the CMV-specific CD8 T cell

388   clonotypes that decreased over time were CD8 binding-independent (Fig. 3G), as all clonotypes

389   were able to bind the CD8-binding deficient NTAmers with a relatively high avidity (mean k_{off}

390   of 0.022 s^{-1}) (Fig. 3F). On the other hand, 75% of increasing clonotypes were CD8 binding-

391   dependent, again with the exception of clono 11 from BCL9, which was CD8 binding-

392   independent (Fig. 3F and 3G). Importantly, each TCR clonotype subgroup (i.e. decreasing,

393   increasing and stable) revealed a similar TCR-pMHC off-rate threshold defining CD8 binding

394   dependency ($k_{off} > 0.0106$ s^{-1}; Fig. 3C and 3F). Collectively, these data indicate that TCR off-

395   rates and CD8 binding dependency have a clear impact on the clonal dominance over time

396   within CMV-specific CD8 T cell repertoires, with the preferential long-term enrichment of

397   clonotypes of fast TCR-pMHC off-rates and greater dependency on CD8 coreceptor binding

398   (i.e. low binding avidity; Fig. 3H). Conversely, CMV-specific clonotypes with slow TCR off-

399   rates and reduced CD8 binding dependency (i.e. high binding avidity) were those that declined

400   in frequency over the 15 years.

401   We also assessed whether this enrichment of low avidity clonotypes over time had an impact

402   on the functional quality of CMV-specific CD8 T cell repertoires. As expected (35), T cell

403   clonotypes of low binding avidity presented decreased functional avidity (i.e. EC$_{50}$) for CD107a

404   degranulation as well as a trend for reduced killing capacity compared to the high avidity ones

405   (Fig. 3I). They produced less TNFα and IFNγ cytokines and were less susceptible to antigen-

14

406 specific activation as shown by the diminished expression of PD-1 following peptide
407 stimulation (Fig. 3I). These results indicate that CMV-specific T cell clonotypes of fast TCR
408 off-rates and increased CD8 binding dependency displayed reduced functional capacity.

409 **TCR binding avidity and CD8 binding dependency of EBV-specific T cell clonotypes are**
410 **associated with particular TRBV family usage**

411 To evaluate the impact of TCR binding avidity on EBV-specific CD8 T cell responses, we next
412 measured k_{off} rates using WT (i.e. NTA) and CD8 binding-deficient (i.e. CD8-null NTA)
413 NTAmers on several clones of each individually identified TCRαβ clonotype (Figure 4). In
414 line with the data obtained for CMV clonotypes, similar k_{off} were found for the same EBV-
415 specific TCRαβ clonotypes between T_n and T_{n+15y} by WT (Fig. 4A) and mutated NTAmers
416 (Fig. 4B). Despite their great stability in terms of frequency (Fig. 4C) over the 15 year period,
417 the different TCR clonotypes covered a large range of binding avidities and CD8 binding-
418 dependency rates between single healthy donors (Fig. 4D and F, Supp. Fig 3). Strikingly, TCR
419 binding avidity and CD8 binding-dependency were closely related to distinct TRBV family
420 usage, but to a weaker extent to TRAV (Supp. Fig. 3E). Specifically, TRBV29 clonotypes
421 (depicted as red symbols) displayed significantly faster TCR off-rates (mean k_{off} of 0.038 s^{-1})
422 and were largely CD8 binding-dependent compared to TRBV20 clonotypes (shown as blue
423 symbols) of slower TCR off-rates (mean k_{off} of 0.0075 s^{-1}) and increased CD8 binding-
424 independency (Fig. 4E and G). TRBV2, TRBV14 and TRBV6 clonotypes presented TCRs of
425 intermediate dissociation rates, (mean k_{off} of 0.010 s^{-1}) and between 33% to 67% were CD8
426 binding-independent (Fig. 4E and G). These differences in TCR binding avidity between EBV-
427 specific T cell clonotypes and related to particular TRBV families were, to some degree, further
428 observed at the functional avidity level. Specifically, TRBV29 clonotypes produced slightly
429 less CD107a and cytokines (IFNγ; TNFα), and were less able to kill target cells than TRBV20
430 clonotypes (Fig. 4H). No major differences were found when assessing fold-change of PD-1
431 expression upon peptide stimulation. In summary, these data indicate that TCR-pMHC-CD8
432 binding avidity differentially impacts on the clonotype evolution of CMV- versus EBV-specific
433 CD8 T cell responses during latent infection over extended periods of time.

434 **Decline in overall avidity of CMV- but not EBV-specific memory CD8 T cell repertoires**
435 **over time**

436 We hypothesized that the enrichment of CMV- but not EBV-specific T cell clonotypes of low
437 TCR binding avidities observed between T_n and T_{n+15y} would lead to an overall decline in TCR
438 avidity of the CMV-specific repertoire. To address this question, we estimated the overall k_{off}

15

439   at the viral epitope-specific CD8 T cell population level for the six healthy donors at T_n and

440   T_{n+15y} (Figure 5). Due to the limited numbers of *ex vivo* antigen-specific T cells, sorted total

441   CMV-specific or EBV-specific CD8 T cells were first non-specifically expanded during short-

442   term *in vitro* cultures before being assessed for their clonal composition by TRBV family

443   staining. We found strong correlations with the TRBV frequencies obtained by *in vitro* cloning,

444   confirming that no major bias was introduced by this strategy (Fig. 5A). We then performed

445   off-rate measurements with NTAmers on CMV-specific bulk T cells from T_n and T_{n+15y} samples

446   and observed faster dissociation rates at the later time-point, revealing a significant decrease in

447   the overall TCR binding avidity over time in three out of four donors (i.e. BCL4, BCL6 and

448   BCL1) (Fig. 5B and C). Off-rates from BCL9 samples were highly heterogenous (Fig. 5C) due

449   to the presence of two distinct NTAmer staining-based dissociation sub-populations (Fig 5B),

450   preventing accurate dissociation fitting and computation. Nonetheless, when we compared the

451   proportion of CMV-specific T cells representative of the slower dissociation curves between

452   the two time-points (Fig. 5B, BCL9, see FACS-gated region), there was also a significant

453   decline in the percentage of these slow dissociating cells over time (Fig. 5D).

454   In most cases, EBV-specific *ex vivo* generated bulk T cell populations were not representative

455   of the clonal repertoire (data not shown), likely due to the high clonotype diversity of EBV-

456   specific repertoires (Fig. 2). Yet, EBV-specific bulk repertoire compositions from donor BCL7

457   correlated well with the clonal ones (Fig. 5E), thus allowing direct overall avidity assessment

458   by NTAmers. For this donor, we observed a high stability of the overall off-rates obtained

459   between T_n and T_{n+15y} (Fig. 5E). We next used indirect methods to estimate the overall TCR

460   binding avidity of EBV-specific repertoires during the observation period of 15 years. First, in

461   donors BCL2 and BCL9, we assessed NTAmer-based k_{off} of 60 *in vitro* generated EBV-specific

462   CD8 T cell clones for each time-point without further clonotype characterization or selection,

463   thus representing an unbiased repertoire, and observed no significant differences in their global

464   TCR off-rates over time (Fig. 5F). Moreover, we reconstituted the overall repertoire avidity of

465   each EBV-positive donor by *in silico* pooling of the k_{off} values obtained for most of the

466   identified TCR$\alpha\beta$ clonotypes according to their respective prevalence. Again, no significant

467   difference in the global TCR off-rates (i.e. k_{off}) was found between both time-points in any of

468   the EBV-positive donors (Fig. 4G). In contrast, similarly reconstituted off-rates of CMV-

469   specific T cell repertoires displayed a comparable overall decline over time as observed by

470   direct NTAmer-based avidity measurements (data not shown).

16

471   Altogether, these observations show that the overall TCR-pMHC binding avidities of the EBV-

472   specific CD8 T cell response were highly stable over time, in contrast to those comprising the

473   CMV-specific repertoire, which were significantly reduced over the 15 year period.

474   **Preferential accumulation of *LILRB1* gene expression in high avidity CMV-specific T cell**

475   **clonotypes over time**

476   To gain further insight into the mechanisms underlying the selection of low avidity clonotypes

477   over time in long-term CMV-specific CD8 T cell responses, we performed a global

478   transcription profiling by RNA sequencing on *ex vivo* sorted CMV/TRBV-specific sub-

479   populations of three CMV-positive donors at T_n and T_{n+15y}. We decided to exclude BCL9 from

480   these screening analyses because this particular donor presented a more diverse clonotype

481   repertoire that was stable over time, contrasting with the preferential accumulation of low

482   binding avidity clonotypes observed in the other donors (Fig. 1 and 3). As demonstrated in Fig.

483   1D, the TRBV-specific sub-populations were highly representative of each clonotype, with the

484   exception of the TRBV6-5-specific sub-population from BCL6, composed of two clonotypes

485   (clono 5 and 6) but sharing similar biological characteristics (i.e. high TCR binding avidity and

486   decreasing frequency over time). As depicted by volcano plots (Fig. 6A) and hierarchical

487   clustering (Fig. 6B, Supp. Fig. 4A), more differentially expressed genes were found over time

488   (i.e. T_n versus T_{n+15y}) than between high (i.e. slow off-rates) versus low (i.e. fast off-rates) TCR

489   binding avidity clonotypes. Nonetheless, hierarchical clustering highlighted the presence of 9

490   genes that were found to be upregulated in high avidity CMV-specific CD8 T cell clonotypes

491   when compared with low TCR binding avidity ones (Fig. 6B). Interestingly, one of these

492   upregulated genes encoded for the inhibitory receptor LILRB1 (CD85j/ILT-2/LIR-1), which

493   expression on CD8 T cells has been shown to increase with age and in the context of chronic

494   CMV infection (44, 45). Moreover, *LILRB1* was not only significantly upregulated in high

495   avidity CMV-specific clonotypes but also at the later T_{n+15y} time-point (Fig. 6C). Consistently,

496   the highest *LILRB1* gene expression was also found in those CMV-specific T cell clonotypes

497   defined as decreasing based on their reduced frequencies over time and mainly consisted of

498   high avidity T cells at both time-points (Fig. 6D). In contrast, expanding TCRαβ clonotypes

499   displayed globally lower normalized *LILRB1* expression. Finally, similar data were obtained

500   when gene expression analyses by NanoString were performed on two representative CMV-

501   specific CD8 T cell clones of different clonotypes from BCL4, i.e. a high avidity/decreasing

502   clonotype (clono 1) and a low avidity/increasing clonotype (clono 3) (Fig. 7A). *LILRB1* was

17

503 among the top genes whose expression was significantly elevated among the high avidity

504 clonotypes, both at rest and upon CMV/pp65-specific-stimulation (Fig. 7A).

505 **Differential impact of LILRB1 blockade on proliferation versus cytokine production of**

506 **LILRB1^{high} expressing CMV-specific CD8 T cell clones**

507 To further explore the role of differential *LILRB1* expression on CMV-specific TCRαβ

508 clonotype evolution, we examined LILRB1 surface expression by flow cytometry in our panel

509 of *in vitro*-generated CMV-specific CD8 T cell clones, including donor BCL9. Compatible with

510 mRNA data, levels of LILRB1 were found to be significantly increased in high avidity

511 TCRαβ clonotypes from all CMV donors when compared to low avidity ones, as well as in

512 clonotypes from T_{n+15y} compared to those derived from T_n (Fig. 7B). Comparable trends were

513 observed when we focused our analysis on donor BCL9 alone (Supp. Fig. 4B). We further

514 found that those clonotypes that underwent contraction over time (i.e. high TCR binding

515 avidity) expressed higher levels of LILRB1 than the increasing/expanding ones (i.e. low TCR

516 binding avidity; Fig. 7C). LILRB1 expression was also associated with enhanced levels of the

517 marker of senescence CD57, while PD-1 expression was reduced (Fig. 7D and E). Stable

518 clonotypes showed intermediate levels of LILRB1, CD57 and PD-1 expression, when

519 compared to increasing and decreasing clonotypes (Supp. Fig. 4C, D and E). Finally, various

520 EBV-specific CD8 T cell clonotypes expressed comparable low levels of LILRB1,

521 independently of their preferential TRBV family usage (Fig. 7F), consistent with a previous

522 study (46).

523 Lastly, we evaluated the biological significance of LILRB1 expression on proliferation,

524 CD107a degranulation and cytokine production of LILRB1^{high} expressing CMV-specific T cell

525 clones upon incubation with a LILRB1 blocking antibody or an isotype control. LILRB1

526 blockade induced an increase in the frequency of dividing cells, while it had no major effect on

527 CD107a degranulation or on cytokine (IFNγ$^+$TNFα$^+$) production following pp65-specific

528 stimulation (Fig. 7G). Together, our data are in line with recent findings showing that LILRB1

529 characterizes a population of senescent but not exhausted CMV-specific effector CD8 T cells

530 (44). Moreover, we propose that LILRB1 may play a regulatory role by inhibiting the expansion

531 of CMV-specific CD8 T cell clonotypes of higher TCR binding avidity.

18

DISCUSSION

CD8 T cells play a central role in controlling latent CMV and EBV-mediated infections. In this regard, both herpes viruses provide attractive models to study the parameters associated with the generation and maintenance of long-lived antigen-specific memory T cells. TCR-pMHC avidity has been investigated by several groups, including ours (9, 16-18), and has been proposed as a key parameter underlying TCR clonal selection and dominance in human CD8 T cell populations specific for persistent DNA viruses. Nonetheless, its precise impact on TCR clonal repertoire evolution in longitudinal studies as well as in a comparative clonal repertoire analysis against the two herpes viruses has not previously been investigated. Here, we addressed the questions of whether TCR-ligand avidity can directly drive the long-term maintenance of particular TCRαβ clonotypes and how this process is determined in latent CMV versus EBV infection. Using specifically designed reversible fluorescent pMHC multimeric complexes, we performed a comprehensive study of quantitative TCR-pMHC off-rates combined with individual virus-specific TCRαβ clonotypes in six CMV- and/or EBV-positive healthy donors, followed over a period of 15 years. Our data revealed the progressive loss of CMV/pp65 CD8 T cell clonotypes of high avidity (i.e. slow off-rates, reduced CD8 binding dependency) during long-term antigen exposure (Fig. 3 and 5), which was associated with the preferential expression of *LILRB1*/CD85j in those cells (Fig. 6 and 7). This was not the case for EBV/BMFL1-specific CD8 T cell repertoires, in which the clonal composition and distribution (i.e. dominant versus sub-dominant, slow versus fast TCR off-rates, CD8 binding-independent versus -dependent) are kept highly stable for at least 15 years. Together, these findings indicate that TCR-pMHC-CD8 binding avidity is a determining factor driving the clonal evolution of long-lasting CMV- but not EBV-specific memory CD8 T cell responses in humans.

Our observations could in part be explained by differences in the nature of these viruses during latent infection. EBV reactivation and replication in B cells occurs only sporadically, leading to intermittent cycles of T cell rest and stimulation, in contrast to CMV, which may be considered more as a smoldering chronic infection (47). There is growing evidence that CMV undergoes low-level viral replication, which potentially impacts the virus-specific CD8 T cell response (13). Specifically, the expansion of CMV-specific CD8 T cells, namely those sharing an effector-memory phenotype could be the consequence of repetitive antigen stimulation (48). With the exception of donor BCL6, we did not observe a significant increase in CMV/pp65-specific CD8 T cells over the observation period of 15 years (Fig. 1). It is possible that our study performed on middle-aged individuals (45 +/- 10 years) was still set too early in the

19

565 course of the latent phase to visualize CMV-specific T cell inflation/expansion, as observed in
566 elderly individuals (7). The majority of CD8 T cells specific for CMV were effector-
567 differentiated T_{EM} (CD28^{neg}) or T_{EMRA} and retained an activated phenotype (CD27^{low} CD127^{low}
568 CD57^{high} and Granzyme B^{high}) in contrast to the memory-differentiated T_{CM} or T_{EM} (CD28^{pos})
569 phenotype displayed by EBV-specific T cells ((8, 9, 49); Fig. 7). Importantly, fluctuations
570 within the CMV-specific clonotype composition were observed over time, contrasting with the
571 striking stability observed among EBV-specific CD8 T cell clonotypes. Altogether, these data
572 further emphasize the presence of distinct features in the CD8 T cell responses elicited by these
573 two herpes viral infections, which could to some extent be related to differing mechanisms of
574 viral latency (14).

575 At present, it still remains to be elucidated whether the remarkable stability in the clonal
576 composition and evolution of EBV-specific repertoires is a global characteristic of EBV-
577 specific T cell responses or only of responses against the EBV epitope studied here (i.e. HLA-
578 A2/BMFL$_{280-288}$). Since HLA-A2/BMLF1$_{280-288}$ is an epitope from the early protein BMLF1
579 essentially expressed during the acute phase of infection, the stability of the observed clonotype
580 repertoires over extended periods of time could potentially be explained by the relative absence
581 of epitope expression during the latent phase. Nonetheless, TCR clonotype composition and
582 distribution against HLA-A2/BMLF1$_{280-288}$ were also highly preserved during transient
583 immunological perturbations after non-myeloablative chemotherapy (41) or following lung
584 transplant under immunosuppression in the presence of EBV reactivation (42). Moreover, long-
585 lasting dominance of EBV-specific TCR$\alpha\beta$ clonotypes against two latent epitopes, with no
586 changes in the T cell hierarchy for at least 18 years has been previously reported (25).
587 Collectively, these observations, including our own study (Fig. 2), are consistent with the
588 concept that TCR$\alpha\beta$ clonotype responses against EBV, once established, show steady
589 repertoires over these long periods. Strikingly, CMV-specific T cell repertoires are also
590 maintained stable during several years ((21, 41); Fig. 3B), but extending the studied period to
591 15 years revealed signs of contraction of the clonal repertoire (Fig. 1). This latter observation
592 was especially apparent for three out of the four studied donors, and suggest that distinct
593 mechanisms regulate the long-term outcome of memory CMV- versus EBV-specific CD8 T
594 cell repertoires in healthy individuals.

595 Schober and colleagues (15) recently proposed different theoretical models of TCR repertoire
596 evolution during latent CMV infection, and to which degree this process is controlled by TCR-
597 pMHC binding avidity. One model hypothesizes an initial accumulation of high-avidity virus-

20

598   specific T cells during the early phase of latency, followed by the succession of clones of lower

599   TCR binding avidity over the course of latent infection (50). During this clonal evolution, T

600   cells of higher TCR binding avidity are progressively lost after replicative senescence due to

601   critical telomere length shortening (51, 52). Compatible with this model, we demonstrated the

602   preferential selection and expansion of CMV-specific clonotypes of lower TCR avidity and

603   higher CD8 binding dependency, compared to those that had contracted after 15 years (Fig. 3).

604   Consequently, an overall avidity decline was also observed at the CMV epitope-specific

605   population (Fig. 5). Another study, comparing donors of different age-groups, showed that low

606   avidity CMV-specific CD8 T cells largely contributed to the expanded T cell pool found in

607   older subjects (32). A recent report in the context of MCMV infection (30) revealed that during

608   the acute and early phase of latent infection (i.e. 100 days), low avidity CD8 T cells were

609   replaced by higher avidity CD8 T cells. Nonetheless, similar to human studies, longer

610   observation periods in mice might be required to reveal the contraction of high avidity clones.

611   In summary, our longitudinal analysis largely supports the model of a T cell repertoire skewing

612   towards an overall lower avidity over the course of latent CMV infection, as reported in other

613   settings of chronic antigen exposure (53, 54). This is in contrast to the highly conserved overall

614   TCR binding avidities found in EBV-specific CD8 T cell repertoires over 15 years (Fig. 5),

615   fitting an alternative model (15) which assumes that a TCR hierarchy according to TCR binding

616   avidity is established during the initial response and is kept constant over longer periods.

617   Presently, it would be interesting to compare a larger array of CMV- and EBV-specific epitopes

618   to fully appreciate the impact of TCR-ligand avidity on the long-term clonal evolution of

619   TCR$\alpha\beta$ repertoires against herpes viruses.

620   Robust techniques allowing for the large-scale *ex vivo* assessment of TCR-pMHC binding

621   kinetics at the surface of live T cells have proven technically challenging until recently. Using

622   NTAmers, we demonstrated that the k_{off} parameter represents a powerful biomarker by which

623   the functional potency of antigen-specific CD8 T cell responses can be directly evaluated (34,

624   35) and graded to better characterize their impact on the efficacy of therapeutic vaccines (55).

625   To our knowledge, the use of NTAmers on well-identified virus-specific TCR$\alpha\beta$ clonotypes as

626   shown in this study revealed, for the first time, the differential impact of TCR-pMHC binding

627   kinetics on long-term TCR clonal evolution during CMV/pp65 versus EBV/BMFL1 latent

628   infection. *In vitro* cloning by limiting dilution followed by TCR sequencing currently remains

629   the method of choice to determine TCR$\alpha\beta$ clonotype sequences simultaneously with TCR-

630   pMHC kinetic measurements at the individual T cell level. Importantly, *in vitro* cloning data

21

631 corresponded well to *ex vivo* TRBV staining followed by sorted single clonotype sequencing
632 analyses (Fig. 1 and 2). Consequently, this strategy yields an accurate representation of the
633 clonotype prevalence when studying epitope-specific populations with skewed clonotype
634 repertoires, as is the case for CMV or EBV latent infection (9, 19, 38, 41). Only one report
635 could successfully assess individual TCR-pMHC affinity (based on micropipette adhesion
636 frequency) simultaneously with its corresponding TCR sequence in a high throughput manner
637 (56). Nonetheless, the success rate in recovering paired TCR$\alpha\beta$ sequences was still restricted
638 to 20-50% (56), consistent with the technical limitations in determining TCR$\alpha\beta$ sequence
639 frequencies by other *ex vivo* single-cell RNA-Seq approaches (reviewed in (57, 58)). Moreover,
640 no study has thus far been performed on frozen human samples, therefore precluding
641 longitudinal analyses. Whilst highly promising, combined single cell TCR-pMHC affinity and
642 sequencing technologies still warrant further refinement before becoming widely applicable for
643 the immune profiling of particular TCR$\alpha\beta$ clonotypes in a straightforward manner at any time
644 and body location.

645 Another finding is that the TCR-pMHC dissociation rate further represents a robust and stable
646 determinant for a given TCR$\alpha\beta$ clonotype. For instance, we found highly comparable off-rate
647 (i.e. k_{off}) values for any studied representative of a given CMV-specific clonotype over time
648 (T_n versus T_{n+15y}; Fig. 3). This contrasted to the biological differences observed at the clonotype
649 level with changes in prevalence (Fig. 3) and in gene expression profiling (Fig. 6 and Supp.
650 Fig. 4B) over the study period. Similar data were found for off-rates from EBV-specific TCR$\alpha\beta$
651 clonotypes obtained at both time-points (Fig. 4). These observations are in agreement with
652 previous studies showing highly conserved NTAmer-based off-rates, independently of the
653 activation state (35) or the differentiation stage (55) of antigen-specific CD8 T cells. In addition,
654 Nauerth and coworkers (59) elegantly demonstrated that the TCR is the main driver of
655 measured off-rates by reporting similar off-rate values between T cell clones and TCR-
656 transduced Jurkat cells.

657 Studies performed during immune aging have provided key insights in the processes involved
658 in the long-lasting persistence of memory virus-specific CD8 T cell responses (reviewed in
659 (60)). Such as, the preferential accumulation of the inhibitory receptor LILRB1 on T cells
660 specific for CMV has been proposed as one of the phenotypic hallmarks of aging (45, 61, 62).
661 LILRB1 recognizes a wide range of classical and non-classical MHC class I molecules,
662 including UL18, a human CMV-encoded MHC class I homologue, previously shown to bind
663 LILRB1 with very high affinity (63). Recently, it has been proposed that LILRB1 may function

22

664   as a checkpoint regulator in CD8 T cell differentiation and ageing (44). Notably, blocking

665   LILRB1 binding enhanced the proliferative capacity of CMV-specific CD8 T cells without

666   altering their cytokine production (44). Here, extending on these observations, we demonstrated

667   the preferential upregulation of *LILRB1* in *ex vivo* sorted CMV-specific TCRαβ clonotypes of

668   high avidity as well as during latent infection after 15 years (Fig. 6). Consequently, clonotypes

669   that underwent clonal contraction (i.e. decline in frequency) and which mainly comprised high-

670   avidity T cells, were also those that expressed the highest levels of *LILRB1* at both time-points

671   (T_n and T_{n+15y}). At the protein level, LILRB1 surface expression was also found to be increased

672   in declining CMV-specific T cell clonotypes, correlating with partial proliferative recovery

673   upon LILRB1 blockade (Fig. 7). This was associated with enhanced expression of the

674   senescence marker, CD57, but not of PD-1. In contrast, low and similar LILRB1 expression

675   were observed in all EBV-specific CD8 TCRαβ clonotypes (Fig. 7). In agreement with these

676   findings, others have reported that CMV-specific T cells often maintain cytotoxic and cytokine-

677   producing functions, in contrast to exhausted T cells, but can show various signs of senescence

678   (reviewed in (48, 64, 65)).

679   Collectively, our data reinforce the key role driven by TCR binding avidity in tailoring CMV-

680   but not EBV-specific clonal evolution during long periods of viral latency. We further propose

681   that LILRB1 acts as an inhibitory checkpoint receptor, specifically by limiting the expansion

682   of high avidity clonotypes over the course of latent CMV infection. In the context of CMV

683   infection, repetitive exposure to antigen is a key determinant for memory inflation, and

684   therefore regulatory mechanisms that can brake CD8 T cell expansion are likely beneficial (13).

685   Such mechanisms include regulatory T cells and anti-inflammatory cytokine production, which

686   might otherwise lead to the extensive proliferation of highly antigen-sensitive T cells (i.e. TCR

687   of high binding avidity), possibly overwhelming the global T cell pool. Supporting this notion,

688   LILRB1 could therefore provide another mechanism by which memory inflation of certain

689   CMV-specific TCRαβ clonotypes might be tightly regulated during lifelong latent infection,

690   while preserving the global functional T cell repertoire.

23

691 **FIGURE LEGENDS**

692 **Figure 1. Frequencies of circulating CMV-specific CD8 TCRαβ clonotypes in healthy**

693 **donors over time. A,** Schematic representation of donor sampling. Blood samples from six

694 CMV- and/or EBV-positive healthy donors were analyzed at early (T_n) and late (T_{n+15y}) time-

695 points during latent infection. **B**, Frequencies of CMV (HLA-A2/pp65)- and EBV (HLA-

696 A2/BMFL1)-specific cells within total *ex vivo* CD8 T cells over time as determined by the

697 corresponding peptide/HLA-A2 multimers. **C,** Correlations of CMV-specific TRBV-family

698 frequencies between *ex vivo* TRBV-staining versus *in vitro* single cell cloning, in BCL4, BCL6,

699 BCL1 and BCL9 at T_n and T_{n+15y}. **D,** Frequencies of color-coded CMV-specific clonotypes per

700 TRBV family for BCL4 and BCL6. Specific *TRBV-CDR3* clonotypes were determined

701 following FACS-sorting of positive TRBV family staining and *TRBV-CDR3* sequencing. **E,**

702 Correlation of TRBV-based clonotype frequencies between *in vitro* single cell cloning and *ex*

703 *vivo* sorted single CMV-specific T cells from BCL6 and BCL8 at T_n. **C and E,** Linear

704 regression analysis with 95% confidence intervals. **F**, Quantification of co-dominant CMV-

705 specific TCRαβ clonotypes at T_n and T_{n+15y}. Results are presented as percentages of color-

706 coded clonotype frequencies by *in vitro* single-cell cloning and *TRBV/TRAV-CDR3* analyses.

707 Unique clonotypes are defined as "others" and depicted in white. Over time decreasing CMV-

708 specific T cell clonotypes are highlighted by grey arcs. Number of clones *n* are indicated.

709 **Figure 2. Frequencies of circulating EBV-specific CD8 TCRαβ clonotypes in healthy**

710 **donors over time. A,** Correlation of EBV-specific TRBV-family frequencies between *ex vivo*

711 TRBV-staining versus *in vitro* single cell cloning in BCL2 and BCL9 at T_n and T_{n+15y} (by linear

712 regression analysis with 95% confidence intervals). **B**, Cumulative frequencies of preferential

713 TRBV family usage within EBV-specific clonotypes at T_n as assessed by *in vitro* single cell

714 cloning. **C,** Quantification of co-dominant EBV-specific TCRαβ clonotypes at T_n and T_{n+15y}.

715 Results are depicted as percentages of T cell clonotypes classified according to their TRBV

716 family by *in vitro* single-cell cloning and *TRBV/TRAV-CDR3* analyses. Preferential TRBV

717 family usage is highlighted by colored arcs. Unique clonotypes are defined as "others" and

718 depicted in white. Number of clones *n* are indicated.

719 **Figure 3. Monomeric TCR-pMHC dissociation rates and CD8 binding dependency of**

720 **CMV-specific TCRαβ clonotypes in healthy donors over time. A,** Relative frequencies of

721 each CMV-specific TCRαβ clonotype at T_n and T_{n+15y} defined as decreasing (left panel),

722 increasing (middle panel) or stable (right panel) clonotypes based on their frequency evolution

723 over time from BCL4, BCL6, BCL1 and BCL9. **B,** Relative frequencies (left panel) and TCR-

24

724   pMHC dissociation rates by wild-type NTAmers (k_{off}, right panel) of each color-coded CMV-

725   specific TCRαβ clonotype from donor BCL6 at the indicated time-points. **C and F**, TCR-

726   pMHC off-rates (k_{off}) by wild-type NTAmers (**C**, NTA) or mutated NTAmers (**F**, CD8null

727   NTA) on a representative selection of CMV-specific CD8 T cell clones of each color-coded

728   TCRαβ clonotype. CD8null NTA non-binder clones are represented in the grey boxes. The

729   dotted line represents the threshold of CD8 binding dependency. **D,** Dissociation rates (k_{off}) of

730   decreasing, increasing and stable TCRαβ clonotypes. Data are representative of 5 pooled clones

731   of each clonotype and are depicted as box (25th and 75th percentiles) and whisker (min to max)

732   plots with the middle line indicating the median. Kruskal-Wallis test-derived ($\alpha = 0.05$) P values

733   are indicated with ** $P < 0.01$. **E,** Correlation of TCR-pMHC off-rates (k_{off}) by wild-type

734   NTAmers (NTA) obtained from identical TCRαβ clonotypes between T_n and T_{n+15y} (by linear

735   regression analysis with 95% confidence intervals). **G**, Proportions of CD8 binding-

736   independent TCRαβ clonotypes from decreasing, increasing and stable sub-groups, based on

737   mutated NTAmer assays (see Fig. 3F). **H**, Proportions of CD8 binding-dependent TCRαβ

738   clonotypes within CMV-specific CD8 T cell populations at T_n and T_{n+15y}. **I,** EC_{50} values from

739   CD107a degranulation, IFNγ and TNFα production and killing capacity derived from co-

740   culture assays using CMV-negative HLA-A2$^+$ T2 target cells pulsed with graded concentrations

741   of native CMV (NLV-pp65$_{495-503}$) peptide and fold-increase in PD-1 expression upon CMV

742   (NLV-pp65$_{495-503}$)-specific stimulation. Data are representative of pooled CMV-specific CD8

743   T cell clones (n = 35 to 59) categorized as high (slow off-rates, reduced CD8 binding

744   dependency) versus low (fast off-rates, increased CD8 binding dependency) binding avidity.

745   Significant differences between groups by Mann-Whitney test (two tailed); * $P < 0.05$ and ** P

746   < 0.01.

747   **Figure 4. Monomeric TCR-pMHC dissociation rates and CD8 binding dependency of**

748   **EBV-specific TCRαβ clonotypes in healthy donors over time. A and B,** Correlations of

749   TCR-pMHC dissociation rates (k_{off}) by wild-type NTAmers (**A**, NTA) or mutated NTAmers

750   (**B**, CD8null NTA) obtained from identical TCRαβ clonotypes between T_n and T_{n+15y} (by linear

751   regression analysis with 95% confidence intervals). **C,** Relative frequencies of each EBV-

752   specific color-coded TCRαβ clonotype and classified according to their TRBV family at T_n

753   and T_{n+15y} from BCL4, BCL7, BCL2 and BCL9. **D and F**, TCR-pMHC off-rates (k_{off}) were

754   assessed by wild-type NTAmers (**D**, NTA) or mutated NTAmers (**F**, CD8null NTA) on a

755   representative selection of EBV-specific T cell clones of each TCRαβ clonotype grouped per

756   color-coded TRBV family usage. CD8null NTAmer non-binder clones are represented in the

757   grey boxes. **E,** TCR-pMHC off-rates (k_{off}) of EBV-specific TCRαβ clonotypes classified

758   according to their preferential TRBV family usage. Data are depicted as box (25th and 75th

759   percentiles) and whisker (min to max) plots with the middle line indicating the median. P value

760   by Kruskal-Wallis test-derived (α = 0.05) with **** P < 0.0001. **G,** Proportions of CD8-

761   independent clonotypes TCRαβ classified according to their TRBV family, based on mutated

762   NTAmer assays (see Fig. 4F). **H,** EC_{50} values from CD107a degranulation, IFNγ and TNFα

763   production and killing capacities performed in co-culture assays using EBV-negative HLA-A2$^+$

764   T2 target cells pulsed with graded concentration of native EBV ($BMFL1_{280-288}$) peptide and fold

765   increase in PD-1 expression upon EBV ($BMFL1_{280-288}$)-specific stimulation. Data are

766   representative of pooled EBV-specific CD8 T cell clones (n = 37 to 45) categorized according

767   to their preferential TRBV family usage.

768   **Figure 5. Overall monomeric TCR-pMHC dissociation rates on total CMV- and EBV-**

769   **specific CD8 T cell populations over time. A,** Correlation of CMV-specific TRBV-family

770   frequencies between *in vitro* single cell cloning and TRBV-staining on *ex vivo* expanded CMV-

771   specific bulk T cell populations from BCL4, BCL6, BCL1 and BCL9 at T_n and T_{n+15y} (by linear

772   regression analysis with 95% confidence intervals). **B,** Representative FACS-based wild-type

773   NTAmer dissociation curves obtained from *ex vivo* expanded CMV-specific bulk populations

774   at T_n and T_{n+15y}. Imidazole was added after 30s of baseline recording. Insets show the gating

775   region used to estimate the proportion of CMV-specific T cells of slower off-rates in donor

776   BCL9. **C,** Dissociation rate (k_{off}) values derived from *ex vivo* expanded CMV-specific bulk

777   populations at T_n and T_{n+15y}. Data are representative of pooled values from 1 to 4 independent

778   experiments with the middle line indicating the mean value. P values by Mann-Whitney test

779   (two tailed) with ** P < 0.01 and *** P < 0.001 and by Kruskal-Wallis test (α = 0.05) with * P <

780   0.05 and ** P < 0.01. **D,** Percentage of slow dissociating CMV-specific bulk cells from BCL9

781   at T_n and T_{n+15y} based on the quantification of slow FACS-gated dissociation curves (see Fig.

782   5B, BCL9). P values by Mann-Whitney test with ** P < 0.01. **E,** Data as described for A (top

783   left), B (bottom panel) and C (top right) for EBV-specific bulk populations from donor BCL7.

784   **F,** TCR-pMHC off-rate (k_{off}) values from 60 *in vitro* generated EBV-specific T cell clones

785   without further clonotype characterization or selection at T_n and T_{n+15y}. **G,** Overall repertoire

786   avidity of each donor by *in silico* pooling of k_{off} data for most identified EBV-specific TCRαβ

787   clonotypes according to their prevalence at T_n and T_{n+15y}. **C, E and F,** ns; non significant.

788   **Figure 6: Gene expression of *ex vivo* sorted CMV-specific TRBV-based clonotypes. A,**

789   Volcano plots showing differentially expressed genes between T_n and T_{n+15y} (left panel) and

26

790 between high- and low-avidity (right panel) CMV-specific CD8 clonotypes. Each red dot

791 represents an individual gene with a False Discovery Rate (FDR) < 0.1 (horizontal dotted line).

792 **B**, Heatmap plot based on the 19 differentially expressed genes between high- and low-avidity

793 CMV-specific clonotypes FDR < 0.1). Normalized expression level was transformed (DESeq2

794 function rlog), center and variance scaled by gene. Red indicates overexpression and blue

795 underexpression relative to the gene mean expression. **C**, Direct comparison of *LILRB1*

796 expression (as normalized counts) between low- and high-avidity CMV-specific clonotypes

797 (left panel) and between T_n and T_{n+15y} (right panel). D, *LILRB1* expression (normalized counts)

798 in decreasing (in blue) and increasing (in red) CMV-specific clonotypes at T_n and T_{n+15y}. **C-D**.

799 The middle line indicating the mean and P values by Mann-Whitney test (two tailed) with * P

800 < 0.05 and ** P < 0.01. **A-D.** Gene expression data were generated by RNA sequencing on *ex*

801 *vivo* sorted CMV/TRBV-specific sub-populations from CMV-positive BCL4, BCL6 and BCL1

802 at T_n and T_{n+15y}.

803 **Figure 7: Surface expression of LILRB1 and functional effect of LILRB1 blockade on**

804 **CMV-specific CD8 TCRαβ clonotypes. A**, Nanostring-based gene expression on two

805 representative CMV-specific TCRαβ clonotypes from BCL4, i.e. a high avidity/decreasing

806 clonotype (clono 1) versus a low avidity/increasing clonotype (clono 3), at resting and upon

807 CMV/pp65-specific stimulation. Data are presented as gene expression ratio of clono 1/clono3.

808 **B**, Baseline surface expression levels (geometric mean fluorescence intensity [gMFI]) of

809 LILRB1 in high- and low-avidity CMV-specific clonotypes and in clonotypes from T_n and

810 T_{n+15y}. **C-E,** Representative FACS-based staining (left panels) and baseline surface expression

811 levels (gMFI) (right panels) of LILRB1 (**C**), CD57 (**D**) and PD-1 (**E**) in decreasing (in blue)

812 and increasing (in red) CMV-specific clonotypes at T_n and T_{n+15y}. **B-E**, Data are representative

813 of a selection of pooled clones and are depicted as box (25th and 75th percentiles) and whisker

814 (min to max) plots with the middle line indicating the median. P values by Mann-Whitney test

815 (two-tailed) with * P < 0.05 and ** P < 0.01. **F,** Baseline surface expression levels (gMFI) of

816 LILRB1 in EBV-specific TCRαβ clonotypes classified according to their TRBV family. **G**,

817 Frequencies of CFSE-labeled divided T cell clones (top left) and of CD107a- and IFNγ+TNFα+-

818 expressing T cell clones (bottom panels) after CMV pp65-specific stimulation in the presence

819 of anti-LILRB1 or an isotype control antibody. P values by Wilcoxon matched-pairs signed

820 rank test (two-tailed) with ** P < 0.01; ns, non significant.

27

28
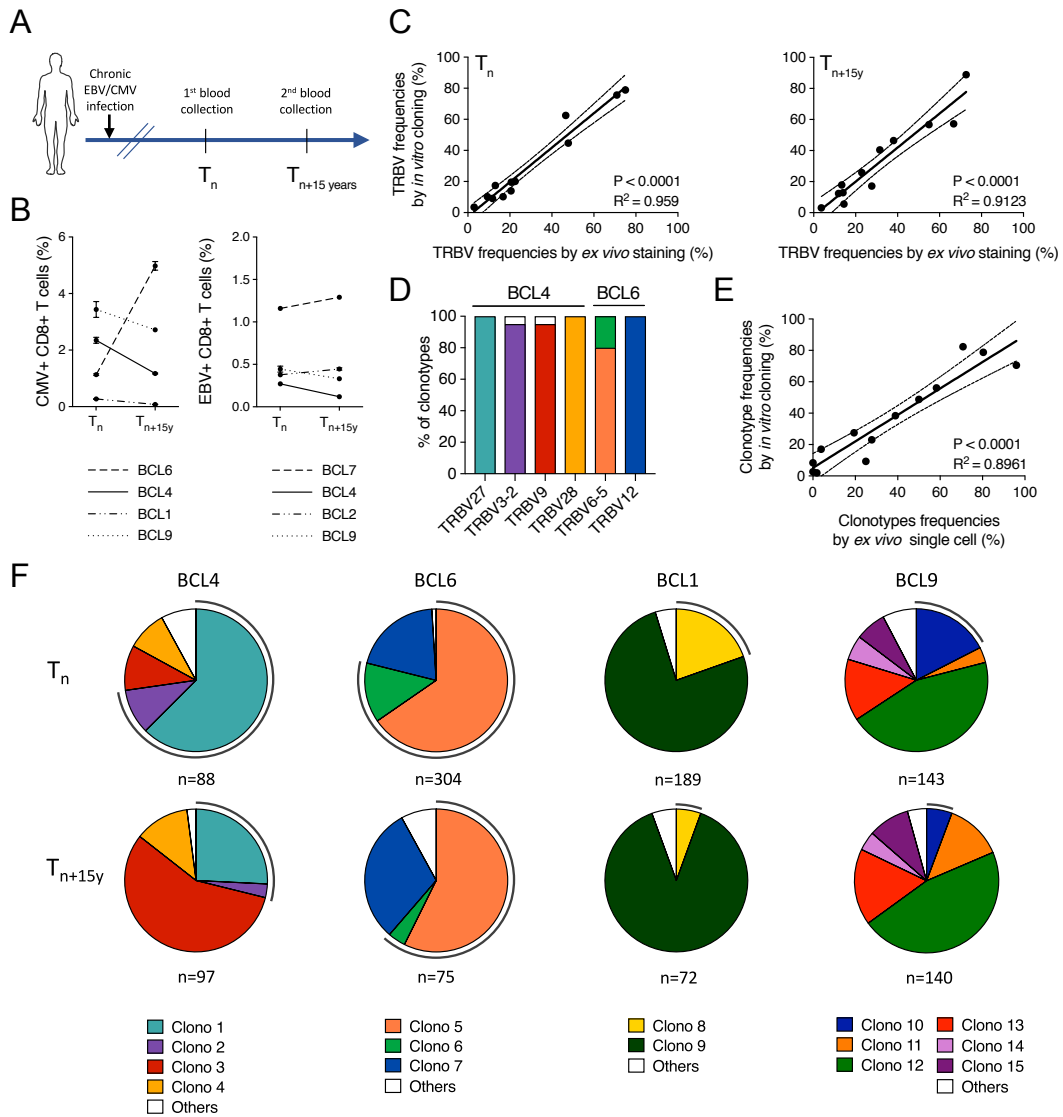
REFERENCES

1. Griffiths P, Baraniak I, and Reeves M. The pathogenesis of human cytomegalovirus. *J Pathol.* 2015;235(2):288-97.
2. Hislop AD, Taylor GS, Sauce D, and Rickinson AB. Cellular responses to viral infection in humans: lessons from Epstein-Barr virus. *Annu Rev Immunol.* 2007;25:587-617.
3. Hislop AD, Annels NE, Gudgeon NH, Leese AM, and Rickinson AB. Epitope-specific evolution of human CD8(+) T cell responses from primary to persistent phases of Epstein-Barr virus infection. *J Exp Med.* 2002;195(7):893-905.
4. Catalina MD, Sullivan JL, Bak KR, and Luzuriaga K. Differential evolution and stability of epitope-specific CD8(+) T cell responses in EBV infection. *J Immunol.* 2001;167(8):4450-7.
5. Karrer U, Sierro S, Wagner M, Oxenius A, Hengel H, Koszinowski UH, et al. Memory inflation: continuous accumulation of antiviral CD8+ T cells over time. *J Immunol.* 2003;170(4):2022-9.
6. Sylwester AW, Mitchell BL, Edgar JB, Taormina C, Pelte C, Ruchti F, et al. Broadly targeted human cytomegalovirus-specific CD4+ and CD8+ T cells dominate the memory compartments of exposed subjects. *J Exp Med.* 2005;202(5):673-85.
7. Vescovini R, Biasini C, Fagnoni FF, Telera AR, Zanlari L, Pedrazzoni M, et al. Massive load of functional effector CD4+ and CD8+ T cells against cytomegalovirus in very old subjects. *J Immunol.* 2007;179(6):4283-91.
8. Appay V, Dunbar PR, Callan M, Klenerman P, Gillespie GM, Papagno L, et al. Memory CD8+ T cells vary in differentiation phenotype in different persistent virus infections. *Nat Med.* 2002;8(4):379-85.
9. Iancu EM, Corthesy P, Baumgaertner P, Devevre E, Voelter V, Romero P, et al. Clonotype selection and composition of human CD8 T cells specific for persistent herpes viruses varies with differentiation but is stable over time. *J Immunol.* 2009;183(1):319-31.
10. Gillespie GM, Wills MR, Appay V, O'Callaghan C, Murphy M, Smith N, et al. Functional heterogeneity and high frequencies of cytomegalovirus-specific CD8(+) T lymphocytes in healthy seropositive donors. *J Virol.* 2000;74(17):8140-50.
11. Snyder CM, Cho KS, Bonnett EL, van Dommelen S, Shellam GR, and Hill AB. Memory inflation during chronic viral infection is maintained by continuous production of short-lived, functional T cells. *Immunity.* 2008;29(4):650-9.
12. Hertoghs KM, Moerland PD, van Stijn A, Remmerswaal EB, Yong SL, van de Berg PJ, et al. Molecular profiling of cytomegalovirus-induced human CD8+ T cell differentiation. *J Clin Invest.* 2010;120(11):4077-90.
13. Welten SPM, Baumann NS, and Oxenius A. Fuel and brake of memory T cell inflation. *Med Microbiol Immunol.* 2019.
14. Torti N, and Oxenius A. T cell memory in the context of persistent herpes viral infections. *Viruses.* 2012;4(7):1116-43.
15. Schober K, Buchholz VR, and Busch DH. TCR repertoire evolution during maintenance of CMV-specific T-cell populations. *Immunol Rev.* 2018;283(1):113-28.
16. Trautmann L, Rimbert M, Echasserieau K, Saulquin X, Neveu B, Dechanet J, et al. Selection of T cell clones expressing high-affinity public TCRs within Human cytomegalovirus-specific CD8 T cell responses. *J Immunol.* 2005;175(9):6123-32.
17. Day EK, Carmichael AJ, ten Berge IJ, Waller EC, Sissons JG, and Wills MR. Rapid CD8+ T cell repertoire focusing and selection of high-affinity clones into memory following primary infection with a persistent human virus: human cytomegalovirus. *J Immunol.* 2007;179(5):3203-13.
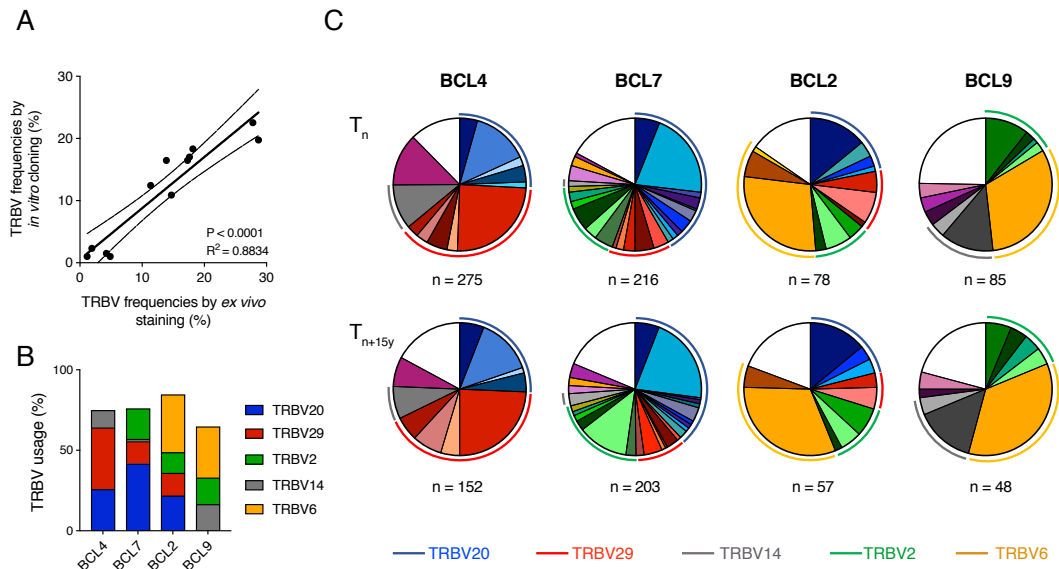
29

886 18. Price DA, Brenchley JM, Ruff LE, Betts MR, Hill BJ, Roederer M, et al. Avidity for
887   antigen shapes clonal dominance in CD8+ T cell populations specific for persistent DNA
888   viruses. *J Exp Med.* 2005;202(10):1349-61.
889 19. Annels NE, Callan MF, Tan L, and Rickinson AB. Changing patterns of dominant TCR
890   usage with maturation of an EBV-specific cytotoxic T cell response. *J Immunol.*
891   2000;165(9):4831-41.
892 20. Cohen GB, Islam SA, Noble MS, Lau C, Brander C, Altfeld MA, et al. Clonotype
893   tracking of TCR repertoires during chronic virus infections. *Virology.* 2002;304(2):474-
894   84.
895 21. Klarenbeek PL, Remmerswaal EB, ten Berge IJ, Doorenspleet ME, van Schaik BD,
896   Esveldt RE, et al. Deep sequencing of antiviral T-cell responses to HCMV and EBV in
897   humans reveals a stable repertoire that is maintained for many years. *PLoS Pathog.*
898   2012;8(9):e1002889.
899 22. Levitsky V, de Campos-Lima PO, Frisan T, and Masucci MG. The clonal composition of
900   a peptide-specific oligoclonal CTL repertoire selected in response to persistent EBV
901   infection is stable over time. *J Immunol.* 1998;161(2):594-601.
902 23. Couedel C, Bodinier M, Peyrat MA, Bonneville M, Davodeau F, and Lang F. Selection
903   and long-term persistence of reactive CTL clones during an EBV chronic response are
904   determined by avidity, CD8 variable contribution compensating for differences in TCR
905   affinities. *J Immunol.* 1999;162(11):6351-8.
906 24. Britanova OV, Shugay M, Merzlyak EM, Staroverov DB, Putintseva EV, Turchaninova
907   MA, et al. Dynamics of Individual T Cell Repertoires: From Cord Blood to Centenarians.
908   *J Immunol.* 2016;196(12):5005-13.
909 25. Miles JJ, Silins SL, Brooks AG, Davis JE, Misko I, and Burrows SR. T-cell grit: large
910   clonal expansions of virus-specific CD8+ T cells can dominate in the peripheral
911   circulation for at least 18 years. *Blood.* 2005;106(13):4412-3.
912 26. Farrington LA, Smith TA, Grey F, Hill AB, and Snyder CM. Competition for antigen at
913   the level of the APC is a major determinant of immunodominance during memory
914   inflation in murine cytomegalovirus infection. *J Immunol.* 2013;190(7):3410-6.
915 27. Turula H, Smith CJ, Grey F, Zurbach KA, and Snyder CM. Competition between T cells
916   maintains clonal dominance during memory inflation induced by MCMV. *Eur J
917   Immunol.* 2013;43(5):1252-63.
918 28. Hutchinson S, Sims S, O'Hara G, Silk J, Gileadi U, Cerundolo V, et al. A dominant role
919   for the immunoproteasome in CD8+ T cell responses to murine cytomegalovirus. *PLoS
920   One.* 2011;6(2):e14646.
921 29. Dekhtiarenko I, Jarvis MA, Ruzsics Z, and Cicin-Sain L. The context of gene expression
922   defines the immunodominance hierarchy of cytomegalovirus antigens. *J Immunol.*
923   2013;190(7):3399-409.
924 30. Baumann NS, Welten SPM, Torti N, Pallmer K, Borsa M, Barnstorf I, et al. Early primed
925   KLRG1- CMV-specific T cells determine the size of the inflationary T cell pool. *PLoS
926   Pathog.* 2019;15(5):e1007785.
927 31. Ouyang Q, Wagner WM, Wikby A, Walter S, Aubert G, Dodi AI, et al. Large numbers of
928   dysfunctional CD8+ T lymphocytes bearing receptors for a single dominant CMV
929   epitope in the very old. *J Clin Immunol.* 2003;23(4):247-57.
930 32. Griffiths SJ, Riddell NE, Masters J, Libri V, Henson SM, Wertheimer A, et al. Age-
931   associated increase of low-avidity cytomegalovirus-specific CD8+ T cells that re-express
932   CD45RA. *J Immunol.* 2013;190(11):5363-72.
933 33. Schwanninger A, Weinberger B, Weiskopf D, Herndler-Brandstetter D, Reitinger S,
934   Gassner C, et al. Age-related appearance of a CMV-specific high-avidity CD8+ T cell
935   clonotype which does not occur in young adults. *Immun Ageing.* 2008;5:14.

30

936 34. Hebeisen M, Schmidt J, Guillaume P, Baumgaertner P, Speiser DE, Luescher I, et al.
937   Identification of Rare High-Avidity, Tumor-Reactive CD8+ T Cells by Monomeric TCR-
938   Ligand Off-Rates Measurements on Living Cells. *Cancer Res.* 2015;75(10):1983-91.
939 35. Allard M, Couturaud B, Carretero-Iglesia L, Duong MN, Schmidt J, Monnot GC, et al.
940   TCR-ligand dissociation rate is a robust and stable biomarker of CD8+ T cell potency.
941   *JCI Insight.* 2017;2(14).
942 36. Nauerth M, Stemberger C, Mohr F, Weissbrich B, Schiemann M, Germeroth L, et al.
943   Flow cytometry-based TCR-ligand Koff -rate assay for fast avidity screening of even
944   very small antigen-specific T cell populations ex vivo. *Cytometry A.* 2016;89(9):816-25.
945 37. Hebeisen M, Allard M, Gannon PO, Schmidt J, Speiser DE, and Rufer N. Identifying
946   Individual T Cell Receptors of Optimal Avidity for Tumor Antigens. *Front Immunol.*
947   2015;6:582.
948 38. Gupta B, Iancu EM, Gannon PO, Wieckowski S, Baitsch L, Speiser DE, et al.
949   Simultaneous coexpression of memory-related and effector-related genes by individual
950   human CD8 T cells depends on antigen specificity and differentiation. *J Immunother.*
951   2012;35(6):488-501.
952 39. Lefranc MP, Pommie C, Ruiz M, Giudicelli V, Foulquier E, Truong L, et al. IMGT
953   unique numbering for immunoglobulin and T cell receptor variable domains and Ig
954   superfamily V-like domains. *Developmental and comparative immunology.*
955   2003;27(1):55-77.
956 40. Schmidt J, Guillaume P, Irving M, Baumgaertner P, Speiser D, and Luescher IF.
957   Reversible major histocompatibility complex I-peptide multimers containing Ni(2+)-
958   nitrilotriacetic acid peptides and histidine tags improve analysis and sorting of CD8(+) T
959   cells. *J Biol Chem.* 2011;286(48):41723-35.
960 41. Iancu EM, Gannon PO, Laurent J, Gupta B, Romero P, Michielin O, et al. Persistence of
961   EBV Antigen-Specific CD8 T Cell Clonotypes during Homeostatic Immune
962   Reconstitution in Cancer Patients. *PLoS One.* 2013;8(10):e78686.
963 42. Nguyen TH, Bird NL, Grant EJ, Miles JJ, Thomas PG, Kotsimbos TC, et al. Maintenance
964   of the EBV-specific CD8(+) TCRalphabeta repertoire in immunosuppressed lung
965   transplant recipients. *Immunol Cell Biol.* 2017;95(1):77-86.
966 43. Trautmann L, Labarriere N, Jotereau F, Karanikas V, Gervois N, Connerotte T, et al.
967   Dominant TCR V alpha usage by virus and tumor-reactive T cells with wide affinity
968   ranges for their specific antigens. *Eur J Immunol.* 2002;32(11):3181-90.
969 44. Gustafson CE, Qi Q, Hutter-Saunders J, Gupta S, Jadhav R, Newell E, et al. Immune
970   Checkpoint Function of CD85j in CD8 T Cell Differentiation and Aging. *Front Immunol.*
971   2017;8:692.
972 45. Northfield J, Lucas M, Jones H, Young NT, and Klenerman P. Does memory improve
973   with age? CD85j (ILT-2/LIR-1) expression on CD8 T cells correlates with 'memory
974   inflation' in human cytomegalovirus infection. *Immunol Cell Biol.* 2005;83(2):182-8.
975 46. Antrobus RD, Khan N, Hislop AD, Montamat-Sicotte D, Garner LI, Rickinson AB, et al.
976   Virus-specific cytotoxic T lymphocytes differentially express cell-surface leukocyte
977   immunoglobulin-like receptor-1, an inhibitory receptor for class I major
978   histocompatibility complex molecules. *J Infect Dis.* 2005;191(11):1842-53.
979 47. Wherry EJ, and Ahmed R. Memory CD8 T-cell differentiation during viral infection. *J
980   Virol.* 2004;78(11):5535-45.
981 48. Klenerman P, and Oxenius A. T cell responses to cytomegalovirus. *Nat Rev Immunol.*
982   2016;16(6):367-77.
983 49. Romero P, Zippelius A, Kurth I, Pittet MJ, Touvrey C, Iancu EM, et al. Four functionally
984   distinct populations of human effector-memory CD8+ T lymphocytes. *J Immunol.*
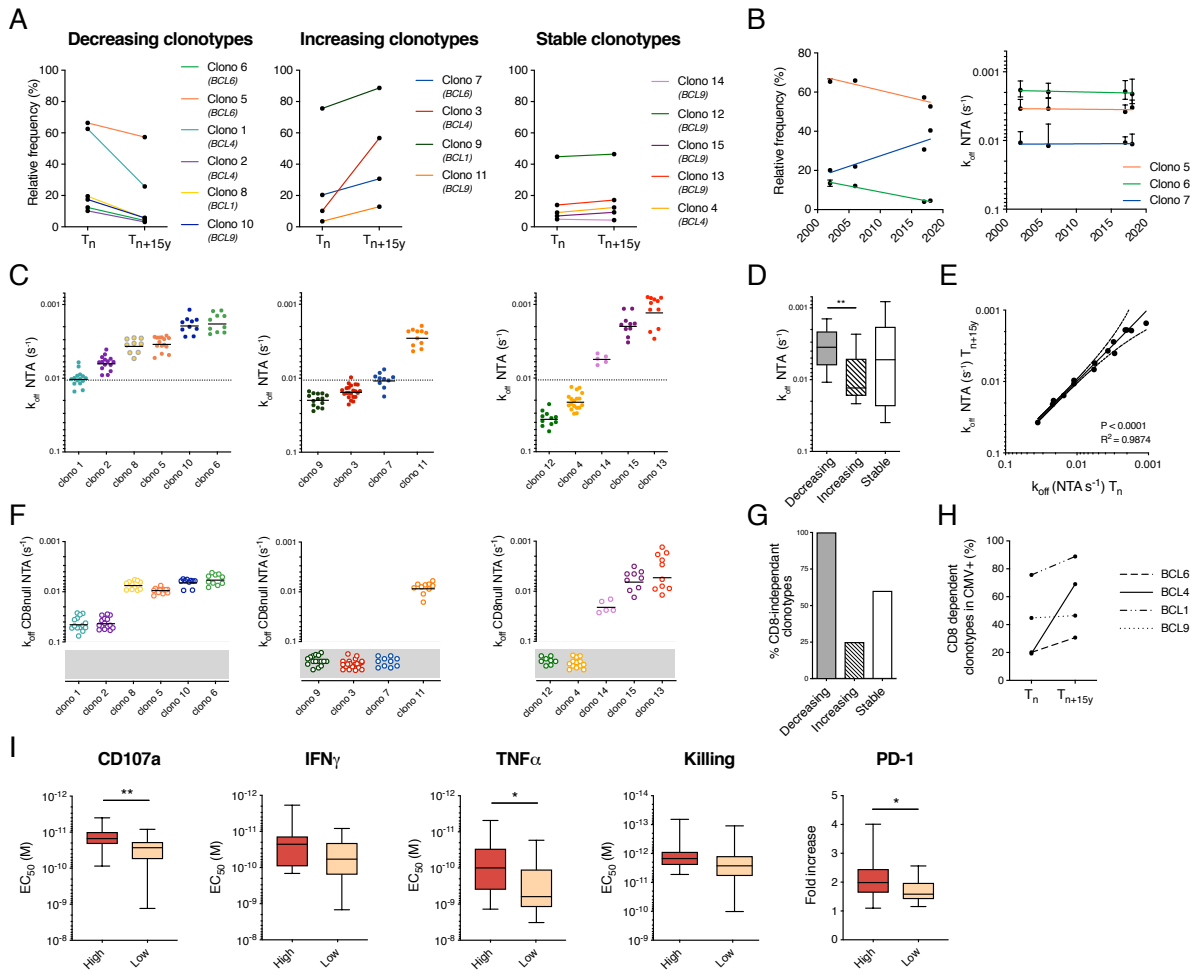985   2007;178(7):4112-9.

986   50. Davenport MP, Fazou C, McMichael AJ, and Callan MF. Clonal selection, clonal
987   senescence, and clonal succession: the evolution of the T cell response to infection with a
988   persistent virus. *J Immunol.* 2002;168(7):3309-17.
989   51. Akbar AN, and Vukmanovic-Stejic M. Telomerase in T lymphocytes: use it and lose it? *J*
990   *Immunol.* 2007;178(11):6689-94.
991   52. Buchholz VR, Neuenhahn M, and Busch DH. CD8+ T cell differentiation in the aging
992   immune system: until the last clone standing. *Curr Opin Immunol.* 2011;23(4):549-54.
993   53. Brentville VA, Metheringham RL, Gunn B, and Durrant LG. High avidity cytotoxic T
994   lymphocytes can be selected into the memory pool but they are exquisitely sensitive to
995   functional impairment. *PLoS One.* 2012;7(7):e41112.
996   54. Vigano S, Bellutti Enders F, Miconnet I, Cellerai C, Savoye AL, Rozot V, et al. Rapid
997   perturbation in viremia levels drives increases in functional avidity of HIV-specific CD8
998   T cells. *PLoS Pathog.* 2013;9(7):e1003423.
999   55. Gannon PO, Wieckowski S, Baumgaertner P, Hebeisen M, Allard M, Speiser DE, et al.
1000   Quantitative TCR:pMHC Dissociation Rate Assessment by NTAmers Reveals
1001   Antimelanoma T Cell Repertoires Enriched for High Functional Competence. *J Immunol.*
1002   2015.
1003   56. Zhang SQ, Parker P, Ma KY, He C, Shi Q, Cui Z, et al. Direct measurement of T cell
1004   receptor affinity and sequence from naive antiviral T cells. *Sci Transl Med.*
1005   2016;8(341):341ra77.
1006   57. De Simone M, Rossetti G, and Pagani M. Single Cell T Cell Receptor Sequencing:
1007   Techniques and Future Challenges. *Front Immunol.* 2018;9:1638.
1008   58. Papalexi E, and Satija R. Single-cell RNA sequencing to explore immune cell
1009   heterogeneity. *Nat Rev Immunol.* 2018;18(1):35-45.
1010   59. Nauerth M, Weissbrich B, and Busch DH. The clinical potential for koff-rate
1011   measurement in adoptive immunotherapy. *Expert Rev Clin Immunol.* 2013;9(12):1151-3.
1012   60. Goronzy JJ, and Weyand CM. Successful and Maladaptive T Cell Aging. *Immunity.*
1013   2017;46(3):364-78.
1014   61. Pita-Lopez ML, Gayoso I, DelaRosa O, Casado JG, Alonso C, Munoz-Gomariz E, et al.
1015   Effect of ageing on CMV-specific CD8 T cells from CMV seropositive healthy donors.
1016   *Immun Ageing.* 2009;6:11.
1017   62. Czesnikiewicz-Guzik M, Lee WW, Cui D, Hiruma Y, Lamar DL, Yang ZZ, et al. T cell
1018   subset-specific susceptibility to aging. *Clin Immunol.* 2008;127(1):107-18.
1019   63. Chapman TL, Heikeman AP, and Bjorkman PJ. The inhibitory receptor LIR-1 uses a
1020   common binding interaction to recognize class I MHC molecules and the viral homolog
1021   UL18. *Immunity.* 1999;11(5):603-13.
1022   64. O'Hara GA, Welten SP, Klenerman P, and Arens R. Memory T cell inflation:
1023   understanding cause and effect. *Trends Immunol.* 2012;33(2):84-90.
1024   65. Akbar AN, and Henson SM. Are senescence and exhaustion intertwined or unrelated
1025   processes that compromise immunity? *Nat Rev Immunol.* 2011;11(4):289-95.
1026

32

Couturaud et al.
Figure 1

A

B

C

BCL4   BCL7   BCL2   BCL9

T_n

n = 275   n = 216   n = 78   n = 85

T_{n+15y}

n = 152   n = 203   n = 57   n = 48

TRBV20   TRBV29   TRBV14   TRBV2   TRBV6

Couturaud et al.
Figure 2
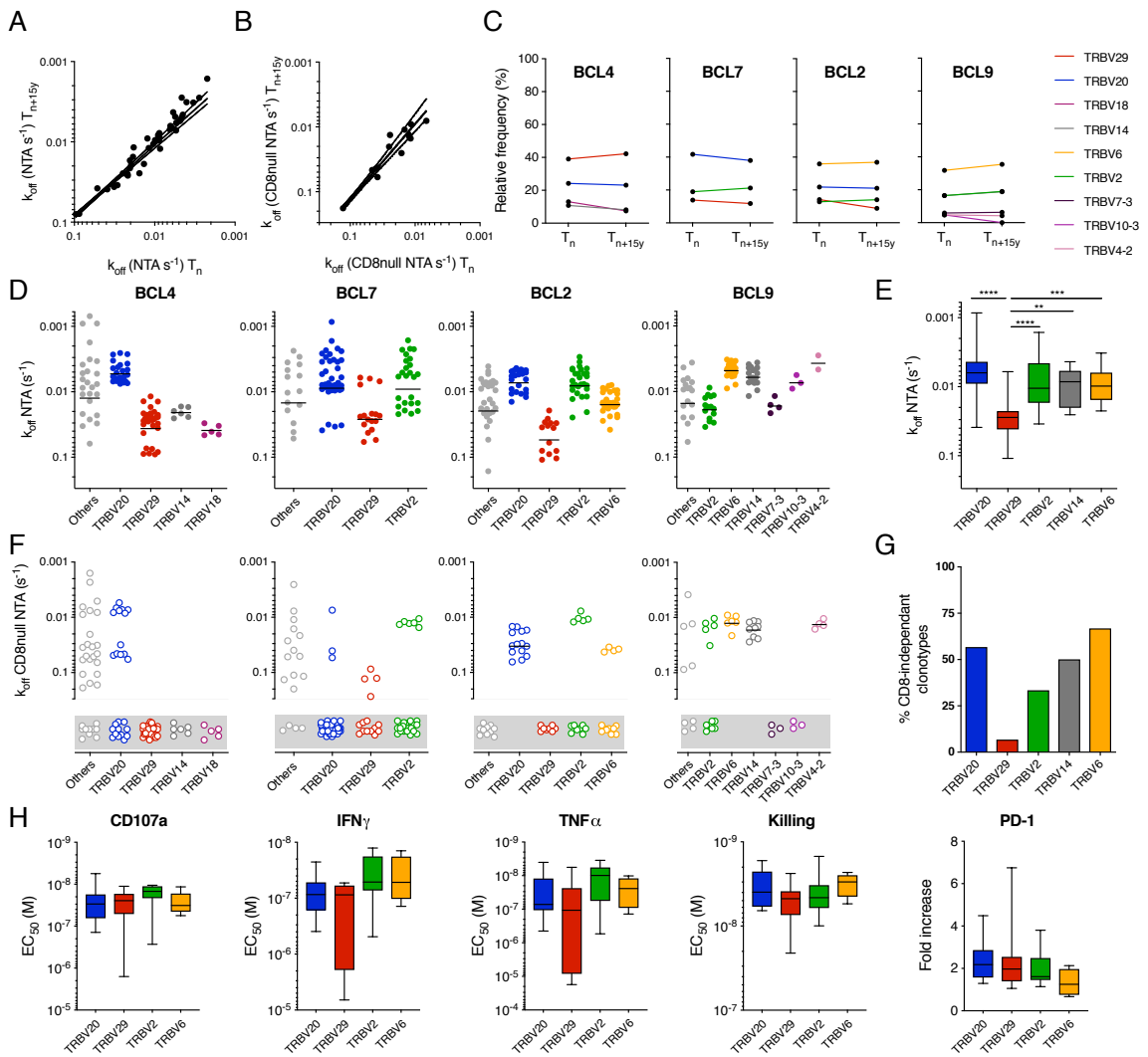
Couturaud et al.
Figure 3

Couturaud et al.
Figure 4
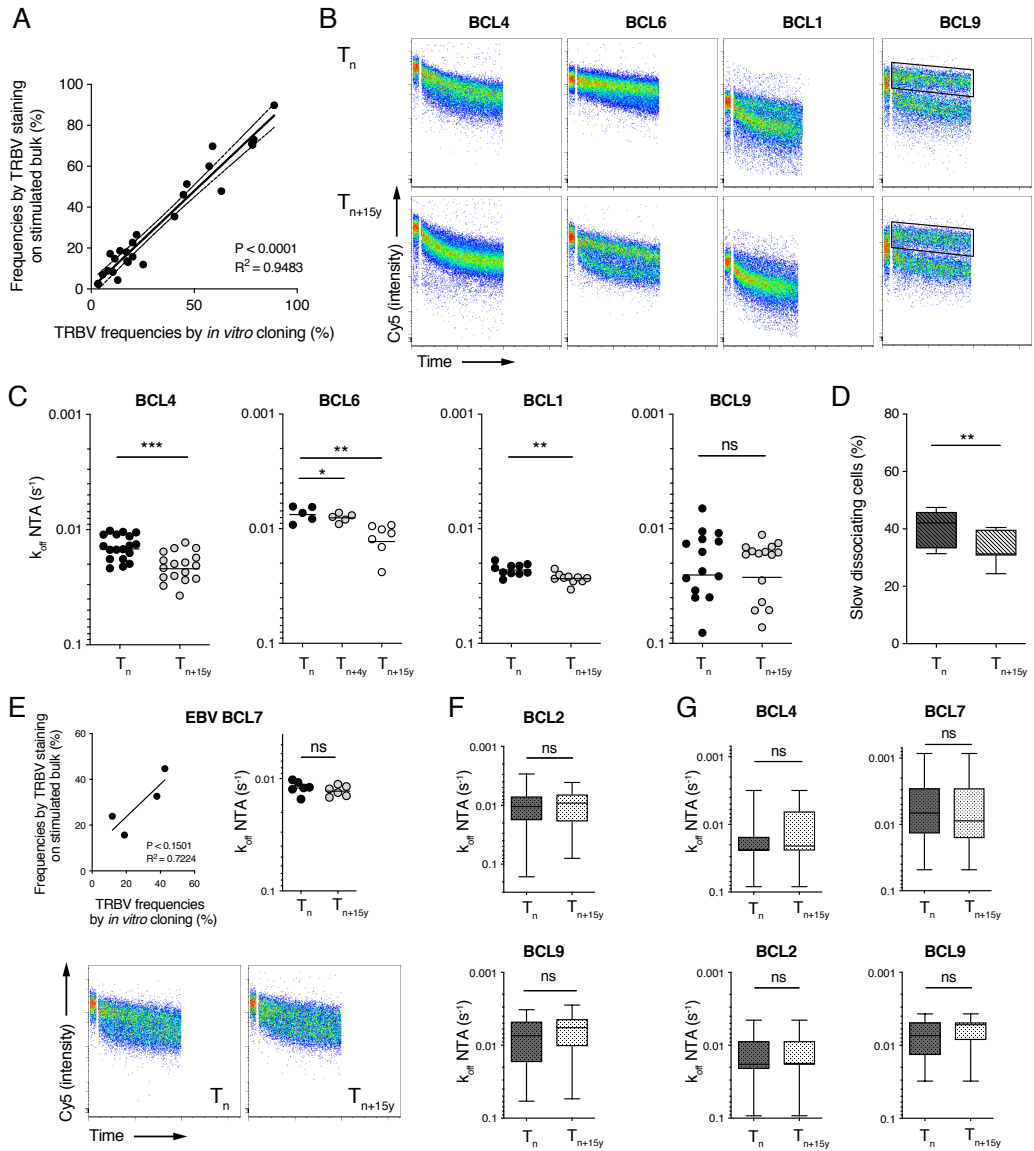
Couturaud et al.
Figure 5
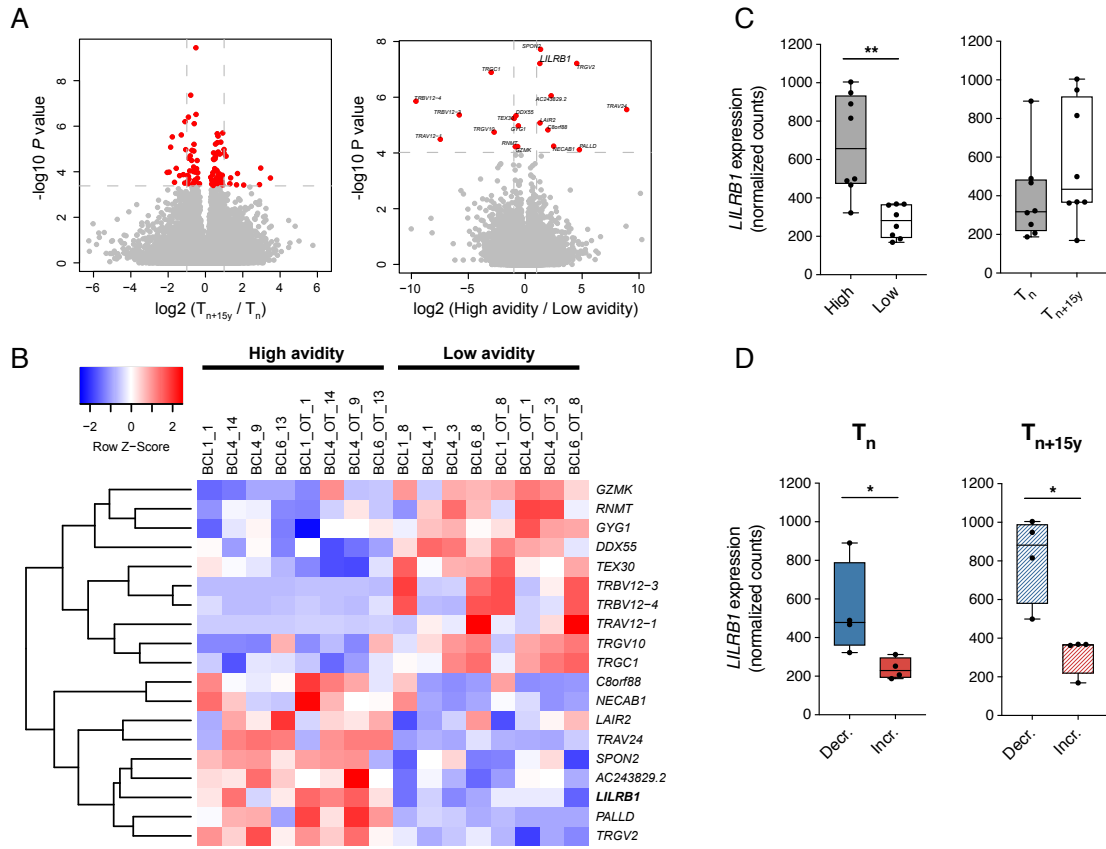
Couturaud et al.
Figure 6
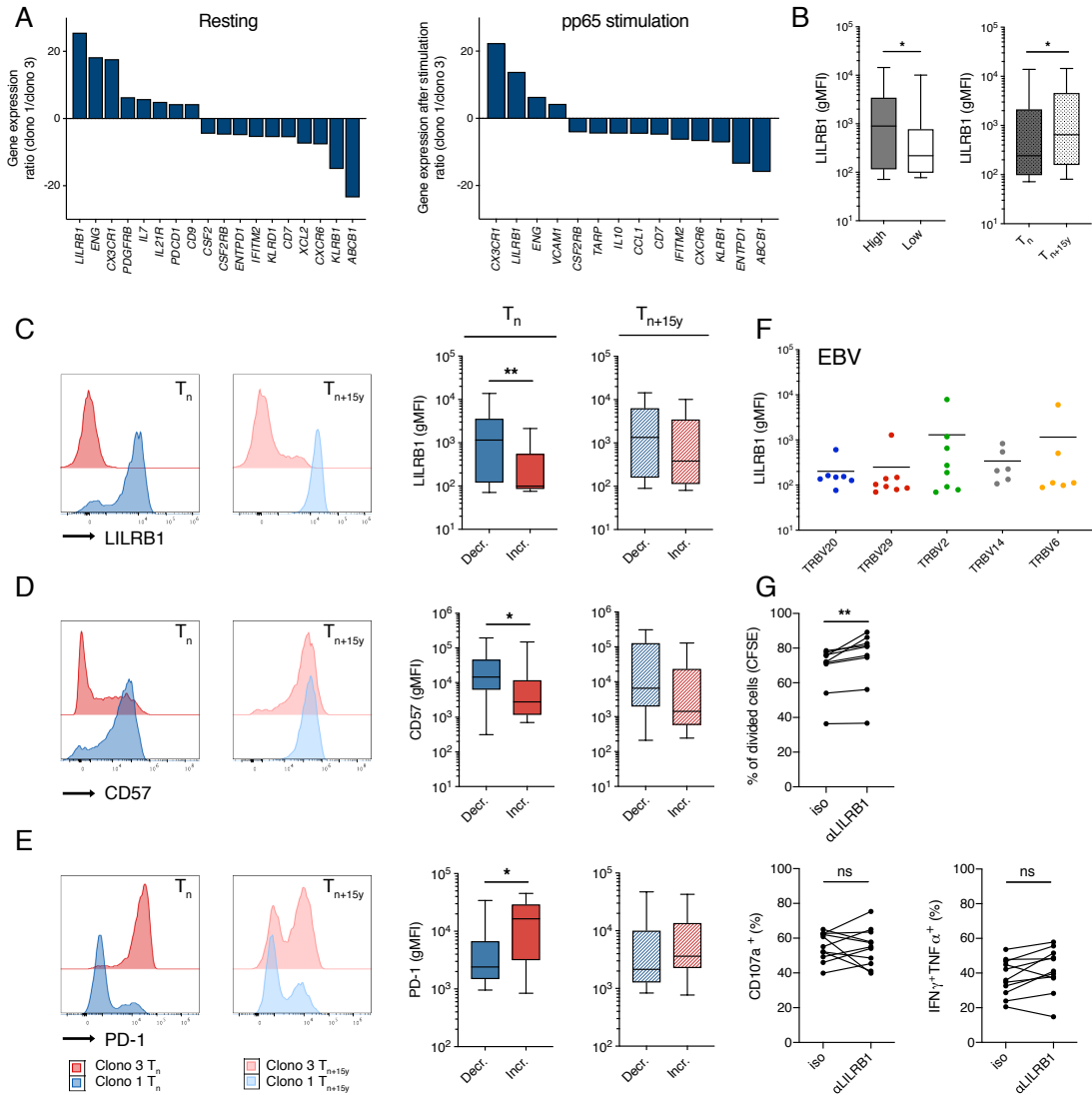
Couturaud et al.
Figure 7

SUPPLEMENTAL DATA

SUPPLEMENTAL MATERIALS AND METHODS

RNA sequencing analysis

Purity-filtered reads were adapters and quality trimmed with Cutadapt (v.1.8, (1)). Reads matching to ribosomal RNA sequences were removed with fastq_screen (v.0.11.1). Remaining reads were further filtered for low complexity with reaper (v.15-065, (2)). Reads were aligned against Homo sapiens.GRCh38.92 genome using STAR (v.2.5.3a, (3)). The number of read counts per gene locus was summarized with htseq-count (v.0.9.1, (4)) using Homo sapiens.GRCh38.92 gene annotation. Quality of the RNA-seq data alignment was assessed using RSeQC (v.2.3.7, (5)). The effect TCR avidity and time were tested in R (v.3.4.0) using the likelihood ratio test implemented in the DESeq2 package (6). A linear model with the TCR binding avidity (low and high avidity), the time-point (T_n, 2002 and T_{n+15y}, 2017) and the donors (BCL1, BCL4, BCL6) was compared to reduced models with (i) the TCR avidity factor removed or (ii) the time-point factor removed. Parameters 'cooksCutoff' and 'independentFiltering' were set to 'false'.

1

Supplemental Table 1. List of TRBV antibodies

Name*	IMGT nomenclature	Company	Catalog #	Clone
Pe-Vio770 anti-Vβ1	TRBV9	Miltenyi	130-110-020	REA662
APC-Vio770 anti-Vβ2	TRBV20	Miltenyi	130-110-098	REA654
FITC anti-Vβ3	TRBV28	Beckman Coulter	IM2372	CH92
FITC anti-Vβ4	TRBV29	Beckman Coulter	B07084	WJF24
FITC anti-Vβ8	TRBV12	Beckman Coulter	IM1233	56C5.2
APC anti-Vβ9	TRBV3	Invitrogen	17-4899-41	AMKB1-2
FITC anti-Vβ13.1	TRBV6-5	Invitrogen	11-5792-41	H131
APC anti-Vβ14	TRBV27	Miltenyi	130-108-738	REA557
FITC anti-Vβ22	TRBV2	Beckman Coulter	IM1484	IMMU546

*TCR Vβ-chain according to Arden's nomenclature (7).

Supplemental Table 2. Biological characteristics of the studied healthy donors

Donors			1st sample			2nd sample			Virus-specificity studied
ID	Sexe	Age	%CMV in CD8+ T cells	%EBV in CD8+ T cells	Age	%CMV in CD8+ T cells	%EBV in CD8+ T cells	
BCL1	F	25.9	0.21	0.12	41.2	0.07	0.09	CMV
BCL2	M	39.1	na	0.38	54.6	na	0.45	EBV
BCL4	F	29.9	2.11	0.27	44.7	1.14	0.12	CMV and EBV
BCL6	F	37.0	1.06	0.21	51.3	4.08	nd	CMV
BCL7	M	27.1	0.08	1.16	42.1	na	1.29	EBV
BCL8	F	28.6	3.07	0.24	na	na	na	CMV
BCL9	M	20.0	1.99	0.45	35.3	1.82	0.33	CMV and EBV

Supplemental Table 3. CMV-specific TCRαβ clonotypes from healthy donors

Donor	Clonotype	IMGT	BV Arden	CDR3β	BJ	IMGT	AV Arden	CDR3α	AJ	TCR avidity
BCL4	Clono 1	TRBV27	14	RLLAGGRSAQ	2.5	TRAV24	18	EGGNQF	49	High
CMV	Clono 2	TRBV3-2	9S2	SLLLGTAAEA	1.1	TRAV24	18	IAGNQF	49	HIgh
	Clono 3	TRBV9	1	SVYGGAGNSPL	1.6	TRAV14	6	KNFNKF	21	Low
	Clono 4	TRBV28	3	SFLGYTEA	1.1	TRAV3	16	YYGQNF	26	Low
BCL6	Clono 5	TRBV6-5	13S1	SRQTGAAYGY	1.2	TRAV24	18	NTGNQF	49	High
CMV	Clono 6	TRBV6-5	13S1	SYATGTAYGY	1.2	TRAV24	18	NTGNQF	49	High
	Clono 7	TRBV12-3/4	8S1/2	SSANYGY	1.2	TRAV35	25	PRETSYDKV	50	Low
BCL1	Clono 8	TRBV9	1	SVVGLWTDTQ	2.3	TRAV14	6	PMKTSYDKV	50	High
CMV	Clono 9	TRBV12-3/4	8S1/2	SSANYGY	1.2	TRAV35	25	EPENSGGSNYKL	53	Low
BCL9	Clono 10	TRBV7-3	6	SLMALGAGANVL	2.6			na		High
CMV	Clono 11	TRBV28	3	SFQGYTEA	1.1			na		High
	Clono 12	TRBV9	1	SPLGGAGLADTQ	2.3	TRAV14	6	REGIIQGAQKL	54	Low
	Clono 13	TRBV27	14	SLTPGSPGSPL	1.6			na		High
	Clono 14	TRBV6-5/1	13	SPTTGTGYFGY	1.2	TRAV24	18	NTGNQF	49	High
	Clono 15	TRBV6-5	13	SLVSGSGSYGY	1.2	TRAV24	18	NTGNQF	49	High
BCL8	Clono 16	TRBV6	13	SSVSGGASNEQ	2.1	TRAV3	16	NYGNML	39	na
CMV	Clono 17	TRBV24-1	15	SDPLTASYEQ	2.5	TRAV29	2	GSQGNL	42	na

2

Supplemental Table 4. EBV-specific TCRαβ clonotypes from healthy donors

Donor	Clonotype	IMGT	BV Arden	CDR3β	BJ	IMGT	AV Arden	CDR3α	AJ
BCL4	2 clono 1	TRBV20	2	RDRIGNGY	1.2	TRAV5	15	DNNARL	31
EBV	2 clono 2*	TRBV20	2	RDRTGNGY	1.2	TRAV5	15	DNNARL	31
	2 clono 3	TRBV20	2	RDSVGNGY	1.2	TRAV5	15	DNNARL	31
	2 clono 4	TRBV20	2	RDRVGNGY	1.2	TRAV5	15	DNNARL	31
	2 clono 5	TRBV20	2	RDSTGNGY	1.2	TRAV5	15	DNNARL	31
	4 clono 1	TRBV29	4	FQEASYGY	1.2	TRAV29	21	SGGSQGNL	42
	4 clono 2**	TRBV29	4	VGTGGTNEKL	1.4	TRAV5	15	STGKL	37
	4 clono 3	TRBV29	4	VGYGGTNEKL	1.4	TRAV5	15	STGKL	37
	4 clono 4	TRBV29	4	VGSGGTNEKL	1.4	TRAV5	15	DNNARL	31
	4 clono 5	TRBV29	4	TPGQLMETQ	2.5	TRAV5	15	TLGNTGKL	37
	16 clono 1	TRBV14	16	SQSPGGTQ	2.5	TRAV5	15	SPPSSASKI	2
	18 clono 1	TRBV18	18	SPPAVSYEQ	2.7	TRAV29	21	IHNQAGTAL	15
BCL7	2 clono 1	TRBV20	2	RDTIGNGY	1.2	TRAV5	15	DNNARL	31
EBV	2 clono 2***	TRBV20	2	RVGVGNTI	1.3	TRVA5	15	DNNARL	31
	2 clono 3	TRBV20	2	RDRVGNTI	1.3	TRAV5	15	DQSPRV	31
	2 clono 4*	TRBV20	2	RDRTGNGY	1.2	TRAV5	15	DNNARL	31
	2 clono 5	TRBV20	2	RSETGNTI	1.3	TRAV5	15	DNNARL	31
	2 clono 6	TRBV20	2	RGSVGNTI	1.3	TRAV5	15	DSNARL	31
	2 clono 7	TRBV20	2	RIGVGNTI	1.3	TRAV5	15	DNNARL	31
	2 clono 8	TRBV20	2	RDRVGNGY	1.2	TRAV5	15	DVNARL	31
	2 clono 9	TRBV20	2	RDETGNGY	1.2	TRAV5	15	DNNARL	31
	2 clono 10	TRBV20	2	WDREVMGGNTI	1.3	TRAV5	15	TSSASKI	3
	4 clono 1	TRBV29	4	VGSGGTNEKL	1.4	TRAV5	15	SIGKL	34
	4 clono 2	TRBV29	4	TTGSGDRGA	1.1	TRAV5	15	DRYSTL	11
	4 clono 3	TRBV29	4	VEGLTYNEQ	2.1	TRAV12-2	2S1	ITGGTYKY	40
	4 clono 4	TRBV29	4	VGEGGTNEKL	1.4	TRAV5	15	SIGKL	37
	4 clono 5	TRBV29	4	VEDSLWGAGDEKKASTDTQ	2.3	TRAV9-2	22	NGGFKT	9
	4 clono 6**	TRBV29	4	VGTGGTNEKL	1.4	TRAV5	15	STGKL	37
	22 clono 1	TRBV2	22	TSGQISPSAI	1.3	TRAV12-1	2S3	NGGDSSYKL	12
	22 clono 2	TRBV2	22	TAGGTLPGEQ	2.7	TRAV12-1	2S3	NGMDSSYKL	12
	22 clono 3	TRBV2	22	SGGQVAPSEQ	2.1	TRAV12-1	2S3	NGEDSSYKL	12
	22 clono 4	TRBV2	22	SSGSVAPGEL	2.2	TRAV12-1	2S3	NGRDSSYKL	12
	22 clono 5	TRBV2	22	SSLEVSPSEQ	2.7	TRAV12-1	2S3	NGKDSSYKL	12
	22 clono 6	TRBV2	22	TSGTVAPGEQ	2.7	TRAV12-1	2S3	NGMDSSYKL	12
BCL2	2 clono 1	TRBV20	2	RDEVSGSWNEQ	2.1	TRAV9-2	22	SGDRDDKI	30
EBV	2 clono 2	TRBV20	2	RDQTGNGY	1.2	TRAV5	15	DNNARL	31
	2 clono 3	TRBV20	2	RDREFGNTI	1.3	TRAV5	15	DSNARL	31
	2 clono 4***	TRBV20	2	RVGVGNTI	1.3	TRAV5	15	DNNARL	31
	4 clono 1	TRBV29	4	VGTGGTNEKL	1.4	TRAV5	15	SVGKL	8
	4 clono 2	TRBV29	4	VEDSIAGFTDTQ	1.4	TRAV9-2	22	NGGFKT	9
	4 clono 3	TRBV29	4	VGQGGTNEKL	1.4	TRAV5	15	SSSVGY	40
	22 clono 1	TRBV2	22	SEGAVAPGEQ	2.7	TRAV12-1	2S3	NGMDSSYKL	12
	22 clono 2	TRBV2	22	TDPRLLPGEQ	2.7	TRAV12-1	2S3	NGADSSYKL	12
	22 clono 3	TRBV2	22	SVGEILPGEQ	2.7	TRAV12-1	2S3	NGRDSSYKL	12
	13 clono 1	TRBV6-5	13	KTGTGNEKL	1.4	TRAV5	15	PNNAGNML	39
	13 clono 2	TRBV6-5	13	PPMGTPNYGY	1.2	TRAV5	15	DNNARL	31
	13 clono 3	TRBV6-5	13	SEWTGYQPQ	1.5	TRAV29	21	SGGGADGL	45
BCL9	13 cl.1	TRBV6-5	13	TPDVNTEA	1.1	TRAV5	15	SMDGYAL	41
EBV	16 cl.1	TRBV14	16	SQSPGGTQ	2.5	TRAV5	15	SRETAL	15
	16 cl.2	TRBV14	16	SQSPGGIQ	2.4	TRAV5	15	GGADGL	45
	22 cl.1	TRBV2	22	SPPGLAPNEQ	2.1	TRAV12-1	2	NGKDSSYKL	12
	22 cl. 2	TRBV2	22	SGGRVAPGEL	2.2	TRAV12-1	2	NGRDSSYKL	12
	22 cl. 3	TRBV2	22	SDGAVAPNEQ	2.1	TRAV12-1	2	NGRDSSYKL	12
	22 cl.4	TRBV2	22	SEGQVWPGEL	2.2	TRAV12-1	2	NGMDSSYKL	12
	6 cl.1	TRBV7-3	6	SSGGNIDTQ	2.3			na	
	12 cl.1	TRBV10-3	12	KSFRHRYSE	2.3	TRAV5	15	DNNARL	31
	7 cl.1	TRBV4-2	7	SQDGAGGLGEQ	2.1	TRAV12-1	2	NIPNDYKL	20

*, **, ***: Public αβ TCR clonotypes

3

SUPPLEMENTAL FIGURE LEGENDS

Supplemental Figure 1. Frequencies of *ex vivo* CMV-specific TRBV family-based CD8 T cell clonotypes from healthy donors. A, Representative FACS dot plots obtained after *ex vivo* labeling with anti-TRBV family antibodies on CMV$^+$CD8$^+$ T cells from BCL4, BCL6, BCL1 and BCL9. Percentages of positively stained cells are indicated. **B,** Quantification of dominant CMV-specific TRBV-family based T cell clonotypes at T_n and T_{n+15y} for each healthy donor. Results are depicted as percentages of color-coded TRBV family frequencies by *ex vivo* TRBV family-based staining. TRBV-unlabeled CMV-specific T cells are depicted in white.

Supplemental Figure 2. Monomeric TCR-pMHC dissociation rates of CMV-specific CD8 TCR$\alpha\beta$ clonotypes over time. A, Correlation of monomeric TCR-pMHC dissociation rate (k_{off}) values by mutated NTAmers (CD8null NTA) obtained from identical TCR$\alpha\beta$ clonotypes between T_n and T_{n+15y} (by linear regression analysis with 95% confidence intervals). **B,** TCR-pMHC dissociation rate (k_{off}) by mutated NTAmers (CD8null NTA) of each color-coded CMV-specific TCR$\alpha\beta$ clonotype from donor BCL6 at the indicated time-points.

Supplemental Figure 3. Monomeric TCR-pMHC dissociation rates and CD8 binding dependency of EBV-specific CD8 TCR$\alpha\beta$ clonotypes per healthy donor. A-D, TCR-pMHC dissociation rates (k_{off}) by wild-type NTAmers (NTA) or mutated NTAmers (CD8null NTA) on a representative selection of EBV-specific T cell clones of each color-coded TCR$\alpha\beta$ clonotype from the four healthy donors. Unique clonotypes are defined as "others" and depicted in grey. CD8null NTAmer non-binder clones are represented in the grey boxes. **E,** TCR-pMHC dissociation rates (k_{off}) by wild-type NTAmers (NTA) of EBV-specific TCR$\alpha\beta$ clonotypes classified according to their preferential TRAV family usage. A representative selection of EBV-specific T cell clones of each TCR$\alpha\beta$ clonotype is shown. Data are depicted as box (25th and 75th percentiles) and whisker (min to max) plots with the middle line indicating the median. Kruskal-Wallis test-derived ($\alpha = 0.05$) P values are indicated with * P < 0.05.

Supplemental Figure 4: Gene and surface molecule expression in CMV-specific CD8 TCR$\alpha\beta$ clonotypes. A, Heatmap plot of 52 differentially expressed genes between CMV-specific clonotypes at T_n versus T_{n+15y} (FDR < 0.1). Normalized expression level was transformed (DESeq2 function rlog), center and variance scaled by gene. Red indicates overexpression and blue underexpression relative to the gene mean expression. Gene expression data were generated by RNA sequencing on *ex vivo* sorted CMV/TRBV-specific sub-populations of CMV-positive BCL4, BCL6 and BCL1 donors at T_n and T_{n+15y}. **B,** Baseline

4

surface expression levels of LILRB1 (gMFI) in high- and low-avidity CMV-specific clonotypes and in clonotypes from T_n and T_{n+15y} from donor BCL9. **C-E,** Baseline surface expression levels (gMFI) of LILRB1 (**C**), CD57 (**D**) and PD-1 (**E**) in decreasing (in blue), increasing (in red) and stable (grey) CMV-specific TCRαβ clonotypes at T_n and T_{n+15y}. Data are representative of a selection of pooled clones and are depicted as box (25th and 75th percentiles) and whisker (min to max) plots with the middle line indicating the median.

REFERENCES

1. Martin M. Cutadapt removes adapter sequences from high-throughput sequencing reads. *2011*. 2011;17(1):3.
2. Davis MP, van Dongen S, Abreu-Goodger C, Bartonicek N, and Enright AJ. Kraken: a set of tools for quality control and analysis of high-throughput sequence data. *Methods.* 2013;63(1):41-9.
3. Dobin A, Davis CA, Schlesinger F, Drenkow J, Zaleski C, Jha S, et al. STAR: ultrafast universal RNA-seq aligner. *Bioinformatics.* 2013;29(1):15-21.
4. Anders S, Pyl PT, and Huber W. HTSeq--a Python framework to work with high-throughput sequencing data. *Bioinformatics.* 2015;31(2):166-9.
5. Wang L, Wang S, and Li W. RSeQC: quality control of RNA-seq experiments. *Bioinformatics.* 2012;28(16):2184-5.
6. Love MI, Huber W, and Anders S. Moderated estimation of fold change and dispersion for RNA-seq data with DESeq2. *Genome Biol.* 2014;15(12):550.
7. Arden B, Clark SP, Kabelitz D, and Mak TW. Human T-cell receptor variable gene segment families. *Immunogenetics.* 1995;42(6):455-500.

5

A

B
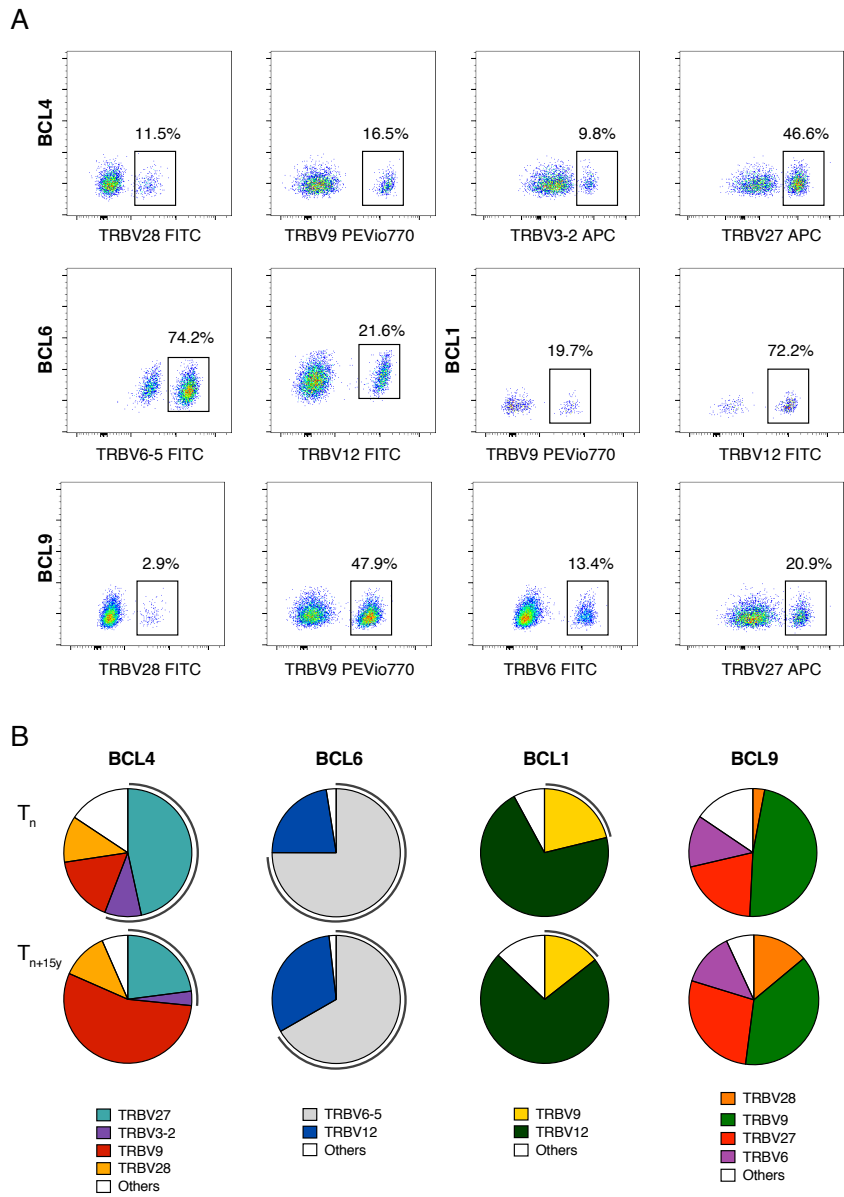
Couturaud et al.
Supplemental Figure 1
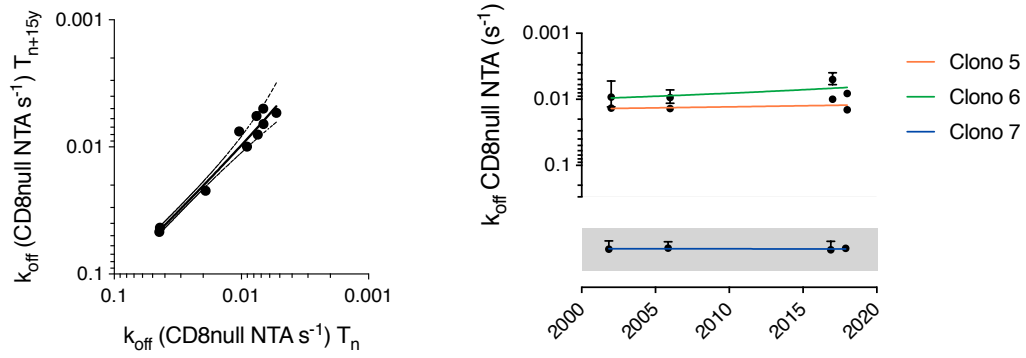
Couturaud et al.
Supplemental Figure 2
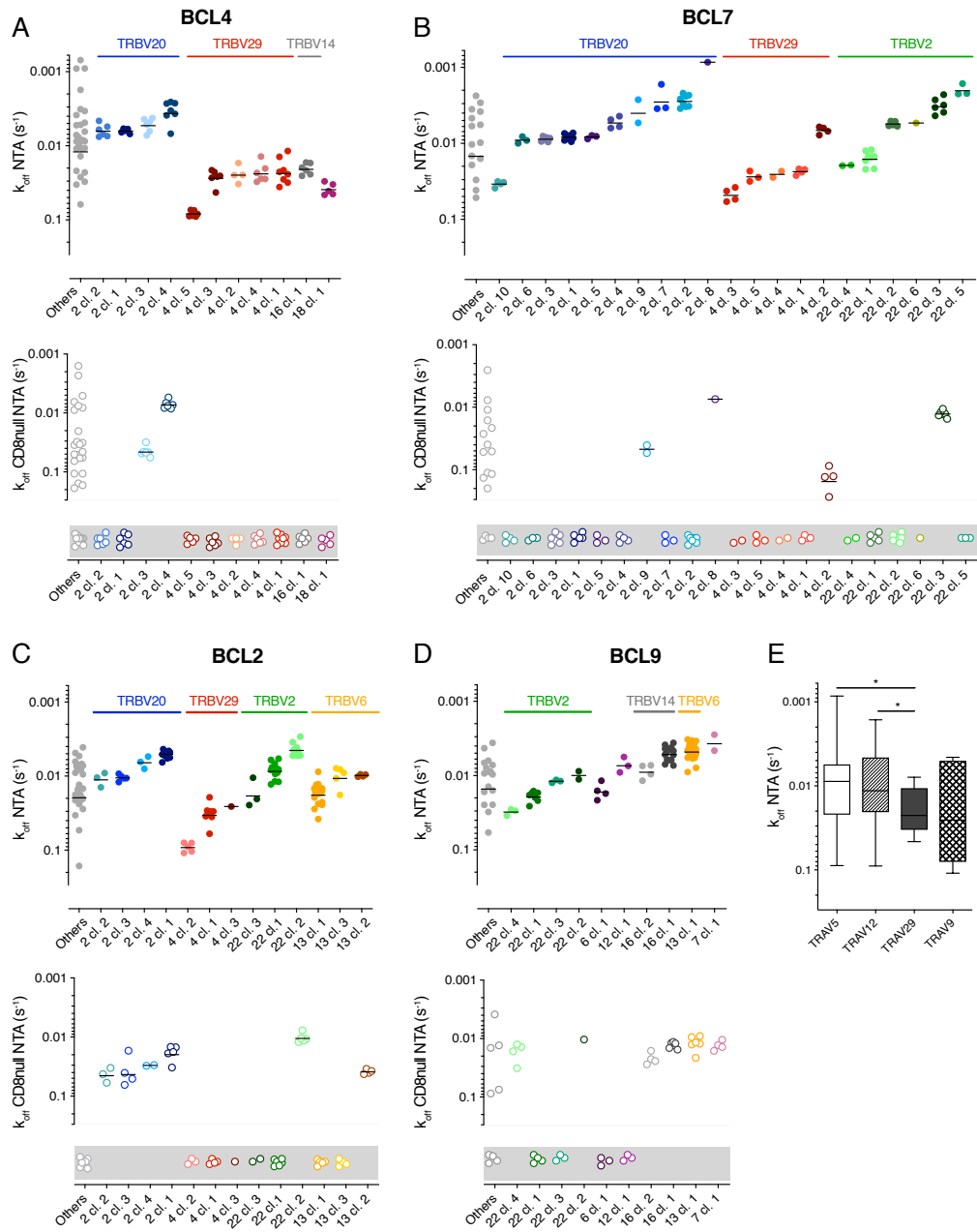
Couturaud et al.
Supplemental Figure 3

Couturaud et al.
Supplemental Figure 4

Discussion

1. Impact of TCR binding avidity on CD8 T cell function among different antigenic specificities

1.1. T cell-based therapies against malignant and infectious diseases
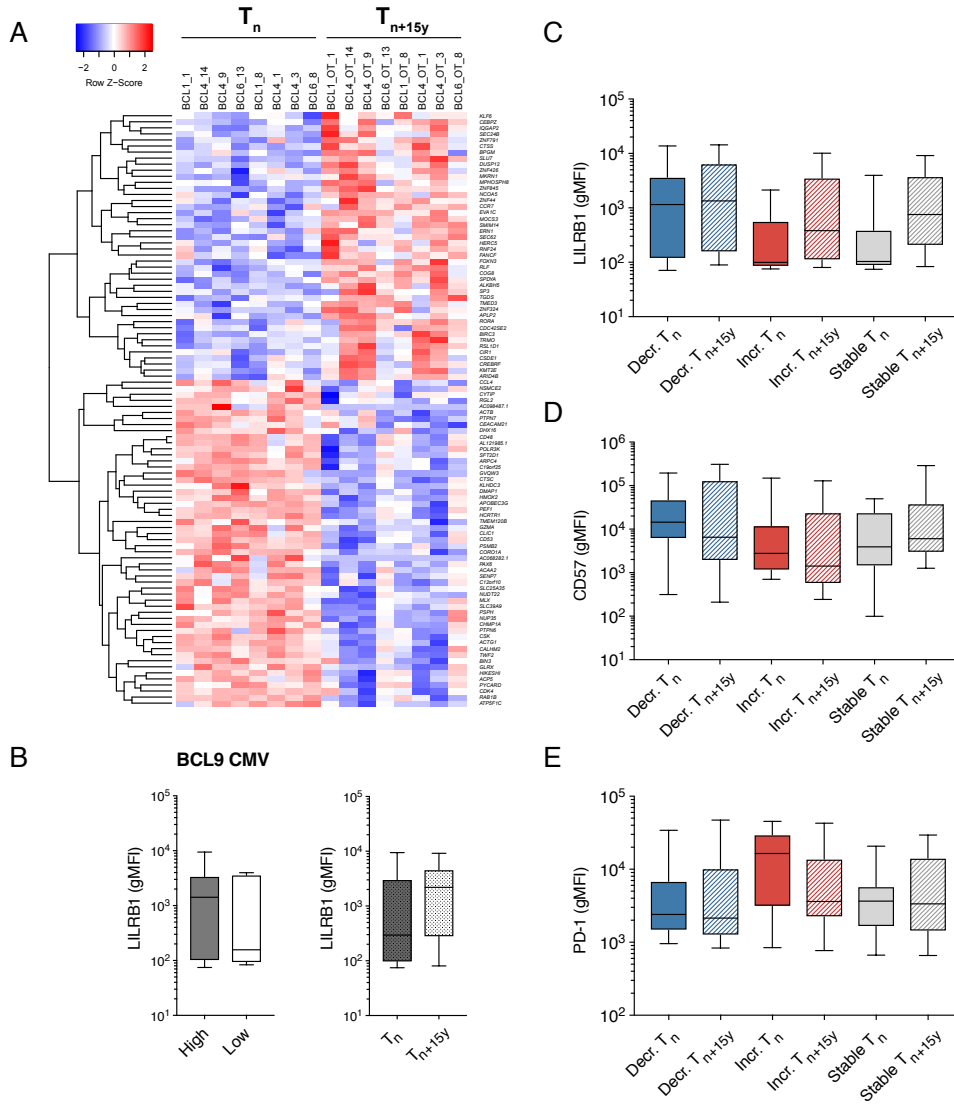
Recent success in T cell-based immunotherapy strategies have demonstrated the therapeutic potential of tumor- and viral-specific T cells. Among these, therapeutic vaccination aims to generating and/or boosting a strong and persistent immune response to destroy tumor or infected cells. Vaccination relies on the identification of immunogenic antigens, and can be delivered in the form of peptide or protein vaccine, or via viral or DNA-based vectors. In the tumor context, a large number of clinicals trials have demonstrated that this immunotherapeutic approach is feasible and safe. However, most phase 3 clinical trials have not shown significant clinical benefit [264]. These failures were in part due to the advanced metastatic state and to the strong immunosuppressive environment of the targeted cancers. Indeed, therapeutic vaccines against non-metastatic prostate cancer have shown enhanced CD8 T cell infiltration [265] and partial clinical efficacy [266]. In addition, the identification of neo-antigens has opened the door for novel vaccine strategies. In this context, the reinfusion of autologous dendritic cells pulsed with autologous whole-tumor cell lysate in the patient, has shown promising results in the treatment of ovarian cancer with the specific amplification of T cells directed against previously recognized and unrecognized neo-epitopes [267]. In the context of viral infection, numerous therapeutic vaccines for patients with CMV-infected allografts, either stem cell or solid organ, have been developed and evaluated. While no vaccine has yet been licensed [268], several candidates in clinical trials have shown promising results [269-271].

Another immunotherapeutic strategy is to restore the functional capacities of exhausted T cells through the administration of antibodies targeting inhibitory receptors or their ligands. Impressive results in cancer patients have been obtained using immune checkpoint blockade targeting immunosuppressive molecules like PD-1, PD ligand-1 (PDL-1) or CTLA-4. These treatments have all led to significant improvement of clinical outcome in metastatic melanoma patients [272, 273].

Finally, adoptive transfer of patient- or donor-derived T cells is of significant interest for the treatment of cancer or viral infection following stem cell or solid organ transplants. Adoptive cell transfer was initially developed by Rosenberg *et al.* more than 30 years ago for the treatment of melanoma [274]. More recently these treatments have been modernized with the development of genetically modified T-cells expressing chimeric antigen receptors (CARs) which have shown encouraging clinical results despite potential high toxicity [275, 276]. In the context of viral infection, the isolation of virus-specific T cells from a healthy donor and subsequent infusion into an immunocompromised patient to control the reactivation of persistent pathogens such as CMV or EBV has been investigated in many patients [277]. While conventional antiviral agents have limited efficacy with frequent reactivation after cessation of treatment as well as significant toxicity, several clinical trials have established the safety and efficacy of adoptive transfer of CMV- or EBV-specific T cells to control those infections [152, 153, 278, 279]. All these strategies rely on the identification and/or the robust activation of powerful T cells to efficiently fight against cancer or infected cells. Hence, there is a strong need to define those parameters that characterize potent T cells and how to assess them in order to further improve current therapies and to reach significant clinical benefit in a larger proportion of treated patients.

1.2. Identifying high-quality individual CD8 T cells

Since T cells play a major role in immune protection against cancer and infection, and are at the forefront of the development of immunotherapies, it is important to determine which T cell properties are essential to predict *in vivo* efficacy. In this regard, the functional capacity of T cells has been widely used as a correlate of protection. Indeed, it is now commonly accepted that CD8 T cells of higher functional avidity (defined as the peptide concentration mediating half-maximal activity, EC_{50}) confer superior viral protection or anti-tumor responses than T cells of lower functional avidity. However, the assessment of *ex vivo* functional avidity (i.e. specific T cell responses when exposed to increasing antigen concentrations) often requires a large number of cells and remain laborious and time consuming. It is also quite clear that significant variability of EC_{50} exists depending on the laboratory protocols and reagents used to assess them [70]. In addition, in the present study we showed that the T cell activation state (Manuscript 1, Figure 6) has a significant impact on the functional avidity, thus introducing additional experimental bias. Indeed, in line with previous studies [280, 281], we observed a gradual increase of functional avidity with time after *in vitro* re-stimulation (up to 20 days) for

identical individual clones. This was consistent with the increased expression of TCRαβ and the co-receptor CD8αβ as well as the very late antigen-1 (VLA-1) (Manuscript 1, Figure 6). The latter is known to be up regulated following several days of T cell stimulation [282] and to interact with collagen to increase TCR-mediated proliferation and cytokine secretion [283, 284] as well as to activate signaling pathways that promote cell survival [285]. This increase in functional avidity also correlated with a reduced expression of CD28 and the inhibitory receptors lymphocyte-activation gene-3 (LAG-3) and T cell immunoreceptor with Ig and ITIM domains (TIGIT) (Manuscript 1, Figure 6).

Finally, we observed a large variability in the peptide dose required to reach the EC_{50} for a given antigen specificity depending on the chosen functional readout (Manuscript 1, Figure 1 and Supp. Figure 4), reflecting different activation thresholds (cytotoxicity < cytokine production). These observations reinforce the need to identify a robust T cell-based biomarker that would allow for the rapid and efficient screening and identification of tumor- and viral-specific cytolytic T cells of high potential for immunotherapy. In this respect, TCR-pMHC binding avidity has been proposed as a potential candidate since it controls numerous aspects of T cell biology such as T-cell activation, differentiation, and functional efficacy (reviewed in [255]). So far technical limitations are the major reason why the TCR-pMHC binding avidity is still infrequently determined in research or patient monitoring, or in the selection of T cells used for adoptive cell therapy. Indeed, pMHC multimers ("tetramers") are biased by their multivalent nature and accurate measurements of TCR-pMHC binding parameters (i.e. 2D surface-based kinetics), while offering important membrane-associated kinetic insights, are not well suited for the high-throughput characterization of living antigen-specific CD8 T cells (reviewed in [94]). To overcome these limitations, reversible multimers have been recently developed which allow for the accurate measurements of monomeric TCR-pMHC dissociation-rates directly on CD8 T cells and on a wide avidity spectrum [99, 108].

1.3.   TCR-pMHC binding avidity is a robust and stable biomarker of CD8 T cell potency

Using reversible multimers NTAmers, our group recently demonstrated that TCR-pMHC dissociation rates robustly correlate with those obtained by SPR [108]. Moreover, the half-lives determined by NTAmers accurately correlated to the killing capacity (i.e. EC_{50}) of tumor-specific T cell clones that were isolated from patients with melanoma [108] as well as following

therapeutic vaccination [109]. In a viral setting using a microscopy and reversible Streptamer-based assay, Nauerth *et al.* [99] have shown that virus-specific CD8 T cells bearing TCRs of high avidity were associated with improved function (i.e. killing capacity) and conferred better protection against *Listeria monocytogenes* infection in mice.

Here we performed a comprehensive study of TCR-pMHC off-rates combined with multiple functional assays on large representative libraries of human self/tumor- and non-self/virus-specific CD8 T cell clones (n > 600). We demonstrated that TCR-pMHC off-rates accurately predict CD107a degranulation, cytokine production, cell proliferation, stimulatory/inhibitory receptor expression (Manuscript 1, Figure 1 and 3), polyfunctionality (Manuscript 1, Figure 2), as well as *in vivo* anti-tumor activity (Manuscript 1, Figure 4). These data confirm that the TCR-pMHC off-rate is a major determinant controlling CD8 T cell function. Our findings are of particular scientific and practical importance as we also found that the TCR-ligand dissociation-rate is a highly stable biomarker, independent of the activation state of the cell and its assessment is highly reproducible for a given clone between different experiments. These features are advantageous compared with frequently used functional assays or multimer staining intensity (Manuscript 1, Figure 6). Together, these data show the potential of TCR-pMHC dissociation-rate measurements as a broadly applicable research method and as a highly promising biomarker to determine the potency of specific-T cells for immunotherapy.

1.4. Therapeutic implications: impact of peptide vaccines on TCR-pMHC binding avidity

Within the scope of cancer immunotherapy, and as shown above, TCR-ligand avidity represents a powerful and robust biomarker that can be used to monitor and study vaccine trials with the aim to determine the treatment regimen that offers the best clinical efficacy in patients. In this regard, NTAmer-based TCR-pMHC off-rates have recently been used by our group to accurately characterize the quality of vaccination-induced self/tumor–specific T cell responses in melanoma patients. First, Gannon *et al.* [109] found differences in the TCR-pMHC binding avidity of Melan-A specific clones depending on the type of Melan-$A_{26\text{-}35}$ peptide used for vaccination. Specifically, they observed the selective enrichment of clones with increased TCR-pMHC binding avidity and stronger tumor reactivity following vaccination with the native Melan-$A^{MART\text{-}1}_{26\text{–}35}$ peptide compared to those derived from patients vaccinated with the analog Melan-$A^{MART\text{-}1}_{26\text{–}35\ (A27L)}$ peptide [109], despite the latter having a 10-fold increased

binding to HLA-A2 compared to the natural peptide [286]. Secondly, during my PhD thesis work, I took part in a project which aimed to evaluate the impact of the analog Melan-A$^{MART-1}_{26-35 (A27L)}$ peptide and CpG-B adjuvant dosage on the induction of tumor-specific CD8 T cell responses in melanoma patients in relation to TCR binding avidity and functional potency (Carretero-Iglesia L, Couturaud B *et al.*, manuscript in preparation). Indeed, as antigenic peptides are poorly immunogenic by themselves, they are administrated in conjunction with strong adjuvants such as the TLR9-mediated agonist CpG B-ODN 7909 and oil emulsion (i.e. incomplete Freund adjuvant, IFA) to generate a robust immune response [48, 287]. Such vaccines have been shown to generate functionally competent T cells *in vivo* [47, 288] and to correlate with favorable clinical outcome [289].

Here (Carretero-Iglesia L, Couturaud B *et al.*, manuscript in preparation), we found that increased peptide dose vaccine (i.e. 0.5 mg) promoted the more rapid selection (after only 4-vaccines) of Melan-A-specific CD8 T cells of enhanced TCR binding avidity (i.e. measured by NTAmer-based dissociation rates and frequency of CD8 binding-independent clones assessed using CD8-null NTAmers) and functional avidity. Comparable results were achieved with lower peptide doses (i.e. 0.1 mg) but required additional serial vaccinations (i.e. 8-vaccines), independently of the CpG-B dose (2-2.6 mg vs 1-1.3 mg). Finally, and in line with our results in Manuscript 1, strong correlations between dissociation rates measured by NTAmers and functional capacity were observed for vaccine-induced CD8 binding-dependent tumor-specific T cell clones. In contrast, these correlations were lost in the CD8 binding-independent group due to the increased proportion of higher avidity clones, despite sharing similar functional avidities to many clones bearing TCRs of lower avidity. This suggests that vaccine-induced CD8 T cell clones bearing high avidity TCRs reach a plateau of maximal response (Carretero-Iglesia L, Couturaud B *et al.*, manuscript in preparation). These results are in line with several studies showing that T cell activation and function are limited to a given TCR-pMHC affinity/avidity window, both in pathogen and tumor-specific T cell responses (reviewed in [94, 290]). Above a given TCR-pMHC affinity/avidity threshold in the upper part or beyond the natural TCR affinity range, T cell functionality does no longer correlate to TCR-pMHC affinity or off-rate [114, 117, 118, 290-295]. This phenomenon could in part explain our observation (Manuscript 1, Figure 1) of weaker, although statistically significant, correlations between TCR binding and functional avidity displayed by virus-specific T cells compared to tumor-specific T cells. Indeed, the overall virus-specific repertoire is of higher TCR-pMHC binding avidity compared to the tumor-specific repertoire.

In summary, TCR binding avidity represents a robust biomarker for the high-throughput assessment of tumor-specific CD8 T cell responses following therapeutic peptide vaccination.

1.5. TCR-pMHC binding avidity varies according to the antigenic specificity of CD8 T cells

One of the great advantages of the NTAmer technology is the possibility to accurately assess a wide spectrum of TCR binding avidities on living CD8 T cells (reviewed in [94]). Indeed, unlike the equivalent Streptamer technology which is limited to the analysis of non-self/virus-specific T cells of high TCR binding avidity due to the lag time (60 sec) in the switch from multimeric to monomeric form, NTAmer complexes dissociate in just a few seconds and allow the analysis of, for example, tumor-specific CD8 T cells of lower TCR avidity. Using this powerful technology, we were able to directly compare large T cell clonotype repertoires ($n >$ 300) across four different antigenic specificities. Comparison of off-rates for antigens of different origin revealed significantly slower off-rates (i.e. low k_{off}/high avidity TCRs) against non-self/viral antigens (i.e. CMV/pp65 and EBV/BMFL1) compared to self/tumor antigens (Melan-A and NY-ESO-1) (Manuscript 1, Figure 5). These results were in line with previous studies showing that while non-self/pathogen specific T cells covered a large range of TCR affinities [111], they are generally of high avidity [54, 55] (Figure 12). Of note, nonetheless, non-self-specific CD8 T cells of very low affinity have been shown to significantly participate in the immune response against pathogens [111]. Specifically, low affinity T cells exit the lymphatic system and enter blood circulation earlier than high avidity ones, and are thus essential for the early control of infection [111]. However, high affinity T cells expand more during the acute phase of infection, thus dominating the peak of the acute response and during memory, as observed in our study. On the other hand, self/tumor-specific T cells are generally of low TCR avidity (Figure 12), which can be explained by mechanisms of central and peripheral tolerance. Indeed, most tumor antigens are expressed in the thymus thus leading to the negative selection of thymocytes with high TCR affinity/avidity for those antigens [296]. In addition, self/tumor-specific T cells can be eliminated in the periphery through mechanisms of peripheral tolerance [297]. Nonetheless, a fraction of cytotoxic T cells reactive to self/tumors antigens with low TCR–pMHC affinity/avidity evade these mechanisms and are found in the periphery [298-301]. Despite being of low TCR avidity, these tumor-reactive T cells are capable of eliminating cancer cells [302, 303]. However, low avidity T cells generally need a stronger signal to be activated and do not exhibit extensive expansion, thus highlighting

the necessity to find better strategies to efficiently and sustainably activate tumor-specific T cells for immunotherapy [304, 305].

Figure 12: Representative TCR-pMHC binding affinity/avidity according to the antigenic specificity of CD8 T cells. *A. CD8 T cells specific for non-self/pathogen cover a large range of TCR affinities/avidities with a large proportion (depicted as dark blue gradients) of cells bearing intermediate to high affinity/avidity TCRs (depicted as orange-red arcs). B. Self/tumor-specific T cells are mainly of low TCR affinity/avidity (depicted as yellow arcs) which can be explained by mechanisms of central and peripheral tolerance. C. Neoantigen-specific T cells are more likely to escape thymic negative selection, as neoantigens are "non-self like" epitopes, thus potentially having a higher proportion of high affinity/avidity TCRs compared to tumor-specific T cells. Adapted from Hebeisen et al. 2015 [94].*

Moreover, we showed for the first time a significant difference in the TCR-pMHC binding avidity among different types of tumor antigens, with TCRs of cancer testis NY-ESO-1-specific T cells having a stronger binding to their pMHC than TCRs of differentiation antigen Melan-A-specific T cells from healthy individuals or unvaccinated melanoma patients (Manuscript 1, Figure 5). Yet, several clones of slower off-rates could still be detected, indicating the presence of rare self/Melan-A specific T cells of high binding avidity within the endogenous unvaccinated repertoire. We could have hypothesized that a large proportion of Melan-A specific CD8 T cells would be of high avidity as a recent study reported that medullary thymic epithelial cells express a truncated Melan-A transcript, lacking the expression of the immunodominant 26–35 epitope, thus precluding clonal deletion of specific CD8 T cells to this antigen during central tolerance [306]. This particular thymic expression in part explains the unusually high frequency of naive A2/Melan-A$_{26-35}$–specific CD8 T cells observed in melanoma patients as well as in healthy donors [307-309]. In addition, Melan-A multimer+ T

cells have been shown to be highly cross-reactive with several self- and pathogen-specific epitopes thus further increasing the size of the subset of Melan-A-specific naive T cells [310]. Nonetheless, differentiation antigens such as Melan-A are not highly tumor specific, as they are expressed in both tumor cells and normal tissues (e.g. healthy melanocytes), thus presumably leading to the deletion of high affinity Melan-A-specific T cells in blood circulation by peripheral tolerance mechanisms. Nevertheless, several clones with enhanced TCR binding avidity could still be detected in vaccinated melanoma patients (Manuscript 1, Figure 5), indicating the presence of rare self/Melan-A-specific CD8 T cells that are selected upon vaccination, in line with a previous study [311]. These results highlight the relevance of therapeutic vaccination approaches to enhance the quality of the tumor-specific T cell repertoire. Contrary to Melan-A, cancer testis antigens such as NY-ESO-1 are strictly tumor-specific. Although these antigens are naturally expressed in trophoblastic cells and male germ cells, they do not lead to auto-immune responses because in the healthy state these cells are devoid of HLA class I molecules and cannot present antigens to T cells [312]. These results further highlight the importance of optimizing the choice of tumor antigens for the development of cancer-based immunotherapies.

1.6.   Perspectives for immunotherapy

The ability to accurately measure the TCR-pMHC binding avidity of tumor-specific T cells could be of great potential for cancer immunotherapy. Specifically, NTAmer technology is an easy-to-use approach that can be readily standardized to identify rare naturally occurring tumor-specific TCRs of high avidity in order to use them for adoptive cell transfer and/or T cell engineering. In addition, it is of particular interest to investigate the TCR-pMHC avidity of neoantigen-specific CD8 T cells. These exclusively tumor-specific T cells are more likely to escape thymic negative selection [313] and are, thus, potentially of high TCR avidity (Figure 12) [314] while being unlikely to drive immune tolerance. Moreover, CD4 and CD8 neoantigen-specific T cells have been associated with favorable clinical outcome in several human cancer types (reviewed in [315]).

TCR-pMHC avidity has long been underestimated as a clinically relevant biomarker due to technical limitations for its precise assessment. Here, we demonstrated that NTAmer-based TCR-pMHC off-rate parameters represent a powerful biomarker to characterize *in vitro* and *in vivo* CD8 T cell potency within antigen-specific CD8 T cell responses. Nonetheless, a high-

throughput method to identify high avidity T cells at the single cell level, directly *ex vivo*, with minimal manipulation and with the potential to recover the sample for amplification and/or genetic engineering before re-employment for treatment is still lacking. In that regard, Soler *et al.* [316] recently developed a label-free 2D affinity analysis of TCR-pMHC by employing a multiparametric Surface Plasmon Resonance (MP-SPR) biosensor functionalized with artificial cell membranes. Another approach consists in the single cell serial determination of 2D TCR-pMHC affinity (based on micropipette adhesion frequency) and TCR clonotyping [256]. Such promising technological progress is of significant interest and clinical importance for the near future.

2. Impact of TCR-ligand binding avidity on the persistence of viral-specific CD8 T cell clonotypes over time

2.1. T cell responses in chronic infections

Contrary to acute infections where the virus is eliminated, chronic infections are characterized by the persistence of a certain level of viremia. The long-term persistence of chronic infections may manifest itself in different ways, from chronic infection with high and sustained viremia (e.g., hepatitis B and C virus or HIV), to infections with periodic reactivation (e.g., herpes simplex virus, VZV or EBV), or to low but continuous chronic infections such as CMV [197]. Gaining insight into the development of memory T cell responses against these viruses and their fine regulation is of fundamental interest to better understand how the human immune system works, as well as of medical importance for the development of preventive and therapeutic treatments such as viral vaccines. For this purpose, animal models of chronic infections such as lymphocytic choriomeningitis virus (LCMV) or MCMV are highly valuable tools as they allow for the tight control of many parameters such as the time of infection, the viral load or co-infections, and allow analyses of all organs [317]. Nonetheless, mice can generally only be studied for a maximum period of several months, while chronic infections in humans may persist for several decades. In addition, recent studies have shown that laboratory pathogen free mice used in many studies are not ideal models to mimic real life infections [318] as they lack differentiated memory cells [319], as well as physical and psychosocial natural stressors [320] that could have an impact on chronic infections and their regulation. Therefore, gaining better insight into CD8 T-cell responses to persistent infections in humans is of utmost importance.

In this regard, T cell immune responses against CMV and EBV have been widely investigated over the last two decades. These herpes viruses are genetically stable agents with double stranded DNA genomes that co-exist with their infected host in a finely orchestrated balance. The high prevalence of these infections in the world (reaching 100% in some populations) and their important contribution to mortality in immunosuppressed individuals, as well as the key role of T cells in controlling these latent infections, make them attractive models to study long-term immune responses. Moreover, during latency, EBV is thought to sporadically reactivate and replicate in B cells, leading to intermittent cycles of T cell rest and stimulation, while CMV could be considered more as a smoldering chronic infection. This difference in biology provides an interesting setting to compare the impact of continuous T cell stimulation versus resting memory T cells with infrequent stimulation, on the evolution of TCRαβ repertoires over time.

In this study (see Manuscript 2), we compared the TCRαβ clonal evolution between CMV (A2/pp65) and EBV (A2/BMFL1) latent infections in a human longitudinal study (over a period of 15 years). Specifically, we aimed at investigating the degree to which this process is determined by TCR-pMHC binding avidity in both viral models. Our findings reveal a progressive long-term avidity decline of CMV- but not EBV-specific memory CD8 T cell clonotype repertoires. This was associated with the preferential expression of the checkpoint inhibitor LILRB1 in high-avidity CMV-specific T cell clonotypes. These data highlight the critical role played by TCR avidity-driven repertoire evolution in the long-term outcome of CMV-specific, compared to EBV-specific, CD8 T cell responses in healthy individuals.

2.2.   TCRαβ clonotype repertoire assessments

TCR repertoire analyses are challenging due to the immense diversity and complexity of the TCR alpha-beta chain that composes each TCR, and especially the CDR3 region, but also due to several technical limitations. In humans, most analyses are done from a few hundred milliliters of blood and ignore the T cell repertoires found in lymphoid organs or tissues, thus leading to an incomplete picture of overall TCR usage.

A direct and pioneering approach to characterize TCR repertoire usage is the use of TRBV-specific antibodies combined to virus- or tumor-specific multimers [257, 321]. This method has been widely exploited [90, 213, 322, 323], even if it only assesses the BV usage and does not reveal the level of heterogeneity at the clonotype level. Nonetheless, it can be used as a first

screening analysis as well as a tool to validate clonal repertoires assessed by other methods. In our study, we used this technology for the latter purpose (Manuscript 2, Figure 1C and 2A) and found a strong correlation between the percentage of cells *ex vivo* stained with specific TRBV antibodies and the percentage of TRBV clonotypes assessed by *in vitro* cloning. Indeed, *in vitro* cloning by limiting dilutions followed by sequencing of the TCRs of the generated clones is an alternative and more precise approach to study TCR repertoires as it allows sequence determination for paired TCR α and β chains for each clone. Nowadays, it is still one of the methods of choice to characterize TCRαβ repertoires. One drawback of this approach is the potential bias introduced by the different capacity of each clone to proliferate or not during *in vitro* culture. In addition, this method is not sufficiently powerful and high-throughput to estimate a complete TCR repertoire diversity. Nonetheless, to study epitope-specific populations with skewed repertoires composed of a maximum of a few dozen dominant clonotypes, this method has shown robust results [90, 324]. Here, we observed a strong correlation between repertoires assessed by the *in vitro* cloning strategy and both *ex vivo* TRBV staining and *ex vivo* sorted-single cell sequencing (Manuscript 2, Figure 1C-E and 2A). Finally, a significant advantage of the generation of *in vitro* clones is the possibility to precisely assess TCR-pMHC binding avidity on living T cells. Together, *in vitro* cloning by limiting dilution followed by TCR sequencing is a robust method to determine TCRαβ clonotype sequences and TCR-pMHC kinetic measurements simultaneously at the individual T cell level.

A major breakthrough in TCR repertoire analyses was the development of high-throughput sequencing techniques that allow for the sequencing of millions of DNA molecules in parallel. While being very informative on the TCR diversity in healthy individuals [13, 325, 326] or in the tumor setting [327], these techniques have several limitations especially for the quantitative analysis of the TCR clonal repertoire due to inconsistent PCR efficiency, PCR and sequencing errors or the impact of the level of TCR expression (reviewed in [328]). In addition, only the TCR β chain is generally sequenced thus not giving information about the α/β pairing. It is only very recently that high-throughput sequencing for paired α and β chains has started to become possible with the development of single cell sequencing (reviewed in [329, 330]). Several groups have used full-length single-cell RNA-sequencing with TCR reconstruction methods to study T cell clonality and fate [331-334]. Others have used tag-based strategies where a "barcode" is introduced during the reverse transcription reaction thus "tagging" the whole cDNA of a single cell [335-337]. These methods increase the high-throughput potential as all tagged-cDNAs can be pooled and prepared together for sequencing. Nonetheless, they

are less informative and sensitive compared to full-length strategies. These state-of-the-art technologies have so far only been used by a few research groups and not on frozen human samples, thus precluding longitudinal studies. Moreover, only one group has successfully assessed single cell 2D TCR-pMHC affinity (based on micropipette adhesion frequency) simultaneously with TCR sequencing in a high-throughput manner [256]. In addition, so far this technology recovered the paired TCR$\alpha\beta$ sequence in only 20% to 50% of cases. Whilst highly promising, these techniques need refinement to become more accessible and widespread in the coming years and to succeed classical *in vitro* cloning approaches.

2.3.   TCR off-rate is a stable biomarker for a given TCR$\alpha\beta$ clonotype

We showed that NTAmer-based TCR off-rates are highly stable for the same Melan-A-specific CD8 T cell clones in intra- and inter-experimental measurements (Manuscript 1, Fig. 6). In addition, off-rate measurements for a given clone at different time-points post-stimulation were highly stable when compared to functional assays (Manuscript 1, Fig. 6), in line with a previous study by Nauerth *et al.* [99] characterizing given CMV/pp65-specific clones using Streptamer technology. Using this approach, they further demonstrated that k_{off} data of two CMV/IE1-specific clones were highly similar to the k_{off} data obtained from Jurkat-76 cells transduced with the TCR α and β chains isolated from the clones. Gannon *et al.* [109] further demonstrated the robustness of the reversible NTAmer-based technique to analyse tumor-specific T cell clones from early- (EM28+) and late- (EM28-) differentiation subsets bearing the same TCR$\alpha\beta$. Highly similar off-rates between T cell subsets were again found, independently of the differentiation status of the T cell clones. Together these results indicate that the TCR is the main driver of TCR-pMHC binding avidity with only marginal impact of other cell-specific parameters such as the differentiation state or cell activation background.

In our second study (Manuscript 2), we strengthened this concept as we found highly comparable off-rate measurements for a given virus-specific TCR$\alpha\beta$ clonotype (Manuscript 2, Fig.3 and Supp. Fig. 3), indicative of the strong stability of TCR off-rates for a given clonotype. Moreover, while a given clonotype displayed significant biological differences over time, i.e. between T_n and 15 years later (i.e. T_{n+15y}), as shown by *ex vivo* RNA sequencing (Manuscript 2, Fig. 6A and Supp. Fig. 4A), NTAmer-based off-rates were again highly conserved. Indeed, strong positive correlations were observed between NTAmer-based off-rates from EBV- and CMV-specific T cell clones bearing the same TCR$\alpha\beta$ obtained at T_n and T_{n+15y} from the six

studied healthy donors, both with wild-type (WT)- and CD8null-NTAmers (Manuscript 2, Fig. 3B, E, Supp. Fig2A and Fig. 4 A, B). Collectively, these data demonstrate that the TCRαβ is a highly stable determinant of the TCR-pMHC structural/binding avidity of living CD8 T cells measured by reversible multimers.

2.4.   TRVB but not TRAV usage of EBV-specific T cells is linked to different TCR avidity

Here, we characterized the TCR repertoire diversity and composition of EBV- and CMV-specific CD8 T cell repertoires from 6 healthy donors. In line with previous studies [90, 91, 199, 202, 203, 205] , in A2/EBV-BMFL1-specific CD8 T cell repertoires, we observed the preferential usage of some TRBV families, i.e. TRBV20, TRBV29, TRBV2 and to a lesser extent TRBV6 and TRBV14 (Manuscript 2, Fig. 2). There was also a marked preferential usage of TRAV families with, in all EBV-positive donors combined, 34 clonotypes out of 57 using TRAV5 with a recurrent TRAV5-DNNARL-AJ31 motif, followed by 14 clonotypes using TRAV12-1 with the frequent motif TRAV12-1-NGxDSSYKL-AJ12. Moreover, we identified three public TCR sequences defined by identical α/β TCRs shared between different healthy donors (Manuscript 2, Supp. Table 4). On the other hand, A2/CMV-pp65-specific repertoires did not show striking TRBV usage preference even though several TCR clonotypes bearing TRBV6-5 and TRBV12 gene segments were each identified in two different healthy individuals (Manuscript, Supp. Table 3). TRAV usage was more biased with the preferential usage of TRAV18 observed in 3 out of 4 individuals (Manuscript, Supp. Table 3), with a recurrent TRAV18-xxGNQF-AJ49 motif. Finally, while we did not identify "true" CMV-specific α/β public TCRs, we found an identical β chain, i.e. TRBV12-SSANYGY-BJ1.2, in two donors, that has previously been described by others [91, 202, 205]. The less stringent TCR bias in the CMV-specific response compared to EBV can in part be explained by highly restricted repertoires with only a few dominant clonotypes in each individual.

TCR bias can arise for various different reasons. The peptide accessibility in the MHC could bias the selection of naive T cells bearing TCRs with conserved structural motifs. Specifically, peptides deeply encapsulated in the MHC groove in a featureless conformation may select restricted TCRs with specific structural pattern [338], while protruding peptides would drive the selection of a broader TCR diversity (reviewed in [339]). However, TCR bias cannot be exclusively attributed to a featureless pMHC, as we observed striking TCR bias of

the A2/EBV-BMFL1 specific response despite it being a protuberant peptide [340]. Indeed, it has been shown that the commonly observed biased TRAV5 and TRBV20 gene usage in the A2/EBV-BMFL1 specific response is related to unique residues encoded only by these genes which lead to specific pMHC contacts [340]. Finally, antigen-driven selection and amplification of clones bearing TCRs of high avidity/affinity based on a particular pMHC recognition model may occur. In this context, Gras *et al.* [219] demonstrated that the immunodominance of a high avidity TCR (based on CD8null multimer staining and multimer dissociation assay) [205] in the pp65/CMV-specific response could be explained by the fact that it forms tight contacts with 3 peptide residues and one HLA-A*0201 amino acid, and is thus of high structural complementarity with the entire peptide. However, this cannot be the main parameter driving TCR bias as we and others [205] observed the preferential selection of TCRs covering a large range of TCR-pMHC avidities. Many other factors can have an impact on TCR selection and bias such as convergent recombination, bias in TCR α and β chain pairing for optimal interaction with MHC or an individual's MHC haplotype (reviewed in [341]). The number of parameters impacting TCR selection and their synergy renders the understanding of mechanisms underlying TCR usage bias very challenging.

In our study we also demonstrated in four EBV-positive healthy donors that TCR-pMHC binding avidity and CD8-binding dependency measured by NTAmers and CD8null NTAmers, respectively, were closely related to distinct TRBV family usage but to a weaker extent to TRAV usage (Manuscript 2, Fig. 4, Supp. Fig. 3). Indeed, substantial TCR avidity differences were observed between the two highly dominant TRBV families, with TRBV20 clonotypes bearing significantly higher avidity TCRs (slower off-rates) and being mainly CD8-binding independent compared to TRBV29 clonotypes which were generally of low avidity (fast off-rates) and largely CD8-binding dependent (Manuscript 2, Fig. 4). These differences in TCR binding avidity related to particular TRBV families were to some extent further reflected at the functional avidity level. Specifically, TRBV29 clonotypes produced slightly less CD107a and cytokines (IFNγ; TNFα), and were less able to kill target cells than TRBV20 clonotypes (Manuscript 2, Fig. 4H). These functional analyses could in part be biased by the relatively broad avidity range of each TRBV family, precluding the assessment of clear functional differences. Nonetheless, these data are in line with the strong positive correlation observed between TCR-pMHC binding avidity and functional capacities at the clonal level in our first manuscript (Manuscript 1, [254]). On the other hand, the highly dominant TRAV5 and TRAV12 families were not

associated with distinct TCR-pMHC binding avidity and clones bearing such TCRs covered a large range of avidity (Manuscript 2, Supp. Fig. 3E). Together, we have shown that in EBV/BMLF1-specific responses, the TCR-pMHC binding avidity was linked to preferential TRBV but not TRAV usage and had no impact on clonotype prevalence over time which was found to be highly stable, independent of the clonotypes' TCR avidity.

2.5. Virus-specific TCRαβ clonal repertoire over time

Previous longitudinal studies have reported that the clonal repertoire specific for CMV and EBV infections, once established, did not evolve for at least several years [91, 198, 216, 217, 342, 343]. Nonetheless, the maximal time span analyzed in those studies was 5 years, whereas CMV and EBV immune responses persist for decades and small changes in the TCR repertoire may only be observed over longer periods of time. To gain deeper insight into the persistence and/or evolution of EBV- and CMV-specific CD8 T cell clonal repertoires over extended periods of time, we analyzed the TCRαβ clonotype composition and selection of large panels of CMV- and EBV-specific CD8 T-cell clones from our cohort of chronically infected healthy donors over a period of 15 years.

2.5.1. Differences between EBV- and CMV-specific clonal repertoires

EBV-specific responses studied in four healthy donors revealed a remarkable stability in the clonal repertoire composition and distribution between the two time-points, suggesting that, once established, EBV-specific repertoires are kept strikingly constant over time (Manuscript 2, Fig. 2C). Whether this clonal repertoire stability is a global characteristic of EBV-specific responses or only of responses against the studied EBV epitope, i.e. $A2/BMLF1_{280-288}$, remains to be elucidated. Indeed, $A2/BMLF1_{280-288}$ is an epitope from the early protein BMLF1 of the lytic cycle. Immediate early and early protein-derived epitopes are preferentially expressed on the infected cell surface during the acute phase of EBV infection and lead to the amplification of T cells specific for those epitopes. During the latent phase, highly restricted latent gene expression in infected cells avoids immune detection by minimizing antigen exposure [127]. The remarkable stability of the EBV-specific CD8 T cell repertoire observed here could be due to the absence of targeted-epitope expression in healthy donors during the latent phase. Nonetheless, Miles *et al.* [92] also demonstrated the persistence of single CD8 T cell clonotypes against two latent epitopes, i.e. HLA B*0801/FLR and HLA B*4405/EEN, for 18 and 11 years, respectively, in two healthy individuals.

In the four CMV-positive healthy donors, we observed that CMV-specific TCRαβ repertoire composition was also maintained, but fluctuations in the clonotypes' distribution were still observed over the 15 year observation period (Manuscript 2, Fig. 1F). Indeed, preferential selection of certain clonotypes over others occurred throughout the course of persistent CMV infection. This phenomenon was especially apparent in three donors (BCL4, 6 and 1), while the CMV-specific TCR repertoire analysis of donor BCL9 showed a relatively more stable repertoire with only two clonotypes out of seven showing frequency variation over time (Manuscript 2, Fig. 1F). These findings suggest that distinct mechanisms regulate the long-term outcome of memory CMV versus EBV-specific CD8 T cell repertoires.

These two contrasting models of repertoire evolution over long periods time during the latent phase of EBV- and CMV-specific memory CD8 T cell responses could, in part, be due to differences in the biology of the two viruses. Indeed, as represented in figure 13, during latency, EBV reactivation and replication in B cells occurs only sporadically, leading to cycles of T cell rest and stimulation thus maintaining a pool of functional CD8 T cells over time [197]. On the contrary, CMV latent infection is thought to be characterized by a continuous low level of transcriptional activity leading to the constant stimulation of CD8 T cells with infrequent rest [196, 197]. While we did not observe a significant increase of CMV+ cells in the CD8 T cell compartment of our donors over time, the continual CD8 T cell stimulation observed in CMV responses is thought to be the main driver of memory inflation observed in chronic CMV infection, and will be discussed in detail in the section 2.5.3.
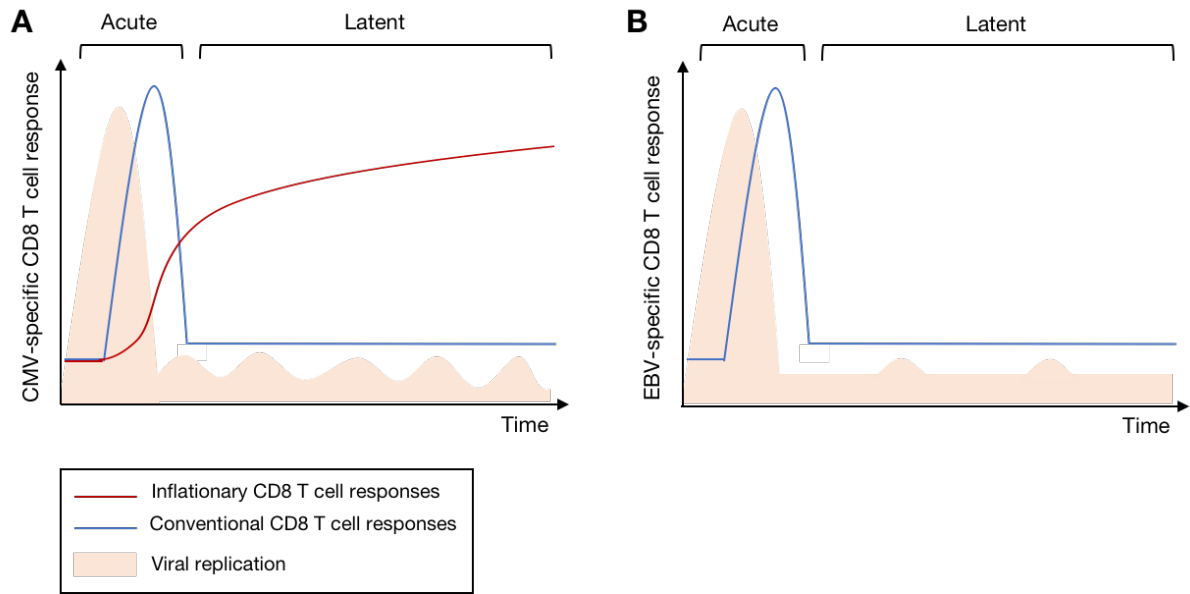
Figure 13: Model of CMV- and EBV-specific CD8 T cell response dynamics. *Representative kinetics of (A) CMV- and (B) EBV-specific CD8 T cells during the acute and latent phases of infection. A. CMV latent infection is characterized by regular transcriptional activity leading to continuous T cell stimulation and the memory inflation of some CMV-specific CD8 T cells. B. EBV reactivation events are only sporadic, leading to the maintenance of a constant pool of CD8 T cells over time. Adapted from Torti, Oxenius 2012, Wherry, Ahmed 2004, and O'Hara G et al. 2012 [171, 196, 197].*

2.5.2. Role of TCR avidity in CMV-specific clonal selection

Despite major efforts, the parameters underlying the long-term maintenance or the selection of some virus-specific CD8 T cell clones during the latent phase of infection remain poorly understood. TCR avidity/affinity has been investigated by several groups, including ours [91, 202, 342, 344], and proposed as a major determinant of TCR repertoire selection and dominance in CMV-specific CD8 T cell responses. Nonetheless, its precise impact on long-term TCR clonal repertoire evolution in healthy individuals has so far not been investigated.

Recently, Schober *et al.* [345] proposed three theoretical models for the evolution of CMV-specific CD8 T cell clonotype repertoires during latency, according to TCR-pMHC binding avidity. The first one assumes that a TCR hierarchy according to TCR avidity is established during the initial response with an avidity maturation similar to secondary T-cell responses, and it is subsequently stably maintained over long periods of time (Figure 14, model A). However, an alternative hypothesis is that CMV-specific T cell clones bearing high avidity TCRs are continuously preferentially selected over time as shown in the second model (Figure 14, model

B). Finally, as Davenport *et al.* [220] have already proposed, a third model hypothesizes an initial accumulation of high-avidity virus-specific T cells followed by the succession of clones of lower TCR avidities due to the proliferative senescence of high avidity T cells by frequent antigenic stimulation (Figure 14, model C).
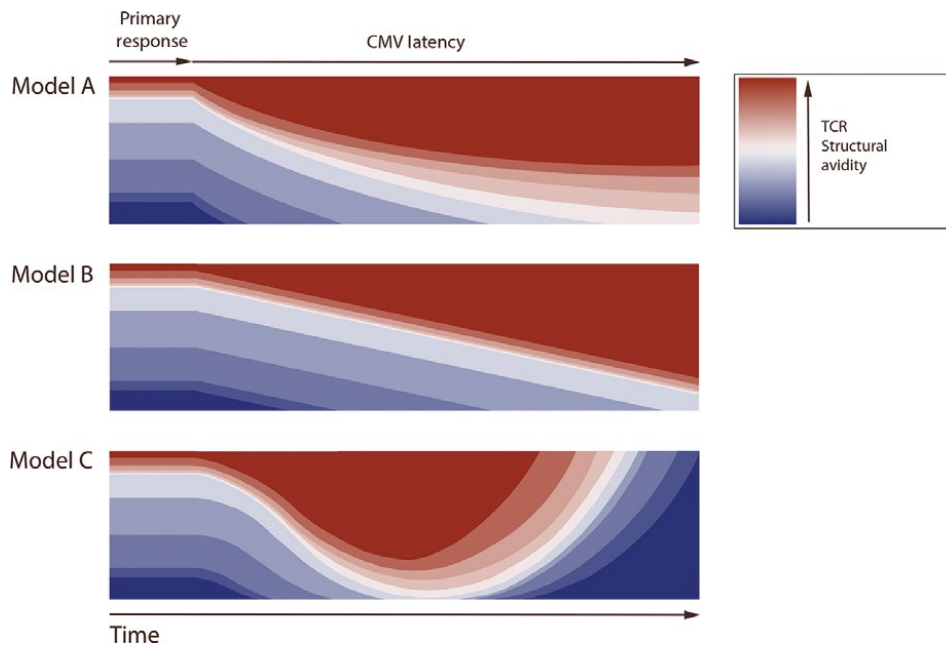

Figure 14: Models of TCR avidity-dependent repertoire evolution during CMV latency. *During CMV latency, a TCR repertoire hierarchy according to TCR avidity could be established and then maintained in a state of equilibrium (model A), or lead to the continued selection of high avidity clones over time (model B). Alternatively, high avidity clones could by more prone to proliferative senescence after an initial accumulation, and thus be succeeded by clones with lower avidity TCRs over time (model C). Adapted from Schober et al. 2018 [345].*

In our study, we took advantage of NTAmer and CD8null NTAmer based off-rate measurements to assess the impact of TCR-ligand avidity on the evolution of clonal repertoires specific for latent herpes viruses over extended periods of time (i.e. 15 years). We observed, at the clonal level, the preferential selection and expansion over time of clonotypes of relatively lower TCR-pMHC avidity and higher CD8 binding dependency compared to clonotypes that tended to decrease in frequency over time (Manuscript 2, Fig. 3). Consequently, at the CMV+CD8+ population level, we also observed a significant overall avidity decline over time (Manuscript 2, Fig. 5). These results are in line with the third model proposed by Schober *et al.*

[345] (Figure 14) and are supported by studies that have investigated TCR repertoire evolution during aging, by comparing groups of individuals of different ages, and revealed an accumulation of lower avidity CMV-specific CD8 T cells [221, 222]. Together, our data and others [221, 222] indicate a T cell repertoire skewing towards an overall lower avidity over extended periods of time and during aging in CMV chronic infection. This was strikingly contrasting with EBV-specific repertoires which were highly stable in terms of repertoire composition and distribution, as well as in overall avidity (Manuscript 2, Fig. 5). Indeed, EBV-specific repertoire evolution fits with the 1st model proposed by Schober *et al.* [345] (Figure 14, model A), which assumes that clones bearing TCRs covering a large range of affinities are selected during the primary response and early during the latent phase and are subsequently stably maintained over long periods of time.

2.5.3. CMV memory inflation

CMV-specific immune responses have been largely investigated in recent decades for their particular capacity to accumulate over time in hosts, in a phenomenon called memory inflation. In our study, we did not observe clear signs of T cell expansion as only one donor, BCL6, showed an increase in the frequency of CMV/pp65+ cells in the pool of CD8 T cells over time (Manuscript 2, Fig. 1). Several studies [156, 346], but not all [347, 348], have observed that both major CMV immunodominant proteins, pp65 and IE1, can drive the accumulation of antigen-specific T cells in humans with aging. Nonetheless, our observation could in part be explained by the pattern of expression of the studied epitope, pp65, compared with IE1, during latency [348-350]. Indeed, immediate early proteins such as IE1 are the first proteins to be expressed during latent CMV replication and even the only one in some instances as CMV replication has been shown to be arrested before early proteins are made in monocytic precursor cells [351]. As a result, IE1-specific T cells would be the first to be activated and to kill infected cells before the production of early and late proteins such as pp65. Therefore, pp65-specific T cells may be less prone to constant stimulation and more dependent on productive CMV reactivation. The importance of the targeted epitope in memory inflation has been extensively studied in mice, where it has been shown that its location in the CMV genome and its ability to be processed by the constitutive proteasome of infected cells influence the degree of memory inflation (reviewed in [352]). In addition, in humans, memory inflation has been particularly described in populations over 60 years old [156, 353] while the studied CMV positive healthy donors here had an average age of 45 years (+/- 10 years) at the time of the second sample collection

(Manuscript 2, Supp. Table 2). Thus, one hypothesis is that in our setting it is too early in the course of the latent phase to observe significant T cell expansion/inflation.

Importantly, it should be noted that whether CMV memory inflation really occurs in humans is still a matter of debate (reviewed in [354]). While several studies observed an accumulation of CMV-specific T cells in humans, others have shown no such accumulation. These discrepancies could be link to several parameters such as (i) the choice of the studied epitope-specific response, (ii) the setting, i.e. longitudinal versus cross-sectional studies and the lack of knowledge of when primary hCMV infection occurred, (iii) the method (*ex vivo* multimer staining or quantitative functional assay) or (iv) the readout (absolute number or frequency of virus-specific T cells). Additional long-term longitudinal studies with the precise quantification of T cells specific for a large array of CMV epitopes in human are still required.

Nonetheless, in our study, we observed the decline in frequency of clones of higher TCR-pMHC binding avidity. In addition to the theory of proliferative senescence of high avidity T cells previously described (Figure 14, Model C), additional and non-exclusive factors could further account for a slow repertoire avidity decline over time in the context of CMV memory inflation. For example, it has been shown in mice that the inflationary repertoire is highly dynamic with the continuous production of short-lived EM T cells recruited from a pool of CM cells [173]. One could hypothesize that naive T cells with high avidity TCRs would generate a larger pool of CM T cells during the acute phase thus leading to the maintenance of a repertoire of mainly high avidity EM T cells over time. Nonetheless, high avidity CM T cells might also have higher chances of differentiating into EM T cells with no further backup of memory cells. Thus, high avidity T cells would gradually disappear from the long-term maintained memory pool and be replaced by cells of lower TCR avidity. Many other parameters such as virus-specific factors have been described to impact the degree of memory inflation (reviewed in [352]) and thus potentially the extent of repertoire shift. For instance, a high initial viral inoculum and, thus, an increased number of latently CMV-infected cells lead to increased memory inflation in mice [355] (Figure 15). In addition, instances of complete CMV reactivation or CMV re-infection, even if well controlled by immunocompetent hosts, could also significantly impact the repertoire clonal dominance.
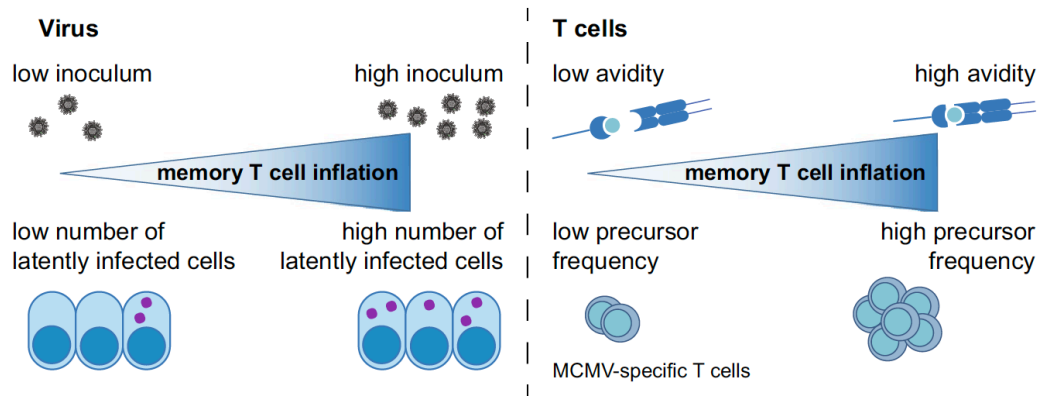
Figure 15: Parameters driving the degree of MCMV memory inflation. *From the virus perspective, the size of the initial viral inoculum and the number of latently infected cells impact the extent of memory inflation. From the host perspective, the inflationary T cell precursor frequency as well as their TCR avidity for the pMHC can influence the degree of memory inflation. Adapted from Welten, Bauman and Oxenius, 2019 [352].*

2.5.4.   Mechanisms for overall repertoire avidity decline over time

To gain further insight into the mechanisms underlying the selection of low avidity clonotypes over time in chronic CMV-specific CD8 T cell responses, we performed a global transcription profiling by RNA sequencing on *ex vivo* sorted populations representative of each of the main clonotypes isolated at T_n and T_{n+15y}. BCL9 was excluded from this screening since this particular donor presented a more diverse as well as a more stable clonotype repertoire over time, in contrast to the preferential accumulation of low binding avidity clonotypes observed in the other three donors. Only a limited number of genes were significantly differentially expressed between high and low avidity samples as well as between samples from T_n and T_{n+15y} (Manuscript 2, Figure 6, Supp. Fig. 4). One still has to keep in mind that the analyzed cells were *ex vivo* sorted quiescent cells from long term cryopreserved samples, with no *in vitro* culture nor stimulation. Thus, the extraction of good quality RNA and identification of few differentially expressed genes was not a foregone conclusion. Interestingly, one of the genes upregulated in high avidity clonotypes as well as at late time points encodes for the inhibitory receptor, LILRB1 (CD85j/ILT-2/LIR-1). Consistently, clonotypes that decreased in frequency over time, which are mainly of high avidity, were also those that expressed higher levels of *LILRB1* compare to clonotypes that increased, at both T_n and T_{n+15y}.

LILRB1 is a receptor expressed in various immune cell types including monocytes, B and T cells, NK cells and dendritic cells, but at different levels depending on the cell type [356]. It acts as an inhibitory receptor through its cytoplasmic tail which contains several immunoreceptor tyrosine-based inhibitory motifs (ITIMs) that are able to recruit the tyrosine phosphatases Src homology region 2 domain-containing phosphatase-1 and -2 (SHP-1 and SHP-2) [357]. LILRB1 recognizes MHC class I molecules and interacts with especially high affinity with HLA-G molecules [358]. In addition, it binds with high affinity to the hCMV-UL18 molecule [359], which is an MHC-I homologue expressed by CMV infected cells, and which has been proposed to act as a decoy molecule to avoid immune recognition by NK cells [360]. Indeed, LILRB1 has been shown to be expressed by CMV-specific CD8 T cells [172, 263, 353, 361] and its expression has been described to increase with age and to be associated with the senescence marker, CD57 [172, 263]. In this context, Gustafson *et al.* recently showed that LILRB1 characterized a population of senescent cells with altered proliferative capacity but conserved cytokine production capacities [263]. They proposed LILRB1 as a checkpoint regulator to control virus-specific T cell expansion during ageing.

Expanding on this study, we observed in all CMV-positive donors including BCL9, increased LILRB1 expression at the protein level in high avidity CMV-specific clonotypes that decreased over time (Manuscript 2, Fig. 7), associated with increased expression of CD57 but not PD-1. In addition, by blocking LILRB1 with a specific antibody we were able to increase the proliferative potential of LILRB1^{high} clones upon pp65-specific stimulation while no significant differences were observed on CD107a degranulation or on IFNγ and TNFα production. Collectively, our data suggest that LILRB1 has an important function as an inhibitory checkpoint receptor, specifically in controlling the expansion of high avidity clonotypes over the course of latent CMV infection (Figure 16). In contrast to CMV-specific T cell clonotypes, similar and low LILRB1 expression was found among the different EBV-specific T cell clonotypes and was not related to specific TRBV family usage. Collectively, our data reinforce the key role of TCR binding avidity in tailoring CMV- but not EBV-specific clonal evolution during long periods of viral latency.
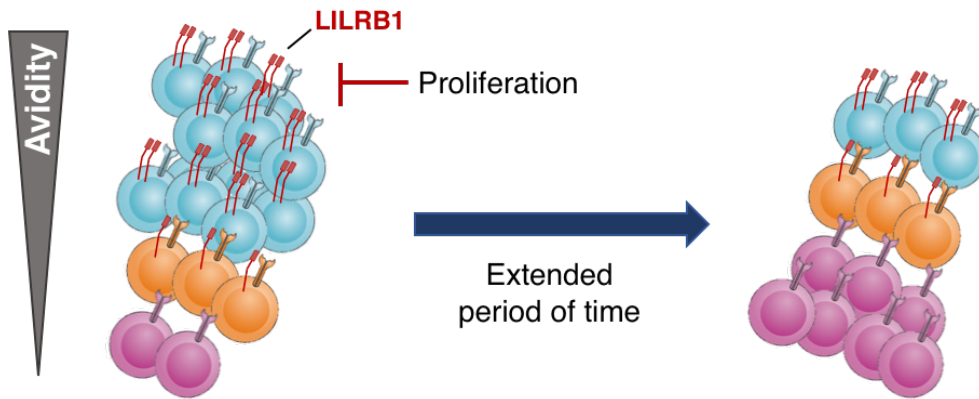
Figure 16: Representative model of LILRB1 in shaping CMV-specific repertoires over time. *Expression of the inhibitory receptor LILRB1 by high avidity T cells (i.e. blue cells) could be a mechanism for overall repertoire avidity decline over the course of latent CMV infection, specifically by regulating the expansion of high avidity clonotypes.*

The role of LILRB1 as an inhibitory checkpoint receptor might be even more pronounced in the context of CMV memory inflation. Indeed, as the main factor driving memory inflation has been shown to be repetitive antigen exposure [177, 362], one could hypothesize that high avidity T cells would be more sensitive to this constant stimulation and thus more susceptible to express inhibitory receptors such as LILRB1. This could lead to an even more drastic phenomenon of repertoire shift and overall avidity decline over time in the context of memory inflation. This hypothesis is in line with the recently published study by Baumann *et al.* who showed in mice that T cells recruited early into the inflationary pool are mainly of high avidity [363] (Figure 15), thus being potentially more prone to increased LILRB1 expression in response to chronic stimulation and subsequent slow replacement by cells of lower TCR avidity over extend periods of time. Nonetheless, whether this mechanism can be observed in short-lived models such as mice remains unclear.

In addition to the expression of LILRB1, we could hypothesize that high avidity CMV-specific T cells might be more subject to replicative senescence. The increased expression of the marker of senescence CD57, but not PD-1, observed in high avidity CMV-specific T cells clonotypes (Manuscript 2, Fig. 7) is in line with a senescent phenotype and not an exhausted one. Others have also reported that CMV-specific CD8 T cells often maintain effector function, in contrast to exhausted T cells [177, 364], but can show signs of replicative senescence due to shortened

telomeres [231]. Together, this suggest that CMV-specific CD8 T cells of high TCR avidity are more susceptible to become senescent, i.e. high functionality but a decreased proliferative potential, than low avidity T cells during CMV latency. This mechanism would be in line with the previously presented model (Figure 14, Model C) of replicative senescence of high avidity T cells leading to the progressive decline of the overall repertoire avidity, as observed in our study. This hypothesis will be investigated in the future by assessing the telomere length of CMV+ TRBV+ clonotypes directly *ex vivo* by quantitative PCR.

One could imagine that the loss of high avidity CMV-specific T cells in aging with persistent CMV infection would be detrimental for the host and would increase the chances of clinically dangerous CMV reactivation. On the other hand, mechanisms that dampen immune responses might also be highly beneficial. In the context of CMV infection likely characterized as a smoldering infection with continuous T cell stimulation, we could imagine that without regulatory mechanisms, highly antigen sensitive T cells, i.e. high avidity T cells, would extensively proliferate and overwhelm the T cell compartment. Such an outgrowth of only few epitope-specific T cells could severely impair CD8-mediated immune responses against other pathogens. Expression of inhibitory receptors such as LILRB1 may provide another mechanism by which excessive expansion of some virus-specific T cells during lifelong latent infection might be tightly regulated, while preserving a global functional repertoire. Along these lines and despite being of relatively lower TCR-pMHC binding avidity, we observed that clonotypes enriched over time were nonetheless of high functional quality and able to efficiently kill target cells, thereby providing long term protection from CMV reactivation or re-infection.

2.6.   Perspectives

In our study, we are able to demonstrate the decline of CMV- but not EBV-specific CD8 T cells of high TCR avidity over time. This decline was associated with increased expression of the inhibitory receptor LILRB1, both at the gene level by *ex vivo* RNA sequencing and at the protein level in *in vitro* generated clones. Nonetheless, the assessment of protein expression in *in vitro* maintained clones is often tricky and does not necessarily reflect *in vivo* expression. *In vitro* culture can induce significant bias depending on the culture conditions, the activation state of the cells, or the number of rounds of *in vitro* stimulation they have been subjected to. In our study, although LILRB1 expression profiles in clones were in line with the gene expression

assessed by *ex vivo* RNA sequencing, we observed a great diversity of LILRB1 expression levels among clones sharing the same TCRαβ clonotype. This could indicate a bias of culture and clone selection and potentially not reflecting the protein expression at the population level. To overcome this limitation, we plan to assess the level of LILRB1 expression, as well as CD57 and PD-1, directly *ex vivo* on the cell surface of CMV/TRBV-specific populations of selected healthy donors at T_n and T_{n+15y}. These data should further confirm the preferential expression of LILRB1 in high avidity CMV-specific T cells *in vivo*.

LILRB1 interacts with MHC class I molecules and acts as an inhibitory receptor through several ITIM motifs which can transmit inhibitory signals and inhibit the activity of immune cells [365]. In the context of CMV, LILRB1 interacts with high affinity with the MHC-I homologue UL18 expressed by CMV infected cells and inhibits LILRB1^{high} NK cell function [360], thus potentially protecting CMV infected cells from LILRB1^{high} NK cell attack. Based on our data, we could speculate a similar role of UL18 expression by CMV-infected cells to limit LILRB1^{high} CD8 T cell function. Similarly, LILRB1 is thought to be important for the evasion from immune surveillance of HLA-G positive tumor cells [366, 367]. Indeed, HLA-G is a high affinity ligand of LILRB1, and elevated expression of both markers in tumor tissue has been associated with advanced tumor stage [368]. In addition, HLA-G-LILRB1 signaling has been studied in NK cells and shown to inhibit the proliferation and cytotoxic activity of infiltrating NK cells in gastric cancer, thus limiting their anti-tumor activity [369]. Finally, LILRB1 interaction with the common MHC class I component β2-microglobulin, expressed on the cell surface of macrophages and cancer cells, respectively, has been shown to act as a "don't eat" me signal that prevents cancer cell phagocytosis [370]. Together, these studies suggest that LILRB1 could be an important immunological target for engaging immune cells such as NK cells and macrophages to attack cancer cells. In addition, one could hypothesize that LILRB1 expressing tumor infiltrating CD8 T cells would be hindered by tumor cells expressing common MHC class I component β2-microglobulin or HLA-G, thus impairing efficient T cell-mediated anti-tumor immunity. Thereby, agents directed against the MHC-class I-LILRB1 signaling axis might sensitize tumors to immune attack. Nonetheless, MHC-I is ubiquitously expressed by normal cells, thus raising questions regarding the safety and specificity of potential MHC-1-LILRB1 targeted immunotherapy. Additional studies are necessary to better understand the role of LILRB1 in both the viral and tumor contexts, and to explore the MHC-l-LILRB1 axis as a target for immunotherapy.

Bibliography

1.   Murphy, K., *Janeway's Immunobiology 8th edition.* 2012.
2.   Zuniga-Pflucker, J.C., *T-cell development made simple.* Nat Rev Immunol, 2004. 4(1): p. 67-72.
3.   Klein, L., et al., *Positive and negative selection of the T cell repertoire: what thymocytes see (and don't see).* Nat Rev Immunol, 2014. 14(6): p. 377-91.
4.   Pittet, M.J., et al., *Melan-A/MART-1-specific CD8 T cells: from thymus to tumor.* Trends Immunol, 2002. 23(7): p. 325-8.
5.   Vignali, D.A., L.W. Collison, and C.J. Workman, *How regulatory T cells work.* Nat Rev Immunol, 2008. 8(7): p. 523-32.
6.   Bassing, C.H., W. Swat, and F.W. Alt, *The mechanism and regulation of chromosomal V(D)J recombination.* Cell, 2002. 109 Suppl: p. S45-55.
7.   Nikolich-Zugich, J., M.K. Slifka, and I. Messaoudi, *The many important facets of T-cell repertoire diversity.* Nat Rev Immunol, 2004. 4(2): p. 123-32.
8.   Davis, M.M. and P.J. Bjorkman, *T-cell antigen receptor genes and T-cell recognition.* Nature, 1988. 334(6181): p. 395-402.
9.   Miles, J.J., D.C. Douek, and D.A. Price, *Bias in the alphabeta T-cell repertoire: implications for disease pathogenesis and vaccination.* Immunol Cell Biol, 2011. 89(3): p. 375-87.
10.   Mora, T. and A.M. Walczak, *Quantifying lymphocyte receptor diversity.* bioRxiv, 2016.
11.   Bianconi, E., et al., *An estimation of the number of cells in the human body.* Ann Hum Biol, 2013. 40(6): p. 463-71.
12.   Arstila, T.P., et al., *A direct estimate of the human alphabeta T cell receptor diversity.* Science, 1999. 286(5441): p. 958-61.
13.   Qi, Q., et al., *Diversity and clonal selection in the human T-cell repertoire.* Proc Natl Acad Sci U S A, 2014. 111(36): p. 13139-44.
14.   Call, M.E. and K.W. Wucherpfennig, *The T cell receptor: critical role of the membrane environment in receptor assembly and function.* Annu Rev Immunol, 2005. 23: p. 101-25.
15.   Holler, P.D. and D.M. Kranz, *Quantitative analysis of the contribution of TCR/pepMHC affinity and CD8 to T cell activation.* Immunity, 2003. 18(2): p. 255-64.
16.   Miceli, M.C. and J.R. Parnes, *The roles of CD4 and CD8 in T cell activation.* Semin Immunol, 1991. 3(3): p. 133-41.
17.   Wooldridge, L., et al., *Interaction between the CD8 coreceptor and major histocompatibility complex class I stabilizes T cell receptor-antigen complexes at the cell surface.* J Biol Chem, 2005. 280(30): p. 27491-501.
18.   Salter, R.D., et al., *A binding site for the T-cell co-receptor CD8 on the alpha 3 domain of HLA-A2.* Nature, 1990. 345(6270): p. 41-6.
19.   Arcaro, A., et al., *Essential role of CD8 palmitoylation in CD8 coreceptor function.* J Immunol, 2000. 165(4): p. 2068-76.
20.   Nunes, J.A., et al., *Signal transduction by CD28 costimulatory receptor on T cells. B7-1 and B7-2 regulation of tyrosine kinase adaptor molecules.* J Biol Chem, 1996. 271(3): p. 1591-8.
21.   Acuto, O. and F. Michel, *CD28-mediated co-stimulation: a quantitative support for TCR signalling.* Nat Rev Immunol, 2003. 3(12): p. 939-51.
22.   McNeill, L., et al., *The differential regulation of Lck kinase phosphorylation sites by CD45 is critical for T cell receptor signaling responses.* Immunity, 2007. 27(3): p. 425-37.
23.   Hamann, D., et al., *Phenotypic and functional separation of memory and effector human CD8+ T cells.* J Exp Med, 1997. 186(9): p. 1407-18.
24.   Champagne, P., et al., *Skewed maturation of memory HIV-specific CD8 T lymphocytes.* Nature, 2001. 410(6824): p. 106-11.
25.   Akbar, A.N., et al., *Loss of CD45R and gain of UCHL1 reactivity is a feature of primed T cells.* J Immunol, 1988. 140(7): p. 2171-8.

26.   Raghavan, M., et al., *MHC class I assembly: out and about.* Trends Immunol, 2008. 29(9): p. 436-43.

27.   Bontrop, R.E., *Comparative genetics of MHC polymorphisms in different primate species: duplications and deletions.* Hum Immunol, 2006. 67(6): p. 388-97.

28.   Neefjes, J., et al., *Towards a systems understanding of MHC class I and MHC class II antigen presentation.* Nat Rev Immunol, 2011. 11(12): p. 823-36.

29.   Grakoui, A., et al., *The immunological synapse: a molecular machine controlling T cell activation.* Science, 1999. 285(5425): p. 221-7.

30.   Monks, C.R., et al., *Three-dimensional segregation of supramolecular activation clusters in T cells.* Nature, 1998. 395(6697): p. 82-6.

31.   Freiberg, B.A., et al., *Staging and resetting T cell activation in SMACs.* Nat Immunol, 2002. 3(10): p. 911-7.

32.   Pentcheva-Hoang, T., et al., *Programmed death-1 concentration at the immunological synapse is determined by ligand affinity and availability.* Proc Natl Acad Sci U S A, 2007. 104(45): p. 17765-70.

33.   Huppa, J.B. and M.M. Davis, *T-cell-antigen recognition and the immunological synapse.* Nat Rev Immunol, 2003. 3(12): p. 973-83.

34.   Love, P.E. and S.M. Hayes, *ITAM-mediated signaling by the T-cell antigen receptor.* Cold Spring Harb Perspect Biol, 2010. 2(6): p. a002485.

35.   Courtney, A.H., W.L. Lo, and A. Weiss, *TCR Signaling: Mechanisms of Initiation and Propagation.* Trends Biochem Sci, 2018. 43(2): p. 108-123.

36.   Smith-Garvin, J.E., G.A. Koretzky, and M.S. Jordan, *T cell activation.* Annu Rev Immunol, 2009. 27: p. 591-619.

37.   Kaech, S.M. and W. Cui, *Transcriptional control of effector and memory CD8+ T cell differentiation.* Nat Rev Immunol, 2012. 12(11): p. 749-61.

38.   Rufer, N., et al., *Ex vivo characterization of human CD8+ T subsets with distinct replicative history and partial effector functions.* Blood, 2003. 102(5): p. 1779-87.

39.   Sallusto, F., et al., *Two subsets of memory T lymphocytes with distinct homing potentials and effector functions.* Nature, 1999. 401(6754): p. 708-12.

40.   Romero, P., et al., *Four functionally distinct populations of human effector-memory CD8+ T lymphocytes.* J Immunol, 2007. 178(7): p. 4112-9.

41.   Schenkel, J.M. and D. Masopust, *Tissue-resident memory T cells.* Immunity, 2014. 41(6): p. 886-97.

42.   Shresta, S., et al., *How do cytotoxic lymphocytes kill their targets?* Curr Opin Immunol, 1998. 10(5): p. 581-7.

43.   Voskoboinik, I., J.C. Whisstock, and J.A. Trapani, *Perforin and granzymes: function, dysfunction and human pathology.* Nat Rev Immunol, 2015. 15(6): p. 388-400.

44.   Nagata, S., *Apoptosis by death factor.* Cell, 1997. 88(3): p. 355-65.

45.   Kuwano, K., T. Kawashima, and S. Arai, *Antiviral effect of TNF-alpha and IFN-gamma secreted from a CD8+ influenza virus-specific CTL clone.* Viral Immunol, 1993. 6(1): p. 1-11.

46.   Appay, V., et al., *New generation vaccine induces effective melanoma-specific CD8+ T cells in the circulation but not in the tumor site.* J Immunol, 2006. 177(3): p. 1670-8.

47.   Gannon, P.O., et al., *Rapid and Continued T-Cell Differentiation into Long-term Effector and Memory Stem Cells in Vaccinated Melanoma Patients.* Clin Cancer Res, 2017. 23(13): p. 3285-3296.

48.   Speiser, D.E., et al., *Rapid and strong human CD8+ T cell responses to vaccination with peptide, IFA, and CpG oligodeoxynucleotide 7909.* J Clin Invest, 2005. 115(3): p. 739-46.

49.   Goldszmid, R.S., A. Dzutsev, and G. Trinchieri, *Host immune response to infection and cancer: unexpected commonalities.* Cell Host Microbe, 2014. 15(3): p. 295-305.

50.   Tormoen, G.W., M.R. Crittenden, and M.J. Gough, *Role of the immunosuppressive microenvironment in immunotherapy.* Adv Radiat Oncol, 2018. 3(4): p. 520-526.

51.   Pasche, B., *Role of transforming growth factor beta in cancer.* J Cell Physiol, 2001. 186(2): p. 153-68.

52.   Colegio, O.R., et al., *Functional polarization of tumour-associated macrophages by tumour-derived lactic acid.* Nature, 2014. 513(7519): p. 559-63.

53.   Munn, D.H. and A.L. Mellor, *Indoleamine 2,3-dioxygenase and tumor-induced tolerance.* J Clin Invest, 2007. 117(5): p. 1147-54.

54.   Cole, D.K., et al., *Human TCR-binding affinity is governed by MHC class restriction.* J Immunol, 2007. 178(9): p. 5727-34.

55.   Aleksic, M., et al., *Different affinity windows for virus and cancer-specific T-cell receptors: implications for therapeutic strategies.* Eur J Immunol, 2012. 42(12): p. 3174-9.

56.   Tscharke, D.C., et al., *Sizing up the key determinants of the CD8(+) T cell response.* Nat Rev Immunol, 2015. 15(11): p. 705-16.

57.   Verdeil, G., et al., *From T cell "exhaustion" to anti-cancer immunity.* Biochim Biophys Acta, 2016. 1865(1): p. 49-57.

58.   Seder, R.A., P.A. Darrah, and M. Roederer, *T-cell quality in memory and protection: implications for vaccine design.* Nat Rev Immunol, 2008. 8(4): p. 247-58.

59.   Jenkins, M.K. and J.J. Moon, *The role of naive T cell precursor frequency and recruitment in dictating immune response magnitude.* J Immunol, 2012. 188(9): p. 4135-40.

60.   Iglesias, M.C., et al., *Immunodominance of HLA-B27-restricted HIV KK10-specific CD8(+) T-cells is not related to naive precursor frequency.* Immunol Lett, 2013. 149(1-2): p. 119-22.

61.   Obar, J.J., K.M. Khanna, and L. Lefrancois, *Endogenous naive CD8+ T cell precursor frequency regulates primary and memory responses to infection.* Immunity, 2008. 28(6): p. 859-69.

62.   Schmidt, J., et al., *Rapid antigen processing and presentation of a protective and immunodominant HLA-B*27-restricted hepatitis C virus-specific CD8+ T-cell epitope.* PLoS Pathog, 2012. 8(11): p. e1003042.

63.   Andersson, A.C. and P.J. Holst, *Increased T cell breadth and antibody response elicited in prime-boost regimen by viral vector encoded homologous SIV Gag/Env in outbred CD1 mice.* J Transl Med, 2016. 14(1): p. 343.

64.   Hervas-Stubbs, S., et al., *High frequency of CD4+ T cells specific for the TB10.4 protein correlates with protection against Mycobacterium tuberculosis infection.* Infect Immun, 2006. 74(6): p. 3396-407.

65.   Radebe, M., et al., *Broad and persistent Gag-specific CD8+ T-cell responses are associated with viral control but rarely drive viral escape during primary HIV-1 infection.* Aids, 2015. 29(1): p. 23-33.

66.   Elias, D., H. Akuffo, and S. Britton, *PPD induced in vitro interferon gamma production is not a reliable correlate of protection against Mycobacterium tuberculosis.* Trans R Soc Trop Med Hyg, 2005. 99(5): p. 363-8.

67.   Skinner, M.A., et al., *A DNA prime-live vaccine boost strategy in mice can augment IFN-gamma responses to mycobacterial antigens but does not increase the protective efficacy of two attenuated strains of Mycobacterium bovis against bovine tuberculosis.* Immunology, 2003. 108(4): p. 548-55.

68.   Engels, B., et al., *Relapse or eradication of cancer is predicted by peptide-major histocompatibility complex affinity.* Cancer Cell, 2013. 23(4): p. 516-26.

69.   Kotturi, M.F., et al., *Naive precursor frequencies and MHC binding rather than the degree of epitope diversity shape CD8+ T cell immunodominance.* J Immunol, 2008. 181(3): p. 2124-33.

70.   Vigano, S., et al., *Functional avidity: a measure to predict the efficacy of effector T cells?* Clin Dev Immunol, 2012. 2012: p. 153863.

71.   Alexander-Miller, M.A., G.R. Leggatt, and J.A. Berzofsky, *Selective expansion of high- or low-avidity cytotoxic T lymphocytes and efficacy for adoptive immunotherapy.* Proc Natl Acad Sci U S A, 1996. 93(9): p. 4102-7.

72.   Derby, M., et al., *High-avidity CTL exploit two complementary mechanisms to provide better protection against viral infection than low-avidity CTL.* J Immunol, 2001. 166(3): p. 1690-7.

73. Speiser, D.E., et al., *Discrepancy between in vitro measurable and in vivo virus neutralizing cytotoxic T cell reactivities. Low T cell receptor specificity and avidity sufficient for in vitro proliferation or cytotoxicity to peptide-coated target cells but not for in vivo protection.* J Immunol, 1992. 149(3): p. 972-80.

74. Almeida, J.R., et al., *Superior control of HIV-1 replication by CD8+ T cells is reflected by their avidity, polyfunctionality, and clonal turnover.* J Exp Med, 2007. 204(10): p. 2473-85.

75. Berger, C.T., et al., *High-functional-avidity cytotoxic T lymphocyte responses to HLA-B-restricted Gag-derived epitopes associated with relative HIV control.* J Virol, 2011. 85(18): p. 9334-45.

76. Abdel-Hakeem, M.S., et al., *Selective expansion of high functional avidity memory CD8 T cell clonotypes during hepatitis C virus reinfection and clearance.* PLoS Pathog, 2017. 13(2): p. e1006191.

77. Neveu, B., et al., *Selection of high-avidity CD8 T cells correlates with control of hepatitis C virus infection.* Hepatology, 2008. 48(3): p. 713-22.

78. Yerly, D., et al., *Increased cytotoxic T-lymphocyte epitope variant cross-recognition and functional avidity are associated with hepatitis C virus clearance.* J Virol, 2008. 82(6): p. 3147-53.

79. Bullock, T.N., et al., *Manipulation of avidity to improve effectiveness of adoptively transferred CD8(+) T cells for melanoma immunotherapy in human MHC class I-transgenic mice.* J Immunol, 2001. 167(10): p. 5824-31.

80. Zeh, H.J., 3rd, et al., *High avidity CTLs for two self-antigens demonstrate superior in vitro and in vivo antitumor efficacy.* J Immunol, 1999. 162(2): p. 989-94.

81. Dutoit, V., et al., *Heterogeneous T-cell response to MAGE-A10(254-262): high avidity-specific cytolytic T lymphocytes show superior antitumor activity.* Cancer Res, 2001. 61(15): p. 5850-6.

82. Speiser, D.E., et al., *A Novel Approach to Characterize Clonality and Differentiation of Human Melanoma-Specific T Cell Responses: Spontaneous Priming and Efficient Boosting by Vaccination.* The Journal of Immunology, 2006. 177(2): p. 1338-1348.

83. Betts, M.R., et al., *HIV nonprogressors preferentially maintain highly functional HIV-specific CD8+ T cells.* Blood, 2006. 107(12): p. 4781-9.

84. Harari, A., et al., *Skewed representation of functionally distinct populations of virus-specific CD4 T cells in HIV-1-infected subjects with progressive disease: changes after antiretroviral therapy.* Blood, 2004. 103(3): p. 966-72.

85. Ciuffreda, D., et al., *Polyfunctional HCV-specific T-cell responses are associated with effective control of HCV replication.* Eur J Immunol, 2008. 38(10): p. 2665-77.

86. Snyder, L.D., et al., *Polyfunctional T-Cell Signatures to Predict Protection from Cytomegalovirus after Lung Transplantation.* Am J Respir Crit Care Med, 2016. 193(1): p. 78-85.

87. Attaf, M., E. Huseby, and A.K. Sewell, *alphabeta T cell receptors as predictors of health and disease.* Cell Mol Immunol, 2015. 12(4): p. 391-9.

88. Meyer-Olson, D., et al., *Limited T cell receptor diversity of HCV-specific T cell responses is associated with CTL escape.* J Exp Med, 2004. 200(3): p. 307-19.

89. Messaoudi, I., et al., *Direct link between mhc polymorphism, T cell avidity, and diversity in immune defense.* Science, 2002. 298(5599): p. 1797-800.

90. Annels, N.E., et al., *Changing patterns of dominant TCR usage with maturation of an EBV-specific cytotoxic T cell response.* J Immunol, 2000. 165(9): p. 4831-41.

91. Iancu, E.M., et al., *Clonotype selection and composition of human CD8 T cells specific for persistent herpes viruses varies with differentiation but is stable over time.* J Immunol, 2009. 183(1): p. 319-31.

92. Miles, J.J., et al., *T-cell grit: large clonal expansions of virus-specific CD8+ T cells can dominate in the peripheral circulation for at least 18 years.* Blood, 2005. 106(13): p. 4412-3.

93. Chen, H., et al., *TCR clonotypes modulate the protective effect of HLA class I molecules in HIV-1 infection.* Nat Immunol, 2012. 13(7): p. 691-700.

94. Hebeisen, M., et al., *Identifying Individual T Cell Receptors of Optimal Avidity for Tumor Antigens.* Front Immunol, 2015. 6: p. 582.

95. Zehn, D., et al., *TCR signaling requirements for activating T cells and for generating memory.* Cell Mol Life Sci, 2012. 69(10): p. 1565-75.

96. Corse, E., R.A. Gottschalk, and J.P. Allison, *Strength of TCR-peptide/MHC interactions and in vivo T cell responses.* J Immunol, 2011. 186(9): p. 5039-45.

97. Schmidt, J., et al., *Reversible major histocompatibility complex I-peptide multimers containing Ni(2+)-nitrilotriacetic acid peptides and histidine tags improve analysis and sorting of CD8(+) T cells.* J Biol Chem, 2011. 286(48): p. 41723-35.

98. Schmidt, J., et al., *Analysis, Isolation, and Activation of Antigen-Specific CD4(+) and CD8(+) T Cells by Soluble MHC-Peptide Complexes.* Front Immunol, 2013. 4: p. 218.

99. Nauerth, M., et al., *TCR-ligand koff rate correlates with the protective capacity of antigen-specific CD8+ T cells for adoptive transfer.* Sci Transl Med, 2013. 5(192): p. 192ra87.

100. Edwards, L.J., et al., *Insights into T cell recognition of antigen: significance of two-dimensional kinetic parameters.* Front Immunol, 2012. 3: p. 86.

101. Huang, J., et al., *The kinetics of two-dimensional TCR and pMHC interactions determine T-cell responsiveness.* Nature, 2010. 464(7290): p. 932-6.

102. Liu, B., et al., *2D TCR-pMHC-CD8 kinetics determines T-cell responses in a self-antigen-specific TCR system.* Eur J Immunol, 2014. 44(1): p. 239-50.

103. Pryshchep, S., et al., *Accumulation of serial forces on TCR and CD8 frequently applied by agonist antigenic peptides embedded in MHC molecules triggers calcium in T cells.* J Immunol, 2014. 193(1): p. 68-76.

104. Dolton, G., et al., *Comparison of peptide-major histocompatibility complex tetramers and dextramers for the identification of antigen-specific T cells.* Clin Exp Immunol, 2014. 177(1): p. 47-63.

105. Hombrink, P., et al., *Mixed functional characteristics correlating with TCR-ligand koff -rate of MHC-tetramer reactive T cells within the naive T-cell repertoire.* Eur J Immunol, 2013. 43(11): p. 3038-50.

106. Wilde, S., et al., *Human antitumor CD8+ T cells producing Th1 polycytokines show superior antigen sensitivity and tumor recognition.* J Immunol, 2012. 189(2): p. 598-605.

107. Wang, X.L. and J.D. Altman, *Caveats in the design of MHC class I tetramer/antigen-specific T lymphocytes dissociation assays.* J Immunol Methods, 2003. 280(1-2): p. 25-35.

108. Hebeisen, M., et al., *Identification of Rare High-Avidity, Tumor-Reactive CD8+ T Cells by Monomeric TCR-Ligand Off-Rates Measurements on Living Cells.* Cancer Res, 2015. 75(10): p. 1983-91.

109. Gannon, P.O., et al., *Quantitative TCR:pMHC Dissociation Rate Assessment by NTAmers Reveals Antimelanoma T Cell Repertoires Enriched for High Functional Competence.* J Immunol, 2015. 195(1): p. 356-66.

110. Ozga, A.J., et al., *pMHC affinity controls duration of CD8+ T cell-DC interactions and imprints timing of effector differentiation versus expansion.* J Exp Med, 2016. 213(12): p. 2811-2829.

111. Zehn, D., S.Y. Lee, and M.J. Bevan, *Complete but curtailed T-cell response to very low-affinity antigen.* Nature, 2009. 458(7235): p. 211-4.

112. van Gisbergen, K.P., et al., *The costimulatory molecule CD27 maintains clonally diverse CD8(+) T cell responses of low antigen affinity to protect against viral variants.* Immunity, 2011. 35(1): p. 97-108.

113. Chen, J.L., et al., *Ca2+ release from the endoplasmic reticulum of NY-ESO-1-specific T cells is modulated by the affinity of TCR and by the use of the CD8 coreceptor.* J Immunol, 2010. 184(4): p. 1829-1839.

114. Kalergis, A.M., et al., *Efficient T cell activation requires an optimal dwell-time of interaction between the TCR and the pMHC complex.* Nat Immunol, 2001. 2(3): p. 229-34.

115. Malecek, K., et al., *Specific increase in potency via structure-based design of a TCR.* J Immunol, 2014. 193(5): p. 2587-99.

116. Robbins, P.F., et al., *Single and dual amino acid substitutions in TCR CDRs can enhance antigen-specific T cell functions.* J Immunol, 2008. 180(9): p. 6116-31.

117. Schmid, D.A., et al., *Evidence for a TCR affinity threshold delimiting maximal CD8 T cell function.* J Immunol, 2010. 184(9): p. 4936-46.

118. Tan, M.P., et al., *T cell receptor binding affinity governs the functional profile of cancer-specific CD8+ T cells.* Clin Exp Immunol, 2015. 180(2): p. 255-70.

119. Johnson, L.A. and C.H. June, *Driving gene-engineered T cell immunotherapy of cancer.* Cell Res, 2017. 27(1): p. 38-58.

120. Rapoport, A.P., et al., *NY-ESO-1-specific TCR-engineered T cells mediate sustained antigen-specific antitumor effects in myeloma.* Nat Med, 2015. 21(8): p. 914-921.

121. Robbins, P.F., et al., *A pilot trial using lymphocytes genetically engineered with an NY-ESO-1-reactive T-cell receptor: long-term follow-up and correlates with response.* Clin Cancer Res, 2015. 21(5): p. 1019-27.

122. Robbins, P.F., et al., *Tumor regression in patients with metastatic synovial cell sarcoma and melanoma using genetically engineered lymphocytes reactive with NY-ESO-1.* J Clin Oncol, 2011. 29(7): p. 917-24.

123. Cohen, J.I., *Epstein-Barr virus infection.* N Engl J Med, 2000. 343(7): p. 481-92.

124. Pembrey, L., et al., *Seroprevalence of cytomegalovirus, Epstein Barr virus and varicella zoster virus among pregnant women in Bradford: a cohort study.* PLoS One, 2013. 8(11): p. e81881.

125. Higgins, C.D., et al., *A study of risk factors for acquisition of Epstein-Barr virus and its subtypes.* J Infect Dis, 2007. 195(4): p. 474-82.

126. McAulay, K.A., et al., *HLA class I polymorphisms are associated with development of infectious mononucleosis upon primary EBV infection.* J Clin Invest, 2007. 117(10): p. 3042-8.

127. Rowe, M. and J. Zuo, *Immune responses to Epstein-Barr virus: molecular interactions in the virus evasion of CD8+ T cell immunity.* Microbes Infect, 2010. 12(3): p. 173-81.

128. Andrei, G., E. Trompet, and R. Snoeck, *Novel Therapeutics for Epstein(-)Barr Virus.* Molecules, 2019. 24(5).

129. Balfour, H.H., Jr., et al., *Behavioral, virologic, and immunologic factors associated with acquisition and severity of primary Epstein-Barr virus infection in university students.* J Infect Dis, 2013. 207(1): p. 80-8.

130. Lunemann, A., et al., *A distinct subpopulation of human NK cells restricts B cell transformation by EBV.* J Immunol, 2013. 191(10): p. 4989-95.

131. Strowig, T., et al., *Tonsilar NK cells restrict B cell transformation by the Epstein-Barr virus via IFN-gamma.* PLoS Pathog, 2008. 4(2): p. e27.

132. Hislop, A.D., et al., *Tonsillar homing of Epstein-Barr virus-specific CD8+ T cells and the virus-host balance.* J Clin Invest, 2005. 115(9): p. 2546-55.

133. Catalina, M.D., et al., *Differential evolution and stability of epitope-specific CD8(+) T cell responses in EBV infection.* J Immunol, 2001. 167(8): p. 4450-7.

134. Hislop, A.D., et al., *Epitope-specific evolution of human CD8(+) T cell responses from primary to persistent phases of Epstein-Barr virus infection.* J Exp Med, 2002. 195(7): p. 893-905.

135. Woodberry, T., et al., *Differential targeting and shifts in the immunodominance of Epstein-Barr virus-specific CD8 and CD4 T cell responses during acute and persistent infection.* J Infect Dis, 2005. 192(9): p. 1513-24.

136. Guerrero-Ramos, A., et al., *Performance of the architect EBV antibody panel for determination of Epstein-Barr virus infection stage in immunocompetent adolescents and young adults with clinical suspicion of infectious mononucleosis.* Clin Vaccine Immunol, 2014. 21(6): p. 817-23.

137. Cannon, M.J., D.S. Schmid, and T.B. Hyde, *Review of cytomegalovirus seroprevalence and demographic characteristics associated with infection.* Rev Med Virol, 2010. 20(4): p. 202-13.

138. Kahl, M., et al., *Efficient lytic infection of human arterial endothelial cells by human cytomegalovirus strains.* J Virol, 2000. 74(16): p. 7628-35.

139. Scrivano, L., et al., *HCMV spread and cell tropism are determined by distinct virus populations.* PLoS Pathog, 2011. 7(1): p. e1001256.

140. Sinzger, C., M. Digel, and G. Jahn, *Cytomegalovirus cell tropism.* Curr Top Microbiol Immunol, 2008. 325: p. 63-83.

141. Poole, E., et al., *Virally induced changes in cellular microRNAs maintain latency of human cytomegalovirus in CD34(+) progenitors.* J Gen Virol, 2011. 92(Pt 7): p. 1539-49.

142. Taylor-Wiedeman, J., et al., *Monocytes are a major site of persistence of human cytomegalovirus in peripheral blood mononuclear cells.* Journal of General Virology, 1991. 72(9): p. 2059-2064.

143. Reeves, M.B., et al., *An in vitro model for the regulation of human cytomegalovirus latency and reactivation in dendritic cells by chromatin remodelling.* J Gen Virol, 2005. 86(Pt 11): p. 2949-54.

144. Soderberg-Naucler, C., K.N. Fish, and J.A. Nelson, *Reactivation of latent human cytomegalovirus by allogeneic stimulation of blood cells from healthy donors.* Cell, 1997. 91(1): p. 119-26.

145. Marsico, C. and D.W. Kimberlin, *Congenital Cytomegalovirus infection: advances and challenges in diagnosis, prevention and treatment.* Ital J Pediatr, 2017. 43(1): p. 38.

146. Kanj, S.S., et al., *Cytomegalovirus infection following liver transplantation: review of the literature.* Clin Infect Dis, 1996. 22(3): p. 537-49.

147. Pereyra, F. and R.H. Rubin, *Prevention and treatment of cytomegalovirus infection in solid organ transplant recipients.* Curr Opin Infect Dis, 2004. 17(4): p. 357-61.

148. Meyers, J.D., N. Flournoy, and E.D. Thomas, *Risk factors for cytomegalovirus infection after human marrow transplantation.* J Infect Dis, 1986. 153(3): p. 478-88.

149. Peterson, P.K., et al., *Cytomegalovirus disease in renal allograft recipients: a prospective study of the clinical features, risk factors and impact on renal transplantation.* Medicine (Baltimore), 1980. 59(4): p. 283-300.

150. Heagy, W., et al., *Inhibition of immune functions by antiviral drugs.* J Clin Invest, 1991. 87(6): p. 1916-24.

151. Blyth, E., et al., *Donor-derived CMV-specific T cells reduce the requirement for CMV-directed pharmacotherapy after allogeneic stem cell transplantation.* Blood, 2013. 121(18): p. 3745-58.

152. Peggs, K.S., *Adoptive T cell immunotherapy for cytomegalovirus.* Expert Opin Biol Ther, 2009. 9(6): p. 725-36.

153. Rauser, G., et al., *Rapid generation of combined CMV-specific CD4+ and CD8+ T-cell lines for adoptive transfer into recipients of allogeneic stem cell transplants.* Blood, 2004. 103(9): p. 3565-72.

154. Walter, E.A., et al., *Reconstitution of cellular immunity against cytomegalovirus in recipients of allogeneic bone marrow by transfer of T-cell clones from the donor.* N Engl J Med, 1995. 333(16): p. 1038-44.

155. Nichols, W.G., et al., *High risk of death due to bacterial and fungal infection among cytomegalovirus (CMV)-seronegative recipients of stem cell transplants from seropositive donors: evidence for indirect effects of primary CMV infection.* J Infect Dis, 2002. 185(3): p. 273-82.

156. Khan, N., et al., *Herpesvirus-specific CD8 T cell immunity in old age: cytomegalovirus impairs the response to a coresident EBV infection.* J Immunol, 2004. 173(12): p. 7481-9.

157. Jonjic, S., et al., *Antibodies are not essential for the resolution of primary cytomegalovirus infection but limit dissemination of recurrent virus.* J Exp Med, 1994. 179(5): p. 1713-7.

158. Vanarsdall, A.L. and D.C. Johnson, *Human cytomegalovirus entry into cells.* Curr Opin Virol, 2012. 2(1): p. 37-42.

159. Jonjic, S., et al., *Site-restricted persistent cytomegalovirus infection after selective long-term depletion of CD4+ T lymphocytes.* J Exp Med, 1989. 169(4): p. 1199-212.

160. Walton, S.M., et al., *Absence of cross-presenting cells in the salivary gland and viral immune evasion confine cytomegalovirus immune control to effector CD4 T cells.* PLoS Pathog, 2011. 7(8): p. e1002214.

161. Elkington, R., et al., *Ex vivo profiling of CD8+-T-cell responses to human cytomegalovirus reveals broad and multispecific reactivities in healthy virus carriers.* J Virol, 2003. 77(9): p. 5226-40.

162. Sylwester, A.W., et al., *Broadly targeted human cytomegalovirus-specific CD4+ and CD8+ T cells dominate the memory compartments of exposed subjects.* J Exp Med, 2005. 202(5): p. 673-85.

163. Holtappels, R., et al., *Enrichment of immediate-early 1 (m123/pp89) peptide-specific CD8 T cells in a pulmonary CD62L(lo) memory-effector cell pool during latent murine cytomegalovirus infection of the lungs.* J Virol, 2000. 74(24): p. 11495-503.

164. Klenerman, P., *The (gradual) rise of memory inflation.* Immunol Rev, 2018. 283(1): p. 99-112.

165.   Sylwester, A., et al., *A new perspective of the structural complexity of HCMV-specific T-cell responses.* Mech Ageing Dev, 2016. 158: p. 14-22.

166.   Karrer, U., et al., *Memory inflation: continuous accumulation of antiviral CD8+ T cells over time.* J Immunol, 2003. 170(4): p. 2022-9.

167.   Munks, M.W., et al., *Four distinct patterns of memory CD8 T cell responses to chronic murine cytomegalovirus infection.* J Immunol, 2006. 177(1): p. 450-8.

168.   Hosie, L., et al., *Cytomegalovirus-Specific T Cells Restricted by HLA-Cw*0702 Increase Markedly with Age and Dominate the CD8+ T-Cell Repertoire in Older People.* Frontiers in Immunology, 2017. 8(1776).

169.   Komatsu, H., et al., *Population analysis of antiviral T cell responses using MHC class I-peptide tetramers.* Clin Exp Immunol, 2003. 134(1): p. 9-12.

170.   Luo, X.H., et al., *The impact of inflationary cytomegalovirus-specific memory T cells on anti-tumour immune responses in patients with cancer.* Immunology, 2018. 155(3): p. 294-308.

171.   O'Hara, G.A., et al., *Memory T cell inflation: understanding cause and effect.* Trends Immunol, 2012. 33(2): p. 84-90.

172.   Northfield, J., et al., *Does memory improve with age? CD85j (ILT-2/LIR-1) expression on CD8 T cells correlates with 'memory inflation' in human cytomegalovirus infection.* Immunol Cell Biol, 2005. 83(2): p. 182-8.

173.   Snyder, C.M., et al., *Memory inflation during chronic viral infection is maintained by continuous production of short-lived, functional T cells.* Immunity, 2008. 29(4): p. 650-9.

174.   Appay, V., et al., *Memory CD8+ T cells vary in differentiation phenotype in different persistent virus infections.* Nat Med, 2002. 8(4): p. 379-85.

175.   Vieira Braga, F.A., et al., *Molecular characterization of HCMV-specific immune responses: Parallels between CD8(+) T cells, CD4(+) T cells, and NK cells.* Eur J Immunol, 2015. 45(9): p. 2433-45.

176.   Wherry, E.J. and M. Kurachi, *Molecular and cellular insights into T cell exhaustion.* Nat Rev Immunol, 2015. 15(8): p. 486-99.

177.   Klenerman, P. and A. Oxenius, *T cell responses to cytomegalovirus.* Nat Rev Immunol, 2016. 16(6): p. 367-77.

178.   Polic, B., et al., *Hierarchical and redundant lymphocyte subset control precludes cytomegalovirus replication during latent infection.* J Exp Med, 1998. 188(6): p. 1047-54.

179.   Simon, C.O., et al., *CD8 T cells control cytomegalovirus latency by epitope-specific sensing of transcriptional reactivation.* J Virol, 2006. 80(21): p. 10436-56.

180.   Torti, N., et al., *Non-hematopoietic cells in lymph nodes drive memory CD8 T cell inflation during murine cytomegalovirus infection.* PLoS Pathog, 2011. 7(10): p. e1002313.

181.   Smith, C.J., H. Turula, and C.M. Snyder, *Systemic hematogenous maintenance of memory inflation by MCMV infection.* PLoS Pathog, 2014. 10(7): p. e1004233.

182.   Stern-Ginossar, N., et al., *Decoding Human Cytomegalovirus.* Science, 2012. 338(6110): p. 1088-1093.

183.   Miller-Kittrell, M. and T.E. Sparer, *Feeling manipulated: cytomegalovirus immune manipulation.* Virol J, 2009. 6: p. 4.

184.   Browne, E.P. and T. Shenk, *Human cytomegalovirus UL83-coded pp65 virion protein inhibits antiviral gene expression in infected cells.* Proceedings of the National Academy of Sciences, 2003. 100(20): p. 11439-11444.

185.   Hegde, N.R., et al., *Inhibition of HLA-DR Assembly, Transport, and Loading by Human Cytomegalovirus Glycoprotein US3: a Novel Mechanism for Evading Major Histocompatibility Complex Class II Antigen Presentation.* Journal of Virology, 2002. 76(21): p. 10929-10941.

186.   Noriega, V.M., et al., *Human cytomegalovirus US3 modulates destruction of MHC class I molecules.* Molecular Immunology, 2012. 51(2): p. 245-253.

187.   Odeberg, J., et al., *The Human Cytomegalovirus Protein UL16 Mediates Increased Resistance to Natural Killer Cell Cytotoxicity through Resistance to Cytolytic Proteins.* Journal of Virology, 2003. 77(8): p. 4539-4545.

188. Kotenko, S.V., et al., *Human cytomegalovirus harbors its own unique IL-10 homolog (cmvIL-10).* Proceedings of the National Academy of Sciences, 2000. 97(4): p. 1695-1700.

189. Callan, M.F., et al., *Direct visualization of antigen-specific CD8+ T cells during the primary immune response to Epstein-Barr virus In vivo.* J Exp Med, 1998. 187(9): p. 1395-402.

190. Chen, G., et al., *CD8 T cells specific for human immunodeficiency virus, Epstein-Barr virus, and cytomegalovirus lack molecules for homing to lymphoid sites of infection.* Blood, 2001. 98(1): p. 156-64.

191. Dunne, P.J., et al., *Epstein-Barr virus-specific CD8(+) T cells that re-express CD45RA are apoptosis-resistant memory cells that retain replicative potential.* Blood, 2002. 100(3): p. 933-40.

192. Vescovini, R., et al., *Different contribution of EBV and CMV infections in very long-term carriers to age-related alterations of CD8+ T cells.* Exp Gerontol, 2004. 39(8): p. 1233-43.

193. Brenchley, J.M., et al., *Expression of CD57 defines replicative senescence and antigen-induced apoptotic death of CD8+ T cells.* Blood, 2003. 101(7): p. 2711-20.

194. Gillespie, G.M., et al., *Functional heterogeneity and high frequencies of cytomegalovirus-specific CD8(+) T lymphocytes in healthy seropositive donors.* J Virol, 2000. 74(17): p. 8140-50.

195. Catalina, M.D., et al., *Phenotypic and functional heterogeneity of EBV epitope-specific CD8+ T cells.* J Immunol, 2002. 168(8): p. 4184-91.

196. Torti, N. and A. Oxenius, *T cell memory in the context of persistent herpes viral infections.* Viruses, 2012. 4(7): p. 1116-43.

197. Wherry, E.J. and R. Ahmed, *Memory CD8 T-cell differentiation during viral infection.* J Virol, 2004. 78(11): p. 5535-45.

198. Couedel, C., et al., *Selection and long-term persistence of reactive CTL clones during an EBV chronic response are determined by avidity, CD8 variable contribution compensating for differences in TCR affinities.* J Immunol, 1999. 162(11): p. 6351-8.

199. Koning, D., et al., *CD8⁺ TCR Repertoire Formation Is Guided Primarily by the Peptide Component of the Antigenic Complex.* The Journal of Immunology, 2013. 190(3): p. 931-939.

200. Miles, J.J., et al., *CTL recognition of a bulged viral peptide involves biased TCR selection.* J Immunol, 2005. 175(6): p. 3826-34.

201. Nguyen, T.H., et al., *Maintenance of the EBV-specific CD8(+) TCRalphabeta repertoire in immunosuppressed lung transplant recipients.* Immunol Cell Biol, 2017. 95(1): p. 77-86.

202. Price, D.A., et al., *Avidity for antigen shapes clonal dominance in CD8+ T cell populations specific for persistent DNA viruses.* J Exp Med, 2005. 202(10): p. 1349-61.

203. Trautmann, L., et al., *Dominant TCR V alpha usage by virus and tumor-reactive T cells with wide affinity ranges for their specific antigens.* Eur J Immunol, 2002. 32(11): p. 3181-90.

204. Attaf, M., et al., *Major TCR Repertoire Perturbation by Immunodominant HLA-B(*)44:03-Restricted CMV-Specific T Cells.* Front Immunol, 2018. 9: p. 2539.

205. Trautmann, L., et al., *Selection of T Cell Clones Expressing High-Affinity Public TCRs within Human Cytomegalovirus-Specific CD8 T Cell Responses.* The Journal of Immunology, 2005. 175(9): p. 6123-6132.

206. Miconnet, I., et al., *Large TCR Diversity of Virus-Specific CD8 T Cells Provides the Mechanistic Basis for Massive TCR Renewal after Antigen Exposure.* The Journal of Immunology, 2011. 186(12): p. 7039-7049.

207. Arden, B., et al., *Human T-cell receptor variable gene segment families.* Immunogenetics, 1995. 42(6): p. 455-500.

208. Chen, G., et al., *Sequence and Structural Analyses Reveal Distinct and Highly Diverse Human CD8(+) TCR Repertoires to Immunodominant Viral Antigens.* Cell reports, 2017. 19(3): p. 569-583.

209. Lim, A., et al., *Frequent contribution of T cell clonotypes with public TCR features to the chronic response against a dominant EBV-derived epitope: application to direct detection of their molecular imprint on the human peripheral T cell repertoire.* J Immunol, 2000. 165(4): p. 2001-11.

210. Venturi, V., et al., *The molecular basis for public T-cell responses?* Nat Rev Immunol, 2008. 8(3): p. 231-8.

211. Wang, G.C., et al., *T cell receptor alphabeta diversity inversely correlates with pathogen-specific antibody levels in human cytomegalovirus infection.* Sci Transl Med, 2012. 4(128): p. 128ra42.

212. Day, E.K., et al., *Rapid CD8+ T Cell Repertoire Focusing and Selection of High-Affinity Clones into Memory Following Primary Infection with a Persistent Human Virus: Human Cytomegalovirus.* The Journal of Immunology, 2007. 179(5): p. 3203-3213.

213. Callan, M.F., et al., *CD8(+) T-cell selection, function, and death in the primary immune response in vivo.* J Clin Invest, 2000. 106(10): p. 1251-61.

214. Silins, S.L., et al., *Development of Epstein-Barr virus-specific memory T cell receptor clonotypes in acute infectious mononucleosis.* J Exp Med, 1996. 184(5): p. 1815-24.

215. Cohen, G.B., et al., *Clonotype Tracking of TCR Repertoires during Chronic Virus Infections.* Virology, 2002. 304(2): p. 474-484.

216. Klarenbeek, P.L., et al., *Deep sequencing of antiviral T-cell responses to HCMV and EBV in humans reveals a stable repertoire that is maintained for many years.* PLoS Pathog, 2012. 8(9): p. e1002889.

217. Levitsky, V., et al., *The clonal composition of a peptide-specific oligoclonal CTL repertoire selected in response to persistent EBV infection is stable over time.* J Immunol, 1998. 161(2): p. 594-601.

218. Iancu, E.M., et al., *Persistence of EBV antigen-specific CD8 T cell clonotypes during homeostatic immune reconstitution in cancer patients.* PLoS One, 2013. 8(10): p. e78686.

219. Gras, S., et al., *Structural bases for the affinity-driven selection of a public TCR against a dominant human cytomegalovirus epitope.* J Immunol, 2009. 183(1): p. 430-7.

220. Davenport, M.P., et al., *Clonal Selection, Clonal Senescence, and Clonal Succession: The Evolution of the T Cell Response to Infection with a Persistent Virus.* The Journal of Immunology, 2002. 168(7): p. 3309-3317.

221. Griffiths, S.J., et al., *Age-associated increase of low-avidity cytomegalovirus-specific CD8+ T cells that re-express CD45RA.* J Immunol, 2013. 190(11): p. 5363-72.

222. Ouyang, Q., et al., *Large numbers of dysfunctional CD8+ T lymphocytes bearing receptors for a single dominant CMV epitope in the very old.* J Clin Immunol, 2003. 23(4): p. 247-57.

223. Poland, G.A., et al., *A systems biology approach to the effect of aging, immunosenescence and vaccine response.* Curr Opin Immunol, 2014. 29: p. 62-8.

224. Weinberger, B., et al., *Healthy aging and latent infection with CMV lead to distinct changes in CD8+ and CD4+ T-cell subsets in the elderly.* Hum Immunol, 2007. 68(2): p. 86-90.

225. Aw, D., A.B. Silva, and D.B. Palmer, *Immunosenescence: emerging challenges for an ageing population.* Immunology, 2007. 120(4): p. 435-46.

226. Vescovini, R., et al., *Naïve and memory CD8 T cell pool homeostasis in advanced aging: impact of age and of antigen-specific responses to cytomegalovirus.* AGE, 2014. 36(2): p. 625-640.

227. Wertheimer, A.M., et al., *Aging and Cytomegalovirus Infection Differentially and Jointly Affect Distinct Circulating T Cell Subsets in Humans.* The Journal of Immunology, 2014. 192(5): p. 2143-2155.

228. Briceno, O., et al., *Reduced naive CD8(+) T-cell priming efficacy in elderly adults.* Aging Cell, 2016. 15(1): p. 14-21.

229. Fagnoni, F.F., et al., *Shortage of circulating naive CD8(+) T cells provides new insights on immunodeficiency in aging.* Blood, 2000. 95(9): p. 2860-8.

230. Fulop, T., A. Larbi, and G. Pawelec, *Human T Cell Aging and the Impact of Persistent Viral Infections.* Frontiers in Immunology, 2013. 4(271).

231. Akbar, A.N. and M. Vukmanovic-Stejic, *Telomerase in T lymphocytes: use it and lose it?* J Immunol, 2007. 178(11): p. 6689-94.

232. Fulop, T., et al., *Immunosenescence and Inflamm-Aging As Two Sides of the Same Coin: Friends or Foes?* Front Immunol, 2017. 8: p. 1960.

233. Nikolich-Zugich, J., et al., *Age-related changes in CD8 T cell homeostasis and immunity to infection.* Semin Immunol, 2012. 24(5): p. 356-64.

234.   Goronzy, J.J. and C.M. Weyand, *Successful and Maladaptive T Cell Aging.* Immunity, 2017. 46(3): p. 364-378.

235.   Thompson, H.L., et al., *Functional and Homeostatic Impact of Age-Related Changes in Lymph Node Stroma.* Front Immunol, 2017. 8: p. 706.

236.   Kostense, S., et al., *Persistent numbers of tetramer+ CD8(+) T cells, but loss of interferon-gamma+ HIV-specific T cells during progression to AIDS.* Blood, 2002. 99(7): p. 2505-11.

237.   Oxenius, A., et al., *Functional discrepancies in HIV-specific CD8+ T-lymphocyte populations are related to plasma virus load.* J Clin Immunol, 2002. 22(6): p. 363-74.

238.   Shankar, P., et al., *Impaired function of circulating HIV-specific CD8(+) T cells in chronic human immunodeficiency virus infection.* Blood, 2000. 96(9): p. 3094-101.

239.   Gruener, N.H., et al., *Sustained Dysfunction of Antiviral CD8+ T Lymphocytes after Infection with Hepatitis C Virus.* Journal of Virology, 2001. 75(12): p. 5550-5558.

240.   Almanzar, G., et al., *Long-term cytomegalovirus infection leads to significant changes in the composition of the CD8+ T-cell repertoire, which may be the basis for an imbalance in the cytokine production profile in elderly persons.* J Virol, 2005. 79(6): p. 3675-83.

241.   Britanova, O.V., et al., *Age-related decrease in TCR repertoire diversity measured with deep and normalized sequence profiling.* J Immunol, 2014. 192(6): p. 2689-98.

242.   Thome, J.J., et al., *Longterm maintenance of human naive T cells through in situ homeostasis in lymphoid tissue sites.* Sci Immunol, 2016. 1(6).

243.   Yoshida, K., et al., *Aging-related changes in human T-cell repertoire over 20years delineated by deep sequencing of peripheral T-cell receptors.* Exp Gerontol, 2017. 96: p. 29-37.

244.   Khan, N., et al., *Cytomegalovirus Seropositivity Drives the CD8 T Cell Repertoire Toward Greater Clonality in Healthy Elderly Individuals.* The Journal of Immunology, 2002. 169(4): p. 1984-1992.

245.   Yang, T.Y., Y.F. Chuang, and Y.L. Chiu, *T-cell aging in end-stage renal disease: an evolving story with CMV.* Med Microbiol Immunol, 2019.

246.   van de Berg, P.J., et al., *Cytomegalovirus-induced effector T cells cause endothelial cell damage.* Clin Vaccine Immunol, 2012. 19(5): p. 772-9.

247.   Roberts, E.T., et al., *Cytomegalovirus antibody levels, inflammation, and mortality among elderly Latinos over 9 years of follow-up.* Am J Epidemiol, 2010. 172(4): p. 363-71.

248.   Gkrania-Klotsas, E., et al., *Higher immunoglobulin G antibody levels against cytomegalovirus are associated with incident ischemic heart disease in the population-based EPIC-Norfolk cohort.* J Infect Dis, 2012. 206(12): p. 1897-903.

249.   Smithey, M.J., et al., *Lifelong CMV infection improves immune defense in old mice by broadening the mobilized TCR repertoire against third-party infection.* Proc Natl Acad Sci U S A, 2018. 115(29): p. E6817-E6825.

250.   Arai, Y., et al., *Inflammation, But Not Telomere Length, Predicts Successful Ageing at Extreme Old Age: A Longitudinal Study of Semi-supercentenarians.* EBioMedicine, 2015. 2(10): p. 1549-58.

251.   Barton, E.S., et al., *Herpesvirus latency confers symbiotic protection from bacterial infection.* Nature, 2007. 447(7142): p. 326-9.

252.   Furman, D., et al., *Cytomegalovirus infection enhances the immune response to influenza.* Sci Transl Med, 2015. 7(281): p. 281ra43.

253.   Frasca, D., et al., *Cytomegalovirus (CMV) seropositivity decreases B cell responses to the influenza vaccine.* Vaccine, 2015. 33(12): p. 1433-9.

254.   Allard, M., et al., *TCR-ligand dissociation rate is a robust and stable biomarker of CD8+ T cell potency.* JCI Insight, 2017. 2(14).

255.   Stone, J.D., A.S. Chervin, and D.M. Kranz, *T-cell receptor binding affinities and kinetics: impact on T-cell activity and specificity.* Immunology, 2009. 126(2): p. 165-76.

256.   Zhang, S.Q., et al., *Direct measurement of T cell receptor affinity and sequence from naive antiviral T cells.* Sci Transl Med, 2016. 8(341): p. 341ra77.

257. Rufer, N., *Molecular tracking of antigen-specific T-cell clones during immune responses.* Curr Opin Immunol, 2005. 17(4): p. 441-7.

258. Busch, D.H. and E.G. Pamer, *T cell affinity maturation by selective expansion during infection.* J Exp Med, 1999. 189(4): p. 701-10.

259. Cukalac, T., et al., *Reproducible selection of high avidity CD8+ T-cell clones following secondary acute virus infection.* Proc Natl Acad Sci U S A, 2014. 111(4): p. 1485-90.

260. Savage, P.A., J.J. Boniface, and M.M. Davis, *A kinetic basis for T cell receptor repertoire selection during an immune response.* Immunity, 1999. 10(4): p. 485-92.

261. Legat, A., et al., *Inhibitory Receptor Expression Depends More Dominantly on Differentiation and Activation than "Exhaustion" of Human CD8 T Cells.* Front Immunol, 2013. 4: p. 455.

262. Fuertes Marraco, S.A., et al., *Inhibitory Receptors Beyond T Cell Exhaustion.* Front Immunol, 2015. 6: p. 310.

263. Gustafson, C.E., et al., *Immune Checkpoint Function of CD85j in CD8 T Cell Differentiation and Aging.* Front Immunol, 2017. 8: p. 692.

264. Kissick, H.T. and M.G. Sanda, *The role of active vaccination in cancer immunotherapy: lessons from clinical trials.* Curr Opin Immunol, 2015. 35: p. 15-22.

265. Fong, L., et al., *Activated lymphocyte recruitment into the tumor microenvironment following preoperative sipuleucel-T for localized prostate cancer.* J Natl Cancer Inst, 2014. 106(11).

266. Kantoff, P.W., et al., *Sipuleucel-T immunotherapy for castration-resistant prostate cancer.* N Engl J Med, 2010. 363(5): p. 411-22.

267. Tanyi, J.L., et al., *Personalized cancer vaccine effectively mobilizes antitumor T cell immunity in ovarian cancer.* Sci Transl Med, 2018. 10(436).

268. Schleiss, M.R., *Cytomegalovirus vaccines under clinical development.* J Virus Erad, 2016. 2(4): p. 198-207.

269. Griffiths, P.D., et al., *Cytomegalovirus glycoprotein-B vaccine with MF59 adjuvant in transplant recipients: a phase 2 randomised placebo-controlled trial.* Lancet, 2011. 377(9773): p. 1256-63.

270. Kharfan-Dabaja, M.A., et al., *A novel therapeutic cytomegalovirus DNA vaccine in allogeneic haemopoietic stem-cell transplantation: a randomised, double-blind, placebo-controlled, phase 2 trial.* Lancet Infect Dis, 2012. 12(4): p. 290-9.

271. Nakamura, R., et al., *Viraemia, immunogenicity, and survival outcomes of cytomegalovirus chimeric epitope vaccine supplemented with PF03512676 (CMVPepVax) in allogeneic haemopoietic stem-cell transplantation: randomised phase 1b trial.* Lancet Haematol, 2016. 3(2): p. e87-98.

272. Robert, C., et al., *Nivolumab in previously untreated melanoma without BRAF mutation.* N Engl J Med, 2015. 372(4): p. 320-30.

273. Schadendorf, D., et al., *Pooled Analysis of Long-Term Survival Data From Phase II and Phase III Trials of Ipilimumab in Unresectable or Metastatic Melanoma.* J Clin Oncol, 2015. 33(17): p. 1889-94.

274. Rosenberg, S.A., et al., *Use of tumor-infiltrating lymphocytes and interleukin-2 in the immunotherapy of patients with metastatic melanoma. A preliminary report.* N Engl J Med, 1988. 319(25): p. 1676-80.

275. Gill, S., M.V. Maus, and D.L. Porter, *Chimeric antigen receptor T cell therapy: 25years in the making.* Blood Rev, 2016. 30(3): p. 157-67.

276. Schubert, M.L., et al., *Chimeric antigen receptor transduced T cells: Tuning up for the next generation.* Int J Cancer, 2018. 142(9): p. 1738-1747.

277. Kaeuferle, T., et al., *Strategies of adoptive T-cell transfer to treat refractory viral infections post allogeneic stem cell transplantation.* J Hematol Oncol, 2019. 12(1): p. 13.

278. Haque, T., et al., *Allogeneic cytotoxic T-cell therapy for EBV-positive posttransplantation lymphoproliferative disease: results of a phase 2 multicenter clinical trial.* Blood, 2007. 110(4): p. 1123-31.

279. Icheva, V., et al., *Adoptive transfer of epstein-barr virus (EBV) nuclear antigen 1-specific t cells as treatment for EBV reactivation and lymphoproliferative disorders after allogeneic stem-cell transplantation.* J Clin Oncol, 2013. 31(1): p. 39-48.

280. Falcioni, F., et al., *Influence of CD26 and integrins on the antigen sensitivity of human memory T cells.* Hum Immunol, 1996. 50(2): p. 79-90.

281. Hesse, M.D., et al., *A T cell clone's avidity is a function of its activation state.* J Immunol, 2001. 167(3): p. 1353-61.

282. Hemler, M.E., et al., *VLA-1: a T cell surface antigen which defines a novel late stage of human T cell activation.* Eur J Immunol, 1985. 15(5): p. 502-8.

283. Bank, I., et al., *Expression and functions of very late antigen 1 in inflammatory joint diseases.* J Clin Immunol, 1991. 11(1): p. 29-38.

284. Rao, W.H., J.M. Hales, and R.D. Camp, *Potent costimulation of effector T lymphocytes by human collagen type I.* J Immunol, 2000. 165(9): p. 4935-40.

285. Giancotti, F.G. and E. Ruoslahti, *Integrin signaling.* Science, 1999. 285(5430): p. 1028-32.

286. Valmori, D., et al., *Enhanced generation of specific tumor-reactive CTL in vitro by selected Melan-A/MART-1 immunodominant peptide analogues.* J Immunol, 1998. 160(4): p. 1750-8.

287. Fourcade, J., et al., *Immunization with analog peptide in combination with CpG and montanide expands tumor antigen-specific CD8+ T cells in melanoma patients.* J Immunother, 2008. 31(8): p. 781-91.

288. Baumgaertner, P., et al., *Vaccination-induced functional competence of circulating human tumor-specific CD8 T-cells.* Int J Cancer, 2012. 130(11): p. 2607-17.

289. Karbach, J., et al., *Tumor-reactive CD8+ T-cell responses after vaccination with NY-ESO-1 peptide, CpG 7909 and Montanide ISA-51: association with survival.* Int J Cancer, 2010. 126(4): p. 909-18.

290. Hebeisen, M., et al., *Molecular insights for optimizing T cell receptor specificity against cancer.* Front Immunol, 2013. 4: p. 154.

291. Corse, E., et al., *Attenuated T cell responses to a high-potency ligand in vivo.* PLoS Biol, 2010. 8(9).

292. Hebeisen, M., et al., *SHP-1 phosphatase activity counteracts increased T cell receptor affinity.* J Clin Invest, 2013. 123(3): p. 1044-56.

293. Irving, M., et al., *Interplay between T cell receptor binding kinetics and the level of cognate peptide presented by major histocompatibility complexes governs CD8+ T cell responsiveness.* J Biol Chem, 2012. 287(27): p. 23068-78.

294. Presotto, D., et al., *Fine-Tuning of Optimal TCR Signaling in Tumor-Redirected CD8 T Cells by Distinct TCR Affinity-Mediated Mechanisms.* Front Immunol, 2017. 8: p. 1564.

295. Riquelme, E., et al., *The duration of TCR/pMHC interactions regulates CTL effector function and tumor-killing capacity.* Eur J Immunol, 2009. 39(8): p. 2259-69.

296. Kyewski, B. and L. Klein, *A central role for central tolerance.* Annu Rev Immunol, 2006. 24: p. 571-606.

297. Kurts, C., et al., *Class I-restricted cross-presentation of exogenous self-antigens leads to deletion of autoreactive CD8(+) T cells.* J Exp Med, 1997. 186(2): p. 239-45.

298. Bouneaud, C., P. Kourilsky, and P. Bousso, *Impact of negative selection on the T cell repertoire reactive to a self-peptide: a large fraction of T cell clones escapes clonal deletion.* Immunity, 2000. 13(6): p. 829-40.

299. Turner, M.J., et al., *Avidity maturation of memory CD8 T cells is limited by self-antigen expression.* J Exp Med, 2008. 205(8): p. 1859-68.

300. Yu, W., et al., *Clonal Deletion Prunes but Does Not Eliminate Self-Specific alphabeta CD8(+) T Lymphocytes.* Immunity, 2015. 42(5): p. 929-41.

301. Zehn, D. and M.J. Bevan, *T cells with low avidity for a tissue-restricted antigen routinely evade central and peripheral tolerance and cause autoimmunity.* Immunity, 2006. 25(2): p. 261-70.

302. Boon, T., et al., *Human T cell responses against melanoma.* Annu Rev Immunol, 2006. 24: p. 175-208.

303. McMahan, R.H. and J.E. Slansky, *Mobilizing the low-avidity T cell repertoire to kill tumors.* Semin Cancer Biol, 2007. 17(4): p. 317-29.

304. Liechtenstein, T., et al., Modulating co-stimulation during antigen presentation to enhance cancer immunotherapy. Immunol Endocr Metab Agents Med Chem, 2012. 12(3): p. 224-235.

305. Restifo, N.P., M.E. Dudley, and S.A. Rosenberg, *Adoptive immunotherapy for cancer: harnessing the T cell response.* Nat Rev Immunol, 2012. 12(4): p. 269-81.

306. Pinto, S., et al., *Misinitiation of intrathymic MART-1 transcription and biased TCR usage explain the high frequency of MART-1-specific T cells.* Eur J Immunol, 2014. 44(9): p. 2811-21.

307. Pittet, M.J., et al., *High frequencies of naive Melan-A/MART-1-specific CD8(+) T cells in a large proportion of human histocompatibility leukocyte antigen (HLA)-A2 individuals.* J Exp Med, 1999. 190(5): p. 705-15.

308. Romero, P., D.E. Speiser, and N. Rufer, *Deciphering the unusual HLA-A2/Melan-A/MART-1-specific TCR repertoire in humans.* Eur J Immunol, 2014. 44(9): p. 2567-70.

309. Voelter, V., et al., *Characterization of Melan-A reactive memory CD8+ T cells in a healthy donor.* Int Immunol, 2008. 20(8): p. 1087-96.

310. Dutoit, V., et al., *Degeneracy of antigen recognition as the molecular basis for the high frequency of naive A2/Melan-a peptide multimer(+) CD8(+) T cells in humans.* J Exp Med, 2002. 196(2): p. 207-16.

311. Pittet, M.J., et al., *Alpha 3 domain mutants of peptide/MHC class I multimers allow the selective isolation of high avidity tumor-reactive CD8 T cells.* J Immunol, 2003. 171(4): p. 1844-9.

312. Gnjatic, S., et al., *NY-ESO-1: review of an immunogenic tumor antigen.* Adv Cancer Res, 2006. 95: p. 1-30.

313. Schumacher, T.N. and R.D. Schreiber, *Neoantigens in cancer immunotherapy.* Science, 2015. 348(6230): p. 69-74.

314. Bobisse, S., et al., *Sensitive and frequent identification of high avidity neo-epitope specific CD8 (+) T cells in immunotherapy-naive ovarian cancer.* Nat Commun, 2018. 9(1): p. 1092.

315. Bobisse, S., et al., *Neoantigen-based cancer immunotherapy.* Ann Transl Med, 2016. 4(14): p. 262.

316. Soler, M., et al., *Two-Dimensional Label-Free Affinity Analysis of Tumor-Specific CD8 T Cells with a Biomimetic Plasmonic Sensor.* ACS Sens, 2018. 3(11): p. 2286-2295.

317. Wong, P. and E.G. Pamer, *CD8 T cell responses to infectious pathogens.* Annu Rev Immunol, 2003. 21: p. 29-70.

318. Jergovic, M., N.A. Contreras, and J. Nikolich-Zugich, *Impact of CMV upon immune aging: facts and fiction.* Med Microbiol Immunol, 2019.

319. Beura, L.K., et al., *Normalizing the environment recapitulates adult human immune traits in laboratory mice.* Nature, 2016. 532(7600): p. 512-6.

320. Rector, J.L., et al., *Consistent associations between measures of psychological stress and CMV antibody levels in a large occupational sample.* Brain Behav Immun, 2014. 38: p. 133-41.

321. Faint, J.M., et al., *Quantitative flow cytometry for the analysis of T cell receptor Vbeta chain expression.* J Immunol Methods, 1999. 225(1-2): p. 53-60.

322. Dietrich, P.Y., et al., *Melanoma patients respond to a cytotoxic T lymphocyte-defined self-peptide with diverse and nonoverlapping T-cell receptor repertoires.* Cancer Res, 2001. 61(5): p. 2047-54.

323. Valmori, D., et al., *Tetramer-guided analysis of TCR beta-chain usage reveals a large repertoire of melan-A-specific CD8+ T cells in melanoma patients.* J Immunol, 2000. 165(1): p. 533-8.

324. Gupta, B., et al., *Simultaneous coexpression of memory-related and effector-related genes by individual human CD8 T cells depends on antigen specificity and differentiation.* J Immunother, 2012. 35(6): p. 488-501.

325. Robins, H.S., et al., *Comprehensive assessment of T-cell receptor beta-chain diversity in alphabeta T cells.* Blood, 2009. 114(19): p. 4099-107.

326. Ruggiero, E., et al., *High-resolution analysis of the human T-cell receptor repertoire.* Nat Commun, 2015. 6: p. 8081.

327. Sherwood, A.M., et al., *Tumor-infiltrating lymphocytes in colorectal tumors display a diversity of T cell receptor sequences that differ from the T cells in adjacent mucosal tissue.* Cancer Immunol Immunother, 2013. 62(9): p. 1453-61.

328. Laydon, D.J., C.R. Bangham, and B. Asquith, *Estimating T-cell repertoire diversity: limitations of classical estimators and a new approach.* Philos Trans R Soc Lond B Biol Sci, 2015. 370(1675).

329. De Simone, M., G. Rossetti, and M. Pagani, *Single Cell T Cell Receptor Sequencing: Techniques and Future Challenges.* Front Immunol, 2018. 9: p. 1638.

330. Papalexi, E. and R. Satija, *Single-cell RNA sequencing to explore immune cell heterogeneity.* Nat Rev Immunol, 2018. 18(1): p. 35-45.

331. Afik, S., et al., *Targeted reconstruction of T cell receptor sequence from single cell RNA-sequencing links CDR3 length to T cell differentiation state.* bioRxiv, 2016: p. 072744.

332. Lonnberg, T., et al., *Single-cell RNA-seq and computational analysis using temporal mixture modelling resolves Th1/Tfh fate bifurcation in malaria.* Sci Immunol, 2017. 2(9).

333. Redmond, D., A. Poran, and O. Elemento, *Single-cell TCRseq: paired recovery of entire T-cell alpha and beta chain transcripts in T-cell receptors from single-cell RNAseq.* Genome Med, 2016. 8(1): p. 80.

334. Stubbington, M.J.T., et al., *T cell fate and clonality inference from single-cell transcriptomes.* Nat Methods, 2016. 13(4): p. 329-332.

335. Klein, A.M., et al., *Droplet barcoding for single-cell transcriptomics applied to embryonic stem cells.* Cell, 2015. 161(5): p. 1187-1201.

336. Macosko, E.Z., et al., *Highly Parallel Genome-wide Expression Profiling of Individual Cells Using Nanoliter Droplets.* Cell, 2015. 161(5): p. 1202-1214.

337. Zemmour, D., et al., *Single-cell gene expression reveals a landscape of regulatory T cell phenotypes shaped by the TCR.* Nat Immunol, 2018. 19(3): p. 291-301.

338. Turner, S.J., et al., *Lack of prominent peptide-major histocompatibility complex features limits repertoire diversity in virus-specific CD8+ T cell populations.* Nat Immunol, 2005. 6(4): p. 382-9.

339. Rossjohn, J., et al., *T cell antigen receptor recognition of antigen-presenting molecules.* Annu Rev Immunol, 2015. 33: p. 169-200.

340. Miles, J.J., et al., *Genetic and structural basis for selection of a ubiquitous T cell receptor deployed in Epstein-Barr virus infection.* PLoS Pathog, 2010. 6(11): p. e1001198.

341. Turner, S.J., et al., *Structural determinants of T-cell receptor bias in immunity.* Nat Rev Immunol, 2006. 6(12): p. 883-94.

342. Day, E.K., et al., *Rapid CD8+ T cell repertoire focusing and selection of high-affinity clones into memory following primary infection with a persistent human virus: human cytomegalovirus.* J Immunol, 2007. 179(5): p. 3203-13.

343. Britanova, O.V., et al., *Dynamics of Individual T Cell Repertoires: From Cord Blood to Centenarians.* J Immunol, 2016. 196(12): p. 5005-13.

344. Trautmann, L., et al., *Selection of T cell clones expressing high-affinity public TCRs within Human cytomegalovirus-specific CD8 T cell responses.* J Immunol, 2005. 175(9): p. 6123-32.

345. Schober, K., V.R. Buchholz, and D.H. Busch, *TCR repertoire evolution during maintenance of CMV-specific T-cell populations.* Immunol Rev, 2018. 283(1): p. 113-128.

346. Vescovini, R., et al., *Massive load of functional effector CD4+ and CD8+ T cells against cytomegalovirus in very old subjects.* J Immunol, 2007. 179(6): p. 4283-91.

347. Jackson, S.E., et al., *Latent Cytomegalovirus (CMV) Infection Does Not Detrimentally Alter T Cell Responses in the Healthy Old, But Increased Latent CMV Carriage Is Related to Expanded CMV-Specific T Cells.* Front Immunol, 2017. 8: p. 733.

348. Khan, N., et al., *T cell recognition patterns of immunodominant cytomegalovirus antigens in primary and persistent infection.* J Immunol, 2007. 178(7): p. 4455-65.

349. Bunde, T., et al., *Protection from cytomegalovirus after transplantation is correlated with immediate early 1-specific CD8 T cells.* J Exp Med, 2005. 201(7): p. 1031-6.

350. Stinski, M.F., *Sequence of protein synthesis in cells infected by human cytomegalovirus: early and late virus-induced polypeptides.* J Virol, 1978. 26(3): p. 686-701.

351. Rice, G.P., R.D. Schrier, and M.B. Oldstone, *Cytomegalovirus infects human lymphocytes and monocytes: virus expression is restricted to immediate-early gene products.* Proc Natl Acad Sci U S A, 1984. 81(19): p. 6134-8.

352. Welten, S.P.M., N.S. Baumann, and A. Oxenius, *Fuel and brake of memory T cell inflation.* Med Microbiol Immunol, 2019.

353. Pita-Lopez, M.L., et al., *Effect of ageing on CMV-specific CD8 T cells from CMV seropositive healthy donors.* Immun Ageing, 2009. 6: p. 11.

354. Jackson, S.E., et al., *Generation, maintenance and tissue distribution of T cell responses to human cytomegalovirus in lytic and latent infection.* Med Microbiol Immunol, 2019.

355. Redeker, A., S.P. Welten, and R. Arens, *Viral inoculum dose impacts memory T-cell inflation.* Eur J Immunol, 2014. 44(4): p. 1046-57.

356. Lamar, D.L., C.M. Weyand, and J.J. Goronzy, *Promoter choice and translational repression determine cell type-specific cell surface density of the inhibitory receptor CD85j expressed on different hematopoietic lineages.* Blood, 2010. 115(16): p. 3278-86.

357. Dietrich, J., M. Cella, and M. Colonna, *Ig-like transcript 2 (ILT2)/leukocyte Ig-like receptor 1 (LIR1) inhibits TCR signaling and actin cytoskeleton reorganization.* J Immunol, 2001. 166(4): p. 2514-21.

358. Shiroishi, M., et al., *Human inhibitory receptors Ig-like transcript 2 (ILT2) and ILT4 compete with CD8 for MHC class I binding and bind preferentially to HLA-G.* Proc Natl Acad Sci U S A, 2003. 100(15): p. 8856-61.

359. Chapman, T.L., A.P. Heikeman, and P.J. Bjorkman, *The inhibitory receptor LIR-1 uses a common binding interaction to recognize class I MHC molecules and the viral homolog UL18.* Immunity, 1999. 11(5): p. 603-13.

360. Prod'homme, V., et al., *The human cytomegalovirus MHC class I homolog UL18 inhibits LIR-1+ but activates LIR-1- NK cells.* J Immunol, 2007. 178(7): p. 4473-81.

361. Antrobus, R.D., et al., *Virus-specific cytotoxic T lymphocytes differentially express cell-surface leukocyte immunoglobulin-like receptor-1, an inhibitory receptor for class I major histocompatibility complex molecules.* J Infect Dis, 2005. 191(11): p. 1842-53.

362. Seckert, C.K., et al., *Viral latency drives 'memory inflation': a unifying hypothesis linking two hallmarks of cytomegalovirus infection.* Med Microbiol Immunol, 2012. 201(4): p. 551-66.

363. Baumann, N.S., et al., *Early primed KLRG1- CMV-specific T cells determine the size of the inflationary T cell pool.* PLoS Pathog, 2019. 15(5): p. e1007785.

364. O'Hara, G.A., et al., *Memory T cell inflation: understanding cause and effect.* Trends in Immunology, 2012. 33(2): p. 84-90.

365. Colonna, M., et al., *A common inhibitory receptor for major histocompatibility complex class I molecules on human lymphoid and myelomonocytic cells.* J Exp Med, 1997. 186(11): p. 1809-18.

366. Carosella, E.D., et al., *HLA-G: An Immune Checkpoint Molecule.* Adv Immunol, 2015. 127: p. 33-144.

367. Kang, X., et al., *Inhibitory leukocyte immunoglobulin-like receptors: Immune checkpoint proteins and tumor sustaining factors.* Cell Cycle, 2016. 15(1): p. 25-40.

368. Wisniewski, A., et al., *Genetic polymorphisms and expression of HLA-G and its receptors, KIR2DL4 and LILRB1, in non-small cell lung cancer.* Tissue Antigens, 2015. 85(6): p. 466-75.

369. Wan, R., et al., *Human Leukocyte Antigen-G Inhibits the Anti-Tumor Effect of Natural Killer Cells via Immunoglobulin-Like Transcript 2 in Gastric Cancer.* Cell Physiol Biochem, 2017. 44(5): p. 1828-1841.

370. Barkal, A.A., et al., *Engagement of MHC class I by the inhibitory receptor LILRB1 suppresses macrophages and is a target of cancer immunotherapy.* Nat Immunol, 2018. 19(1): p. 76-84.

Acknowledgements

First, I would like to warmly thank Dr. Nathalie Rufer, for giving me the opportunity to do my PhD in her group and for believing in my skills. Thank you for your supervision and support during these 4 years and all the confidence you have put in me. I feel very lucky to have had the chance to work in such a great environment and to have been able to develop my scientific skills and to grow up personally in the Rufer lab.

I also kindly thank all the members of the Rufer lab, starting from Michael Hebeisen for his communicative motivation and passion for science, his fatherly support, and all his advice. It was a pleasure, although too rare, to work with you! Thank you, Minh Ngoc Duong, for your scientific input and nice chats together. Thank you, almost-Dr. Efe Erdes for your sincere kindness and generosity and for all the fun we shared in and outside the lab! I am especially thankful to Mathilde Allard, who taught me so much in the first years of my thesis and for whom I have immense scientific and personal respect. I hope we will continue our catch-up sessions over a drink for many years to come! Finally, I am especially thankful to Laura Carretero-Iglesia, for all her help and advice in the lab, her true friendship and endless support. I could not have dreamed of a better partner in crime to share the last 4 years with. While it is without doubt that our friendship paths won't split, I hope our scientific paths will cross again!

I also wish to acknowledge Prof. Fabienne Tacchini-Cottier, Prof. Annette Oxenius, Prof. Daniel Speiser, Prof. Pedro Romero and Prof. Renaud Du Pasquier for participating in my PhD jury during the different steps of my thesis and for all their precious advice and suggestions to improve my research.

I would also like to thank Anne Wilson, Romain Bedel, Francisco Saladeoyangure, and Danny Labes for their assistance with the flow cytometry facility, Patricia Werffeli, Françoise Flejszman and Natasa Jovanovic for their administrative support, Nicole Montandon and Anthony Cornu for their magic hands to take blood and all the blood donors without who I could not have carried out this project!

I am extremely grateful to all the people of the 2nd floor of the Biopole 3 and especially colleagues from the Romero and Speiser lab, for all the science, reagents, stress, hopelessness but most importantly successes, lunches, laughs, beers, parties and amazing adventures we shared together. I would like to also particularly thank the people from the Verdeil group

(Laure, Claire, Marine, Connie and Daniela) who became much more than just my office mates during the last year of my thesis. Thank you girls for our daily conversations, for your caring support and encouragement!

Thank you so much to all my friends here in Lausanne, from the Limousin and Bordeaux for their warm support and for having been my best allies to escape from the everyday PhD life.

Finally, I would like to particularly thank my family, mom, Luc, Théo, Sarah, Tom, Cassandre, Mamiette and Dude for their support since the beginning, their constant encouragement and for always having believed in me. Our regular phone calls and reunions in Limousin were an essential source of joy and an energy boost. A special thanks to my sister Sarah for her daily support, fun, confidence, help and much more. Having you next to me during this journey was invaluable.

Last but not least, I would like to thank Timothy Murray for his unfailing and constant support. I can never thank you enough for all your help during these years and while writing this thesis. Thank you for always being able to pick me up during the difficult times, and for always looking at the bright side of "la petite vie". Thank you for your kindness, your love and all the wonderful moments we shared and all the new ones I look forward to share with mon chaton in a PhD-free mind!

Appendix 1 – Curriculum Vitae

Barbara COUTURAUD

Rue de Bourg 35 – 1003 Lausanne, Switzerland

+41 (0) 76 418 11 35 – couturaud.barbara@gmail.com

Education

2015 - present **– PhD in Cancer and Immunology** – *University of Lausanne (UNIL) and Lausanne university hospital (CHUV) – SWITZERLAND*
T cell biology and engineering group, Dr. Nathalie Rufer
Impact of TCR-ligand avidity for viral and tumor antigens on human CD8 T cell potency and long-term persistence

2012 - 2015 **– Master's degree in Biotechnology** – *ENSTBB (Bordeaux National School of Biomolecular Technology) – FRANCE*

2010 - 2012 **– Associate's Degree in Biology of Human Health, specialty biological and biochemical analysis** – *University of Technology - Angers, FRANCE*

Relevant work experience

2015 - present
(4 years)

PhD student **– PhD in Cancer and Immunology - *University of Lausanne (UNIL) and Lausanne university hospital (CHUV) – SWITZERLAND***

- Research on the impact of TCR-pMHC-CD8 avidity on T cell potency and long-term persistence in human
- Generation and culture of primary antigen-specific CD8+ T cell clones
- Multichromatic flow cytometry and NTAmers staining and dissociation kinetics measurements
- DNA and RNA extraction – PCR and RT-PCR – TCR Spectratyping
- T cells functional assays (Chromium release cytotoxic T lymphocytes assay; CD107a degranulation and intracellular cytokine staining; surface marker expression and modulation assay)

2014 - 2015
(7 months)

Intern **– Biopharm Research and Development – *GlaxoSmithKline, UK***

- Selection of domain antibodies by phage display as building blocks for bispecific antibodies generation
- Phage display selection on soluble antigen - Phage ELISA - Sequencing analysis - Protein expression
- Protein purification (Protein A and Size Exclusion Chromatography) – SDS-PAGE – LC/MS analysis
- Cell-based binding assay by FACS

2013
(2 months)

Intern **– Conlon Research laboratory – *University of North Carolina at Chapel Hill, USA***

- Study of the implication of the transcription factor LIM homeobox 9 during epicardial development in *Xenopus laevis*
- Whole-mount *in situ* hybridization – Immunohistochemistry – Scanning Electron Microscopy
- Molecular Biology: PCR – Construction of over expressing plasmid
- Cell culture (HEK-293) – Cell transfection – Scratch assay

2012
(3 months)

Intern **– Academic Research Laboratory –** *Medical University of Limoges, FRANCE*

- Study of the potential role of p75NTR and TrkB neurotrophin receptors in human glioblastoma cell line (U-87 MG) grown in normoxia or hypoxia
- Cell culture - ELISA cell death – BrdU Cell Proliferation Assay
- Molecular Biology: RNA extraction (Qiagen RNeasy Mini kit) – RT PCR
- *In vivo* study: Cells grafted in a chick chorioallantoic membrane model

Skills

Informatics: Extensive experience with Microsoft Office packages (Windows & OSX), FLowJo, Snapgene, GraphPad prism, Navigation on public Data Bank (NCBI), sequence alignment (BLAST, FASTA)

Quality: Compliance with GLP (Good Laboratory Practice) and GMP (Good Manufacturing Practice) guidelines

Language: Native French speaker, fluent in English

Scientific publications and presentations

Publications

- Allard M, **Couturaud B**, Carretero-Iglesia L, Duong MN, Schmidt J, Monnot GC, Romero P, Speiser DE, Hebeisen M, and Rufer N. TCR-ligand dissociation rate is a robust and stable biomarker of CD8+ T cell potency. *JCI Insight.* 2017;2(14).
- **Couturaud B**, Carretero-Iglesia L, Allard M, Pradervand S, Hebeisen M and Rufer N. Progressive long-term avidity decline of CMV- but not EBV-specific memory CD8 T cell clonotype repertoires. *Manuscript in preparation.*
- Carretero-Iglesia L, **Couturaud B**, Baumgaertner P, Schmidt J, Maby-El Hajjami H, Speiser DE, Hebeisen M and Rufer N. Increased peptide dose vaccine promotes the rapid selection of tumor-reactive CD8 T cells of enhanced TCR binding and functional avidity. *Manuscript in preparation.*

Presentations

- Symposium Fourth Faculty and Staff Retreat 2015, EPFL – Poster presentation
- 6th EPFL-UNIL PhD retreat, 2016 – Oral presentation
- Symposium Fifth Faculty and Staff Retreat 2016, EPFL – Poster presentation
- 7th EPFL-UNIL PhD retreat, 2017 – Oral presentation
- Symposium Sixth Faculty and Staff Retreat, 2017, EPFL – Poster presentation
- 30th meeting of the Swiss Immunology PhD students 2018 – Oral presentation
- 5th European Congress of Immunology (ECI), 2018 – Poster presentation